Transport and Hydrodynamics in Holography, Strange Metals and Graphene

a dissertation presented

by

Andrew Lucas

to

The Department of Physics

in partial fulfillment of the requirements for the degree of Doctor of Philosophy in the subject of

Physics

Harvard University
Cambridge, Massachusetts
April 2016

 $\bigodot{2016}$ – Andrew Lucas

All rights reserved.

Transport and Hydrodynamics in Holography, Strange Metals and Graphene

ABSTRACT

This dissertation provides an overview of what gauge-gravity duality, often called holography, has taught us about quantum condensed matter physics, with particular emphasis on the problem of thermoelectric transport. A comprehensive theory of transport in weakly disordered metals is subsequently developed using a variety of techniques, all of which precisely agree. The theory in its present form may be applied directly to realistic models of transport in strongly interacting strange metallic phases, and also serves as a point of direct contact between gauge-gravity duality and more traditional theories of condensed matter physics. Next, novel techniques are developed to demonstrate the absence of disorder-driven metal-insulator transitions in holographic metals in two spatial dimensions. Finally, experimental evidence is presented for hydrodynamic transport in charge neutral graphene, and new theories are developed to understanding the resulting data.

Contents

Acknowledgements

I would like to thank the many collaborators and friends at Harvard who have made my stay so wonderful. First and foremost, my advisor Subir Sachdev has been a fantastic mentor and through his support I have become a much better scientist. Secondly, I am indebted to my fellow graduate students, for good times and support: Alex Thomson, Shubhayu Chatterjee, Seth Whitsitt, Wenbo Fu, Julia Steinberg, Aavishkar Patel and Debanjan Chowdhury in Subir's group, and Kartiek Agarwal, Monica Kang, Temple He, Dan Kapec, Yuliya Dovzhenko, Arthur Safira and Tom Rudelius in the broader department. I have appreciated collaboration and discussions with Joe Bhaseen, Ben Doyon, Philipp Strack, Piotr Surowka, Tatsuhiko Ikeda, Yuichiro Nakai, Richard Davison, Will Witzcak-Krempa, Philip Kim and Saso Grozdanov. I would also like to especially thank the collaborators Sean Hartnoll, Koenraad Schalm, Paul Chesler, Kin Chung Fong and Jesse Crossno for many excellent conversations and discoveries over the years. Many of the aforementioned have also become friends and I hope to maintain professional and personal communication with them.

Most of all, I am grateful to my parents Bob and Sara Lucas for personal and financial support during my graduate studies. I am looking forward to the next chapter of my life as a postdoctoral fellow at Stanford and will always look back fondly on these past four years for the intensive personal and professional growth they have afforded me.

Chapter 1

Overview

Here we present a brief summary of the contents of this thesis.

Part I of this thesis consists of a large portion of a comprehensive upcoming review article, co-authored with Sean Hartnoll and Subir Sachdev. Especially on the problem of transport in strange metals, such rapid advances have occurred in the past two years that the field is badly lacking a comprehensive overview of these advances, which may place them into their proper context. I hope that this work will ultimately provide an excellent reference, and may serve as a compass to newcomers to a large body of recent literature. An extensive and pedagogical introduction to the subject is found here.

Part II of this thesis consists of a selection of the original papers [?, ?, ?] which have led to the development of a comprehensive theory of transport in weakly disordered metals. In a formal sense, this problem is now solved. Part III of this thesis consists of a pair of short papers [?, ?] which discuss bounds on thermoelectric transport coefficients in holographic models of metals in two spatial dimensions. Part IV of this thesis discusses the application of many of these theoretical ideas – in particular, the concept of hydrodynamic transport in electron fluids – to the Dirac fluid in graphene, which appeared in [?, ?]. This is the first time that such concrete contact has been made between a "string theory"-inspired approach to condensed matter physics, and a solid-state experiment.

Part I

Review and Introduction

Chapter 2

Holographic quantum matter

The holographic correspondence

Introducing 'AdS/CMT'

This review is about a particular interface between condensed matter physics, gravitational physics and string and quantum field theory. The defining feature of this interface is that it is made possible by holographic duality, to be introduced briefly in this first section. This interface has been called 'AdS/CMT' – a pun on the name of the best understood version of holography, the AdS/CFT correspondence. Let us be clear from the outset, however, that neither AdS nor CFT are essential features of the framework that we will develop.

Holographic condensed matter physics encompasses a body of work with a wide range of motivations and objectives. Here are three different informal and zeroth order descriptions of the remit of this review:

- For the condensed matter physicist: AdS/CMT is the study of condensed matter systems without quasiparticles. In particular, AdS/CMT provides a class of models without an underlying quasiparticle description in which controlled computations can nonetheless be performed.
- For the relativist: AdS/CMT is the study of event horizons in spacetimes whose asymptopia acts as a confining box. Asymptotically AdS spacetime is the simplest such box. Of particular interest are charged horizons, as well as various flavors of novel 'hairy' black holes.
- For the string or field theorist: AdS/CMT is the study of certain properties of large N field theories and their corresponding holographically dual spacetimes. Of particular interest are dissipative properties and the phases of the theory as a function of temperature and chemical potentials.

Of course our reader should feel no need to place herself in a particular category! The point is that under the umbrella of 'AdS/CMT' one will find, for example, discussions of experimental features of non-quasiparticle transport, ways around no-hair theorems for black holes, and discussions of objects from string theory such as D-branes. We aim to address all these perspectives in the following. While we have tried to make our discussion intelligible to readers from different backgrounds, for basic introductory material we will refer the reader to the literature.

Historical context I: horizons are dissipative

The most interesting results in holographic condensed matter physics are made possible by the fact that the classical dynamics of black hole horizons is thermodynamic and dissipative. This is the single most powerful and unique aspect of the holographic approach. In this subsection we briefly outline these basic intrinsic properties of event horizons, independently of any holographic interpretation. Later, via the holographic correspondence, the classical dynamics of event horizons will be reinterpreted as statements about the deconfined phase of gauge theories in the 't Hooft matrix large N limit. The 't Hooft limit will be the subject of the following subsection.

To emphasize the central points, we discuss stationary, neutral and non-rotating black holes. The important quantities characterizing the black hole are then its area A, mass M and surface gravity κ . The surface gravity is the force required at infinity to hold a unit mass in place just above the horizon. The horizon is the surface of no return – this irreversibility inherent in classical gravity underpins the connection with thermodynamics. Bardeen, Carter and Hawking showed that the classical Einstein equations imply [?]:

- 1. The surface gravity κ is constant over the horizon.
- 2. Adiabatic changes to the mass and size of the black hole are related by

$$\delta M = \frac{\kappa}{8\pi G_N} \, \delta A \,. \tag{2.1}$$

Here G_N is Newton's constant.

3. The horizon area always increases: $\delta A \geq 0$.

These are clearly analogous to the zeroth through second laws of thermodynamics. Hawking subsequently showed that black holes semiclassically radiate thermal quanta, and thereby obtained the temperature and entropy [?]

$$T = \frac{\hbar \kappa}{2\pi}, \qquad S = \frac{1}{4} \frac{A}{\hbar G_N} = \frac{1}{4} \frac{A}{L_p^2}.$$
 (2.2)

Note the explicit factors of Planck's constant \hbar . This shows that while Hawking radiation is a quantum mechanical effect, the entropy of the black hole is so large (the area is measured in Planck units L_p) that the thermodynamic nature of black holes is imprinted on the classical equation (??) – the factors of \hbar in the temperature and entropy have cancelled. This is an important lesson for our purposes: black holes are able to geometrize thermodynamics because they describe systems with a huge number of degrees of freedom.

Granted that black holes in equilibrium behave as a thermodynamic system, the next question is whether perturbations of stationary black holes are described by dissipative linear response theory. Early work in the 70s by Hawking, Hartle, Damour and Znajek showed that perturbed black holes exhibited dissipative processes such as Joule heating. These observations were formalized as the 'membrane paradigm' of black holes [?, ?, ?]. For example, near an event horizon electromagnetic radiation must be 'infalling' (that is, directed into rather than out of the black hole). Maxwell's equations then relate the electric and magnetic fields parallel to the horizon as

$$E_{\parallel} = \hat{n} \times B_{\parallel} \,, \tag{2.3}$$

where \hat{n} is a spacelike outward pointing unit normal to the horizon. Because the horizon acts a boundary of the spacetime, properly satisfying the variational principle leading to the Maxwell equations requires the association of charge and current densities to the horizon. The charge density is found to be proportional to the electric flux through the horizon while the current density j along the horizon is related to the magnetic field at the horizon via

$$B_{\parallel} = g_H^2 \, j \times \hat{n} \,, \tag{2.4}$$

where g_H^2 is the electromagnetic coupling evaluated at the horizon (allowing in general for a space-dependent 'dilaton' coupling). Putting the previous two equations together gives Ohm's law on the horizon

$$E_{\parallel} = g_H^2 j. \tag{2.5}$$

Hence the two dimensional spatial slice of the horizon has a universal dimensionless resistivity of g_H^2 , much like a two dimensional quantum critical medium. Solving the Einstein equations at quadratic order in the electromagnetic fields one finds that the area of the horizon increases in precisely the way required to describe the entropy generated by this current and resistivity.

The membrane description of black hole dissipation in asymptotically flat spacetime was complicated by the fact that such black holes have an unstable underlying thermodynamics (in particular, a negative specific heat) as well as finite size horizons. As we shall see, the holographic correspondence gives a clean framework for making sense of – and putting to use – the dissipative dynamics of horizons. The membrane paradigm

was directly incorporated into holography in [?, ?], to be discussed below.

Historical context II: the 't Hooft matrix large N limit

The essential fact about useful large N limits of quantum fields theories is that there exists a set of operators $\{\mathcal{O}_i\}$ with no fluctuations to leading order at large N [?, ?]:

$$\langle \mathcal{O}_{i_1} \mathcal{O}_{i_2} \cdots \mathcal{O}_{i_n} \rangle = \langle \mathcal{O}_{i_1} \rangle \langle \mathcal{O}_{i_2} \rangle \cdots \langle \mathcal{O}_{i_n} \rangle. \tag{2.6}$$

Operators that obey this large N factorization are classical in the large N limit. One might generally hope that, for a theory with many degrees of freedom 'per site', each configuration in the path integral has a large action, and so the overall partition function is well approximated by a saddle point computation. However, the many local fields appearing in the path integral will each be fluctuating wildly. To exhibit the classical nature of the large N limit one must therefore identify a set of 'collective' operators $\{\mathcal{O}_i\}$ that do not fluctuate, but instead behave classically according to (??). Even if one can identify the classical collective operators, it will typically be challenging to find the effective action for these operators whose saddle point determines their expectation values. The complexity of different large N limits depends on the complexity of this effective action for the collective operators.

A simple set of examples are given by vector large N limits. One has, for instance, a bosonic field $\vec{\Phi}$ with N components and, crucially, interactions are restricted to be O(N) symmetric. This means the interaction terms must be functions of

$$\sigma \equiv \vec{\Phi} \cdot \vec{\Phi} \,. \tag{2.7}$$

(Slightly more generally, they could also be functions of $\vec{\Phi} \cdot \partial_{\mu_1} \cdots \partial_{\mu_2} \vec{\Phi}$.) While the individual vector components of $\vec{\Phi}$ fluctuate about zero, σ is a sum of the square of N such fluctuating fields. We thus expect that σ behaves classically up to fluctuations which are subleading in N, analogous to the central limit theorem. Indeed, by means of a Hubbard-Stratonovich transformation that introduces σ as an auxiliary field, the action can be represented as a quadratric function of $\vec{\Phi}$ coupled to σ . Performing the path integral over $\vec{\Phi}$ exactly, one then obtains an effective action for σ alone with an order N overall prefactor (from the N functional determinants arising upon integrating out $\vec{\Phi}$). This is the desired effective action for the collective field σ that can now be treated in a saddle point approximation in the large N limit, see e.g. [?].

For our purposes the vector large N limits are too simple. The fact that one can obtain the effective action for σ from a few functional determinants translates into the fact that the theory is essentially a weakly interacting theory in the large N limit. As we will emphasize repeatedly throughout this review,

weak interactions means long lived quasiparticles, which in turn mean essentially conventional phases of matter and conventional Boltzmann descriptions of transport. The point of holographic condensed matter is precisely to realize inherently strongly interacting phases of matter and transport that are not built around quasiparticles. Thus, while vector large N limits do admit interesting holographic duals [?], they will not be further discussed here. As we will explain below, strongly interacting large N theories are necessary to connect directly with the classical dissipative dynamics of event horizons discussed in the previous section.

The 't Hooft matrix large N limit [?], in contrast to the vector large N limit, has the virtue of admitting a strongly interacting saddle point description. The fields in the theory now transform in the adjoint rather than the vector representation of some large group such as U(N). Thus the fields are large $N \times N$ matrices Φ_I and interactions are functions of traces of these fields

$$\mathcal{O}_i = \operatorname{tr}\left(\Phi_{I_1}\Phi_{I_2}\cdots\Phi_{I_m}\right). \tag{2.8}$$

These 'single trace' operators are straightforwardly seen to factorize and hence become classical in the large N limit [?, ?]. There are vastly more classical operators of the form (??) than there were in the vector large N limit case (??). Furthermore there is no obvious prescription for obtaining the effective action whose classical equations of motion will determine the values of these operators. For certain special theories in the 't Hooft limit, this is precisely what the holographic correspondence achieves. The fact that was unanticipated in the 70s is that the effective classical description involves fields propagating on a higher dimensional curved spacetime.

In the simplest cases, the strength of interactions in the matrix large N limit is controlled by the 't Hooft coupling λ [?]. When the Lagrangian is itself a single trace operator then this coupling appears in the overall normalization as, schematically,

$$\mathcal{L} = \frac{N}{\lambda} \operatorname{tr} \left(\partial^{\mu} \Phi \, \partial_{\mu} \Phi + \cdots \right). \tag{2.9}$$

When λ is small, the large N limit remains weakly coupled and can be treated perturbatively. In this limit the theory is similar to the vector large N limit. When λ is large, however, solving the theory would require summing a very large class of so-called planar diagrams. Through the holographic examples to be considered below, we will see that the large λ limit is indeed strongly coupled: there are no quasiparticles and the single trace operators, while classical, acquire significant anomalous dimensions. This review is a study of the phenomenology of these strongly interacting large N theories

Maldacena's argument and the canonical examples

We will now outline Maldacena's argument that connects the physics of event horizons described in \S ?? with the 't Hooft matrix large N limit of \S ?? [?, ?]. This argument involves concepts from string theory. Experimentalists have our permission to skip this section on a first reading. However, we will only attempt to get across the essential logic of the argument, which we hope will be broadly accessible. This argument is the source of the best understood, canonical examples of holographic duality.

The central idea is to describe a certain physical system in two different limits. Specifically, we consider a large number N of 'Dp branes' stacked on top of each other, in an otherwise empty spacetime. Dp branes are objects in string theory with p spatial dimensions. Thus a D0 brane is a point particle, a D1 brane is an extended string, a D2 brane is a membrane, and so on. As a physical system, the coincident Dp branes have certain low energy excitations. We proceed to describe these excitations in two limits. These limits are illustrated in figure $\ref{eq:process}$ below and explained in more detail in the following.

Figure 1: Low energy excitations of a stack of D3 branes at weak and strong 't Hooft coupling. Weak coupling: N^2 light string states connecting the N D3 branes. Strong coupling: classical gravitational excitations that are strongly redshifted by an event horizon.

The simplest case of all is for D3 branes, so we will start with these. D3 branes are objects with three spatial dimensions, extended within the nine spatial dimensions of (type IIB) string theory. Like all objects, the D3 branes gravitate. How strongly they gravitate depends on their tension and the strength of the gravitational force. The gravitational backreaction turns out to be determined by the number N of superimposed D3 branes and the dimensionless string coupling constant g_s . It is found that when

$$\lambda \equiv 4\pi g_s N \ll 1 \,, \tag{2.10}$$

then the gravitational effects of the D3 branes are negligible. This is because the tension of the N D3 branes

goes like N/g_s , whereas the strength of gravity goes like g_s^2 . In this limit we can just imagine the D3 branes sitting in (nine dimensional) flat space. The low energy degrees of freedom in this case are known to be strings stretching between pairs of D3 branes. The lightest string states are massless because the D3 branes are coincident in space. There are N^2 such strings, corresponding to the different ways the N D3 branes can be paired up. At the lowest energy scales, it is known that these N^2 massless strings are described by a field theory called $\mathcal{N}=4$ super Yang-Mills theory. This theory describes excitations that propagate on the three spatial dimensions of the D3 branes and, schematically, has Lagrangian density

$$\mathcal{L} \sim \frac{N}{\lambda} \operatorname{tr} \left(F^2 + (\nabla \Phi)^2 + i \bar{\Psi} \not\!\!{D} \Psi + i \bar{\Psi} [\Phi, \Psi] - [\Phi, \Phi]^2 \right). \tag{2.11}$$

This expression describes a theory with an SU(N) field strength F coupled to bosonic fields Φ and fermionic fields Ψ , all in the adjoint representation. In $\mathcal{N}=4$ super Yang-Mills there are six bosonic fields and four fermionic fields. All of these fields are $N \times N$ matrices. The above Lagrangian therefore takes the form we discussed previously in $(\ref{eq:total_strength})$, with λ in $(\ref{eq:total_strength})$ now revealed as the 't Hooft coupling! Therefore, we have found that the low energy excitations of the D3 branes in the regime $(\ref{eq:total_strength})$ are described by a weakly interacting matrix large N theory.

In the opposite regime

$$\lambda \equiv 4\pi g_s N \gg 1\,, (2.12)$$

the D3 branes gravitate very strongly. Under the strong effects of gravity the branes collapse upon themselves and form what is known as a black brane. These black branes are described by an appropriate analogue of well-known black hole solutions of general relativity. The horizon of the black brane is, by definition, a surface of infinite gravitational redshift. Therefore, for a far away observer, the low energy excitations of the system are any excitations that occur very close to the horizon. This region is called the near horizon geometry. This (ten dimensional) geometry is known to be a solution called $AdS_5 \times S^5$, with spacetime metric

$$ds^{2} = L^{2} \left(\frac{-dt^{2} + d\vec{x}_{3}^{2} + dr^{2}}{r^{2}} + d\Omega_{5}^{2} \right).$$
 (2.13)

The coordinates $\{t, \vec{x}\}$ are those along the D3 brane worldvolume, the 'radial' coordinate r is orthogonal to the D3 branes, while the five sphere with round metric $d\Omega_5^2$ surrounds the D3 branes. The horizon itself is at $r \to \infty$ in these coordinates. The scale L is called the AdS radius and can be related (see e.g. [?]) to the two fundamental scales in string theory, the string length L_s and the Planck length L_p

$$L = \lambda^{1/4} L_s = (4\pi N)^{1/4} L_p.$$
(2.14)

In particular, in the strong 't Hooft coupling regime (??) and at large $N \gg 1$, the radius of curvature L of the $AdS_5 \times S^5$ geometry is very large compared to both the string and the Planck lengths. It follows that for many purposes we can neglect effects due to highly excited string states (controlled by L_s) as well as quantum gravity effects (controlled by L_p). The excitations of the near horizon region will simply be described by classical gravitational perturbations of the background (??).

The upshot of the previous two paragraphs is that the low energy excitations of N D3 branes look very different in two different limits. At weak 't Hooft coupling they are described by a weakly interacting matrix large N field theory. At strong 't Hooft coupling they are described by gravitational perturbations about $AdS_5 \times S^5$ spacetime (??). The original version of the holographic correspondence [?] was the conjecture that there existed a decoupled set of degrees of freedom that interpolated between these weak and strong coupling descriptions. In particular, this implies that the classical gravitational dynamics of $AdS_5 \times S^5$ is precisely the strong coupling description of large N N = 4 super Yang-Mills theory. This is the long-sought effective classical description of a matrix large N limit. Remarkably, the effective classical fields are gravitating and live in a higher number of spacetime dimensions! We now gain our first glimpse of a microscopic understanding of the dissipative dynamics of horizons that we discussed §??: gravity is in fact the dynamics of a strongly interacting matrix large N quantum field theory in disguise.

The logic of the above argument can be applied to a very large number of configurations of branes in string theory. Many 'dual pairs' of quantum field theories and classical gravitational theories are obtained in this way. In Table ?? below we list what might be considered the canonical, best understood examples of holographic duality for field theories in 3+1, 2+1 and 1+1 spacetime dimensions. We will not explain the terminology appearing in this table. Entry points to the literature include the original papers [?, ?] and the review [?]. Our main objective here is to make clear that explicit examples of the duality are known in various dimensions and that they are found by using string theory as a bridge between quantum field theory and gravity.

The essential dictionary

The GKPW formula

While string theory is useful in furnishing explicit examples of holographic duality, much of the machinery of the duality is quite general and can be described using only concepts from quantum field theory (QFT) and gravity.

The basic observables that characterize the QFT are the multi-point functions of operators in the QFT. In particular, at large N, the basic observables are multi-point functions of the single trace operators \mathcal{O}_i ,

String theory system	Quantum field theory	Gravitational theory
N D3 branes in IIB string theory on $\mathbb{R}^{1,9}$	$\mathcal{N} = 4$ SYM theory (3+1)	IIB supergravity on $AdS_5 \times S^5$
N M2 branes in M theory on $\mathbb{R}^{1,2} \times \mathbb{R}^8/\mathbb{Z}_k$	ABJM theory (2+1)	11d supergravity on $AdS_4 \times S^7/\mathbb{Z}_k$
Q_1 D1 branes and Q_5 D5 branes in IIB string theory on $\mathbb{R}^{1,5} \times M^4$	$\mathcal{N} = (4,4) \text{ SCFT } (1+1)$	IIB supergravity on $AdS_3 \times S^3 \times M^4$

Table 1: The canonical examples of holographic duality for field theories in 3+1, 2+1 and 1+1 spacetime dimensions. The first column shows the string theory setup of which one should consider the low energy excitations. In the limit of no gravitational backreaction the low energy degrees of freedom are described by a quantum field theory, given in the second column. In the limit of strong gravitational back reaction, the low energy degrees of freedom are described by classical gravitational dynamics about the backgrounds shown in the third column.

described above in (??). As examples of such operators, we can keep in mind charge densities j^t and current densities \vec{j} , associated with symmetries of the theory. The multi-point functions can be obtained if we know the generating functional

$$Z_{\text{QFT}}[\{h_i(x)\}] \equiv \left\langle e^{i\sum_i \int dx \, h_i(x)\mathcal{O}_i(x)} \right\rangle_{\text{QFT}}.$$
 (2.15)

Observables in gravitating systems can be difficult to characterize, because the spacetime itself is dynamical. In the case where the spacetime has a boundary, however, observables can be defined on the boundary of the spacetime. We can, for instance, consider a Dirichlet problem in which the values of all the 'bulk' fields (i.e. the dynamical fields in the theory of gravity) are fixed on the boundary. The boundary itself is not dynamical, giving the observer a 'place to stand'. We can then construct the partition function of the theory as a function of the boundary values $\{h_i(x)\}$ of all the bulk fields $\{\phi_i\}$

$$Z_{\text{Grav.}}[\{h_i(x)\}] \equiv \int^{\phi_i \to h_i} \left(\prod_i \mathcal{D}\phi_i\right) e^{iS[\{\phi_i\}]}. \tag{2.16}$$

It is a nontrivial mathematical problem to show that the Dirichlet problem for gravity is in fact well-posed, even in the classical limit (see e.g. [?] for a recent discussion). However, we will see below how in practice the boundary data determines the bulk spacetime.

Suppose that a given QFT and theory of gravity are holographically dual. The essential fact relating observables in the two dual descriptions (of the same theory) is that there must be a one-to-one correspondence between single trace operators \mathcal{O}_i in the QFT, and dynamical fields ϕ_i of the bulk theory. For example, a given scalar operator such as tr (Φ^2) in the QFT with schematic Lagrangian (??) will be dual to a particular scalar field ϕ in the bulk theory. The scalar ϕ will have its own bulk dynamics given by the action S in (??). We will be more explicit about the bulk action shortly. Having matched up bulk operators and

boundary fields in this way, we can write the essential entry in the holographic dictionary, as first formulated by Gubser-Klebanov-Polyakov and Witten (GKPW) [?, ?]:

$$Z_{\text{QFT}}[\{h_i(x)\}] = Z_{\text{Grav.}}[\{h_i(x)\}].$$
 (2.17)

That is, the generating functional of the QFT with source h_i for the single trace operator \mathcal{O}_i is equal to the bulk partition function with the bulk field ϕ_i corresponding to \mathcal{O}_i taking boundary value h_i . This relationship is illustrated in figure ?? below.

Figure 2: **Essential dictionary:** The boundary value h of a bulk field ϕ is a source for an operator \mathcal{O} in the dual QFT.

The reader may have many immediate questions: How do we know which bulk field corresponds to which operator? There are a very large number of single trace operators, and so won't the bulk description involve a very large number of fields and hence be unwieldy? Before addressing these questions, we will illustrate the dictionary (??) at work.

Fields in AdS spacetime

The large N limit is supposed to be a classical limit, so let us evaluate the bulk partition function semiclassically

$$Z_{\text{Grav.}}[\{h_i(x)\}] = e^{iS[\{\phi_i^* \to h_i\}]}.$$
 (2.18)

Here $S[\{\phi_i^{\star} \to h_i\}]$ is the bulk action evaluated on a saddle point, i.e. a solution to the bulk equations of motion, $\{\phi_i^{\star}\}$, subject to the boundary condition that $\phi_i^{\star} \to h_i$.

We need to specify the bulk acton. The most important bulk field is the metric g_{ab} . The QFT operator corresponding to this bulk field will be the energy momentum tensor $T^{\mu\nu}$. This means that the boundary value of the bulk metric (more precisely, the induced metric on the boundary) is a source for the energy momentum tensor in the dual QFT, which seems natural. In writing down an action for the bulk metric, we will consider an expansion in derivatives, as one usually does in effective field theory. Later in this section we describe the circumstances in which this is a correct approach. The general bulk action for the metric

involving terms that are at most quadratic in derivatives of the metric is

$$S[g] = \frac{1}{2\kappa^2} \int d^{d+2}x \sqrt{-g} \left(R + \frac{d(d+1)}{L^2} \right). \tag{2.19}$$

The first term is the Einstein-Hilbert action, with R the Ricci scalar and $\kappa^2 = 8\pi G_{\rm N} \propto L_p^d$ defines the Planck length in the bulk d+2 dimensions (i.e. the boundary QFT has d spatial dimensions). The second term is a negative cosmological constant characterized by a lengthscale L. The equations of motion following from this action are

$$R_{ab} = -\frac{d+1}{L^2} g_{ab} \,. \tag{2.20}$$

The simplest solution to these equations is AdS_{d+2} :

$$ds^{2} = L^{2} \left(\frac{-dt^{2} + d\vec{x}_{d}^{2} + dr^{2}}{r^{2}} \right). \tag{2.21}$$

This spacetime has multiple symmetries. The easiest to see is the dilatation symmetry: $\{r, t, \vec{x}\} \to \lambda\{r, t, \vec{x}\}$. In fact there is an SO(d+1,2) isometry group [?]. This is precisely the conformal group in d+1 spacetime dimensions. The solution (??) describes the vacuum of the dual QFT. If we now perturb the solution by turning on sources $\{h_i\}$, these perturbations will need to transform under the SO(d+1,2) symmetry group of the background. This suggests that the d+2 dimensional metric (??) dually describes a 'boundary' conformal field theory (CFT) in d+1 spacetime dimensions. Let us see this explicitly.

Perturbing the metric itself is a little complicated, so consider instead an additional field ϕ in the bulk with an illustrative simple action

$$S[\phi] = -\int d^{d+2}x \sqrt{-g} \left(\frac{1}{2} (\nabla \phi)^2 + \frac{m^2}{2} \phi^2 \right).$$
 (2.22)

As noted above, ϕ will correspond to some particular scalar operator in the dual quantum field theory. For concreteness we can have in the back of our mind an operator like tr (Φ^2) . To see the effects of adding a source h for this operator, we must solve the classical bulk equations of motion

$$\nabla^2 \phi = m^2 \phi \,, \tag{2.23}$$

subject to the boundary condition $\phi \to h$, and then evaluate the action on the solution as specified in (??). We have already noted that the horizon of AdS_{d+2} is the surface $r \to \infty$ in (??) – this is properly called the Poincaré horizon. This is the surface of infinite redshift where $g_{tt} \to 0$. The 'conformal boundary' at

which we impose $\phi \to h$ is the opposite limit, $r \to 0$. In the metric (??) this corresponds to an asymptotic region where the volume of constant r slices of the spacetime are becoming arbitrarily large. This should be thought of as imposing boundary conditions 'at infinity'.

The equation of motion (??) is a wave equation in the AdS_{d+2} background (??). We can solve this equation by decomposing the field into plane waves in the t and x directions

$$\phi = \phi(r)e^{-i\omega t + ik \cdot x} \,. \tag{2.24}$$

The equation for the radial dependence then becomes

$$\phi'' - \frac{d}{r}\phi' + \left(\omega^2 - k^2 - \frac{(mL)^2}{r^2}\right)\phi = 0.$$
 (2.25)

To understand the asymptotic boundary conditions, we should solve this equation in a series expansion as $r \to 0$. This is easily seen to take the form¹

$$\phi = \frac{\phi_{(0)}}{L^{d/2}} r^{d+1-\Delta} + \dots + \frac{\phi_{(1)}}{L^{d/2}} r^{\Delta} + \dots \quad (as \quad r \to 0),$$
(2.26)

where

$$\Delta(\Delta - d - 1) = (mL)^2. \tag{2.27}$$

There are two constants of integration $\phi_{(0)}$ and $\phi_{(1)}$. The first of these is what we previously called the boundary value h of ϕ . We shall understand the meaning of the remaining constant $\phi_{(1)}$ shortly. In (??) we see that in order to extract the boundary value h of the field, one must first strip away some powers of the radial direction r. These powers of r will now be seen to have an immediate physical content. We noted below (??) that rescaling $\{r,t,\vec{x}\} \to \lambda\{r,t,\vec{x}\}$ is a symmetry of the background AdS_{d+2} bulk spacetime. Like the metric, the scalar field ϕ itself must remain invariant under this transformation (the symmetry is a property of a particular solution, not of the fields themselves). Therefore the source must scale as $\phi_{(0)} = h \to \lambda^{\Delta - d - 1} h$ in order for (??) to be invariant. Recalling that the source h couples to the dual operator \mathcal{O} as in (??), we learn that the dual operator must rescale as

$$\mathcal{O}(x) \to \lambda^{-\Delta} \mathcal{O}(\lambda x)$$
. (2.28)

Therefore Δ is nothing other than the scaling dimension of the operator \mathcal{O} . Equation (??) is a very important

¹With the factors of L appearing as in $(\ref{eq:condition})$, the leading coefficient explicitly has the mass dimension $[\phi_{(0)}] = [h] = d + 1 - \Delta$, as expected for the source in the dual field theory.

result that relates the mass of a bulk scalar field to the scaling dimension of the dual operator in a CFT. We can see that for relevant perturbations ($\Delta < d+1$), the $\phi_{(0)}$ term in (??) goes to zero at the boundary $r \to 0$, while for irrelevant perturbations ($\Delta > d+1$), this term grows towards the boundary. This will fit perfectly with our interpretation in section ?? below of the radial direction as capturing the renormalization group of the dual quantum field theory, with $r \to 0$ describing the UV.

For a given bulk mass, equation (??) has two solutions for Δ . For most masses we must take the larger solution Δ_+ in order for $\phi_{(0)}$ to be interpreted as the boundary value of the field in (??). Exceptions to this statement will be discussed later. Note that $d + 1 - \Delta_{\pm} = \Delta_{\mp}$.

Simplification in the limit of strong QFT coupling

We can now address the concern above that a generic matrix large N quantum field theory has a very large number of single trace operators. For instance, with only two matrix valued fields one can construct operators of the schematic form tr $(\Phi_1^{n_1}\Phi_2^{n_2}\Phi_1^{n_3}\Phi_2^{n_4}\cdots)$. These each correspond to a bulk field. The bulk action should therefore be extremely complicated. In theories with tractable gravity duals an unexpected simplification takes place: in the limit of large 't Hooft coupling, $\lambda \to \infty$, all except a small number of operators acquire parametrically large anomalous dimensions. According to the relation (??) this implies that all but a small number of the bulk fields have very large masses.² The heavy fields can be neglected for many purposes. This leads to a tractable bulk theory. In the concrete string theory realizations of holographic duality discussed above in section ??, the hierarchy in the bulk can be easily understood. The excitations of the theory are string states. From the relation quoted in (??) we see that large 't Hooft coupling $\lambda \gg 1$ implies that $L/L_s \gg 1$. The mass of a typical excited string state is $m \sim 1/L_s$, and therefore $Lm \gg 1$ for these states. Only a handful of low energy string states survive. This perspective also justifies a derivative expansion of the bulk action (and hence the neglect of higher derivative terms in (??) and (??)). Higher derivative terms are suppressed by powers of L_s/L , as they arise due to integrating out heavy string states.³

Beyond specific string theory realizations, the lesson of the previous paragraph is that a holographic

²We are ignoring the presence of so-called bulk Kaluza-Klein modes in this discussion. These modes can lead to many light bulk fields even in the strong 't Hooft coupling limit $\lambda \to \infty$. They will be addressed in section ??.

 $^{^3}$ A handful of higher derivative terms with unsuppressed couplings are in principle allowed, and can be traded for additional fields. This often leads to ghosts (fields with wrong-sign kinetic terms), which can be problematic. A finite number of unsuppressed and well-behaved higher derivative terms correspond to fine tuning the bulk theory. For instance, to obtain the basic AdS_{d+2} solution (??), the cosmological constant term in the action balances the Ricci scalar term, which has more derivatives. This is only possible because the cosmological constant has been tuned to be very small in Planck units $(L/L_p \gg 1)$. In the dual QFT, this tuning is just the fact that we have taken N to be large! The correct statement for a bulk theory dual to a QFT with an operator gap is that there cannot be an infinite number of unsuppressed higher derivative terms in the bulk, which would lead to a non-local bulk action [?].

approach is useful for QFTs in which two simplifications occur:

Large N limit

$$\Leftrightarrow$$
 Classical bulk theory. (2.29)

Gap in single trace operator spectrum (e.g. large λ limit)

$$\Leftrightarrow$$
 Derivative expansion in bulk, small number of bulk fields. (2.30)

While the second condition may appear restrictive, string theory constructions show that these simplifications do indeed arise in concrete models. The most important point is that this is a way (a large N limit with a gap in the operator spectrum) to simplify the description of QFTs without going to a weakly interacting quasiparticle regime. We will repeatedly see below how this fact allows holographic theories to capture generic behavior of, for instance, transport in strongly interacting systems that is not accessible otherwise. In contrast, weakly interacting large N limits, such as the vector large N limit, cannot have such a gap in the operator spectrum. This is because to leading order in large N the dimensions of operators add, and in particular operators such as $\vec{\Phi} \cdot \partial_{\mu_1} \cdots \partial_{\mu_2} \vec{\Phi}$ give an evenly spaced spectrum of conserved currents with no gap. Beyond the holographic approach discussed here, the development of purely quantum field theoretic methods exploiting the existence of an operator gap has recently been initiated [?, ?, ?, ?].

Expectation values and Green's functions

A second result that can be obtained from the asymptotic expansion (??) is a formula for the expectation value of an operator. From (??), (??) and (??) above

$$\langle \mathcal{O}_i(x) \rangle = \frac{1}{Z_{\text{QFT}}} \frac{\delta Z_{\text{QFT}}}{\delta h_i(x)} = i \frac{\delta}{\delta h_i(x)} S\left[\{ \phi_i^{\star} \to h_i \} \right].$$
 (2.31)

The scalar action (??) becomes a boundary term when evaluated on a solution. Because the volume of the boundary is diverging as $r \to 0$, we take a cutoff boundary at $r = \epsilon$. Then

$$\langle \mathcal{O}(x) \rangle = -\frac{i}{2} \frac{\delta}{\delta \phi_{(0)}} \int_{r=\epsilon} d^{d+1} x \sqrt{-\gamma} \, \phi \, n^a \nabla_a \phi \tag{2.32}$$

$$= \frac{i}{2} \frac{\delta}{\delta \phi_{(0)}} \int_{r=\epsilon}^{\infty} d^{d+1}x \left(\frac{L}{\epsilon}\right)^d \left((d+1-\Delta) \frac{\epsilon^{2d+1-2\Delta}}{L^d} \phi_{(0)}^2 + (d+1) \frac{\phi_{(0)}\phi_{(1)}}{L^d} + \cdots \right). \tag{2.33}$$

In the first line γ is the induced metric on the boundary (i.e. put $r = \epsilon$ in (??)) and n is an outward pointing unit normal (i.e. $n^r = -\epsilon/L$). In the second line we have used the boundary expansion (??). Upon taking

 $\epsilon \to 0$, the first term diverges, the second is finite, and the remaining terms all go to zero. The divergent term is an uninteresting contact term, to be dealt with more carefully in the following section. We ignore it here. In evaluating the second term, note that because the bulk field ϕ satisfies a linear equation of motion, then $\delta \phi_{(1)}/\delta \phi_{(0)} = \phi_{(1)}/\phi_{(0)}$. Thus we obtain

$$\langle \mathcal{O}(x) \rangle \propto \phi_{(1)} \,. \tag{2.34}$$

We have not given the constant of proportionality here, as obtaining the correct answer requires a more careful computation, which will appear in the following section. The important point is that we have discovered the following basic relations:

Field theory source h

$$\Leftrightarrow$$
 Leading behavior $\phi_{(0)}$ of bulk field. (2.35)

Field theory expectation value $\langle \mathcal{O} \rangle$

$$\Leftrightarrow$$
 Subleading behavior $\phi_{(1)}$ of bulk field. (2.36)

This connection will turn out to be completely general. For instance, the source could be the chemical potential and the expectation value the charge density. Or, the source could be an electric field and the expectation value could be the electric current.

For a given set of sources $\{h_i\}$ at $r \to 0$, regularity of the fields in the interior of the spacetime (e.g. at the horizon $r \to \infty$) will fix the bulk solution completely. In particular, the subleading behavior near the boundary will be fixed. Therefore, by solving the bulk equations of motion subject to specified sources and regularity in the interior, we will be able to solve for the expectation values $\langle \mathcal{O}_i \rangle$. We can illustrate this with the simple case of the scalar field. The radial equation of motion (??) is solved by Bessel functions. The boundary condition at the horizon is that the modes of the bulk wave equation must be 'infalling', that is, energy flux must fall into rather than come out of the horizon. We will discuss infalling boundary conditions in detail below. For now, we quote the fact that the boundary conditions at the horizon and near the asymptotic boundary pick out the solution (let us emphasize that t here is real time, we will also be discussing imaginary time later)

$$\phi \propto h \, r^{(d+1)/2} K_{\Delta - \frac{d+1}{2}} \left(r \sqrt{k^2 - \omega^2} \right) e^{-i\omega t + ik \cdot x} \,. \tag{2.37}$$

The overall normalization is easily computed but unnecessary and not illuminating. Here K is a modified

Bessel function and Δ is the larger of the two solutions to (??). By expanding this solution near the boundary $r \to 0$, we can extract the expectation value (??). Taking the ratio of the expectation value by the source gives the retarded Green's function of the boundary theory

$$G_{\mathcal{O}\mathcal{O}}^{R}(\omega,k) = \frac{\langle \mathcal{O} \rangle}{h} \propto \frac{\phi_{(1)}}{\phi_{(0)}} \propto \left(k^2 - \omega^2\right)^{\Delta - (d+1)/2}. \tag{2.38}$$

This is precisely the retarded Green's function of an operator \mathcal{O} with dimension Δ in a CFT. This confirms our expectation that perturbations about the AdS_{d+2} background (??) will dually describe the excitations of a CFT.

Bulk gauge symmetries are global symmetries of the dual QFT

The computation of the Green's function (??) illustrates how knowing the bulk action and the bulk background allows us to obtain correlators of operators in the dual strongly interacting theory. For this to be useful, we would like to know which bulk fields correspond to which QFT operators. This can be complicated, even when the dual pair of theories are known explicitly. Symmetry is an important guide. In particular, gauge symmetries in the bulk are described by bulk gauge fields. These include Maxwell fields A_a , the metric g_{ab} and also nonabelian gauge bosons. The theory must be invariant under gauge transformations of these fields, including 'large' gauge transformations, where the generator of the transformation remains constant on the asymptotic boundary. We can illustrate this point easily with a bulk gauge field A_a , which transforms to $A_a \to A_a + \nabla_a \chi$ for a scalar function χ . If χ is nonzero on the boundary, then the boundary coupling in the action transforms to

$$\int d^{d+1}x\sqrt{-\gamma}(A_{\mu} + \nabla_{\mu}\chi)J^{\mu} = \int d^{d+1}x\sqrt{-\gamma}(A_{\mu}J^{\mu} - \chi\nabla_{\mu}J^{\mu}), \qquad (2.39)$$

where we integrated by parts in the last step. Invariance under the bulk gauge transformation requires that the current is conserved (in all correlation functions). Therefore

Bulk gauge field (e.g.
$$A_a, g_{ab}$$
)

 \Leftrightarrow Conserved current of global symmetry in QFT (e.g. $J^{\mu}, T^{\mu\nu}$). (2.40)

Similarly, fields that are charged under a bulk gauge field will be dual to operators in the QFT that carry the corresponding global charge. Thus quantities such as electric charge and spin must directly match up in the two descriptions. Matching up operators beyond their symmetries is often not possible in practice, and indeed is not really the right question to ask. The bulk is a self-contained description of the strongly coupled theory. The spectrum and interactions of bulk fields define the correlators and all other properties of a set of dual operators. Reference to a weakly interacting QFT Lagrangian description is not necessary and potentially misleading. Nonetheless, it can be comforting to have in the back of our minds some familiar operators. Thus a low mass scalar field ϕ in the bulk might be dual to QFT operators such as $\operatorname{tr} F^2$, $\operatorname{tr} \Phi^2$ or $\operatorname{tr} \overline{\Psi} \Psi$. Here we are using the notation of the schematic QFT action (??). A low mass fermion ψ in the bulk will be dual to an operator such as $\operatorname{tr} \Phi \Psi$.

The general condensed matter systems we wish to study are not CFTs (although CFTs do comprise an interesting subset). Instead there will be multiple scales of interest: temperature, chemical potential, and scales generated by renormalization group flow of relevant operators. These are all understood within the framework of holographic renormalization, that we turn to next.

The emergent dimension I: Wilsonian holographic renormalization

An essential aspect of the duality map (??) is that the gravitating 'bulk' spacetime has an extra spatial dimension relative to the dual 'boundary' CFT. In this section and the following we will gain some intuition for the meaning of this extra 'radial' dimension. The short answer is that the radial dimension geometrizes the renormalization group: processes close to the boundary of the bulk correspond to high energy physics in the dual QFT while dynamics deep in the interior of the bulk describes low energy physics in the QFT. This will be one of the conceptual pillars of holographic condensed matter physics, another being the already mentioned fact that horizons geometrize dissipation. The relation is illustrated in the following figure ??.

The radial or 'holographic' dimension captures all of the standard renormalization physics: (i) isolating universal low energy dynamics while parameterizing our ignorance about short distance physics, (ii) computing beta functions for running couplings and (iii) determining the structure of short distance divergences as a UV regulator is removed. In this section we work through the illustrative case of a scalar field in a fixed background geometry, as in the previous section. We will develop the concepts further as we need them throughout the review.

⁴ Single trace operators in QFT are dual to fields in the bulk. What about multi-trace operators? The insertion of multi-trace operators in the action in the sense of (??) will be discussed in the following section on holographic renormalization. A simpler aspect of multi-trace operators relates to the operator-state correspondence for CFTs. Here the single trace operator \mathcal{O} corresponds to the state created by a quantum of the dual field ϕ . The double-trace operator \mathcal{O}^2 corresponds to creating two quanta of the dual field. In the bulk, quantum effects are suppressed at large N and so these different quanta are simply superimposed solutions of free bulk wave equations. For this reason, single trace operators in large N theories (whose dimension does not scale with N) are sometimes referred to as generalized free fields, e.g. [?].

Figure 3: **The radial direction:** Events in the interior of the bulk capture long distance, low energy dynamics of the dual field theory. Events near the boundary of the bulk describe short distance, UV dynamics in the field theory dual. The simplest way to think about this is that the interior events are increasingly redshifted relative to the boundary energy scales (a similar logic was used in the decoupling argument of section ?? to derive holographic duality, here we are discussing redshifts within the near horizon AdS region itself).

Bulk volume divergences and boundary counterterms

We have already encountered a divergence when we tried to evaluate the on-shell action in (??). This divergence is due to the infinite volume of the bulk spacetime, that is integrated over in evaluating the action. In (??) we regulated the divergence by cutting off the spacetime close to the boundary at $r = \epsilon$. We will see momentarily that this cutoff appears in the dual field theory as a short distance regulator of UV divergences. This connection between infinitely large scales in the bulk and infinitesimally short scales in the field theory is sometimes called the UV/IR correspondence [?]. Taking our cue from perturbative renormalization in field theory, we can regulate the bulk action by adding a 'counterterm' boundary action. For the case of the scalar, let

$$S \to S + S_{\text{ct.}} = S + \frac{a}{2L} \int_{r-\epsilon} d^{d+1}x \sqrt{-\gamma} \phi^2$$
. (2.41)

Choosing $a = \Delta - d - 1$, the counterterm precisely cancels the divergent term in (??). Because it is a boundary term defined in terms of purely intrinsic boundary data, it neither changes the bulk equations of motion nor the boundary conditions of the bulk field. The counterterm action furthermore contributes to the finite term in the expectation value of the dual operator: We can now write (??) more precisely as

$$\langle \mathcal{O}(x) \rangle = (2\Delta - d - 1)\phi_{(1)}. \tag{2.42}$$

The counterterm boundary action is a crucial part of the theory if we wish the dual field theory to be well-defined in the 'continuum' limit $\epsilon \to 0$. A bulk action that is finite as $\epsilon \to 0$ allows us to think of the dual field theory as being defined by starting from a UV fixed point. This is the first of several instances we will encounter in holography where boundary terms in the action must be considered in more detail than one might be accustomed to.

The counterterm action (??) is a local functional of boundary data. It is a nontrivial fact that all divergences that arise in evaluating on shell actions in holography can be regularized with counterterms that are local functionals of the boundary data. The terms that arise precisely mimic the structure of UV divergences in quantum field theory in one lower dimension, even though the bulk divergences are entirely classical. This identification of the counterterm action is called holographic renormalization. Entry points into the vast literature include [?, ?]. An important conceptual fact is that in order for the bulk volume divergences to be local in boundary data, the growth of the volume towards the boundary must be sufficiently fast. Spacetimes that asymptote to AdS spacetime are the best understood case where such UV locality holds.

Wilsonian renormalization as the Hamilton-Jacobi equation

In this review we will frequently be interested in universal emergent low energy dynamics. For such questions, as in conventional quantum field theory, the precise short distance regularization or completion of the theory is unimportant. To understand the running of couplings and emergent dynamics we require a Wilsonian perspective on holographic theories. We outline how this works following [?, ?].

Recall that a QFT is defined below some UV cutoff Λ by the path integral

$$Z = \int_{\Lambda} \mathcal{D}\Phi e^{i(I_0[\Phi] + I_{\Lambda}[\Phi])}. \tag{2.43}$$

Here $I_0[\Phi]$ is the microscopic action and $I_{\Lambda}[\Phi]$ are the terms obtained by integrating out all degrees of freedom at energy scales above the cutoff scale Λ . By requiring that the partition function Z is independent of Λ we obtain the renormalization group equations for $I_{\Lambda}[\Phi]$. By taking the cutoff to low energies we can obtain (in principle) the emergent low energy dynamics. By seeing how this structure emerges in holography we can gain some intuition for the meaning of the radial direction.

In the presence of a UV cutoff, there is a generalization of the fundamental holographic dictionary (??). Consider a radial cutoff in the bulk at $r = \epsilon$. The cutoff gravitational partition function is now expressed in terms of the values of fields $\phi_i^{\epsilon} \equiv \phi_i(\epsilon)$ at the cutoff. Considering a single bulk field ϕ for notational

simplicity, the gravity partition function (??) becomes

$$Z^{\epsilon}[\phi^{\epsilon}] \equiv \int^{\phi \to \phi_{\epsilon}} \mathcal{D}\phi \, e^{iS[\phi]} \,. \tag{2.44}$$

This quantity is naturally related to the partition function of the dual QFT integrated only over modes below some UV cutoff Λ . In particular, it is natural to generalize (??) to

$$Z^{\epsilon}[\phi^{\epsilon}] = \int_{\Lambda} \mathcal{D}\Phi \, e^{iI_0[\Phi] + i \int dx \, \phi^{\epsilon}(x) \mathcal{O}(x)} \,. \tag{2.45}$$

Here $\int_{\Lambda} \mathcal{D}\Phi$ is the regulated field theory path integral as in (??). Thus, the values of the bulk fields at the cutoff boundary are now interpreted as sources in an effective QFT valid at scales below a field theoretic cutoff Λ . While we schematically write $\Lambda \sim 1/\epsilon$, the precise nature of the field theory cutoff Λ corresponding to the bulk cutoff ϵ is not known. For instance, the regulator preserves any gauge invariance of the boundary field theory and is therefore not a hard momentum cutoff. Determining precisely the field theory renormalization group scheme defined by a cutoff in the bulk would probably amount to a proof of holography. The perspective we will take is that the radial cutoff is a natural UV regulator in theories with holographic gravity duals, and we wish to check now that it leads to sensible consequences. In particular, we proceed to derive the renormalization group equations from the bulk. The following few paragraphs are a little technical, but allow us to show how the second order bulk equations of motion are related to first order renormalization group flow equations.

The full bulk partition function (??) with source h at the boundary is related to the truncated partition function (??) by gluing path integrals together in the usual way (see Fig. ??):

$$Z[h] = \int \mathcal{D}\phi^{\epsilon} Z^{\epsilon}[\phi^{\epsilon}] Z_{\text{UV}}^{\epsilon}[\phi^{\epsilon}, h] \equiv \int \mathcal{D}\phi^{\epsilon} \left[Z^{\epsilon}[\phi^{\epsilon}] \int_{\phi \to \phi_{\epsilon}}^{\phi \to h} \mathcal{D}\phi \, e^{iS[\phi]} \right] . \tag{2.46}$$

Here $Z_{\text{UV}}^{\epsilon}[\phi^{\epsilon}, h]$ is the bulk path integral over the UV modes between the cutoff ϵ and the boundary at r = 0, with boundary conditions at both ends. Putting this previous equation together with (??) and (??) we obtain

$$e^{iI_{\Lambda}[\mathcal{O}]} = \int \mathcal{D}\phi^{\epsilon} e^{i\int dx \,\phi^{\epsilon}(x)\mathcal{O}(x)} Z_{\text{UV}}^{\epsilon}[\phi^{\epsilon}, h]$$
 (2.47)

This equation gives a holographic expression for the effective action for the QFT operator \mathcal{O} (a single trace operator built from the field theory degrees of freedom Φ) obtained by integrating out high energy modes above the cutoff Λ . It is given by an integral transform of the bulk partition function where we only integrate over modes living on the bulk spacetime between the boundary at r = 0 and $r = \epsilon$, subject to boundary

Figure 4: **The Wilsonian cutoff:** The cutoff is at $r = \epsilon$, while the UV fixed point theory is at r = 0. The partition function $Z^{\epsilon}[\phi^{\epsilon}]$ is over all modes at $r > \epsilon$, subject to the boundary condition $\phi(\epsilon) = \phi^{\epsilon}$. The partition function $Z^{\epsilon}_{\text{UV}}[\phi^{\epsilon}, h]$ is over all modes between $r = \epsilon$ and r = 0, with boundary conditions at both ends.

conditions at both ends.

The semiclassical limit of (??) is the Legendre transform relation

$$I_{\Lambda}[\mathcal{O}] = \int d^{d+1}x \,\phi_{\star}^{\epsilon}(x)\mathcal{O}(x) + S[\phi_{\star}^{\epsilon} \leftarrow \phi_{\star} \to h], \qquad \mathcal{O} = -\frac{\delta S_{\star}}{\delta \phi_{\star}^{\epsilon}}. \tag{2.48}$$

Here $S_{\star} \equiv S[\phi_{\star}^{\epsilon} \leftarrow \phi_{\star} \rightarrow h]$ is the action evaluated on a solution ϕ_{\star} subject to the boundary conditions indicated. The action is the integral of a Lagrangian density $S = \int d^{d+2}x \sqrt{-g}\mathcal{L}$, together with any boundary counterterms of the type we discussed above. It follows that

$$\partial_{\epsilon} I_{\Lambda}[\mathcal{O}] = \int_{r=\epsilon} d^{d+1}x \left(\mathcal{O} \partial_r \phi_{\star} - \sqrt{-g} \mathcal{L} \right) . \tag{2.49}$$

From Hamilton-Jacobi theory, we see that \mathcal{O} in (??) is precisely the momentum conjugate to ϕ under radial evolution. We can then recognize the right hand side of (??) as the Hamiltonian generating radial evolution.

To be concrete, consider the previous bulk action for the scalar (??) generalized to arbitrary potential

$$\mathcal{L} = -\frac{1}{2} \left(\nabla \phi \right)^2 - V(\phi) \,. \tag{2.50}$$

Using this expression in (??), we obtain the Hamilton-Jacobi functional equation

$$\sqrt{g^{rr}}\partial_{\epsilon}I_{\Lambda}[\mathcal{O}] = \int d^{d+1}x\sqrt{-\gamma}\left(\frac{1}{2\gamma}\mathcal{O}^{2} + \frac{1}{2}\left(\nabla_{(d+1)}\phi_{\star}^{\epsilon}\right)^{2} + V(\phi_{\star}^{\epsilon})\right), \qquad \phi_{\star}^{\epsilon} = \frac{\delta I_{\Lambda}[\mathcal{O}]}{\delta\mathcal{O}}. \tag{2.51}$$

Here we assumed for simplicity that the metric takes the form $ds^2 = g_{rr}dr^2 + \gamma_{\mu\nu}(r)dx^{\mu}dx^{\nu}$, with no

cross terms between the radial and boundary directions. $\nabla_{(d+1)}$ denotes the derivative along the boundary directions only. The second equation in (??) follows from (??).

The functional equation (??) is to be solved for $I_{\Lambda}[\mathcal{O}]$, and gives the evolution of the effective field theory action as a function of the cutoff ϵ . If we expand the action in powers of \mathcal{O} then we can write

$$I_{\Lambda}[\mathcal{O}] = \sum_{n} \int d^{d+1}x \sqrt{-\gamma} \,\lambda_n(x,\Lambda) \mathcal{O}(x)^n \,. \tag{2.52}$$

Plugging this expansion in the flow equation (??), we obtain the beta functions for all of the couplings λ_n . Therefore, we have shown that varying the bulk cutoff ϵ leads to explicit first order flow equations of exactly the kind we anticipate for couplings in quantum field theories as function of some Wilsonian cutoff Λ . As we noted below (??) above, the exact nature of the QFT cutoff Λ is not known.

Multi-trace operators

It is useful to note that the Wilsonian effective action (??) includes multi-trace operators \mathcal{O}^n . Even – as is often the case – we start with a single trace action in the UV, these terms are generated under renormalization. Explicit holographic computations typically only make use of the bulk field ϕ , which is dual to the single trace operator \mathcal{O} . However, ϕ satisfies a second order equation in the bulk. What has happened is that the first order beta function equations for all the couplings (including the multi-trace couplings) have been repacked into a second order equation for a single bulk field ϕ . This approach, which is useful at large N, has been called the quantum renormalization group in [?].

Multi-trace operators can also be inserted directly into the UV action. It can be shown that these correspond to changing the boundary conditions of the field as $r \to 0$ [?, ?]. To deform the field theory action by

$$\Delta S = W[\mathcal{O}], \tag{2.53}$$

where W is some functional of the single trace operator $\mathcal{O}(x)$, we must impose a specific relation between the coefficients $\phi_{(0)}$ and $\phi_{(1)}$ appearing in the near boundary expansion (??). This boundary condition is

$$\phi_{(0)} = \left. \frac{\delta W[\mathcal{O}]}{\delta \mathcal{O}} \right|_{\mathcal{O} = \frac{2\Delta - d - 1}{L} \phi_{(1)}}.$$
(2.54)

This general prescription includes the case of deformations by single trace operators we had considered previously in (??). That case corresponds to the simple linear relation $W[\mathcal{O}] = \int d^{d+1}x \phi_{(0)}(x) \mathcal{O}(x)$.

An important special case is the double trace deformation $W[\mathcal{O}] \propto \int d^{d+1}x \mathcal{O}(x)^2$, in the case when the operator dimension (??) of \mathcal{O} is in the range $\frac{d+1}{2} \leq \Delta_+ \leq \frac{d+1}{2} + 1$. It is a general fact about large N conformal

field theories that such an irrelevant double trace deformation induces a flow leading to a new UV fixed point theory [?]. Under this flow, the dimension of the operator \mathcal{O} changes from the larger root Δ_+ of (??) to the smaller root Δ_- , while no other single trace operators receive any change in dimension to leading order at large N. This new theory therefore corresponds precisely to what is known as the alternate quantization of the bulk [?]. That is, the role of Δ_+ and Δ_- are exchanged – one can also think of this as the roles of $\phi_{(0)}$ and $\phi_{(1)}$ being exchanged, keeping Δ fixed, although we will prefer not to. The alternate quantization of the bulk is possible when the mass of the scalar field (??) is in the range $-\frac{(d+1)^2}{4} \leq m^2 \leq -\frac{(d+1)^2}{4} + 1$ (note that slightly negative values of the mass squared are stable in anti-de Sitter spacetime, so long as Δ is real – we will discuss this in more detail later). The important fact about this range of masses is that both modes in (??) fall off sufficiently quickly that either one can be taken to be the 'normalizable' mode, and the other the source. While the standard quantization required the boundary counterterm action (??), the alternate quantization requires instead

$$S_{\text{ct.}}^{(\text{alt})} = \int_{r=\epsilon} d^{d+1}x \sqrt{-\gamma} \left(\phi \, n^a \nabla_a \phi + \frac{\Delta}{2L} \phi^2 \right) \,. \tag{2.55}$$

Here $\Delta = \Delta_{-}$ is now the smaller of the two exponents. Unlike the previous counterterm (??), this expression includes a derivative normal to the boundary. This is the term responsible for changing the boundary conditions so that the Δ_{+} rather than Δ_{-} term becomes the source. The expression (??) for the expectation value still holds.

Geometrized versus non-geometrized low energy degrees of freedom

From the Wilsonian holographic renormalization picture outlined above it is clear, in principle, how to zoom in on the low energy universal physics. We need to consider the dynamics of the fields in the far interior of the bulk spacetime. We will also need to understand how to match this interior dynamics to the sources that appear as boundary conditions on the asymptotic spacetime. We shall do this explicitly several times later in this review.

There is an interesting caveat to the previous paragraph. Holography geometrizes the renormalization of the order N^2 matrix degrees of freedom in the dual large N field theory. Sometimes, however, there can be order $1 \ll N^2$ light degrees of freedom that are missed by this procedure. These degrees of freedom are extended throughout the bulk spacetime and not localized in the far interior. Effectively, they are not fully geometrized. An example are Goldstone modes of spontaneously broken symmetries. A framework, known as semi-holography, has been developed to characterize these cases, e.g. [?, ?, ?]. We shall describe these methods later, as the various modes manifest themselves as poles in Green's functions that we will be

computing. The contribution of these (low energy, non geometrized) modes running in loops in the bulk can lead to non-analyticities in low energy observables at subleading order in the 1/N expansion, causing subtle breakdowns of the large N expansion. Examples are quantum oscillations due to bulk Fermi surfaces ??, destruction of long-range order in low dimensions by fluctuating Goldstone modes ?? and long time tails in hydrodynamics ??.

The emergent dimension II: Entanglement entropy

The previous section showed how the radial direction of the bulk spacetime geometrized the energy scale of the dual quantum field theory. The energy scale was understood within a functional integral, Wilsonian perspective on the QFT. An alternative way to conceive the bulk radial direction is as a certain geometric re-organization of the QFT Hilbert space.

Shortly after the discovery of the holographic correspondence, it was realized that the bulk can be thought of as being made up of order N^2 QFT degrees of freedom per AdS radius [?]. The recent discovery [?, ?, ?] and proof [?] of the Ryu-Takayangi formula for entanglement entropy in theories with holographic duals suggests that a more refined understanding of how the bulk reorganizes the QFT degrees of freedom is within reach. In the simplest case, in which the bulk is described by classical Einstein gravity coupled to matter, the Ryu-Takayanagi formula states that the entanglement entropy of a region A in the QFT is given by

$$S_E = \frac{A_\Gamma}{4G_N} \,, \tag{2.56}$$

where G_N is the bulk Newton's constant and A_{Γ} is the area of a minimal surface (i.e. a soap bubble) Γ in the bulk that ends on the boundary of the region A. The region A itself is at the boundary of the bulk spacetime. We illustrate this formula in the following figure ??. The formula (??) generalizes the Bekenstein-Hawking

Figure 5: Minimal surface Γ in the bulk, whose area gives the entanglement entropy of the region A on the boundary.

entropy formula (??) for black holes. This last statement is especially clear for black holes describing thermal

equilibrium states, which correspond to entangling the system with a thermofield double [?].

Let us now illustrate the Ryu-Takayanagi formula by computing the entanglement entropy of a spherical region of radius R in a CFT, following [?]. By spherical symmetry, we know that the minimal surface will be of the form $r(\rho)$, where ρ is the radial coordinate on the boundary (so that $d\vec{x}_d^2 = d\rho^2 + \rho^2 d\Omega_{d-1}^2$). The induced metric on this surface is given by putting $r = r(\rho)$ and t = 0 in the AdS_{d+2} spacetime (??) to obtain:

$$ds^{2} = \frac{L^{2}d\rho^{2}}{r^{2}} \left[1 + \left(\frac{dr}{d\rho} \right)^{2} \right] + \frac{L^{2}\rho^{2}}{r^{2}} d\Omega_{d-1}^{2}.$$
 (2.57)

From the determinant of this induced metric, the area of the surface is given by:

$$A_{\Gamma} = L^{d} \Omega_{d-1} \int \frac{\mathrm{d}\rho}{r^{d}} \rho^{d-1} \sqrt{1 + \left(\frac{\mathrm{d}r}{\mathrm{d}\rho}\right)^{2}}.$$
 (2.58)

 Ω_{d-1} denotes the volume of the unit sphere S^{d-1} . It is simple to check that

$$r(\rho) = \sqrt{R^2 - \rho^2},$$
 (2.59)

solves the Euler-Lagrange equations of motion found by minimizing the area (??). This is therefore the Ryu-Takayanagi surface. Note that $dr/d\rho = -\rho/r$.

The entanglement entropy (??) is given by evaluating (??) on the solution (??). For dimensions d > 1,

$$A_{\Gamma} = L^{d} \Omega_{d-1} \int_{0}^{R} d\rho \, \frac{R \rho^{d-1}}{(R^{2} - \rho^{2})^{(d+1)/2}}.$$
 (2.60)

This integral is dominated near r=0. Switching to the variable $y=R-\rho$, we obtain that

$$A_{\Gamma} \approx L^{d} \Omega_{d-1} \int_{s} dy \frac{R^{d}}{(2Ry)^{(d+1)/2}} \sim L^{d} \left(\frac{R}{\delta}\right)^{(d-1)/2}, \qquad (2.61)$$

where δ is a cutoff on the bulk radial dimension near the boundary that, as in the previous Wilsonian section, we will want to interpret as a short distance cutoff in the dual field theory. This result becomes more transparent in terms of the equivalent cutoff on the bulk coordinate $r = \epsilon$; using (??) one has that $\epsilon = \sqrt{2R\delta}$. Hence, the entanglement entropy is

$$S_E \sim \frac{L^d}{G_N} \left(\frac{R}{\epsilon}\right)^{d-1} + \text{subleading.}$$
 (2.62)

The first term is proportional to the area of the boundary sphere R, and hence (??) is called the area

law of entanglement [?]. It can be intuitively understood as follows – entanglement in the vacuum is due to excitations which reside partially inside the sphere, and partially outside. In a local QFT, we expect that the number of these degrees of freedom is proportional to the area of the sphere in units of the short distance cutoff, $(R/\epsilon)^{d-1}$. This is true regardless of whether or not the state is gapped. Equation (??) therefore gives another perspective on the identification of a near-boundary cutoff on the bulk geometry with a short-distance cutoff in the dual QFT. In the holographic result (??), the proportionality coefficient $L^d/G_N \sim (L/L_p)^d \gg 1$. This is consistent with the general expectation that there must be a large number of degrees of freedom "per lattice site" in microscopic QFTs with classical gravitational duals. While the coefficient of the area law is sensitive to the UV cutoff ϵ (since we have to count the number of degrees of freedom residing near the surface), some subleading coefficients are universal [?].

In d = 1, the story is a bit different. Now,

$$A_{\Gamma} = 2L \int_{0}^{R} \frac{\mathrm{d}\rho R}{R^{2} - \rho^{2}} \approx 2L \int_{\delta}^{R} \frac{\mathrm{d}\rho}{2\rho} = L \log \frac{R}{\delta} + \dots = 2L \log \frac{R}{\epsilon} + \dots$$
 (2.63)

The prefactor of 2 is related to the fact that the semicircular minimal surface has two sides. Using the result (beyond the scope of this review) that the central charge c of the dual CFT2, which counts the effective degrees of freedom, is given by [?]

$$c = \frac{3L}{2G_{\rm N}},\tag{2.64}$$

we recover the universal CFT2 result [?]

$$S = \frac{c}{3}\log\frac{R}{\epsilon} + \cdots {2.65}$$

Note that the area law, which would have predicted S = constant, has logarithmic violations in a CFT2. We will see an intuitive argument for this shortly, as shown in Figure ??.

Analogy with tensor networks

It was pointed out in [?] that the Ryu-Takayangi formula resembles the computation of the entanglement entropy in quantum states described by tensor networks. We will now describe this connection, following the exposition of [?]. While, at the time of writing, these ideas remain to be fleshed out in any technical detail, they offer a useful way to think about the emergent spatial dimension in holography. For a succinct introduction to the importance of entanglement in real space renormalization, see [?].

Consider a system with degrees of freedom living on lattice sites labelled by i, taking possible values

 s_i . For instance each s_i could be the value of a spin. Tensor network states (see e.g. [?]) are certain wavefunctions $\psi(\{s_i\})$. The simplest example of a tensor network state is a Matrix Product State (MPS) for a one dimensional system with L sites. For every value that the degrees of freedom s_i can take, construct a $D \times D$ matrix T_{s_i} . Here D is called the bond dimension. The physical wavefunction is now given by

$$\psi(s_1, \dots, s_L) = \text{tr}(T_{s_1} T_{s_2} \dots T_{s_L})$$
 (2.66)

For the case that each s_i describes a spin half, these Matrix Product States parametrize a $2LD^2$ dimensional subspace of the full 2^L dimensional Hilbert space. The importance of these states is that they capture the entanglement structure of the ground state of gapped systems, as we now recall.

To every site i in the lattice, associate two auxiliary vector spaces of dimension D. Let these have basis vectors $|n\rangle_{i1}$ and $|n\rangle_{i2}$ respectively, with $n=1,\dots,D$. Now form a state, in this auxiliary space, made of maximally entangled pairs between neighboring sites

$$|\Psi\rangle = \prod_{i=1}^{L} \left(\sum_{n=1}^{D} |n\rangle_{i2} |n\rangle_{(i+1)1} \right) . \tag{2.67}$$

For periodic boundary conditions we can set $|n\rangle_{(L+1)1} = |n\rangle_{11}$. It is clear that if we trace over some number of adjacent sites, the entanglement entropy of the reduced density matrix will be $2 \log D$, corresponding to maximally entangled pairs at each end of the interval we have traced over. To obtain a state in the physical Hilbert space, we now need to project at each site. That is, let $P_i : \mathbb{R}^D \times \mathbb{R}^D \to \mathbb{R}^2$ be a projection, then the physical state

$$|\psi\rangle = \prod_{i=1}^{L} P_i |\Psi\rangle. \tag{2.68}$$

If we write the projection operators as $P_i = \sum_{m,n,s_i} T_{s_i}^{mn} |s_i\rangle_{i1} \langle m|_{i2} \langle n|$, then we recover precisely the MPS state (??). The advantage of this perspective is that we now see that if we trace out a number of adjacent sites in this physical state ψ , the entanglement entropy of the reduced density matrix is bounded above by $S_E \leq 2 \log D$. In gapped systems, the entanglement entropy of the ground state grows with the correlation length. At a fixed correlation length, the entanglement structure of the state can therefore be well approximated by a MPS state with some fixed bond dimension D (if the inequality $S_E \leq 2 \log D$ is approximately saturated).

⁵This follows from the fact that, focusing on a single cut between two sites for simplicity, the state (??) in the auxiliary space can be written $|\Psi\rangle = \sum_{p=1}^{D} |p\rangle_L |p\rangle_R$ for some set of states $|p\rangle_L$ and $|p\rangle_R$ to the left and right of the cut, respectively. The projectors act independently on the left and right states, and necessarily map each D dimensional subspace onto a vector space of dimension D or lower. Schmidt decomposing the projected state, we have $|\psi\rangle = \sum_{p=1}^{D} c_p |\widetilde{p}\rangle_L |\widetilde{p}\rangle_R$, for coefficients c_p and states $|\widetilde{p}\rangle_{L/R}$ in the physical Hilbert space on either side of the cut. Hence the entanglement entropy is bounded above by $\log D$.

For gapless systems such as CFTs, a more complicated structure of tensor contractions is necessary to capture the large amount of entanglement. A structure that realizes a discrete subgroup of the conformal group is the so-called MERA network, illustrated in figure ?? below. Viewing the network as obtained by

Figure 6: **MERA network** and a network geodesic that cuts a minimal number of links allowing it to enclose a region of the physical lattice at the top of the network. Each line between two points can be thought of as a maximally entangled pair in the auxiliary Hilbert space, while the points themselves correspond to projections that glue the pairs together. At the top of the network, the projectors map the auxiliary Hilbert space into the physical Hilbert space. The entanglement entropy of the physical region is bounded by the number of links cut by the geodesic: $S_E \leq \ell \log D$.

projecting maximally entangled pairs, the entanglement bound discussed above for MPS states generalizes to the statement that the entanglement entropy of a sequence of adjacent sites is bounded above $\ell \log D$, where ℓ is the number of links in the network that must be cut to separate the entangled sites from the rest of the network. The strongest bound is found from the minimal number of such links that can be cut. This effectively defines a 'minimal surface' within the network. As with the minimal surface appearing in the Ryu-Takayanagi formula, the entanglement entropy is proportional (if the bound is saturated) to the length of the surface. Such a surface in a MERA network is illustrated in figure ??.

The similarity between the tensor network computation of the entanglement entropy and the Ryu-Takayangi formula suggests that the extended tensor network needed to capture the entanglement of gapless states can be thought of as an emergent geometry, analogous to that arising in holography [?]. From this perspective, the emergent radial direction is a consequence of the large amount of entanglement in the QFT ground state, and the tensor network describing the highly entangled state is the skeleton of the bulk geometry. Further discussion may be found in [?, ?, ?]. A key challenge for future work is to show how the large N limit can flesh out this skeleton to provide a local geometry at scales below the AdS radius.

Microscopics: Kaluza-Klein modes and consistent truncations

This section may be skipped by readers of a more pragmatic bent. The following discussion is however conceptually and practically important for understanding the simplest explicit holographic dual pairs, such as those in table ?? above.

In our discussion of the gap in the operator spectrum in section ?? we glossed over an important issue. In many explicit examples of holographic duality, e.g. those in table ??, the bulk spacetime has additional spatial dimensions relative to the dual QFT, beyond the 'energy scale' dimension discussed in previous sections. These dimensions are referred to as the 'internal space'. For instance in the $AdS_5 \times S^5$ spacetime (??), the five sphere is the internal space. We can see that near the boundary $r \to 0$, the five sphere remains of constant size while the AdS_5 part of the metric becomes large. This means that the sphere is not part of the boundary dimensions. Here is the complication: while the statement in (??) that there is a small number of bulk fields as $\lambda \to \infty$ remains true, these fields can have an arbitrary dependence on the internal dimensions. Thus, for every field ϕ in the full spacetime we obtain an infinite tower of fields in AdS_5 , one for each 'spherical harmonic' on the internal space. These are called Kaluza-Klein modes and their dimensions do not show a gap (because $LM_{\rm KK} \sim L/L \sim 1$). That is, while the large λ limit does get rid of many operators (those corresponding to excited string states in the bulk), it does not remove the infinitely many Kaluza-Klein modes. These modes are mostly a nuisance from the point of view of condensed matter physics. While emergent locality in the radial direction – explored in the previous two sections – usefully geometrized the renormalization group, emergent locality in the internal space leads to the QFT growing undesired extra spatial dimensions at low energy scales. In this section we discuss these modes and how to avoid them.

The most compelling strategy would be to get rid of the internal space completely. This is difficult because the best understood consistent bulk theories of quantum gravity require ten or eleven spacetime dimensions. However, 'non-critical' string theories – defined directly in a lower number of spacetime dimensions – do exist. In fact, non-critical string theory lead to early intuition about the existence of holographic duality [?]. Holographic backgrounds of non-critical string theory have been considered in, for instance [?, ?, ?]. The technical difficulty with these solutions is that while Kaluza-Klein modes can be eliminated or reduced, the string scale is typically comparable to the AdS radius (i.e. the 't Hooft coupling $\lambda \sim 1$) and therefore the infinite tower of excited string states must be considered – undoing our motivation for considering these models in the first place.

The second best way to get rid of the Kaluza-Klein modes would be to find backgrounds in which the internal space is parametrically smaller than the AdS radius (unlike, e.g. the $AdS_5 \times S^5$ spacetime (??), in which the AdS_5 and the internal space have the same radius of curvature). This way, all the Kaluza-Klein

modes acquire a large bulk mass and can be mostly ignored (i.e. $LM_{\rm KK} \sim L/L_{\rm internal} \gg 1$). The necessary tools to find backgrounds with a hierarchy of lengthscales have been developed in the context of the 'string landscape' [?]. A first application of these methods to holography can be found in [?]. In our opinion this direction of research is underdeveloped relative to its importance.

The most developed method for getting rid of the Kaluza-Klein modes is called consistent truncation. Here, one shows that it is possible to set all but a finite number of harmonics on the internal space to zero and that these harmonics are not sourced by the handful of modes that are kept. Because the equations of motion in the bulk are very nonlinear, and typically all modes are coupled, it can be technically difficult to identify a consistent set of modes that may be retained. While symmetries can certainly help, a general method does not exist – finding consistent truncations is something of an art form. While less satisfactory than the other approaches mentioned above, consistent truncation gives a manageable bulk action with only one extra spatial dimension relative to the dual QFT. Furthermore, the dynamics of this action consistently captures the dynamics of a subset of operators in the full theory. The main, important, drawback of consistent truncations is that they can miss instabilities in modes that have been thrown out in the truncation. They may, therefore, mis-identify the ground state.

We proceed to give a list of simple examples of bulk actions that can be obtained by consistent truncation, referring to the literature for details. These examples have been chosen (from a large literature) to illustrate and motivate the kind of bulk dynamics we will encounter later in this review. These constructions lead to so-called "top-down holography" and are in contrast to "bottom-up" holography, wherein one postulates a reasonable bulk action with convenient properties. The objective of bottom-up holography is to explore the parameter space of possible strong coupling dynamics. It is useful to have a flavor for what descends from string theory and supergravity to build a sensible bottom-up model.

• Einstein-Maxwell theory: The four dimensional bulk action

$$S_{\text{EM4}} = \int d^4x \sqrt{-g} \left[\frac{1}{2\kappa^2} \left(R + \frac{6}{L^2} \right) - \frac{1}{4e^2} F^2 \right],$$
 (2.69)

is a consistent truncation of M theory compactified on any Sasaki-Einstein seven-manifold, see e.g. [?,?,?]. Therefore this action captures the dynamics of a sector of a large class of dual 2+1 dimensional QFTs. The simplest Sasaki-Einstein seven-manifold is S^7 . The bulk Maxwell field, F = dA, is dual to a particular U(1) symmetry current operator J^{μ} , called the R-symmetry, in the dual superconformal field theory. Similarly, the five dimensional action

$$S_{\text{EM5}} = \int d^5 x \sqrt{-g} \left[\frac{1}{2\kappa^2} \left(R + \frac{12}{L^2} \right) - \frac{1}{4e^2} F^2 \right] + \frac{\kappa}{\sqrt{6} e^3} \frac{1}{3!} \int d^5 x \epsilon^{abcde} A_a F_{bc} F_{de} , \qquad (2.70)$$

is a consistent truncation of IIB supergravity compactified on any Sasaki-Einstein five-manifold, e.g. [?]. This theory describes a sector of a large number of dual 3+1 dimensional QFTs. The simplest Sasaki-Einstein five-manifold is S^5 , and so these theories include $\mathcal{N}=4$ SYM theory. The additional Chern-Simons term in the above action is common in five bulk spacetime dimensions and dually describes an anomaly in the global U(1) R-symmetry of the QFT [?].

Einstein-Maxwell theory is the workhorse for much of holographic condensed matter physics.

• Einstein-Maxwell theory with charged scalars: The above consistent truncations to Einstein-Maxwell theory by compactification on Sasaki-Einstein manifolds may be extended to include additional bulk fields. In particular the five dimensional action (??) can be extended to [?, ?]

$$S = S_{\text{EM5}} - \frac{1}{2\kappa^2} \int d^5 x \sqrt{-g} \left[\frac{1}{2} \left(\nabla \eta \right)^2 + V(\eta) + f(\eta) \left(\nabla \theta - \frac{\sqrt{6}\kappa}{eL} A \right)^2 \right]. \tag{2.71}$$

Here η and θ are the magnitude and phase of a complex scalar field that is charged under the Maxwell field A. The two functions appearing in the action are

$$V(\eta) = \frac{3}{L^2} \sinh^2 \frac{\eta}{2} \left(\cosh \eta - 3 \right) \,, \qquad f(\eta) = \frac{1}{2} \sinh^2 \eta \,. \tag{2.72}$$

The expression for V is slightly different compared to that in [?, ?] because we have extracted the cosmological constant term in (??). The complex scalar field is dual to a particular charged scalar operator \mathcal{O} in the dual QFT [?]. Similarly the four dimensional action (??) can be extended to [?, ?, ?, ?]

$$S = \frac{1}{2\kappa^2} \int d^4x \sqrt{-g} \left[R - \frac{1}{2} \left(\nabla \sigma \right)^2 - \frac{\tau(\sigma)}{4e^2} F^2 - \frac{1}{2} \left(\nabla \eta \right)^2 - V(\sigma, \eta) - f(\eta) \left(\nabla \theta - \frac{1}{2eL} A \right)^2 + \frac{1}{8e^2} \vartheta(\sigma) \epsilon^{abcd} F_{ab} F_{cd} \right]. \tag{2.73}$$

Actually this action is not quite an extension of (??) – the Sasaki-Einstein compactification needs to be 'skew-whiffed', as described in the above references. This theory contains a neutral pseudoscalar field σ in addition to the charged scalar $\{\eta,\theta\}$. The functions in the action are now

$$\tau(\sigma) = \frac{1}{\cosh\sqrt{3}\sigma}, \qquad \vartheta(\sigma) = \tanh\sqrt{3}\sigma, \qquad f(\eta) = 2\sinh^2\eta, \qquad (2.74)$$

and

$$V(\sigma, \eta) = -\frac{6}{L^2} \cosh \frac{\sigma}{\sqrt{3}} \cosh^4 \frac{\eta}{2} \left[1 - \frac{4}{3} \tanh^2 \frac{\eta}{2} \cosh^2 \frac{\sigma}{\sqrt{3}} \right]. \tag{2.75}$$

Note that in a background with both electric and magnetic charges, the pseudoscalar is sourced by the final term in the action and hence cannot be set to zero in general. On the other hand we can set $\eta = 0$ and remove the complex scalar.

Charged scalars in the bulk will play a central role in the theory of holographic superconductivity.

• Einstein-Maxwell theory with neutral scalars: Both of the next two examples are taken from [?, ?]. The five dimensional bulk action

$$S = \frac{1}{2\kappa^2} \int d^5x \sqrt{-g} \left[R - \frac{e^{4\alpha}}{4} F^2 - 12 \left(\nabla \alpha \right)^2 + \frac{1}{L^2} \left(8e^{2\alpha} + 4e^{-4\alpha} \right) \right], \tag{2.76}$$

is a consistent truncation of IIB supergravity compactified on S^5 , and therefore describes a sector of $\mathcal{N}=4$ SYM theory. Here α is a neutral scalar field. Similarly the four dimensional action

$$S = \frac{1}{2\kappa^2} \int d^4x \sqrt{-g} \left[R - \frac{e^{\alpha}}{4} F^2 - \frac{3}{2} (\nabla \alpha)^2 + \frac{6}{L^2} \cosh \alpha \right] , \qquad (2.77)$$

is a consistent truncation of M theory compactified on S^7 , provided $\epsilon^{abcd}F_{ab}F_{cd} = 0$. If this last condition does not hold, an additional pseudoscalar must be included – similarly to in (??) above – and the action becomes more complicated [?].

Exponential functions of scalars multiplying the Maxwell action are ubiquitous in consistent truncations and will underpin our discussions of Lifshitz geometries and hyperscaling violation.

The interested reader will find many more instances of consistent truncations by looking through the references in and citations to the papers mentioned above. It is also possible to find consistent truncations in which the four and five bulk dimensional actions above (and others) are coupled to fermionic fields. The resulting actions are a little complicated and we will not give them here, see [?, ?, ?, ?, ?, ?]. Bulk fermion fields will be important in our discussion below of holographic Fermi surfaces.

Zero density matter

The simplest examples of systems without quasiparticle excitations are realized in quantum matter at special densities which are commensurate with an underlying lattice [?]. These are usually modeled by quantum field theories which are particle-hole symmetric, and have a vanishing value of a conserved U(1) charge

linked to the particle number of the lattice model — hence 'zero' density. Even in the lattice systems, it is conventional to measure the particle density in terms of deviations from such a commensurate density.

In this section we will first give some explicit examples of non-quasiparticle zero density field theories arising at quantum critical points in condensed matter systems. This will include an example with emergent gauge fields. We will then discuss how such quantum critical systems can arise holographically. Our discussion in this section will cover quantum critical scaling symmetries as well as deformations away from scaling by temperature and relevant operators. Charge dynamics in these zero density quantum critical theories will be the subject of the following section.

Condensed matter systems

The simplest example of a system modeled by a zero density quantum field theory is graphene. This QFT is furthermore relativistic at low energies.⁶ Graphene consists of a honeycomb lattice of carbon atoms, and the important electronic excitations all reside on a single π -orbital on each atom. 'Zero' density corresponds here to a density of one electron per atom. A simple computation of the band structure of free electrons in such a configuration yields an electronic dispersion identical to massless 2-component Dirac fermions, Ψ , which have a 'flavor' index extending over 4 values. The Dirac 'spin' index is actually a sublattice index, while the flavor indices correspond to the physical S = 1/2 spin and a 'valley' index corresponding to 2 Dirac cones at different points in the Brillouin zone. The density of electrons can be varied by applying a chemical potential, μ , by external gates, so that the dispersion is $\epsilon(\mathbf{k}) = v_F |\mathbf{k}| - \mu$, where v_F is the Fermi velocity [?]. Electronic states with $\epsilon(\mathbf{k}) < 0$ are occupied at T = 0, and zero density corresponds to $\mu = 0$.

At first glance, it would appear that graphene is not a good candidate for holographic study. The interactions between the electrons are instantaneous Coulomb interactions, because the velocity of light $c \gg v_F$. These interactions are then seen to be formally irrelevant at low energies under the renormalization group, so that the electronic quasiparticles are well-defined. However, as we will briefly note later, the interactions become weak only logarithmically slowly [?, ?], and there is a regime with $T \gtrsim \mu$ where graphene can be modeled as a dissipative quantum plasma. Thus, insight from holographic models can prove quite useful. Experimental evidence for this quantum plasma has emerged recently [?], as we will discuss further in this review. More general electronic models with short-range interactions on the honeycomb lattice provide examples of quantum critical points without quasiparticle excitations even at T=0, and we will discuss these shortly below.

For a more clear-cut realization of quantum matter without quasiparticles we turn to a system of ultracold atoms in optical lattices. Consider a collection of bosonic atoms (such as ⁸⁷Rb) placed in a periodic potential,

⁶We will see shortly that Lorentz invariance is by no means essential for holography.

Figure 7: Ground states of bosons on a square lattice with tunneling amplitude between the sites w, and on-site repulsive interactions U. Bosons are condensed in the zero momentum state in the superfluid, and so there are large number fluctuations in a typical component of the wavefunction shown above. The Mott insulator is dominated by a configuration with exactly one particle on each site.

with a density such that there is precisely one atom for each minimum of the periodic potential. The dynamics of the atoms can be described by the boson Hubbard model: this is a lattice model describing the interplay of boson tunneling between the minima of the potential (with amplitude w), and the repulsion between two bosons on the same site (of energy U). For small U/w, we can treat the bosons as nearly free, and so at low temperatures T they condense into a superfluid with macroscopic occupation of the zero momentum single-particle state, as shown in Fig. ??. In the opposite limit of large U/w, the repulsion between the bosons localizes them into a Mott insulator: this is a state adiabatically connected to the product state with one boson in each potential minimum. We are interested here in the quantum phase transition between these states which occurs at a critical value of U/w. Remarkably, it turns out that the low energy physics in the vicinity of this critical point is described by a quantum field theory with an emergent Lorentz invariant structure, but with a velocity of 'light', c, given by the velocity of second sound in the superfluid [?, ?]. In the terms of the long-wavelength boson annihilation operator ψ , the Euclidean time (τ) action for the field theory is

$$S = \int d^2x \, d\tau \left[|\nabla_x \psi|^2 + c^2 |\partial_\tau \psi|^2 + s|\psi|^2 + u|\psi|^4 \right] \,. \tag{2.78}$$

Here s is the coupling which tunes the system across the quantum phase transition at some $s = s_c$. For $s > s_c$, the field theory has a mass gap and no symmetry is broken: this corresponds to the Mott insulator. The gapped particle and anti-particle states associated with the field operator ψ correspond to the 'particle' and 'hole' excitations of the Mott insulator. These can be used as a starting point for a quasiparticle theory of the dynamics of the Mott insulator via the Boltzmann equation. The other phase with $s < s_c$ corresponds to the superfluid: here the global U(1) symmetry of \mathcal{S} is broken, and the massless Goldstone modes correspond

to the second sound excitations. Again, these Goldstone excitations are well-defined quasiparticles, and a quasiclassical theory of the superfluid phase is possible (and is discussed in classic condensed matter texts).

Our primary interest here is in the special critical point $s = s_c$, which provides the first example of a many body quantum state without quasiparticle excitations. And as we shall discuss momentarily, while this is only an isolated point at T = 0, the influence of the non-quasiparticle description widens to a finite range of couplings at non-zero temperatures. Renormalization group analyses show that the $s = s_c$ critical point is described by a fixed point where $u \to u^*$, known as the Wilson-Fisher fixed point [?, ?]. The value of u^* is small in a vector large M expansion in which ψ is generalized to an M-component vector, or for small ϵ in a field theory generalized to $d = 3 - \epsilon$ spatial dimensions. Given only the assumption of scale invariance at such a fixed point, the two-point ψ Green's function obeys

$$G_{\psi\psi}^{R}(\omega,k) = k^{-2+\eta} F\left(\frac{\omega}{k^{z}}\right)$$
 (2.79)

at the quantum critical point. Here η is defined to be the anomalous dimension of the field ψ which has scaling dimension

$$[\psi] = (d + z - 2 + \eta)/2 \tag{2.80}$$

in d spatial dimensions. The exponent z determines the relative scalings of time and space, and is known as the dynamic critical exponent. The function F is a scaling function which depends upon the particular critical point under study. In the present situation, we know from the structure of the underlying field theory in Eq. (??) that $G_{\psi\psi}^R$ has to be Lorentz invariant (ψ is a Lorentz scalar), and so we must have z=1 and a function F consistent with

$$G_{\psi\psi}^{R}(\omega,k) \sim \frac{1}{(c^{2}k^{2} - \omega^{2})^{(2-\eta)/2}}$$
 (2.81)

Indeed, the Wilson-Fisher fixed point is not only Lorentz and scale invariance, it is also conformally invariant and realizes a conformal field theory (CFT), a property we will exploit below.

A crucial feature of G^R in Eq. (??) is that for $\eta \neq 0$ its imaginary part does not have any poles in the ω complex plane, only branch cuts at $\omega = \pm ck$. This is an indication of the absence of quasiparticles at the quantum critical point. However, it is not a proof of absence, because there could be quasiparticles which have zero overlap with the state created by the ψ operator, and which appear only in suitably defined observables. For the case of the Wilson-Fisher fixed point, no such observable has ever been found, and it seems highly unlikely that such an 'integrable' structure is present in this strongly-coupled theory. Certainly, the absence of quasiparticles can be established at all orders in the ϵ or vector 1/M expansions. In the remaining discussion we will assume that no quasiparticle excitations are present, and develop a framework to describe

the physical properties of such systems. We also note in passing that CFTs in 1+1 spacetime dimensions (i.e. CFT2s) are examples of theories in which there are in fact quasiparticles present, but whose presence is not evident in the correlators of most field variables [?]. This is a consequence of integrability properties in CFT2s which do not generalize to higher dimensions.

We can also use a scaling framework to address the ground state properties away from the quantum critical point. In the field theory S we tune away from quantum critical point by varying the value of s away from s_c . This makes $s - s_c$ a relevant perturbation at the fixed point, and its scaling dimension is denoted as

$$[s - s_c] = 1/\nu. \tag{2.82}$$

In other words, the influence of the deviation away from the criticality becomes manifest at distances larger than a correlation length, ξ , which diverges as

$$\xi \sim |s - s_c|^{-\nu}.\tag{2.83}$$

We can also express these scaling results in terms of the dimension of the operator conjugate to $s - s_c$ in the action

$$[|\psi|^2] = d + z - \frac{1}{\nu}. (2.84)$$

For $s > s_c$, the influence of the relevant perturbation to the quantum critical point is particularly simple: the theory acquires a mass gap $\sim c/\xi$ and so

$$G_{\psi\psi}^{R}(\omega,k) \sim \frac{1}{(c^{2}(k^{2}+\xi^{-2})-\omega^{2})}$$
 (2.85)

at frequencies just above the mass gap. Note now that a pole has emerged in G^R , confirming that quasiparticles are present in the $s > s_c$ Mott insulator.

We now also mention the influence of a non-zero temperature, T, on the quantum critical point, and we will have much more to say about this later. In the imaginary time path integral for the field theory, T appears only in boundary conditions for the temporal direction, τ : bosonic (fermionic) fields are periodic (anti-periodic) with period $\hbar/(k_BT)$. At the fixed point, this immediately implies that T should scale as a frequency. So we can generalize the scaling form (??) to include a finite ξ and a non-zero T by

$$G_{\psi\psi}^{R}(\omega,k) = \frac{1}{T^{(2-\eta)/z}} \mathcal{F}\left(\frac{k}{T^{1/z}}, \frac{\xi^{-1}}{T^{1/z}}, \frac{\hbar\omega}{k_{B}T}\right).$$
 (2.86)

We have included fundamental constants in the last argument of the scaling function \mathcal{F} because we expect

Figure 8: Phase diagram of S as a function of s and T. The quantum critical region is bounded by crossovers at $T \sim |s - s_c|^{z\nu}$ indicated by the dashed lines. Conventional quasiparticle or classical-wave dynamics applies in the non-quantum-critical regimes (colored blue) including a Kosterlitz-Thouless phase transition above which the superfluid density is zero. One of our aims in this review is to develop a theory of the non-quasiparticle dynamics within the quantum critical region.

the dependence on $\hbar\omega/(k_BT)$ to be fully determined by the fixed-point theory, with no arbitrary scale factors. Note also that for $T > \xi^{-z} \sim |g - g_c|^{z\nu}$, we can safely set the second argument of \mathcal{F} to zero. So in this "quantum critical" regime, the finite temperature dynamics is described by the non-quasiparticle dynamics of the fixed point CFT3: see Fig. ??. In contrast, for $T < \xi^{-z} \sim |g - g_c|^{z\nu}$ we have the traditional quasiparticle dynamics associated with excitations similar to those described by (??). Our discussion in the next few sections will focus on the quantum-critical region of Fig. ??.

In the remainder of this subsection, we note extensions to other examples of zero density systems without quasiparticles.

Antiferromagnetism on the honeycomb lattice

We return to electronic models defined on the honeycomb lattice, relevant for systems like graphene, mentioned at the beginning of Section ??. In particular, we consider a Hubbard model for spin S = 1/2 fermions ('electrons') on the honeycomb lattice at a density of one fermion per site. As for the boson Hubbard model, the two energy scales are the repulsion energy, U, between two electrons on the same site (which necessarily have opposite spin), and the electron hopping amplitude w between nearest-neighbor sites. For small U/w, the electronic spectrum is that of 4 flavors of massless 2-component Dirac fermions, Ψ , and the short-range interactions only weakly modify the free fermion spectrum. In contrast, for large U/w, the ground state is an insulating antiferromagnet, as illustrated in Fig. ??. This state is best visualized as one with fermions

localized on the sites, with opposite spin orientations on the two sublattices. The excitations of the insulating antiferromagnet come in two varieties, but both are amenable to a quasiparticle description: (i) there are the bosonic Goldstone modes associated with the breaking of spin rotation symmeter, and (ii) there are fermionic quasiparticle excitations with the same quantum numbers as the electron above an energy gap. The quantum field theory for the phase transition [?] between the large U/w and small U/w phases is known in the particle-theory literature as the Gross-Neveu model (where it is a model for chiral symmetry breaking). Its degrees of a freedom are a relativistic scalar φ^a , a = 1, 2, 3 representing the antiferromagnetic order parameter, and the Dirac fermions Ψ . The action for φ^a is similar to that the superfluid order parameter ψ in Eq. (??), and this is coupled to the Dirac fermions via a 'Yukawa' coupling, leading to the field theory

$$S_{\varphi} = \int d^2x \, d\tau \left[(\partial_x \varphi^a)^2 + c^2 (\partial_\tau \varphi^a)^2 + s(\varphi^a)^2 + u \left((\varphi^a)^2 \right)^2 + i \overline{\Psi} \gamma^\mu \partial_\mu \Psi + \lambda \overline{\Psi} \Gamma^a \Psi \varphi^a \right]. \tag{2.87}$$

Here γ^{μ} are suitable 2 × 2 Dirac matrices, while the Γ^{a} are 'flavor matrices' which act on a combination of the valley and sublattice indices of the fermions. The γ^{μ} and the Γ^{a} turn out to commute with each other, and so when the velocity c equals the Fermi velocity v_{F} , the action \mathcal{S}_{φ} becomes invariant under Lorentz transformations. So we find an emergent Lorentz invariance near the quantum critical point, similar to that found above for the superfluid-insulator transition for bosons. The tuning parameter across the quantum critical point, s, is now a function of U/w. The phase with broken spin-rotation symmetry ($s < s_{c}$) has $\langle \varphi^{a} \rangle \neq 0$, we then see that the Yukawa term, λ , endows the Dirac fermions with a 'mass' i.e. there is a gap to fermionic excitations; this 'mass' is analogous to the Higgs boson endowing the fermions with a mass in the Weinberg-Salam model. The quantum critical point at $s = s_{c}$ can be analyzed by renormalization group and other methods, as for the boson-only theory \mathcal{S} in Eq. (??). In this manner, we find that the quantum critical theory is a CFT, described by a renormalization group fixed at $u = u^{*}$ and $\lambda = \lambda^{*}$. This is a state without quasiparticle excitations, with Green's functions for φ^{a} and Ψ similar to those of the other CFT3s noted above.

Emergent gauge fields

Condensed matter models also lead to field theories which have fluctuating dynamic gauge fields, in contrast to those in Eq. (??) and (??). These arise most frequently in theories of quantum antiferromagnets, and can be illustrated most directly using the 'resonating valence bond' model [?, ?]. Fig. ??a shows a component, $|D_i\rangle$, of a wavefunction of an antiferromagnet on the square lattice, in which nearby electrons pair up in to singlet valence bonds—the complete wavefunction is a superposition of numerous components with different

Figure 9: Phase diagram of the Hubbard model for spin S=1/2 fermions on the honeycomb lattice at a density of one fermion per site. The large U/w ($s < s_c$) state breaks spin rotation symmetry, and is an insulating antiferromagnet with a gap to all charged excitations. The small U/w ($s > s_c$) state is described at low energies by a CFT3 of free Dirac fermions.

choices of pairing between the electrons:

$$|\Psi\rangle = \sum_{i} c_i |D_i\rangle \tag{2.88}$$

where the c_i are unspecified complex numbers. In a modern language, such a resonating valence bond wavefunction was the first to realize long-range quantum entanglement [?]. In more practical terms, the long-range entanglement is reflected in the fact that an emergent gauge fields is required to describe the low energy dynamics of such a state [?, ?]. A brief argument illustrating the origin of emergent gauge fields is illustrated in Fig. ??. We label each state by a configuration by a set of integers \hat{n}_i representing the number of singlet valence bonds on each link. As each electron can form only one singlet bond, we have a local constraint on each site, as shown in Fig. ??. Now, introducing an 'electric field' operator on each link defined by $\hat{E}_{i\alpha} = (-1)^{i_x + i_y} \hat{n}_{i\alpha}$ (here *i* labels sites of the square lattice, and $\alpha = x, y$ labels the two directions), this local constraint can be written in the very suggestive form

$$\Delta_{\alpha} \hat{E}_{i\alpha} = \rho_i, \tag{2.89}$$

where Δ_{α} is a discrete lattice derivative, and $\rho_i \equiv (-1)^{i_x+i_y}$ is a background 'charge' density. Eq. (??) is analogous to Gauss's Law in electrodynamics, and a key indication that the physics of resonating valence

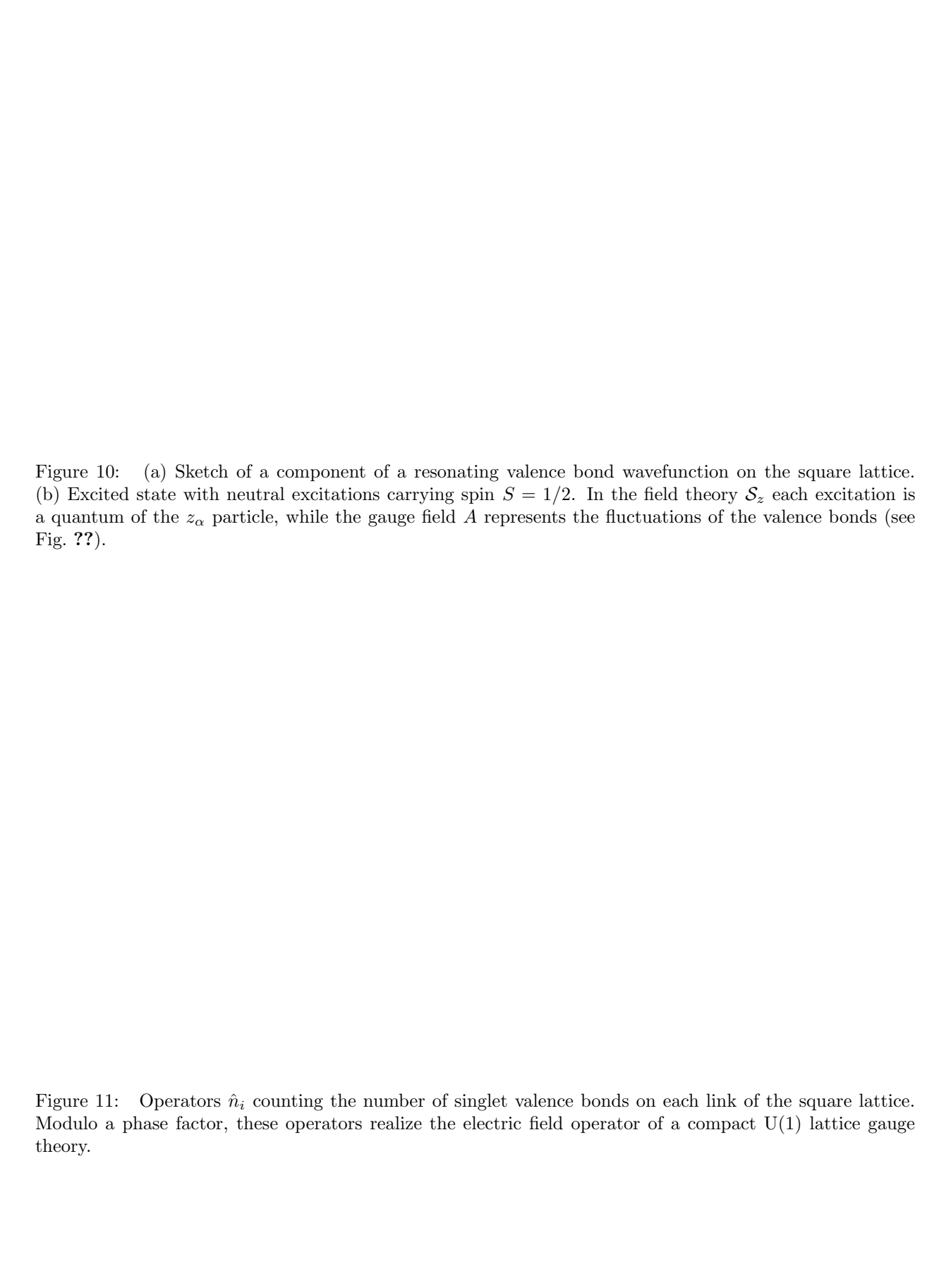


Figure 12: Phases of a square lattice antiferromagnet. The vicinity of the critical point is described by the theory S_z in Eq. (??) (compare Fig. ??). The phase with Néel order is the Higgs phase of the gauge theory, while the Coulomb phase of S_z is destabilized by monopoles, leading to valence bond solid order.

bonds is described by an emergent compact U(1) gauge theory.

CFTs with emergent gauge fields appear when we consider a quantum phase transition out of the resonating valence bond state into an ordered antiferromagnet with broken spin rotation symmetry. To obtain antiferromagnetic order, we need to consider state in which some on the electrons are unpaired, as illustrated in Fig. ??b. For an appropriate spin liquid, these excitations behave like relativistic bosons, z_{α} , at low energy; here $\alpha = \uparrow, \downarrow$ is the 'spin' index, but note here that α does not correspond to spacetime spin, and behaves instead like a 'flavor' index associated with the global SU(2) symmetry of the underlying lattice antiferromagnet. The quantum transition from the resonating valence bond state to the antiferromagnet is described by the condensation of the z_{α} bosons [?, ?], and the quantum critical point is proposed to be a CFT3 [?]; see Fig. ??. Such a transition is best established for a set of quantum antiferromagnetics with a global SU(M) symmetry, as reviewed recently by Kaul and Block [?]. These models are expressed in terms of SU(M) spins, \vec{S} , residing on the sites of various bipartite lattices, with bilinear and biquadratic exchange interactions between nearest neighbor sites. The low energy physics in the vicinity of the critical point is described by a field theory with an emergent U(1) gauge field A and the relativistic scalar z_{α} (now

 $\alpha = 1 \dots M$

$$S_z = \int d^2x \, d\tau \left[|(\nabla_x - iA_x)z_\alpha|^2 + c^2 |(\partial_\tau - iA_\tau)z_\alpha|^2 + s|z_\alpha|^2 + u\left(|z_\alpha|^2\right)^2 + (1/(2e^2)F^2\right],\tag{2.90}$$

where F = dA. The order parameter for the broken symmetry in the antiferromagnet involves a gauge-invariant bilinear of the z_{α} . In the present case, it turns out that resonating valence bond phase where the z_{α} are gapped turns out to be unstable to the proliferation of monopoles in the U(1) gauge field, which leads ultimately to the appearance of a broken lattice symmetry with 'valence bond solid' (VBS) order (see Fig. ??) [?, ?]. However, the monopoles are suppressed at the quantum critical point at $s = s_c$, and then S_z realizes a conformal gauge theory [?]: numerical studies of the lattice Hamiltonian are consistent with many features of the 1/N expansion of the critical properties of the gauge theories.

Our interest here is primarily on the non-quasiparticle dynamics of the T > 0 quantum critical region near $s = s_c$. Here, the scaling structure is very similar to our discussion of the Wilson-Fisher critical theory, with the main difference being that the associated CFT is now also a gauge theory.

Scale invariant geometries

We have already seen in §?? above that the simplest solution to the most minimal bulk theory (??) is the AdS_{d+2} spacetime

$$ds^{2} = L^{2} \left(\frac{-dt^{2} + d\vec{x}_{d}^{2} + dr^{2}}{r^{2}} \right).$$
 (2.91)

We noted that this geometry has the SO(d+1,2) symmetry of a d+1 (spacetime) dimensional CFT. We verified that a scalar field ϕ in this spacetime was dual to an operator \mathcal{O} with a certain scaling dimension Δ determined by the mass of the scalar field via (??). We furthermore verified that the retarded Green's function (??) of \mathcal{O} , as computed holographically, was indeed that of an operator of dimension Δ in a CFT. More generally, the dynamics of perturbations about the bulk background (??) gives a holographic description of zero temperature correlators in a dual CFT.

Dynamical critical exponent z > 1

A CFT has dynamic critical exponent z=1. This section explains the holographic description of general quantum critical systems with z not necessarily equal to 1. The first requirement is a background that geometrically realizes the more general scaling symmetry: $\{t, \vec{x}\} \to \{\lambda^z t, \lambda \vec{x}\}$. The geometry

$$ds^{2} = L^{2} \left(-\frac{dt^{2}}{r^{2z}} + \frac{d\vec{x}_{d}^{2} + dr^{2}}{r^{2}} \right), \qquad (2.92)$$

does the trick [?]. These are called 'Lifshitz' geometries because the case z=2 is dual to a quantum critical theory with the same symmetries as the multicritical Lifshitz theory. These backgrounds do not have additional continuous symmetries beyond the scaling symmetry, spacetime translations and spatial rotations. They are invariant under time reversal $(t \to -t)$. We will shortly see that correlation functions computed from these backgrounds indeed have the expected scaling form (??). Firstly, though, we describe how the spacetime (??) can arise in a gravitational theory.

All Lifshitz metrics have constant curvature invariants. It can be proven that the only effects of quantum corrections in the bulk is to renormalize the values of z and L [?]. In this sense the scaling symmetry is robust beyond the large N limit. However, for $z \neq 1$ these metrics suffer from so-called pp singularities at the 'horizon' as $r \to \infty$. Infalling observers experience infinite tidal forces. See [?] for more discussion. Such null singularities are likely to be acceptable within a string theory framework, see e.g. [?, ?]. So far, no pathologies associated with these singularities has arisen in classical gravity computations of correlators and thermodynamics.

Unlike Anti-de Sitter spacetime, the Lifshitz geometries are not solutions to pure gravity. Therefore, a slightly more complicated bulk theory is needed to describe them. Two simple theories that have Lifshitz geometries (??) as solutions are Einstein-Maxwell-dilaton theory [?, ?] and Einstein-Proca theory [?]. The Einstein-Proca theory couples gravity to a massive vector field:

$$S[g,A] = \frac{1}{2\kappa^2} \int d^{d+2}x \sqrt{-g} \left(R + \Lambda - \frac{1}{4}F^2 - \frac{m_A^2}{2}A^2 \right), \qquad (2.93)$$

with
$$\Lambda = \frac{(d+1)^2 + (d+1)(z-2) + (z-1)^2}{L^2}, \quad m_A^2 = \frac{z d}{L^2}.$$
 (2.94)

It is easily verified that the equations of motion following from this action have (??) as a solution, together with the massive vector

$$A = \sqrt{\frac{2(z-1)}{z}} \frac{L \, dt}{r^z} \,. \tag{2.95}$$

This is only a real solution for $z \ge 1$. We will discuss physically allowed values of z later. The Einstein-Maxwell-dilaton theory

$$S[g, A, \phi] = \frac{1}{2\kappa^2} \int d^{d+2}x \sqrt{-g} \left(R + \Lambda - \frac{1}{4} e^{2\alpha\phi} F^2 - \frac{1}{2} (\nabla \phi)^2 \right), \qquad (2.96)$$

with
$$\Lambda = \frac{(z+d)(z+d-1)}{L^2}$$
, $\alpha = \sqrt{\frac{d}{2(z-1)}}$, (2.97)

has the Lifshitz metric (??) as a solution, together with the dilaton and Maxwell fields

$$A = \sqrt{\frac{2(z-1)}{z+d}} \frac{L \, dt}{r^{z+d}}, \qquad e^{2\alpha\phi} = r^{2d}.$$
 (2.98)

Again, these solutions make sense for z > 1. In these solutions the scalar field ϕ is not scale invariant. We will see below that these kinds of running scalars can lead to interesting anomalous scaling dimensions. Because the Einstein-Mawell-dilaton theory involves a nonzero conserved flux for a bulk gauge field (dual to a charge density in the QFT), it is most naturally interpreted as a finite density solution, and will re-appear in §?? below. There is a large literature constructing Lifshitz spacetimes from consistent truncations of string theory, starting with [?, ?]. In our later discussion of compressible matter, we will describe some further ways to obtain the scaling geometry (??).

Repeating the analysis we did for the CFT case in §??, we can consider the two point function of a scalar operator in these theories. As before, consider a scalar field ϕ (not the dilaton above) that satisfies the Klein-Gordon equation (??), but now in the Lifshitz geometry (??). Once again writing $\phi = \phi(r)e^{-i\omega t + ik \cdot x}$, the radially dependent part must now satisfy

$$\phi'' - \frac{z+d-1}{r}\phi' + \left(\omega^2 r^{2z-2} - k^2 - \frac{(mL)^2}{r^2}\right)\phi = 0.$$
 (2.99)

This equation cannot be solved explicitly in general. Expanding into the UV region, as $r \to 0$, we find that the asymptotic behavior of (??) generalizes to

$$\phi = \phi_{(0)} \left(\frac{r}{L}\right)^{D_{\text{eff.}} - \Delta} + \dots + \phi_{(1)} \left(\frac{r}{L}\right)^{\Delta} + \dots \quad \text{(as} \quad r \to 0).$$
 (2.100)

We introduced the effective number of spacetime dimensions

$$D_{\text{eff.}} = z + d\,, (2.101)$$

because these theories can be thought of as having z rather than 1 time dimensions, and the (momentum) scaling dimension Δ now satisfies

$$\Delta(\Delta - D_{\text{eff.}}) = (mL)^2 . \tag{2.102}$$

As in our discussion of AdS in §??, $\phi_{(0)}$ is dual to a source for the dual operator \mathcal{O} , whereas $\phi_{(1)}$ is the expectation value. By rescaling the radial coordinate of the equation (??), setting $\rho = r\omega^{1/z}$, and then using the asymptotic form (??), we can conclude that the retarded Green's function has the scaling form required

for an operator of dimension Δ in a scale invariant theory with dynamical critical exponent z:

$$G_{\mathcal{O}\mathcal{O}}^{R}(\omega, k) = \frac{2\Delta - D_{\text{eff.}}}{L} \frac{\phi_{(1)}}{\phi_{(0)}} = \omega^{(2\Delta - D_{\text{eff.}})/z} F\left(\frac{\omega}{k^{z}}\right). \tag{2.103}$$

To obtain the correct normalization of the second expression, the discussion of holographic renormalization in section ?? must be adapted to Lifshitz spacetimes [?].

The scaling function F(x) appearing in $(\ref{equation})$ will depend on the theory, it is not constrained by symmetry when $z \neq 1$. Remarkably, a certain asymptotic property of this function has been shown to hold both in strongly coupled holographic models and also in general weakly interacting theories. Specifically, consider the spectral weight (the imaginary part of the retarded Green's function) at low energies $(\omega \to 0)$, but with the momentum k held fixed. We expect this quantity to be vanishingly small, because the scaling of on-shell states as $\omega \sim k^z$ implies that there are no low energy excitations with finite k [?, ?]. The precise holographic result is obtained from a straightforward WKB solution to the differential equation ($\ref{equation}$), in which $\ref{equation}$ is the large WKB parameter. For the interested reader, we will go through some explicit WKB derivations of holographic Green's functions (very similar to the computations that pertain here) in later parts of the review. The essential point is that if the wave equation ($\ref{equation}$) is written in the form of a Schrödinger equation, then the imaginary part of the dual QFT Green's function is given by the probability for the field to tunnel from the boundary of the spacetime through to the horizon. Here we can simply quote the result [$\ref{equation}$]

$$\operatorname{Im} G_{\mathcal{O}\mathcal{O}}^{R}(\omega, k) \sim e^{-A(k^{z}/\omega)^{1/(z-1)}}, \qquad (\omega \to 0, \ k \text{ fixed}).$$
 (2.104)

The positive coefficient A is a certain ratio of gamma functions. Precisely the same relation (??) has been shown to hold in weakly interacting theories [?]. At weak coupling the constant A goes like the logarithm of the coupling. The weak coupling results follows from considering the spectrum of on-shell excitations that are accessible at some given order in perturbation theory. Taking the holographic and weak coupling results together suggests that the limiting behavior (??) may be a robust feature of the momentum dependence of general quantum critical response functions, beyond the existence of quasiparticles.

We should note also that when z = 2, the full Green's function can be found explicitly in terms of gamma functions [?, ?], which is typically a sign of a hidden $SL(2, \mathbb{R})$ symmetry.

Hyperscaling violation

A more general class of scaling metrics than (??) take the form

$$ds^{2} = L^{2} \left(\frac{r}{R}\right)^{2\theta/d} \left(-\frac{dt^{2}}{r^{2z}} + \frac{d\vec{x}_{d}^{2} + dr^{2}}{r^{2}}\right). \tag{2.105}$$

Here L is determined by the bulk theory while R is a constant of integration in the solution. On the face of it, these metrics do not appear to be scale invariant. Under the rescaling $\{t, \vec{x}, r\} \to \{\lambda^z t, \lambda \vec{x}, \lambda r\}$, the metric transforms as $ds^2 \to \lambda^{2\theta/d} ds^2$. However, this covariant transformation of the metric amounts to the fact that the energy density operator (as well as other operators) in the dual field theory has acquired an anomalous dimension. Recall from §?? that the bulk metric is dual to the energy-momentum tensor in the QFT. From the essential holographic dictionary (??), the boundary value $\delta \gamma_{\mu\nu}$ of a bulk metric perturbation sources the dual energy density ε via the field theory coupling

$$\frac{1}{R^{\theta}} \int d^{d+1}x \left(\delta \gamma\right)_{t}^{t} \varepsilon. \tag{2.106}$$

The factors of R appear because the boundary metric is obtained, analogously to $(\ref{eq:condition})$, from $(\ref{eq:condition})$ by stripping off the powers of r and L (but not R, which is a property of the solution) from each component of the induced boundary metric. As in our discussion around $(\ref{eq:condition})$ above, the scaling action $\{t, \vec{x}, r\} \to \{\lambda^z t, \lambda \vec{x}, \lambda r\}$ must be combined with a scaling of parameters in the solution that leave the field (the metric in this case) invariant. Therefore, under this scaling we have $d^{d+1}x \to \lambda^{z+d}d^{d+1}x$, $(\delta\gamma)_t{}^t$ is invariant (because one index is up and the other down), $\varepsilon(x) \to \lambda^{-\Delta_{\varepsilon}} \varepsilon(\lambda x)$ and $R \to \lambda R$. Scale invariance of the coupling $(\ref{eq:condition})$ then requires

$$\Delta_{\varepsilon} = z + d - \theta = \Delta_{\varepsilon,0} - \theta \,, \tag{2.107}$$

where $\Delta_{\varepsilon,0}$ is the canonical dimension of the energy density operator. The existence of such an anomalous dimension is known as hyperscaling violation, and θ is called the hyperscaling violation exponent [?]. We will see later that this anomalous dimension indeed controls thermodynamic quantities and correlation functions of the energy-momentum tensor in the expected way. It is important to note, however, that because of the dimensionful parameter R in the background, typically not all correlators of all operators will be scale covariant. An example is given by scalar fields with a large mass in the bulk [?]. In particular, when z = 1, theories with $\theta \neq 0$ are not CFTs. Hyperscaling violation arises when a UV scale does not decouple from certain IR quantities.

Hyperscaling violating metrics (??) will be important below in the context of compressible phases of

matter. However, they can also describe zero density fixed points and therefore fit into this section of our review. For instance, hyperscaling violating metrics of the form (??) with z = 1 arise as solutions to the Einstein-scalar action [?, ?]:

$$S[g,\phi] = \frac{1}{2\kappa^2} \int d^{d+2}x \sqrt{-g} \left(R + V_0 e^{\beta\phi} - \frac{1}{2} (\nabla\phi)^2 \right), \qquad (2.108)$$

with
$$V_0 = \frac{(d+1-\theta)(d-\theta)}{L^2}$$
, $\beta^2 = \frac{2\theta}{d(\theta-d)}$, (2.109)

where on the solution

$$e^{\beta\phi} = r^{-2\theta/d} \,. \tag{2.110}$$

Thus we find Lorentzian hyperscaling-violating theories. One sees in the above that for β to be real one must have $\theta < 0$ or $\theta > d$. In fact, this is a special case of a more general requirement that we now discuss.

A spacetime satisfies the null energy condition if $G_{ab}n^an^b \geq 0$ for all null vectors n. Here G_{ab} is the Einstein tensor. The null energy condition is a constraint on matter fields sourcing the spacetime (because Einstein's equations are $G_{ab} = 8\pi G_N T_{ab}$). In a holographic context, the null energy condition is especially natural because it seems to be necessary for holographic renormalization to make sense [?]. In particular, it ensures that the spacetime shrinks sufficiently rapidly as one moves into the bulk, cf. [?]. For the hyperscaling violating spacetimes (??), the null energy condition requires the following two inequalities to hold

$$(d-\theta)[d(z-1)-\theta] \ge 0, \tag{2.111}$$

$$(z-1)(d+z-\theta) \ge 0. (2.112)$$

With $\theta = 0$, these inequalities require that $z \ge 1$, consistent with our observations above. While perhaps plausible, this condition on the dynamic critical exponent remains to be understood from a field theory perspective.

Unlike the Lifshitz geometries, hyperscaling-violating spacetimes do not have constant curvature invariants, and these invariants generically (with one potentially interesting exception [?, ?]) diverge at either large or small r. These are more severe singularities than the pp-singularities of the Lifshitz geometries, and likely indicate the hyperscaling-violating spacetime only describes an intermediate energy range of the field theory, with new IR physics needed to resolve the singularity. For instance, microscopic examples of theories with zero density hyperscaling-violating intermediate regimes are non-conformal D-brane theories, such as super Yang-Mills theory in 2+1 dimensions [?].

Galilean-invariant 'non-relativistic CFTs'

None of the scaling geometries we have discussed so far (except for AdS itself) have symmetries beyond dilatations, spacetime translation and rotations. In [?, ?] a gravitational geometry was proposed as a dual to non-relativistic CFTs. These are theories in which the scaling symmetry is enhanced by a Galilean boost symmetry and a particle number symmetry. For the case z = 2, further enhancement by a special conformal symmetry is possible. For this reason these geometries are known as 'Schrödinger' spacetimes. The various algebras are discussed in [?]. The primary motivation of these works was to model strongly interacting critical regimes of cold atomic gases. This body of work is somewhat tangential to the main thrust of our review, so we limit ourselves to some brief comments and pointers to the literature.

The vacuum poses a challenge for gravity duals of Galilean-invariant systems. While vacua of e.g. relativistic field theories are highly nontrivial, the state with zero particle number in a Galilean-invariant system has no dynamics whatsoever. It seems puzzling, therefore, that it could be dually described by an emergent spacetime, which is certainly not trivial. This difficulty manifests itself in the fact that the geometries proposed in [?, ?] involve a compactified null circle, which is well-known to be a delicate thing (see e.g. [?]). It is natural, therefore, to consider states of the theory with a large particle number [?, ?, ?, ?]. While the resulting geometries are better behaved, the underlying compactified null circle in the construction directly results in thermodynamic properties (as a function of temperature and particle number) that are quite unlike those of more conventional Galilean-invariant systems [?]. It is important to see if these difficulties can be overcome by more general holographic constructions [?, ?].

Nonzero temperature

The most universal way to introduce a single scale into the scale invariant theories discussed above is to heat the system up. The thermal partition function is given by the path integral of the theory in Euclidean time with a periodic imaginary time direction, $\tau \sim \tau + 1/T$:

$$Z_{\text{QFT}}(T) = \int_{S^1 \times \mathbb{R}^d} d\Phi \, e^{-I_E[\Phi]} \,. \tag{2.113}$$

Here $I_E[\Phi]$ is the Euclidean action of the quantum field theory.

The essential holographic dictionary (??) identifies the space in which in the field theory lives as the asymptotic conformal boundary of the bulk spacetime. In particular, once we have placed the theory in a nontrivial background geometry ($S^1 \times \mathbb{R}^d$ in this case), then the bulk geometry must asymptote to this form. In order to compute the thermal partition function (??) holographically, in the semiclassical limit (??), we

must therefore find a solution to the Euclidean bulk equations of motion with these boundary conditions.

Thermodynamics

The required solutions are Euclidean black hole geometries. Allowing for general dynamic critical exponent z and hyperscaling violation, the solutions can be written in the form

$$ds^{2} = L^{2} \left(\frac{r}{R}\right)^{2\theta/d} \left(\frac{f(r)d\tau^{2}}{r^{2z}} + \frac{dr^{2}}{f(r)r^{2}} + \frac{d\vec{x}_{d}^{2}}{r^{2}}\right). \tag{2.114}$$

The new aspect of the above metric relative to the scaling geometry (??) is the presence of the function f(r). There is some choice in how the metric is written, because we are free to perform a coordinate transformation: $r \to \rho(r)$. The above form is convenient, however, because often the function f(r) is simple in this case. We will see some examples of f(r) shortly, but will first note some general features.

Asymptotically, as $r \to 0$, the metric must approach the scaling form (??), and therefore f(0) = 1. Recall from the discussion in §?? that the near-boundary metric corresponds to the high energy UV physics of the dual field theory. Therefore, this boundary condition on f(r) is the familiar statement that turning on a finite temperature does not affect the short distance, high energy properties of the theory. The temperature will, however, have a strong effect on the low energy IR dynamics. In fact, we expect the temperature to act as an IR cutoff on the theory, with long wavelength processes being Debye screened. It should not come as a surprise, therefore, that in the interior of the spacetime we find that at a certain radius r_+ we have $f(r_+) = 0$. At this radius the thermal circle τ shrinks to zero size and the spacetime ends. This is the Euclidean version of the black hole event horizon. The radial coordinate extends only over the range $0 \le r \le r_+$.

The radius r_{+} is related to the temperature by imposing that the spacetime be regular at the Euclidean horizon. If we expand the metric near the horizon we find

$$ds^{2} = A_{+} \left(\frac{|f'(r_{+})|(r_{+} - r)d\tau^{2}}{r_{+}^{2z}} + \frac{dr^{2}}{|f'(r_{+})|(r_{+} - r)r_{+}^{2}} + \frac{d\vec{x}_{d}^{2}}{r_{+}^{2}} \right) + \cdots$$
 (2.115)

Performing the change of coordinates

$$r = r_{+} - \frac{r_{+}^{2}|f'(r_{+})|}{4A_{+}}\rho^{2}, \qquad \tau = \frac{2r_{+}^{z-1}}{|f'(r_{+})|}\phi,$$
 (2.116)

the near-horizon geometry becomes

$$ds^{2} = \rho^{2} d\phi^{2} + d\rho^{2} + \frac{d\vec{x}_{d}^{2}}{r_{\perp}^{2}} + \cdots$$
 (2.117)

We immediately recognize this metric as flat space in cylindrical polar coordinates. In order to avoid a conical singularity at $\rho = 0$, we must have the identification $\phi \sim \phi + 2\pi$. But θ is defined in terms of τ in (??), and τ already has the periodicity $\tau \sim \tau + 1/T$. Therefore

$$T = \frac{|f'(r_+)|}{4\pi r_\perp^{z-1}}. (2.118)$$

The (topological) plane parametrized by the τ and r coordinates is called the cigar geometry and is illustrated in figure ??.

Figure 13: Cigar geometry. The r coordinate runs from 0 at the boundary to r_+ at the horizon, where the Euclidean time circle shrinks to zero.

The Einstein-scalar theories with action $(\ref{eq:condition})$ are an example of cases in which the function f(r) can be found analytically. The equations of motion following from this action are found to have a black hole solution given by the metric $(\ref{eq:condition})$, with z=1, with the scalar remaining unchanged from the zero temperature solution $(\ref{eq:condition})$ and

$$f(r) = 1 - \left(\frac{r}{r_{+}}\right)^{d+1-\theta} . {(2.119)}$$

It follows from (??) that for these black holes

$$T = \frac{d+1-\theta}{4\pi r_{+}} \,. \tag{2.120}$$

In particular, when $\theta = 0$ this gives the temperature of the (planar) AdS-Schwarzschild black hole in pure Einstein gravity. In other cases, such as the Einstein-Proca theory considered in the previous section, it will not be possible to find a closed form expression for f(r). In these cases, the Einstein equations will give ODEs for f(r), which will typically be coupled to other unknown functions appearing in the solution. These ODEs must then be solved numerically subject to the boundary conditions at r = 0 and $r = r_+$ that we gave in the previous paragraph. These numerics are straightforward and are commonly performed either with shooting or with spectral methods. In performing the numerics, because the constant r_+ is the only scale, it can be scaled out of the equations by writing $r = r_+\hat{r}$. This scaling symmetry together with the formula (??) for the temperature implies that in generality

$$T \sim r_+^{-z}$$
. (2.121)

With the temperature at hand, we can now compute the entropy as a function of temperature. It is a general result in semiclassical gravity that the entropy is given by the area of the horizon divided by $4G_N$ [?, ?]. In our conventions, Newton's constant $G_N = \kappa^2/(8\pi)$. Therefore, for the black hole spacetime (??) we have the entropy density

$$s = \frac{S}{V_d} = \frac{2\pi L^d}{\kappa^2} \frac{r_+^{\theta - d}}{R^{\theta}} \sim \frac{L^d}{L_p^d} \frac{T^{(d - \theta)/z}}{R^{\theta}} \,. \tag{2.122}$$

The temperature and entropy are especially nice observables in holography because they are determined entirely by horizon data. The free energy is a more complicated quantity because it depends on the whole bulk solution. In particular

$$F = -T\log Z_{\text{OFT}} = -T\log Z_{\text{Grav.}} = TS[g_{\star}]. \tag{2.123}$$

Here we used the equivalence of bulk and QFT partition functions (??) and also the semiclassical limit in the bulk (??). In the final expression, $S[g_{\star}]$ is the bulk Euclidean action evaluated on the black hole solution (??). The action involves an integral over the whole bulk spacetime and diverges due to the infinite volume near the boundary as $r \to 0$. The divergences are precisely of the form of the expected short distance divergences in the free energy of a quantum field theory. This is an instance of the general association of the near boundary region of the bulk with the UV of the dual QFT, illustrated in figure ?? above. If we believe that the scale invariant theory we are studying is a fundamental theory, then it makes sense to holographically

renormalize the theory by adding appropriate boundary counterterms as described in §?? above. However, more typically, we expect in condensed matter physics that the scaling theory is an emergent low energy description with some latticized short distance completion. The divergences we encounter in evaluating the action are then physical and simply remind us that the free energy is sensitive to (and generically dominated by) non-universal short distance degrees of freedom. For this reason we will refrain from explicitly evaluating the on shell action (??) for the moment, and note that the entropy (??) is a better characterization of the universal emergent scale-invariant degrees of freedom at temperatures that are low compared to some UV cutoff.

Thermal screening

Beyond equilibrium thermodynamic quantities, in §?? the Lorentzian signature version of the black hole backgrounds (??) will be the starting point for computations of linear response functions such as conductivities. At this point we can show how black holes cause thermal screening of spatial correlation. Correlators with $\omega = 0$ are the same in Lorentzian and Euclidean signature. To do this, consider the wave equation of a massive scalar field in the black hole background (??). For this computation, let us not consider the effects of hyperscaling violation and so set $\theta = 0$. The wave equation (??), at Euclidean frequency ω_n , becomes

$$\phi'' + \left(\frac{f'}{f} - \frac{z+d-1}{r}\right)\phi' - \frac{1}{f}\left(k^2 + \frac{(mL)^2}{r^2} + \frac{r^{2z}\omega_n^2}{r^2f}\right)\phi = 0.$$
 (2.124)

This equation cannot be solved analytically in general. By rescaling the r coordinate as described above equation (??) above, and with the assumption that r_+ is the only scale in the bulk solution, so that f is a function of r/r_+ , with r_+ related to T via (??), we can again conclude that the Green's function will have the expected scaling form

$$G_{\mathcal{O}\mathcal{O}}^{R}(\omega, k) = \omega^{(2\Delta - D_{\text{eff.}})/z} F\left(\frac{\omega}{k^{z}}, \frac{T}{k^{z}}\right).$$
 (2.125)

Useful intuition for how thermal screening arises is obtained by solving the above equation in the WKB limit and with $\omega_n = 0$. This approximation holds for large $mL \gg 1$. The WKB analysis is especially simple for equation (??) as there are no classical turning points. Imposing an appropriate boundary condition at the horizon (which will be discussed in generality in §??), one finds that the correlator is

$$\langle \mathcal{O}\mathcal{O}\rangle (k) = r_{+}^{-2mL} \exp\left\{-2\int_{0}^{r_{+}} \frac{dr}{r} \left(\sqrt{\frac{(mL)^{2} + (kr)^{2}}{f}} - mL\right)\right\}.$$
 (2.126)

To see thermal screening, consider the real space correlator at large separation. This is found by taking the Fourier transform of (??) and evaluating using a stationary phase approximation for the k integral as

 $x \to \infty$ to obtain:

$$\langle \mathcal{O}\mathcal{O}\rangle(x) = \int_{-\infty}^{\infty} \frac{d^d k}{(2\pi)^d} \langle \mathcal{O}\mathcal{O}\rangle(k) e^{-ik \cdot x} \sim e^{-ik_{\star}x}.$$
 (2.127)

It is simple to determine k_{\star} . From (??) and (??), k_{\star} must satisfy

$$2\int_0^{r_+} \frac{k_{\star} r dr}{\sqrt{f} \sqrt{(mL)^2 + (k_{\star} r)^2}} + ix = 0.$$
 (2.128)

In this expression we see that at large x, k_{\star} will be independent of x to leading order. Specifically: to balance the ix term, the integral must become large. This occurs if the integrand is close to developing a pole at $r = r_+$ (which would give a logarithmically divergent integral). For this to happen it must be that $(mL)^2 + (k_{\star}r)^2$ is close to vanishing at $r = r_+$ (where f already vanishes). To leading order, then, we have $k_{\star} = \pm imL/r_+$. Choosing the physical sign, it follows that at large x

$$\langle \mathcal{O}\mathcal{O}\rangle(x) \sim e^{-mL\,x/r_{+}}, \quad \text{as} \quad x \to \infty.$$
 (2.129)

We have therefore shown that the thermal screening length is

$$L_{\text{thermal}} = \frac{r_{+}}{mL} \sim \frac{1}{T^{1/z}},$$
 (2.130)

as we might have anticipated.

The screening length $(\ref{equation})$ arose because the momentum integral in $(\ref{equation})$ was dominated by momenta at the horizon scale. This can be seen even more directly by recalling that the WKB limit of the Klein-Gordon equation in a geometry describes the motion of very massive particles along geodesics. The correlation function at a separation x is then given by the length of a geodesic in the bulk that connects two points on the boundary separated by distance x. The simplest quantity to consider here is the equal time correlation function. For points separated by much more than the horizon length r_+ , the geodesic essentially falls straight down to the horizon, and runs along the horizon for a distance x. See figure $\ref{equation}$? Thereby one recovers $\ref{equation}$ from

$$\langle \mathcal{OO} \rangle (x) \sim e^{-m \times (\text{Geodesic length})} \sim e^{-mLx/r_{+}}.$$
 (2.131)

Thus we see a very geometric connection between the presence of a horizon and thermal screening.

Figure 14: **Thermal screening**. The geodesic runs along the horizon over a distance x. This contribution to its length dominates the correlation function and leads to an exponentially decaying correlation (??) in space, with scale set by the horizon radius r_+ .

Theories with a mass gap

The geometries we have discussed so far give the holographic duals to quantum critical theories at zero and nonzero temperature. The simplest way to move away from criticality is to deform the theory by a relevant operator. The RG flow triggered by the relevant deformation may lead to another fixed point in the IR, or may gap out the theory.

The essential holographic dictionary discussed in §?? and §?? tells us how to deform a critical theory by a relevant operator \mathcal{O} of dimension $\Delta < D_{\text{eff.}}$. Namely, one introduces a field Φ in the bulk dual to \mathcal{O} and requires that near the boundary $(r \to 0)$, the field behave as $\Phi \sim \Phi_{(0)} r^{d_{\text{efff.}} - \Delta}$. Recall from §?? that $\Phi_{(0)} \equiv s - s_c$ is the dual field theory coupling of the operator \mathcal{O} . This boundary condition, together with $\Delta < D_{\text{eff.}}$, implies that the field Φ grows as one moves into the bulk away from r = 0. This growth corresponds to the growth of the relevant coupling $\Phi_{(0)}$ into the IR as described in §?? above.

As the field Φ grows as a function of the radial coordinate, it will eventually backreact on the metric (as well as any other fields that were present in the scaling solution with $\Phi = 0$). One must therefore solve the coupled equations of motion for the field and the metric. For simplicity, we will focus on the Lorentz invariant case of z = 1 and with hyperscaling holding in the original undeformed theory. Then, we expect to find a (Euclidean) bulk solution that can be written in the general form

$$ds^{2} = e^{2A(r)} \left(d\tau^{2} + dr^{2} + d\vec{x}_{d}^{2} \right), \qquad \Phi = \Phi(r).$$
 (2.132)

This is a general form for a metric that preserves Poincaré invariance along the RG flow. On this ansatz, the equations of motion will become coupled ODEs for $\{A, \Phi\}$ as functions of r. These must be solved subject to the UV boundary condition that $A \to -\log(r/L)$ and $\Phi \to \Phi_{(0)} r^{d+1-\Delta}$ as $r \to 0$.

Two qualitatively different types of IR behavior are possible. One is that the solution extends to $r \to \infty$ and that the function in the metric behaves as $A \sim (\frac{\theta_{\text{IR}}}{d} - 1) \log r$. This signals the emergence of a new far IR

fixed point, possibly with hyperscaling violation. In this case the solutions that interpolate between scaling geometries in the UV and IR are called 'domain wall' spacetimes. For a discussion (without hyperscaling violation) see [?]. We will be greatly interested in the emergence of IR scaling in slightly more general, nonzero charge density, setups in §?? below. The reference [?] also explains how the equations of motion for gravity coupled to a scalar field can be substantially simplified when the potential for the scalar field can be written in terms of a 'superpotential'. Such a rewriting is also useful to construct explicit examples of the gapped physics that we will only outline below.

The other option is that the IR is gapped. In a gapped theory correlators decay exponentially at late Euclidean times. This is similar to our earlier discussion of exponential decay at large spatial separation for thermal screening. In fact, the discussion around (??) above tells us what we need to occur for the geometry (??) to give exponential decay at late Euclidean time. We will need the solution to terminate at some $r = r_o$, and furthermore $A(r_o)$ should be finite. This latter condition ensures that the tension of timelike geodesics running along $r = r_o$ is finite. This is important, because such geodesics determine late time correlations, analogously to how the geodesic in (??) determines large separation correlation. In order for the geometry to terminate at $r = r_o$ with $A(r_o)$ remaining finite, one or both of A'(r) and $\Phi(r)$ should diverge as $r \to r_o$. This indicates a singular solution, and so care is required to determine if the singularity is physical or not. See, for example, the discussion in [?].

In the above scenario, the mass gap will be set by the geodesic tension at $r = r_0$. As the only dimensionful input (from the boundary QFT perspective) into the problem is the UV coupling $\Phi_{(0)} \equiv s - s_c$, it must be this scale that determines the mass gap

$$M \sim e^{A(r_o)} \sim (s - s_c)^{\nu},$$
 (2.133)

with $\nu = 1/(d+1-\Delta)$. As with thermal screening, the termination of the geometry at some finite radial distance is a very natural geometrization of a mass gap. In our discussion of Wilsonian renormalization in §?? we noted that the increasing redshift as one moves into the bulk corresponded to the decreasing energy scale of the dual QFT. If the bulk terminates at some finite redshift, as we have just described, then there simply do not exist holographic degrees of freedom with energies below this lowest redshift scale. That is, the spectrum is gapped.

In fact, the best understood examples of holographic flows to gapped phases are not quite of the form just described. Instead, the best understood solutions involve Kaluza-Klein modes (see §?? above) in an essential way, e.g. [?, ?, ?]. This is because one or several of the internal dimensions can smoothly collapse to zero size at some finite value of the radial coordinate $r \sim r_o$ (in an entirely analogous way to how the

thermal circle collapses to zero at the tip of the Euclidean cigar geometry of figure ??). This description has the advantage of being nonsingular. One disadvantage of this approach is that typically the gap scale will be of order the Kaluza-Klein scale. This makes it difficult to decouple the physics of the gap from microscopic details that pertain to a higher dimensional auxiliary theory.

Most discussion of gaps in holography has been related to the physics of confinement, as the existence of horizons is closely tied to the existence of deconfined phases of large N gauge theories [?]. Some of this discussion may be directly relevant for the description of deconfined quantum critical points. Beyond this connection, the use of holography to study crossovers between quantum critical scaling and gapped regimes appears to be relatively underexplored. See [?] for some preliminary comments. Some caution is called for. The bulk dynamics of fields about a gapped geometry is literally that of fields in a box. The power of holography to describe dissipation classically via event horizons is lost, as the gapped geometry has no regions of infinite redshift. Instead, in the semiclassical bulk limit all excitations are perfectly stable and do not dissipate. This is an artifact of the large N expansion in gapped phases (cf. [?]).

We have characterized the gapped phase by exponential decay of correlators in Euclidean time. One expects the absence of low energy degrees of freedom to manifest itself in the absence of a power law specific heat at low temperatures. To compute the temperature dependence of the specific heat, a solution describing a black hole must be found. For instance, in the framework described above these will be solutions of the form

$$ds^{2} = e^{2A(r)} \left(f(r)d\tau^{2} + \frac{dr^{2}}{f(r)} + d\vec{x}_{d}^{2} \right), \qquad \Phi = \Phi(r).$$
 (2.134)

The functions $\{A, \Phi\}$ will change relative to the zero temperature solution (??), but must still satisfy the same boundary conditions in the UV, namely, that the relevant operator is sourced. It is typically found that a black hole solution satisfying the appropriate boundary conditions either does not exist or is not the dominant saddle point of the path integral at temperatures below some critical temperature $T_c \sim M$. For temperatures $T < T_c$ the dominant saddle is just the zero temperature spacetime (??), but now with the Euclidean thermal circle identified. The absence of a horizon for $T < T_c$ then means that the entropy density, and hence specific heat, will be zero to leading order at large N for $T < T_c$. Thus we see the gap in the low energy degrees of freedom very vividly. For $T > T_c$, the dominant saddle will be a black hole spacetime of the form (??). For an example of such a transition see [?, ?]. These types of transitions between geometries with and without horizons are referred to as Hawking-Page transitions. The original and simplest case of such a transition occurs if the boundary is considered on a spatial sphere rather than a plane [?, ?, ?, ?].

Quantum critical transport

Condensed matter systems and questions

Let us consider the simplest case of transport of a conserved U(1) "charge" density n(x,t) (we will explicitly write out the time coordinate, t, separately from the spatial coordinate x in this section). Its conservation implies that there is a current $J_i(x,t)$ (where i=1...d) such that

$$\partial_t n + \partial_i J_i = 0. (2.135)$$

We are interested here in the consequences of this conservation law at T > 0 for correlators of n and J_i in quantum systems without quasiparticle excitations.

We begin with a simple system in d=1: a narrow wire of electrons which realize a Tomonaga-Luttinger liquid [?]. For simplicity, we ignore the spin of the electron in the present discussion. In field-theoretic terms, such a liquid is a CFT2. In the CFT literature it is conventional to describe its correlators in holomorphic (and anti-holomorphic) variables constructed out of space and Euclidean time, τ . The spacetime coordinate is expressed in terms of a complex number $z = x + i\tau$, and the density and the current combine to yield the holomorphic current \mathcal{J} . A well-known property of all CFT2s with a conserved \mathcal{J} is the correlator

$$\langle \mathcal{J}(z)\mathcal{J}(0)\rangle = \frac{\mathcal{K}}{z^2},$$
 (2.136)

where K is the 'level' on the conserved current. Here we wish to rephrase this correlator in more conventional condensed matter variables using momenta k and Euclidean frequency ω . Fourier transforming (??) we obtain

$$\left\langle \left| n(k,\omega) \right|^2 \right\rangle = \mathcal{K} \frac{c^2 k^2}{c^2 k^2 + \omega^2} \,,$$
 (2.137)

where c is the velocity of 'light' of the CFT2. A curious property of CFT2s is that (??) holds also at T > 0. This is a consequence of the conformal mapping between the T = 0 planar spacetime geometry and the T > 0 cylindrical geometry; as shown in [?], this mapping leads to no change in the Euclidean time correlator in (??) apart from the restriction that ω is an integer multiple of $2\pi T$ (i.e. it is a Masturbara frequency). We can also analytically continue from the Euclidean correlation in (??), via $i\omega \to \omega + i\epsilon$, to obtain the retarded two-point correlator of the density

$$G_{nn}^{R} = \mathcal{K} \frac{c^2 k^2}{c^2 k^2 - (\omega + i\epsilon)^2} \quad , \quad d = 1 \,,$$
 (2.138)

where ϵ is a positive infinitesimal. We emphasize that (??) holds for all CFT2s with a global U(1) symmetry at any temperature T.

Now we make the key observation that (??) is not the expected answer for a generic non-integrable interacting quantum system at T > 0 for small ω and k. Upon applying an external perturbation which creates a local non-uniformity in density, we expect any such system to relax towards the equilibrium maximum entropy state. This relaxation occurs via hydrodynamic diffusion of the conserved density. Namely, we expect that on long time and length scales compared to $\hbar/k_{\rm B}T$ (or analogous thermalization length scale):

$$J_i \approx -D\partial_i n + \mathcal{O}(\partial^3).$$
 (2.139)

We will give a more complete introduction to hydrodynamics in Section ??. As described in some detail by Kadanoff and Martin [?], the (very general) assumption that hydrodynamics is the correct description of the late dynamics forces the retarded density correlator at small k and ω to be

$$G_{nn}^R = \chi \frac{Dk^2}{Dk^2 - i\omega},\tag{2.140}$$

where D is the diffusion constant, and χ is the susceptibility referred to as the compressibility.⁷ The disagreement between (??) and (??) implies that all CFT2s have integrable density correlations, and do not relax to thermal equilibrium.

What is the situation for CFTs in higher dimension? We consider interacting CFT3s, such as the Wilson-Fisher fixed point describing the superfluid-insulator transition in §??. In this case (using a relativistic notation with c = 1), we have a current J_{μ} ($\mu = 0, ...d$), and its conservation and conformal invariance imply that in d spatial dimensions and at zero temperature:

$$\langle J_{\mu}(p)J_{\nu}(-p)\rangle = -\mathcal{K}|p|^{d-1}\left(\delta_{\mu\nu} - \frac{p_{\mu}p_{\nu}}{p^2}\right), \qquad (2.141)$$

where p is a Euclidean spacetime momentum and K is a dimensionless number characteristic of the CFT. The non-analytic power of p above follows from the fact that the n and J_i have scaling dimension d. Taking the $\mu = \nu = 0$ component of the above, and analytically continuing to the retarded correlator, we obtain

$$G_{nn}^{R} = \mathcal{K} \frac{k^{2}}{\sqrt{k^{2} - (\omega + i\epsilon)^{2}}}$$
, $d = 2, T = 0.$ (2.142)

While (??) is the exact result for all CFT3s, now we do not expect it to hold at T > 0. Instead, we expect

⁷In terms of thermodynamic quantities, $\chi = \partial n/\partial \mu$, with μ the chemical potential.

that for $\omega, k \ll T$ CFT3s will behave like generic non-integrable quantum systems and relax diffusively to thermal equilibrium. In other words, we expect a crossover from (??) at $\omega, k \gg T$ to (??) at $\omega, k \ll T$. Furthermore, using the fact that T is the only dimensionful parameter present, dimensional analysis from a comparison of these expressions gives us the T dependence of the compressibility and the diffusivity

$$\chi = \mathcal{C}_{\chi} T \quad , \quad D = \frac{\mathcal{C}_D}{T}, \tag{2.143}$$

where $C_{\chi,D}$ are dimensionless numbers also characteristic of the CFT3. Note that there is no direct relationship between $C_{\chi,D}$ and K other than the fact that they are all numbers obtained from the same CFT3.

The computation of $C_{\chi,T}$ for CFT3s is a difficult task we shall address by several methods in the following sections. For now, we note that these expressions also yield the conductivity σ upon using the Kubo formula [?]

$$\sigma(\omega) = \lim_{\omega \to 0} \lim_{k \to 0} \frac{-i\omega}{k^2} G_{nn}^R(k, \omega). \tag{2.144}$$

From (??) we conclude that

$$\sigma(\omega \gg T) = \mathcal{K},\tag{2.145}$$

while from (??) and (??)

$$\sigma(\omega \ll T) = \mathcal{C}_{\chi} \mathcal{C}_{D}. \tag{2.146}$$

The crossover between these limiting values is determined by a function of ω/T , and understanding the structure of this function is an important aim of the following discussion.

In the application to the boson Hubbard model, we note that the above conductivity is measured in units of $(e^*)^2/\hbar$ where e^* is the charge of a boson. We also note that the above discussion has glossed over subtleties with "hydrodynamic long-time tails": these arise from non-linearities of the equations of hydrodynamics and lead to a subtle frequency dependence of the transport co-efficients at the lowest frequencies [?]. For the present situation, there is a logarithmic frequency dependence whose coefficient has been estimated. Such long-time tails have also been obtained by holographic methods, where they are subleading in the large N expansion [?, ?]. We shall return briefly to long-time tails in section ??.

Before embarking upon various explicit methods for the computation of $\sigma(\omega)$ and $G_{nn}^R(k,\omega)$, it is useful state two exact sum rules that are expected to be obeyed by $\sigma(\omega)$. These sum rules were first noticed in a holographic context, but with the benefit of hindsight, strong arguments can now be made that they are very generally applicable at quantum critical points in d=2, and even at those which are not conformally invariant, and at those which include quenched disorder. The first sum rule is the analog of the optical sum

rule (also referred to as the f-sum rule). This states that the integral of $Re[\sigma(\omega)]$ equals a fixed number proportional to the average kinetic energy of the system. For scale-invariant critical points, the large ω behavior is given by (??), and so the integral is divergent. This is not surprising, because the average kinetic energy of the critical field theory is also an ultraviolet divergent quantity. However, it has been argued that after a simple subtraction of this divergence the integral is finite, and it integrates to a vanishing value [?]. So we have

$$\int_{0}^{\infty} d\omega \left(\operatorname{Re} \left[\sigma(\omega) \right] - \mathcal{K} \right) = 0 \tag{2.147}$$

at all T.

The second sum rule is similar in spirit, but requires a much more subtle argument. As we will see in our discussion of holography below, but as can also be argued more generally [?], CFT3s with a conserved U(1) are expected to have an 'S-dual' formulation in which the U(1) current maps to the flux of a U(1) gauge field A with

$$J_{\mu} = \frac{1}{2\pi} \epsilon_{\mu\nu\lambda} \partial_{\nu} A_{\lambda}. \tag{2.148}$$

In the S-dual theory, conductivity of the particle current equals the resistivity of the original theory. Combining this fact with (??), the existence of the S-dual theory implies that

$$\int_0^\infty d\omega \left(\text{Re} \left[\frac{1}{\sigma(\omega)} \right] - \frac{1}{\mathcal{K}} \right) = 0.$$
 (2.149)

Explicit holographic computations verify this sum rule. As before, this sum rule is expected to be widely applicable, although it is difficult to come up with other explicit computations which fully preserve the non-perturbative S-duality.

Standard approaches and their limitations

We now describe a number of approaches applied to the computation of $\sigma(\omega)$ for CFT3s, and especially to the Wilson-Fisher fixed point of the superfluid-insulator transition described by (??). Similar methods can also be applied to other transport coefficients, and to other CFTs. Each of the methods below has limitations, although their combination does yield significant insight.

Quasiparticle-based methods

We emphasized above that interacting CFT3s do not have any quasiparticle excitations. However, there are the exceptions of free CFT3s which do have infinitely long-lived quasiparticles. So we can hope that we could expand away from these free CFTs and obtain a controlled theory of interacting CFT3s. After all, this is

essentially the approach of the ϵ expansion in dimensionality by Wilson and Fisher for the critical exponents. However, we will see below that the ϵ expansion, and the related vector 1/M expansion, have difficulty in describing transport because they do not hold uniformly in ω . Formally, the $\epsilon \to 0$ and the $\omega \to 0$ limits do not commute.

Let us first perform an explicit computation on a free CFT3: a CFT with M two-component, massless Dirac fermions, C, with Lagrangian

$$\mathcal{L} = \overline{C}\gamma^{\mu}\partial_{\mu}C. \tag{2.150}$$

We consider a conserved flavor U(1) current $J_{\mu} = -i\overline{C}\gamma_{\mu}\rho C$, where ρ is a traceless flavor matrix normalized as $\text{Tr}\rho^2 = 1$. The T = 0 Euclidean correlator of the currents is

$$\langle J_{\mu}(p)J_{\nu}(-p)\rangle = -\int \frac{d^{3}k}{8\pi^{3}} \frac{\text{Tr}\left[\gamma_{\mu}\gamma_{\lambda}k_{\lambda}\gamma_{\nu}\gamma_{\delta}(k_{\delta}+p_{\delta})\right]}{k^{2}(p+k)^{2}}$$

$$= -\frac{1}{2\pi} \left(\delta_{\mu\nu} - \frac{p_{\mu}p_{\nu}}{p^{2}}\right) \int_{0}^{1} dx \sqrt{p^{2}x(1-x)}$$

$$= -\frac{1}{16}|p| \left(\delta_{\mu\nu} - \frac{p_{\mu}p_{\nu}}{p^{2}}\right). \tag{2.151}$$

This is clearly of the form in (??), and determines the value $\mathcal{K} = 1/16$.

The form of the current correlator of the CFT3 is considerably more subtle at T > 0. In principle, this evaluation only requires replacing the frequency integral in (??) by a summation over the Matsubara frequencies, which are quantized by odd multiples of πT . However, after performing this integration by standard methods, the resulting expression should be continued carefully to real frequencies. We quote the final result for $\sigma(\omega)$, obtained from the current correlator via (??)

$$\operatorname{Re}[\sigma(\omega)] = \frac{T \ln 2}{2} \delta(\omega) + \frac{1}{16} \tanh\left(\frac{|\omega|}{4T}\right)$$

$$\operatorname{Im}[\sigma(\omega)] = \int_{-\infty}^{\infty} \frac{d\Omega}{\pi} \mathcal{P}\left(\frac{\operatorname{Re}[\sigma(\Omega)] - 1/16}{\omega - \Omega}\right), \qquad (2.152)$$

where \mathcal{P} is the principal part. Note that in the limit $\omega \gg T$, (??) yields $\sigma(\omega) = \mathcal{K} = 1/16$, as expected. However, the most important new feature of (??) is the delta function at zero frequency in the real part of the conductivity, with weight proportional to T. This is a consequence of the presence of quasiparticles, which have been thermally excited and can transport charge ballistically in the absence of any collisions between them.

We can now ask if the zero frequency delta function is preserved once we move to an interacting CFT. A simple way to realize an interacting CFT3 is to couple the fermions to a dynamical U(1) gauge field,

Figure 15: Schematic of the real part of the conductivity of a CFT3 of M Dirac fermions coupled to a U(1) gauge field in the large M limit. Similar features apply to other CFT3s in the vector large M limit. The peak at zero frequency is a remnant of the quasiparticles present at $M = \infty$, and the total area under this peak equals $(T \ln 2)/2$ as $M \to \infty$.

and examine the theory for large M. It is known that the IR physics is then described by a interacting CFT3 [?, ?, ?, ?, ?, ?, ?, ?, ?, ?] and its T=0 properties can be computed in a systematic 1/M expansion (we emphasize that this is a 'vector' 1/M expansion, unlike the matrix large N models considered elsewhere in this paper). The same remains true at T>0 for the conductivity, provided we focus on the $\omega\gg T$ region of (??) (we will have more to say about this region in the following subsection). However, now collisions are allowed between the quasiparticles that were not present at $M=\infty$, and these collisions cannot be treated in a bare 1/M expansion. Rather, we have to examine the effects of repeated collisions, and ask if they lead to number diffusion and a finite conductivity. This is the precise analog of the question Boltzmann asked for the classical ideal gas, and he introduced the Boltzmann equation to relate the long-time Brownian motion of the molecules to their two-particle collision cross-section. We can apply a quantum generalization of the Boltzmann equation to the CFT3 in the 1/M expansion, where the quasiparticles of the $M=\infty$ CFT3 undergo repeated collisions at order 1/M by exchanging quanta of the U(1) guage field. The collision cross-section can be computed by Fermi's golden rule and this then enters the collision term in the quantum Boltzmann equation [?, ?].

One subtlety should be kept in mind while considering the analogy with the classical ideal gas. The free CFT3 has both particle and anti-particle quasiparticles, and these move in opposite directions in the presence of an applied electric field. So the collision term must also consider collisions between particles and anti-particles. Such collisions have the feature that they can degrade the electrical current while conserving total momentum. Consequently, a solution of the Boltzmann equation shows that the zero-frequency conductivity is finite even at T>0, after particle-anti-particle collisions have been accounted for [?, ?]. As in the usual Drude expression for the conductivity, the zero frequency conductivity is inversely proportional to the collision rate. As the latter is proportional to 1/M, we have $\sigma(0) \sim M$. Similarly, we can consider the frequency dependence of the conductivity at $\omega \ll T$, and find that the width of the peak in the conductivity extends up to frequencies of order T/M. So the zero frequency delta function in (??) has broadened into peak of height M and width T/M, as sketched in Fig. ??. It required a (formally uncontrolled) resummation of the 1/M expansion using the Boltzmann equation to obtain this result. And it should now also be clear from a glance at Fig. ?? that the $\omega \to 0$ and $M \to \infty$ limits do not commute at T>0.

A similar analysis can also be applied to the Wilson-Fisher CFT3 described by (??), using a model

with a global O(M) symmetry. The Boltzmann equation result for the zero frequency conductivity is $\sigma(0) = 0.523M$, where the boson superfluid-insulator transition corresponds to the case M = 2 [?, ?].

Our main conclusion here is that the vector 1/M expansion of CFT3s, which expands away from the quasiparticles present at $M=\infty$, yields fairly convincing evidence that $\sigma(\omega)$ is a non-trivial universal function of ω/T . However, it does not appear to be a reliable way of computing $\sigma(\omega)$ for $\omega < T$ and smaller values of M.

Short time expansion

Transport involves the long time limit of the correlators of conserved quantities, but we can nevertheless ask if any useful information can be obtained from short time correlators. For lattice models with a finite Hilbert space at each site, the short time expansion is straightforward: it can be obtained by expanding the time evolution operator $e^{-iHt/\hbar}$ in powers of t. Consequently, the short time expansion of any correlation function only involves integer powers of t.

The situation is more subtle in theories without an ultraviolet cutoff because the naive expansion of the time evolution operator leads to ultraviolet divergencies. For CFTs these ultraviolet divergencies can be controlled by a renormalization procedure, and this is expressed in terms of a technology known as the operator product expansion (OPE). Detailed reviews of the OPE are available elsewhere [?, ?], and here we only use a few basic results to examine its consequences for the two-point correlator of the current operator at short times. After a Fourier transform from time to energy, the short time expansion translates into a statement for the large frequency behavior of the conductivity of CFT3s, at frequencies much larger than T [?]

$$\sigma(\omega) = \mathcal{K} - b_1 \left(\frac{T}{i\omega}\right)^{3-1/\nu} - b_2 \left(\frac{T}{i\omega}\right)^3 + \dots , \quad \omega \gg T.$$
 (2.153)

The leading term in (??) is clearly in agreement with (??). The first sub-leading term, proportional to the numerical constant b_1 , is determined by the OPE between the currents and a scalar operator with a scaling dimension given in (??). For the Wilson-Fisher CFT3, the exponent ν is the same as that determining the correlation length in the superfluid or insulator phases on either side of the critical point. The value of b_1 is a characteristic property of the CFT3, and can be computed in a vector 1/M expansion, or by the numerical study to be described in the following subsection. The final term displayed above is a consequence of the OPE of the currents with the stress-energy tensor (an operator of dimension 3). The term with coefficient b_2 will be purely imaginary. Similarly, operators with higher dimensions can be used to obtain additional subleading corrections.

The above expansion does not directly place any constraints on the conductivity at low frequencies,

Figure 16: Schematic of the real part of the conductivity of a CFT3 as constrained by the OPE in (??) and the sum rule in (??). The areas of the shaded regions are equal to each other.

 $\omega \ll T$. However, in combination with the sum rule in (??), we can make an interesting observation. The 1/M expansion for the Wilson-Fisher CFT, and the numerical results presented below, show that the constant $b_1 > 0$. Consequently we have $\sigma(\omega) < \mathcal{K}$ at large enough ω . The sum rule in (??) now implies that there must be a region at smaller ω where we have $\sigma(\omega) > \mathcal{K}$. If we make the simple assumption that $\sigma(\omega) - \mathcal{K}$ crosses zero only once, we can conclude that $\sigma(\omega)$ should have the form in Fig. ??, with the two shaded regions having equal area. It is curious that the qualitative form of $\sigma(\omega)$ has similarities to the quasiparticle result in Fig. ??, although we have not made any use of quasiparticles in the present argument.

Quantum Monte Carlo

Quantum Monte Carlo studies perform a statistical sampling of the spacetime configurations of the imaginary time path integral of quantum systems. So they are only able to return information on correlation functions defined at imaginary Matsubara frequencies. However, even in such Euclidean studies there is the potential for a 'sign problem', with non-positive weights, because of the presence of complex Berry phase terms [?]. For the CFT3s being studied here such sign problems are usually absent; however, the problems with a non-zero chemical potential to be considered later in our review invariably do have a sign problem.

For the Wilson-Fisher CFT3 defined by (??), there is an especially elegant model for efficient Monte Carlo studies. This is the lattice regularization provided by the Villain model. This model is defined in terms of integer valued variables, $j_{i,\mu}$, on the links of a cubic lattice. Here i labels the sites of a cubic lattice, and $\mu = \pm x, \pm y, \pm z$ represents the six links emerging from each site. Each link has an orientation, so that $j_{i+\hat{\mu},-\mu} = j_{i,\mu}$, just as conventional in lattice gauge theory. The $j_{i,\mu}$ represent the currents of the complex scalar particle in (??). These currents must be conserved, and so we have the zero divergence condition

$$\Delta_{\mu} j_{i,\mu} = 0 \tag{2.154}$$

where Δ_{μ} is the discrete lattice derivative; this is the analog of Kirchoff's law in circuit theory. Finally, the action of the Villain model is simply [?]

$$S_V = \frac{K}{2} \sum_{i,\mu} j_{i,\mu}^2. \tag{2.155}$$

This model has a phase transition at a critical $K = K_c$, which is in the universality class of the O(2) Wilson-Fisher CFT3.

There have been extensive numerical studies of the Villain model, and sophisticated finite-size scaling methods have yielded detailed information on $\sigma(i\omega_n)$ at the Matsubara frequencies, ω_n , which are integer multiples of $2\pi T$ [?, ?, ?, ?, ?, ?]. Note especially that Monte Carlo does not yield any information at $\omega_n = 0$ (this is consequence of the structure of the Kubo formula for the conductivity, which is only defined at non-zero ω , and reaches $\omega = 0$ by a limiting process). So the smallest possible frequency at which we can determine the conductivity is $2\pi Ti$. The results at these, and higher Matsubara frequencies are all found [?] to be in excellent agreement with OPE expansion in (??). So the conclusion is that the quantum Monte Carlo results are essentially entirely in the large ω regime, where the results of the OPE also apply. The simulations can therefore help determine the values of the numerical constants $b_{1,2}$ in (??). While this agreement is encouraging, the somewhat disappointing conclusion is that quantum Monte Carlo does not yield any more direct information on the low frequency behavior than is available from the OPE.

Holographic spectral functions

In the next few sections we will cover holographic computations of the retarded Green's functions for operators in quantum critical systems at nonzero temperature. In general we will be interested in multiple coupled operators and so we write, in frequency space,

$$\delta \langle \mathcal{O}_A \rangle (\omega, k) = G_{\mathcal{O}_A \mathcal{O}_B}^R(\omega, k) \delta h_B(\omega, k). \tag{2.156}$$

Here $\delta\langle\mathcal{O}_A\rangle$ is the change in the expectation value of the operator \mathcal{O}_A due to the (time and space dependent) change in the sources δh_B . From the holographic dictionary discussed in previous sections, we know that expectation values and sources are given by the near boundary behavior of the bulk fields $\{\phi_A\}$ dual to the operators $\{\mathcal{O}_A\}$. Therefore

$$G_{\mathcal{O}_A \mathcal{O}_B}^R = \frac{\delta \langle \mathcal{O}_A \rangle}{\delta h_B} = \frac{2\Delta - D_{\text{eff.}}}{L^z} \frac{\delta \phi_{A(1)}}{\delta \phi_{B(0)}}.$$
 (2.157)

Here $\phi_{(0)}$ and $\phi_{(1)}$ are as defined in (??) above. The near boundary behavior of the fields has the same form at zero and nonzero temperature because, as we saw in §?? above, putting a black hole in the spacetime changes the geometry in the interior (IR), but not near the boundary (UV).

To compute the Green's function (??) in a given background, one first perturbs the background fields

$$\phi_A(r) \mapsto \phi_A(r) + \delta\phi_A(r)e^{-i\omega t + ik \cdot x}$$
 (2.158)

Linearizing the bulk equations of motion leads to coupled, linear, ordinary differential equations for the perturbations $\delta \phi_A(r)$. Once these linearized equations are solved, the asymptotic behavior of fields can

be read off from the solutions and the Green's function obtained from (??). A crucial part of solving the equations for the perturbations is to impose the correct boundary conditions at the black hole horizon. One way to understand these boundary conditions is to recall that the retarded Green's function is obtained from the Euclidean (imaginary time) Green's function by analytic continuation from the upper half frequency plane (i.e. $\omega_n > 0$). An important virtue of the holographic approach is that this analytic continuation can be performed in a very efficient way, as we now describe.

Infalling boundary conditions at the horizon

Starting with the Euclidean black hole spacetime (??), we described how to zoom in on the spacetime near the horizon in the manipulations following equation (??). To see how fields behave near the horizon, we can consider the massive wave equation in the black hole background (??) at $r \sim r_+$. The equation becomes

$$\phi'' + \frac{1}{r - r_{+}} \phi' - \frac{\omega_{n}^{2}}{(4\pi T)^{2} (r - r_{+})^{2}} \phi = 0.$$
 (2.159)

The temperature T is as given in (??). The two solutions to this equation are

$$\phi_{\pm} = (r - r_{+})^{\pm \omega_{n}/(4\pi T)} \ . \tag{2.160}$$

For $\omega_n > 0$, it is clear that the regular solution is the one that decays as $r \to r_+$ (that is, the positive sign in the above equation). Once this condition is imposed on all fields, the solution is determined up to overall an overall constant, which will drop out upon taking the ratios in (??) to compute the Green's function.

The real time equations of motion are the same as the Euclidean equations, with the substitution $i\omega_n \to \omega$. In particular, the regular boundary condition at the horizon analytically continues to the "infalling" boundary condition

$$\phi_{\text{infalling}} = (r - r_+)^{-i\omega/(4\pi T)} . \qquad (2.161)$$

This behavior at the horizon can also be derived directly from the real time, Lorentzian, equations of motion. Infalling modes are required for regularity in the Kruskal coordinates that extend the black hole spacetime across the horizon (see e.g. [?]). The derivation via the Euclidean modes makes clear, however, that infalling boundary conditions correspond to computing the retarded Green's function.

 expansions, in which $\omega \to 0$ and $N \to \infty$ do not commute at nonzero temperatures, as we explained above. Infalling modes have an energy flux into the horizon that is lost to an exterior observer. The black hole horizon has geometrized the irreversibility of entropy production. Physically, energy crossing the horizon has dissipated into the 'order N^2 ' degrees of freedom of the deconfined gauge theory.

Infalling boundary conditions were first connected to retarded Green's function in [?]. We derived the infalling boundary condition from the Euclidean Green's function. An alternative derivation of this boundary condition starts from the fact that the fully extended Penrose diagram of (Lorentzian) black holes has two boundaries, and that these geometrically realize the thermofield double or Schwinger-Keldysh approach to real time thermal physics [?, ?].

Example: spectral weight $\operatorname{Im} G^R_{\mathcal{OO}}(\omega)$ of a large dimension operator

We will now illustrate the above with a concrete example. We will spell out here in some detail steps that we will go over more quickly in later cases. To start with we will put k = 0 and obtain the dependence of the Green's function on frequency. The scalar wave equation (??) in the Lorentzian signature black hole background becomes

$$\phi'' + \left(\frac{f'}{f} - \frac{z+d-1}{r}\right)\phi' - \frac{1}{f}\left(\frac{(mL)^2}{r^2} - \frac{r^{2z}\omega^2}{r^2f}\right)\phi = 0.$$
 (2.162)

To develop an intuition for an equation like the above, it is often useful to put the equation into a Schrödinger form. To do this we set $\phi = r^{d/2}\psi$, so that (??) becomes

$$-\frac{f}{r^{z-1}}\frac{d}{dr}\left(\frac{f}{r^{z-1}}\frac{d}{dr}\psi\right) + V\psi = \omega^2\psi.$$
 (2.163)

If we define r_* such that $\partial_{r_*} = r^{1-z} f \partial_r$, we immediately recognize the above equation as the time-independent Schrödinger equation in one spatial dimension. All the physics is now contained in the Schrödinger potential

$$V(r) = \frac{f}{r^{2z}} \left((Lm)^2 + \frac{d(d+2z)f}{4} - \frac{drf'}{2} \right).$$
 (2.164)

The Schrödinger equation (??) is to be solved subject to the following boundary conditions. We will discuss first the near-horizon region, $r \to r_+$. The Schrödinger coordinate $r_* = \int dr \left(r^{z-1}/f\right) \to \infty$ as $r \to r_+$, so this is a genuine asymptotic region of the Schrödinger equation. The potential (??) vanishes on the horizon because $f(r_+) = 1$. Therefore for any $\omega^2 > 0$, recall that ω^2 plays the role of the energy in the Schrödinger equation (??), the solution oscillates near the horizon. The infalling boundary condition is thus seen to translate into the boundary condition that modes are purely outgoing as $r_* \to \infty$. This is a scattering

boundary condition of exactly the sort one finds in elementary one dimensional scattering problems.

The boundary at r=0 is not an asymptotic region of the Schrödinger equation. There will be normalizable and non-normalizable behaviors of ϕ as $r \to 0$. To compute the Green's function we will need to fix the coefficient of the non-normalizable mode and solve for the coefficient of the normalizable mode.

A key physical quantity is the imaginary part of the retarded Green's function of the operator \mathcal{O} dual to ϕ (also called the spectral weight). The imaginary part of the retarded Green's function is a direct measure of the entropy generated when the system is subjected to the sources δh_B of equation (??). Specifically, with an assumption of time reversal invariance (see e.g. [?]), the time-averaged rate of work done on the system per unit volume by a spatially homogeneous source driven at frequency ω is given by

$$\frac{\overline{dw}}{dt} = \omega \delta h_A^* \operatorname{Im} G_{AB}^R(\omega) \delta h_B \ge 0.$$
 (2.165)

We now illustrate how this spectral weight is given by the amplitude with which the field can tunnel from the boundary r = 0 through to the horizon. Thus, we will exhibit the direct connection between dissipation in the dual QFT and rate of absorption by the horizon.

The analysis is simplest in the limit of large $mL \gg 1$. Recall that this corresponds to an operator \mathcal{O} with large scaling dimension. In this limit the equation (??) can be solved in a WKB approximation. In the large mass limit, the potential (??) typically decreases monotonically from the boundary towards the horizon. There is therefore a unique turning point r_o at which $V(r_o) = \omega^2$. The infalling boundary condition together with standard WKB matching formulae give the solution

$$\psi = \begin{cases}
\exp\left\{i \int_{r_o}^r \frac{r^{z-1}dr}{f} \sqrt{\omega^2 - V(r)} - \frac{i\pi}{4}\right\} & r_+ > r > r_o, \\
\exp\left\{\int_{r}^{r_o} \frac{r^{z-1}dr}{f} \sqrt{V(r) - \omega^2}\right\} + \frac{i}{2} \exp\left\{-\int_{r}^{r_o} \frac{r^{z-1}dr}{f} \sqrt{V(r) - \omega^2}\right\} & r_0 > r.
\end{cases}$$
(2.166)

In this limit $V = (mL)^2 f/r^{2z}$. Expanding the above solution near the $r \to 0$ boundary, the retarded Green's function is obtained from the general formula (??). In particular, the imaginary part is given by

$$\chi''(\omega) \equiv \operatorname{Im} G_{\mathcal{O}\mathcal{O}}^{R}(\omega) \tag{2.167}$$

$$\propto r_o^{-2mL} \exp\left\{-2\int_0^{r_o} \frac{dr}{r} \left(\sqrt{\frac{(mL)^2}{f} - \frac{r^{2z}\omega^2}{f^2}} - mL\right)\right\}$$
 (2.168)

= Probability for quanta of ϕ to tunnel from boundary into the near horizon region ('transmission probability'). From the above expression the expected limits of high and low frequency are immediately obtained. Note that for $\omega r_+^z \ll 1$ then $r_o \sim r_+$, whereas for $\omega r_+^z \gg 1$, $r_o \sim \omega^{-1/z}$. Thus

$$\chi''(\omega) \sim \begin{cases} \omega^{2\Delta/z} & \omega \gg T, \\ T^{2\Delta/z} & \omega \ll T. \end{cases}$$
 (2.169)

On general grounds χ'' must be an odd function of ω . This can be seen in a more careful WKB computation that includes the order one prefactor. Relatedly, to obtain (??) we used the fact that the scaling dimension (??) is given by $\Delta = mL$ in the limit $mL \gg 1$. We also used the expression (??) for the temperature. The full result (??) gives an explicit and relatively simple crossover between these two limits.

More generally, the equation $(\ref{equation})$ can easily be solved numerically. Later we will give an example of the type of Mathematica code one uses to solve such equations. We should note, however, that for general values of Δ (e.g. not integer, etc.) the boundary conditions often need to be treated to a very high accuracy to get stable results, as discussed in e.g [?]. Also, one should be aware that when the fast and slow falloffs differ by an integer, one can find logarithmic terms in the near boundary expansion. These must also be treated with care and, of course, correspond to the short distance logarithmic running of couplings in the dual QFT that one expects in these cases.

Infalling boundary conditions at zero temperature

In equation (??) above we obtained the infalling boundary condition for finite temperature horizons. Zero temperature geometries that are not gapped will also have horizons in the far interior (or, more generally, as we noted in our discussion of Lifshitz geometries in §?? above, mild null singularities). To compute the retarded Green's function from such spacetimes we will need to know how to impose infalling boundary conditions in these cases. This is done as before, by analytic continuation of the Euclidean mode that is regular in the upper half complex frequency plane. It is not always completely straightforward to find the leading behavior of solutions to the wave equation near a zero temperature horizon, especially when there are many coupled equations. The following three examples illustrate common possibilities. In each case we give the leading solution to $\nabla^2 \phi = m^2 \phi$ near the horizon.

1. Poincaré horizon. Near horizon metric (as $r \to \infty$):

$$ds^{2} = L^{2} \left(\frac{-dt^{2} + dr^{2} + d\vec{x}_{d}^{2}}{r^{2}} \right).$$
 (2.170)

Infalling mode as $r \to \infty$ and with $\omega^2 > k^2$

$$\phi_{\text{infalling}} = r^{d/2} e^{ir\sqrt{\omega^2 - k^2}}.$$
 (2.171)

2. Extremal AdS_2 charged horizon. Near horizon metric (as $r \to \infty$):

$$ds^{2} = L^{2} \left(\frac{-dt^{2} + dr^{2}}{r^{2}} + d\vec{x}_{d}^{2} \right).$$
 (2.172)

Infalling mode as $r \to \infty$

$$\phi_{\text{infalling}} = e^{i\omega r} \,. \tag{2.173}$$

3. Lifshitz 'horizon'. Near horizon metric (as $r \to \infty$):

$$ds^{2} = L^{2} \left(\frac{-dt^{2}}{r^{2z}} + \frac{dr^{2} + d\vec{x}_{d}^{2}}{r^{2}} \right). \tag{2.174}$$

Infalling mode as $r \to \infty$, with z > 1,

$$\phi_{\text{infalling}} = r^{d/2} e^{i\omega r^z/z} \,. \tag{2.175}$$

Finally, occasionally one wants to find the Green's function directly at $\omega = 0$ (for instance, in our discussion of thermal screening around (??) above). The equations at $\omega = 0$ typically exhibit two possible behaviors near the horizon, one divergent and the other regular. At finite temperature the divergence will be logarithmic. Clearly one should use the regular solution to compute the correlator.

Quantum critical charge dynamics

So far we have discussed scalar operators \mathcal{O} as illustrative examples. However, a very important set of operators are instead currents J^{μ} associated to conserved charges. The retarded Green's functions of current operators capture the physics of charge transport in the quantum critical theory. We explained around equation (??) above that a conserved U(1) current J^{μ} in the boundary QFT is dually described by a Maxwell field A_a in the bulk. Therefore, to compute the correlators of J^{μ} , we need an action that determines the bulk dynamics of A_a .

Conductivity from the dynamics of a bulk Maxwell field

As we are considering zero density quantum critical matter in this section, we restrict to situations where the Maxwell field is not turned in the background (we will relax this assumption in §?? below). Therefore, in order to obtain linear response functions in a zero density theory, it is sufficient to consider a quadratic action for the Maxwell field about a fixed background. The simplest such action is the Maxwell action (with F = dA, as usual)

$$S[A] = -\frac{1}{4e^2} \int d^{d+2}x \sqrt{-g} F^2, \qquad (2.176)$$

so we will start with this. We noted in §?? that Einstein-Maxwell theory can be obtained as a consistent truncation of explicit bulk theories with known QFT duals.

Before obtaining the Maxwell equations we should pick a gauge. A very useful choice for many purposes in holography is the 'radial gauge', in which we put $A_r = 0$. Among other things, the bulk Maxwell field in this gauge has the same nonzero components as the boundary current operator J^{μ} . The Maxwell equations about a black hole geometry of the form (??) can now be written out explicitly. Firstly, write the Maxwell field as

$$A_{\mu} = a_{\mu}(r)e^{-i\omega t + ikx}, \qquad (2.177)$$

where without loss of generality we have taken the momentum to be in the x direction. The equations of motion, $\nabla_a F^{ab} = 0$, become coupled ordinary differential equations for the $a_{\mu}(r)$. By considering the discrete symmetry $y \to -y$ of the background, where y is a boundary spatial dimension orthogonal to x, we immediately see that the perturbation will decouple into longitudinal $(a_t \text{ and } a_x)$ and transverse (a_y) modes. It is then useful to introduce the following 'gauge invariant' variables [?], that are invariant under a residual gauge symmetry $A_{\mu} \to A_{\mu} + \partial_{\mu} [\lambda e^{-i\omega t + ikx}]$,

$$a_{\perp}(r) = a_y(r), \qquad a_{\parallel}(r) = \omega a_x(r) + ka_t(r).$$
 (2.178)

In terms of these variables, the Maxwell action becomes:

$$S = -\frac{L^{d-2}}{2e^2} \int dr \left[fr^{3-d-z} a_{\perp}^{\prime 2} + a_{\perp}^2 \left(k^2 r^{3-d-z} - \frac{\omega^2 r^{z+1-d}}{f} \right) + \frac{fr^{3-d-z}}{\omega^2 - k^2 f r^{2-2z}} a_{\parallel}^{\prime 2} - \frac{r^{z+1-d}}{f} a_{\parallel}^2 \right]$$
(2.179)

leading to the following two decoupled second order differential equations

$$\left(\frac{fr^{3-d-z}}{\omega^2 - k^2 fr^{2-2z}} a'_{\parallel}\right)' = -\frac{r^{z+1-d}}{f} a_{\parallel}, \qquad (2.180)$$

$$(fr^{3-d-z}a'_{\perp})' = k^2r^{3-d-z}a_{\perp} - \frac{\omega^2r^{z+1-d}}{f}a_{\perp}.$$
 (2.181)

When k = 0 the transverse and longitudinal equations are the same, as we should expect. These equations with z = 1 have been studied in several important papers [?, ?, ?, ?], sometimes using different notation.

Near the boundary at $r \to 0$, the asymptotic behavior of a_{μ} is given by:

$$a_t = a_t^{(0)} + a_t^{(1)} r^{d-z} + \cdots,$$
 (2.182a)

$$a_i = a_i^{(0)} + a_i^{(1)} r^{d+z-2} + \cdots$$
 (2.182b)

Note that when $z \neq 1$, as expected, the asymptotic falloffs are different for the timelike and spacelike components of a_{μ} . So long as d > z, it is straightforward to add boundary counterterms to make the bulk action finite. We can then, using the general formalism developed previously, obtain the expectation values for the charge and current densities:

$$\langle J^t \rangle = -\frac{L^{d-2}}{e^2} (d-z) a_t^{(1)},$$
 (2.183a)

$$\langle J^i \rangle = \frac{L^{d-2}}{e^2} (d+z-2) a_i^{(1)}.$$
 (2.183b)

If instead d < z, the 'subleading' term in (??) is in fact the largest term near the boundary. This leads to many observables having a strong dependences on short distance physics, we will see an example shortly when we compute the charge diffusivity. A closely related fact is that when d < z there is a relevant (double trace) deformation to the QFT given by $\int d^{d+1}x \, n^2$. As discussed in section ?? above, and first emphasized in [?], this deformation will generically drive a flow to a new fixed point in which the role of $a_t^{(0)}$ and $a_t^{(1)}$ are exchanged. The physics of such a theory is worth further study, as there are known examples (nematic or ferromagnetic critical points in metals, at least when treated at the 'Hertz-Millis' mean field level [?, ?]) of d = 2 and z = 3.

A quantity of particular interest is the frequency dependent conductivity

$$\sigma(\omega) = \frac{\langle J_x(\omega) \rangle}{E_x(\omega)} = \frac{\langle J_x(\omega) \rangle}{i\omega a_x^{(0)}(\omega)} = \frac{G_{J_xJ_x}^R(\omega)}{i\omega}. \tag{2.184}$$

As we have noted above, the dissipative (real) part of the conductivity will control entropy generation due to Joule heating when a current is driven through the system. We shall compute the optical conductivity (??) shortly, but first consider the physics of certain low energy limits.

The dc conductivity

The dc conductivity

$$\sigma = \lim_{\omega \to 0} \, \sigma(\omega) \,, \tag{2.185}$$

determines the dissipation (??) due to an arbitrarily low frequency current being driven through the system. It should therefore be computable in an effective low energy description of the physics. Following our discussion of Wilsonian holographic renormalization in §??, this means that we might hope to obtain the dc conductivity from a computation in purely the near-horizon, far interior, part of the spacetime. Indeed this is the case. We will follow a slightly modernized (in the spirit of [?]) version of the logic in [?], which in turn built on [?]. The upshot is the formula (??) below for the dc conductivity which is expressed purely in terms of data at the horizon itself.

The dc conductivity can be obtained by directly applying a uniform electric field, rather than taking the $k, \omega \to 0$ limit of (??). Consider the bulk Maxwell potential

$$A = (-Et + a_x(r))\mathrm{d}x. \tag{2.186}$$

Given the near boundary expansion (??), the QFT source term is given by the non-normalizable constant term $a_x^{(0)}$ of the bulk field near the boundary $r \to 0$. The boundary electric field is then obtained from (??) as $E = -\partial_t a_x^{(0)} = -F_{tx}(r \to 0)$, and is uniform. To obtain the dc conductivity we must now determine the uniform current response.

The bulk Maxwell equations can be written as $\partial_a(\sqrt{-g}F^{ab}) = 0.8$ For the field (??) one immediately has that

$$\partial_r \left(\sqrt{-g} F^{rx} \right) = 0. \tag{2.187}$$

We have thereby identified a radially conserved quantity. Furthermore, near the boundary

$$\lim_{r \to 0} \sqrt{-g} F^{rx} = L^{d-2} (d+z-2) a_x^{(1)} = e^2 \langle J_x \rangle.$$
 (2.188)

Here we used the near boundary expansion (??), as well as (??) to relate $\langle J_x \rangle$ to $a_x^{(1)}$.

From (??) and (??) it follows that we can obtain the field theory current response $\langle J_x \rangle$ if we are able to evaluate $\sqrt{-g}F^{rx}$ at any radius. It turns out that we can compute it at the horizon. It is a standard trick that physics near black hole horizons is often elucidated by going to infalling coordinates; so we replace t in

⁸For vectors and antisymmetric tensors, covariant derivatives $\nabla_a X^{a\cdots} = (-g)^{-1/2} \partial_a (\sqrt{-g} X^{a\cdots})$.

favor of the 'infalling Eddington-Finkelstein coordinate' v by

$$v = t + \int \frac{\sqrt{g_{rr}}dr}{\sqrt{-g_{tt}}}.$$
 (2.189)

It is easily seen that the (Lorentzian version of the) black hole spacetime (??) is regular at $r = r_+$ in the coordinates $\{v, r, \vec{x}\}$. Therefore, a regular mode should only depend on t and r through the combination v. It follows that, at the horizon,

$$\partial_r A_x \Big|_{r=r_+} = -\sqrt{\frac{g_{rr}}{-g_{tt}}} \partial_t A_x \Big|_{r=r_+}. \tag{2.190}$$

This is exactly the maneuver we used in equation (??) to obtain the 'membrane paradigm' conductivity of an event horizon. We find that

$$a_x'(r_+) = \frac{r_+^{z-1}}{f} E. (2.191)$$

We are now able to compute the conductivity by evaluating

$$\sigma = \frac{\langle J_x \rangle}{E} = \frac{1}{e^2} \lim_{r \to r_+} \sqrt{-g} g^{rr} g^{xx} a_x'(r) = \frac{L^{d-2}}{e^2} \left(f r_+^{3-d-z} \right) \frac{r_+^{z-1}}{f} = \frac{L^{d-2}}{e^2} r_+^{2-d} . \tag{2.192}$$

Using the relation (??) between r_+ and T, we obtain

$$\sigma \sim T^{(d-2)/z}. (2.193)$$

Various comments are in order:

- 1. Equation (??) is an exact, closed form expression for the dc conductivity that comes from evaluating a certain radially conserved quantity at the horizon.
- 2. The temperature scaling of the conductivity is precisely that expected for a quantum critical system (without hyperscaling violation or an anomalous dimension for the charge density operator) [?].
- 3. The derivation above generalizes easily to more complicated quadratic actions for the Maxwell field, such as with a nonminimal coupling to a dilaton [?].
- 4. Infalling boundary conditions played a crucial role in the derivation, connecting with older ideas of the 'black hole membrane paradigm' discussed in §?? above [?, ?]. Once again: this boundary condition is the origin of nontrivial dissipation in holography.

The same argument given above, applied to certain perturbations of the bulk metric rather than a bulk Maxwell field, gives a direct proof of a famous result for the shear viscosity η over entropy density s in a

large class of theories with classical gravity duals [?]:

$$\frac{\eta}{s} = \frac{1}{4\pi} \,. \tag{2.194}$$

Here η plays an analogous role to the dc conductivity σ in the argument above. The shear viscosity was first computed for holographic theories in [?] and the ratio above emphasized in [?, ?].

Diffusive limit

The longitudinal channel includes fluctuations of the charge density. Because the total charge is conserved, this channel is expected to include a collective diffusive mode [?]. This fact is why the longitudinal equation (??) is more complicated than the transverse equation (??). It is instructive to see how the diffusive mode can be explicitly isolated from (??). We will adapt the argument in [?].

Diffusion is a process that will occur at late times and long wavelengths if we apply a source to the system to set up a nontrivial profile for the charge density, turn off the source, and then let the system evolve. Therefore diffusion should appear as a mode in the system that (i) satisfies infalling boundary conditions at the horizon and (ii) has no source at the asymptotic boundary. We will see in §?? below that these are the conditions that define a so-called quasinormal mode, which correspond precisely to the poles of retarded Green's functions in the complex frequency plane. More immediately, we must solve the longitudinal equation (??) with these boundary conditions, and in the limit of small frequency and wavevector.

We cannot simply take the limit $\omega \to 0$ of the longitudinal equation (??). This is because taking $\omega \to 0$ in this equation does not commute with the near horizon limit $r \to r_+$, at which $f \to 0$. As we take the low frequency limit, we need to ensure that the infalling boundary condition as $r \to r_+$ is correctly imposed. This can be achieved by writing

$$a_{\parallel}(r) = f(r)^{-i\omega/(4\pi T)} S(r)$$
. (2.195)

By extracting the infalling behavior (??) in this way, the equation satisfied by S will no longer have a singular point at the horizon. S must tend to a constant at the horizon. We can therefore safely expand S in $\omega, k \to 0$. We do this by setting $\omega = \epsilon \hat{\omega}$ and $k = \epsilon \hat{k}$ and then expanding in small ϵ . With a little benefit of hindsight [?], we look for a solution of the form

$$S(r) = \epsilon \,\hat{\omega} + \epsilon^2 s(r) + \cdots \,. \tag{2.196}$$

The resulting differential equation for s, to leading order as $\epsilon \to 0$, can be integrated explicitly. The solution

that is regular at the horizon is

$$s(r) = -\int_{r}^{r_{+}} \frac{dr'}{f(r')} \left[\frac{i\hat{\omega}^{2} f'(r')}{4\pi T} - \frac{ir'^{d-3-z} f'(r_{+})}{4\pi T r_{+}^{d-3+z}} \left(\hat{\omega}^{2} r'^{2z} - \hat{k}^{2} f(r') r'^{2} \right) \right]. \tag{2.197}$$

To isolate the diffusive regime, consider $\omega \sim k^2$. This corresponds to taking $\hat{\omega}$ small. In this regime we can ignore the $\hat{\omega}^2$ terms in (??). We had to keep these terms in the first instance in order to impose the regularity condition at the horizon and fix a constant of integration in the solution (??). The full solution to the order we are working can now be written

$$S(r) = \omega + \frac{ik^2}{r_+^{d-2}} \int_r^{r_+} r'^{d-z-1} dr'.$$
 (2.198)

Here we used (??) to write $f'(r_+) = -4\pi T r_+^{z-1}$. The remaining boundary condition to impose is the absence of a source $a_{\parallel}^{(0)}$ in the near boundary expansion (??) of the Maxwell field. Thus we require S(0) = 0. Imposing this condition on (??) we obtain a diffusive relationship between frequency and wavevector:

$$\omega = -iDk^2, \qquad D = \frac{r_+^{2-z}}{d-z}.$$
 (2.199)

This is the anticipated diffusive mode. Some comments on this result:

- 1. Beyond finding the diffusive mode (??), one can also find the full diffusive part of the longitudinal channel retarded Green's functions, giving a density Green's function of the form (??), as was originally done in [?, ?].
- 2. The diffusion constant in (??), unlike the dc conductivity (??), is not given purely in terms of horizon data. To find the diffusive mode we had to explicitly solve the Maxwell equations everywhere. This is an example of the phenomenon of semi-holography mentioned in our discussion of Wilsonian holographic renormalization in §??. Because there is only one diffusive mode compared to the many (order N^2) gapless modes of the IR theory, the diffusive mode is 'not powerful' enough to backreact on the dynamics of the IR fixed point theory. To some extent this is an artifact of the large N limit of holography. The consequence is that the diffusive mode is not fully described by the dynamics of the event horizon, but is rather a quasinormal mode in its own right, with support throughout the spacetime. A holographic Wilsonian discussion of the diffusive mode can be found in [?, ?, ?].
- 3. When d < z, the diffusivity is UV divergent and (??) no longer holds [?]. This gives an extreme illustration of the previous comment: in this case the diffusivity is dominated by non-universal short

distance physics, even while the dc conductivity (??) is captured by the universal low energy dynamics of the horizon.

4. A basic property of diffusive processes is the Einstein relation $\sigma = \chi D$, where χ is the charge susceptibility (compressibility). The susceptibility is obtained from the static, homogeneous two point function of a_t . The easiest way to do this is to show that the following a_t perturbation solves the linearized Maxwell equations (with $\omega = 0$):

$$a_t = \mu \left(1 - \frac{r^{d-z}}{r_+^{d-z}} \right),$$
 (2.200)

where μ is a small chemical potential. The susceptibility is given by $\partial_{\mu}n(\mu,T)$ as $\mu \to 0$. Combining $(\ref{eq:condition})$ and $(\ref{eq:condition})$, and using $\langle J^t \rangle = n$ we find

$$\chi = \frac{L^{d-2}}{e^2} \frac{d-z}{r_+^{d-z}}. (2.201)$$

It is immediately verified from (??), (??) and (??) that the Einstein relation holds.

$\sigma(\omega)$ part I: Critical phases

We have emphasized in section ?? and in equation (??) above that the real part of the frequency-dependent conductivity at zero momentum (k = 0)

$$\operatorname{Re}\sigma(\omega) = \frac{\operatorname{Im}G_{J_xJ_x}^R(\omega)}{\omega}, \qquad (2.202)$$

is a direct probe of charged excitations in the system as a function of energy scale. We also emphasized that this quantity is difficult to compute in strongly interacting theories using conventional methods, whereas it is readily accessible holographically. Two key aspects of the holographic computation are firstly the possibility of working directly with real-time frequencies, via the infalling boundary conditions discussed in section ??, and secondly the fact that dissipation occurs at leading, classical, order in the 't-Hooft large N expansion, and that in particular the $N \to \infty$ and $\omega \to 0$ limits commute for the observable (??).

Consider first a bulk Maxwell field in a scaling geometry with exponent z as discussed in section ?? above. Putting k = 0 in the equations of motion (??) or (??) for the Maxwell potential leads leads to

$$(fr^{3-d-z}a_x')' = -\frac{\omega^2 r^{z+1-d}}{f} a_x.$$
 (2.203)

We must solve this equation subject to infalling boundary conditions at the horizon. Given the solution, equations (??) and (??) for the near-boundary behavior of the field imply that the conductivity (??) will be

given by

$$\sigma(\omega) = \frac{L^{d-2}}{e^2} \frac{1}{i\omega} \lim_{r \to 0} \frac{1}{r^{d+z-3}} \frac{a'_x}{a_r}.$$
 (2.204)

The equation (??) can be solved explicitly in two boundary space dimensions, d = 2. This is the most interesting case, in which the conductivity is dimensionless. The solution that satisfies infalling boundary conditions is

$$a(r) = \exp\left(i\omega \int_0^r \frac{s^{z-1}ds}{f(s)}\right). \tag{2.205}$$

The overall normalization is unimportant. It follows immediately from the formula for the conductivity (??), using only the fact that at the boundary f(0) = 1, that

$$\sigma(\omega) = \frac{1}{e^2} \,. \tag{2.206}$$

In particular, there is no dependence on $\omega/T!$ In the language of section ??, this means that the, a priori distinct, constants characterizing the diffusive $(\omega \to 0)$ and zero temperature $(\omega \to \infty)$ limits are equal in this case: $\mathcal{K} = \mathcal{C}_{\chi}\mathcal{C}_{D}$, first noted in [?]. We have obtained this result for all z in d = 2. We will see in section ?? that the lack of ω dependence is due to the electromagnetic duality enjoyed by the equations of motion of the bulk 3+1 dimensional Maxwell field, which translates into a self-duality of the boundary QFT under particle-vortex duality. Meanwhile, however, this means that in order to obtain more generic results for the frequency-dependent conductivity, we will need to depart from pure Maxwell theory in the bulk.

In the remainder of this subsection, we will restrict ourselves to the important case of CFT3s. That is, we put d=2 and z=1. The discussion in section ?? showed that the existence of a relevant deformation of the quantum critical theory plays an important role in the structure of $\sigma(\omega)$, because it determines the leading correction to the constant $\omega/T \to \infty$ limit. Such an operator will always be present if the critical theory is obtained by tuning to a quantum critical point. However, a quantum critical phase, by definition, does not admit relevant perturbations. In such cases one may continue to focus on the universal sector described in the bulk by the metric and Maxwell field. It is an intriguing fact that the simplest holographic theories lead naturally to critical phases rather than critical points.

An especially simple deformation of Maxwell theory that does not introduce any additional bulk fields is given by the action

$$S[A] = \frac{1}{e^2} \int d^4x \sqrt{-g} \left(-\frac{1}{4} F^2 + \gamma L^2 C_{abcd} F^{ab} F^{cd} \right). \tag{2.207}$$

Here $C_{abcd} = R_{abcd} - (g_{a[c}R_{d]b} - g_{b[c}R_{d]a}) + \frac{1}{3}g_{a[c}g_{d]b}$ is the Weyl curvature tensor. There is a new bulk coupling constant γ . Aspects of transport in this theory have been studied in [?, ?, ?, ?, ?]. The theory

(??) has several appealing features. In particular, it is still second order in derivatives of the Maxwell field. Therefore the formalism we have described in the last few sections for computing conductivities does not need to be modified. As we are interested in linear response around a zero density background (that is, with no Maxwell field turned on), for the present purposes it is sufficient to consider actions quadratic in the field strength and evaluated in geometric backgrounds that solve the vacuum Einstein equations (??). The action (??) is the unique such deformation of Maxwell theory that is of fourth order in derivatives of the metric and field strength, see e.g. [?, ?]. The reason to limit the number of total derivatives is that we can then imagine that the new term in (??) is the leading correction to Einstein-Maxwell theory in a bulk derivative expansion. Indeed, such terms will be generated by stringy or quantum effects in the bulk. See the references just cited for entry points into the relevant literature on higher derivative corrections in string theory. The effects on the optical conductivity of terms that are higher order yet in derivatives than those in (??) were studied e.g. [?, ?].

A word of caution is necessary before proceeding to compute in the theory (??). Generically, the bulk derivative expansion will only be controlled if the coupling constant γ is parametrically small. Considering a finite nonzero γ while neglecting other higher derivative terms requires fine tuning that may not be possible in a fully consistent bulk theory. Remarkably, it can be shown, both from the bulk and also from general QFT arguments, that consistency requires [?, ?, ?, ?, ?]

$$|\gamma| \le \frac{1}{12} \,. \tag{2.208}$$

In the concrete model (??) we will see shortly that this bound has the effect of bounding the dc conductivity. However, physically speaking, and thinking of (??) as representative of a broader class of models, the bound (??) is a statement about short rather than long time physics [?, ?, ?]. In particular, γ is directly related to the b_2 coefficient that appears in the large frequency expansion (??) of the conductivity. As we have stressed, the b_1 term in (??) is absent in quantum critical phases. Thus the b_2 term is the leading correction to the asymptotic constant result, although it is pure imaginary and therefore not immediately relevant for sum rules. Specifically, for the class of theories (??) one can show that as $\omega \to \infty$ [?]

$$\sigma(\omega) = \frac{1}{e^2} \left(1 - i \frac{\gamma}{9} \left(\frac{4\pi T}{\omega} \right)^3 + \frac{\gamma(15 + 38\gamma)}{324} \left(\frac{4\pi T}{\omega} \right)^6 + \cdots \right). \tag{2.209}$$

This expansion is obtained by solving (??) below in a WKB expansion. A slight correction to the $1/\omega^6$ term has been made.

Satisfying the bound (??) by no means guarantees that the bulk theory is a classical limit of a well defined

theory of quantum gravity. However, it does mean that no pathology will arise at the level of computing the retarded Green's function for the current operator in linear response theory. Therefore, we can go ahead and use the theory (??) as tool to generate Green's functions that are consistent with all necessary CFT axioms, that satisfy both of the sum rules (??) and (??), and for which we know the parameter b_2 appearing in the large frequency expansion (??).

The equations of motion for the Maxwell potential A following from (??) are easily derived. The background geometry will be the AdS-Schwarzschild spacetime (i.e. the metric (??) with emblackening factor (??), with z = 1, $\theta = 0$ and d = 2). As above, the perturbation takes the form $A = a_x(r)e^{-i\omega t}dx$. The Weyl tensor term in the action (??) changes the previous equation of motion (??) to [?]

$$a_x'' + \left(\frac{f'}{f} + \gamma \frac{12r^2}{r_+^3 + 4\gamma r^3}\right) a_x' + \frac{\omega^2}{f^2} a_x = 0.$$
 (2.210)

The only effect of the coupling γ is to introduce the second term in brackets. To obtain this equation of motion, one should use a Mathematica package that enables simple computation of curvature tensors (such as the Weyl tensor). Examples are the RGTC package or the diffgeo package, both easily found online.

Near the boundary, the spacetime approaches pure AdS_4 , which has vanishing Weyl curvature tensor, and hence the new term in the action (??) does not alter the near boundary expansions of the fields. Therefore, from a solution of the equation of motion (??), with infalling boundary conditions at the horizon, the conductivity is again given by (??). The following Mathematica code solves equation (??) numerically. The output is plots of the conductivity $\sigma(\omega)$ for different values of γ . These plots are shown in figure ?? below. In performing the numerics, it is best to rescale the coordinates and frequencies by setting $r = r_+ \hat{r}$ and $\omega = \hat{\omega}/r_+$. In this way one can put the horizon radius at $r_+ = 1$ in doing calculations. Recall that $r_+ = 3/(4\pi T)$ according to (??). We must remember to restore the factor of r_+ in presenting the final result.

% emblackening factor of background metric

$$fs[r_{-}] = 1 - r^3;$$

% equation of motion

eq[
$$\omega_-$$
, γ_-] = Ax''[r] + $\omega^2/f[r]^2$ Ax[r] + f'[r]/f[r] Ax'[r]

+ (12r^2
$$\gamma$$
 Ax'[r])/(1+4r^3 γ) /.f \rightarrow fs;

% series expansion of Ax near the horizon. Infalling boundary conditions

$$\text{Axnh}[r_-, \omega_-, \gamma_-] = (1-r)^{(-i\omega/3)} (1 + ((3+8\gamma(6-i\omega)-2i\omega)\omega)/(3(1+4\gamma)(3i+2\omega))(1-r));$$

% series expansion of Ax'

$$\texttt{Axnhp}[\texttt{r}_-\,,\omega_-\,,\gamma_-] \ = \ \texttt{D}[\texttt{Axnh}[\texttt{r}\,,\omega\,,\gamma]\,,\texttt{r}]\,;$$

Figure 17: Frequency-dependent conductivity computed from the bulk theory (??). From bottom to top, γ is increased from -1/12 to +1/12.

Figure ?? shows that for γ nonzero, the conductivity acquires a nontrivial frequency dependence. This was the main reason to consider the coupling to the Weyl tensor in (??), which breaks the electromagnetic self-duality of the equations of motion. To leading order in small γ , electromagnetic duality now maps

 $\gamma \to -\gamma$ [?, ?]. Furthermore we see that $\gamma > 0$ is associated to a 'particle-like' peak at low frequencies whereas $\gamma < 0$ is associated with a 'vortex-like' dip. In section ?? below we will phrase these features in terms of the location of a 'quasinormal pole' or zero in the complex frequency plane. We see in the plot that larger $|\gamma|$ results in larger deviations from the constant $\gamma = 0$ result at low frequencies. The magnitude of this deviation is limited by the bound (??) on γ . Therefore, within this simple class of strongly interacting theories, the magnitude of the 'Damle-Sachdev' [?] low frequency peak is bounded.

$\sigma(\omega)$ part II: Critical points and holographic analytic continuation

It was emphasized in [?] that in order to describe quantum critical points rather than critical phases, it is essential to include the scalar relevant operator \mathcal{O} that drives the quantum phase transition. A minimal holographic framework that captures the necessary physics was developed in [?]. The action is

$$S[g, A, \phi] = -\int d^4x \sqrt{-g} \left[\frac{1}{2\kappa^2} \left(R + \frac{6}{L^2} + (\nabla \phi)^2 + m^2 \phi^2 - 2\alpha_1 L^2 \phi C_{abcd} C^{abcd} \right) + \frac{1}{4e^2} (1 + \alpha_2 \phi) F^2 \right]. \tag{2.211}$$

Here the new bulk field ϕ is dual to the relevant operator \mathcal{O} . Relevant means that the operator scaling dimension $\Delta < 3$. The scaling dimension is determined by the mass squared m^2 according to (??) above.

The two couplings α_1 and α_2 in the theory (??) implement two important physical effects. The first, α_1 , ensures that \mathcal{O} acquires a nonzero expectation value at T > 0. This is of course generically expected for a scalar operator, but will not happen unless there is a bulk coupling that sources ϕ . Because $C_{abcd} = 0$ in the T = 0 pure AdS₄ background, this term does not source the scalar field until temperature is turned on. While the Weyl tensor thus is a very natural way to implement a finite temperature expectation value, the $C_{abcd}C^{abcd}$ term is higher order in derivatives and therefore should be treated with caution in a full theory. The second, α_2 , term ensures that there is a nonvanishing $C_{JJ\mathcal{O}}$ OPE coefficient. Both α_1 and α_2 must be nonzero for the anticiapted term to appear in the large frequency expansion of the conductivity – i.e. for the coefficient b_1 in (??) to be nonzero. Plots of the resulting frequency-dependent conductivities can be found in [?].

An exciting use of the theory (??) is as a 'machine' to analytically continue Euclidean Monte Carlo data [?, ?, ?]. The conductivity of realistic quantum critical theories such as the O(2) Wilson-Fisher fixed point can be computed reliably along the imaginary frequency axis, using Monte Carlo techniques. However, analytic continuation of this data to real frequencies poses a serious challenge, as errors are greatly amplified. One way to understand this fact is that, as we will see in section ?? shortly, the analytic structure of the

conductivity in the complex frequency plane in strongly interacting CFTs at finite temperature is very rich [?]. In particular there are an infinite number of 'quasinormal poles' extending down into the lower half frequency plane.

The conductivity of holographic models, in contrast, can be directly computed with both Euclidean signature (imposing regularity at the tip of the Euclidean 'cigar') and Lorentzian signature (with infalling boundary conditions at the horizon). Solving the holographic model thereby provides a method to perform the analytic continuation, which is furthermore guaranteed to satisfy sum rules and all other required formal properties of the conductivity. A general discussion of sum rules in holography can be found in [?]. It is found that the model (??) allows an excellent fit to the imaginary frequency conductivity of the O(2) Wilson-Fisher fixed point. The fit fixes the two parameters α_1 and α_2 in the action. The dimension Δ of the relevant operator at the Wilson-Fisher fixed point is already known and is therefore not a free parameter. Once the parameters in the action are determined, the real frequency conductivity $\sigma(\omega)$ is easily calculated numerically using the same type of Mathematica code as described in the previous subsection.

Further discussion of the use of sum rules and asymptotic expansions to constrain the frequency-dependent conductivity of realistic quantum critical points can be found in [?].

Particle-vortex duality and Maxwell duality

All CFT3s with a global U(1) symmetry have a 'particle-vortex dual' or 'S-dual' CFT3, see e.g. [?]. The name 'particle-vortex' duality can be illustrated with the following simple example. Consider a free compact boson $\theta \sim \theta + 2\pi$, with Lagrangian

$$\mathcal{L} = -\frac{1}{2}\partial_{\mu}\theta\partial^{\mu}\theta. \tag{2.212}$$

Vortices are (spatially) point-like topological defects where θ winds by $2\pi \times$ an integer, and so we write

$$\theta = \tilde{\theta} + \theta_{\text{vortex}} = \tilde{\theta} + \sum w_n \arctan \frac{y - y_n}{x - x_n}.$$
 (2.213)

Here $w_n \in \mathbb{Z}$ denotes the winding number of a vortex located at (x_n, y_n) , and $\tilde{\theta}$ smooth. We now perform a series of exact manipulations to the Lagrangian (??), understood to be inside a path integral. We begin by adding a Lagrange multiplier J^{μ} :

$$\mathcal{L} = -\frac{1}{2}J_{\mu}J^{\mu} - J^{\mu}\partial_{\mu}(\tilde{\theta} + \theta_{\text{vortex}}). \tag{2.214}$$

Now, we integrate out the smooth field $\tilde{\theta}$, which enforces a constraint $\partial_{\mu}J^{\mu}=0$. The constraint is solved by writing $2J^{\mu}=\epsilon^{\mu\nu\rho}\partial_{\nu}A_{\rho}$, and after basic manipulations we obtain

$$\mathcal{L} = -\frac{1}{4}F_{\mu\nu}F^{\mu\nu} + A^{\rho}\epsilon^{\rho\mu\nu}\partial_{\mu}\partial_{\nu}\theta_{\text{vortex}} = -\frac{1}{4}F_{\mu\nu}F^{\mu\nu} + A_{\rho}(x)\sum_{n}w_{n}\delta^{(2)}(x - x_{n})n_{n}^{\rho}, \qquad (2.215)$$

with F = dA and n_n^{ρ} a normal vector parallel to the worldine of the *n*th 'vortex'. Evidently, the compact boson is the same as a free gauge theory interacting with charged particles. The vortices have become the charged particles, which leads to the name of the duality.

Above, we see that (??) and (??) are not the same. In some cases, such as non-compact $\mathbb{C}P^1$ models [?] or supersymmetric QED3 [?], the theory is identical after the particle-vortex transformation. These theories can be called particle-vortex self-dual. We will see that the bulk Einstein-Maxwell theory (??) is also in this class, at least for the purposes of computing current-current correlators. We firstly describe some special features of transport in particle-vortex self-dual theories.

In any system with current conservation and rotational invariance, the correlation functions of the current operators may be expressed as [?]

$$G_{\mu\nu}^{\mathrm{R}}(\omega,k) = \sqrt{k^2 - \omega^2} \left[\left(\eta_{\mu\nu} - \frac{p^{\mu}p^{\nu}}{p^2} \right) K^{\mathrm{L}}(\omega,k) - \left(\delta_{ij} - \frac{k_i k_j}{k^2} \right) (K^{\mathrm{L}}(\omega,k) - K^{\mathrm{T}}(\omega,k) \right]$$
(2.216)

with $p^{\mu}=(\omega,k)$. No Lorentz invariance is assumed. K^L and K^T determine the longitudinal and transverse parts of the correlator. The second term in the above equation is defined to vanish if $\mu=t$ or $\nu=t$. In [?] it was argued that particle-vortex self-duality implies

$$K^{\mathcal{L}}K^{\mathcal{T}} = \mathcal{K}^2, \tag{2.217}$$

at all values of ω , k and temperature T. \mathcal{K} is the constant $\omega \to \infty$ value of the conductivity, as defined in section ?? above, and must be determined for the specific CFT. The key step in the argument of [?] is to note that particle-vortex duality is a type of Legendre transformation in which source and response are exchanged. This occurred in the simple example above when we introduced $2J^{\mu} = \epsilon^{\mu\nu\rho}\partial_{\nu}A_{\rho}$. When sources and responses are exchanged, the Green's functions relating them are then inverted. Self-duality then essentially requires a Green's function to be equal to its inverse, and this is what is expressed in equation (??).

Setting $k \to 0$ in the above discussion, spatial isotropy demands that $K_L(\omega) = K_T(\omega) = \sigma(\omega)$. Hence,

(??) in fact implies that for the self-dual theories:

$$\sigma\left(\frac{\omega}{T}\right) = \mathcal{K}\,,\tag{2.218}$$

for any value of $\omega/T!$

The absence of a frequency dependence in (??) mirrors what we found for Einstein-Maxwell theory in (??). Let us rederive that result from the perspective of self-duality [?]. Recall that in any background four dimensional spacetime, the Maxwell equations of motion are invariant under the exchange

$$F_{ab} \leftrightarrow G_{ab} = \frac{1}{2} \epsilon_{abcd} F^{cd} \,. \tag{2.219}$$

This is not a symmetry of the full quantum mechanical Maxwell theory partition function, as electromagnetic duality inverts the Maxwell coupling. However, all we are interested in here are the equations of motion. To see how (??) acts on the function $\sigma(\omega)$ we can write

$$e^{2} \sigma(\omega) = \frac{1}{i\omega} \lim_{r \to 0} \frac{a'_{x}}{a_{x}} = \lim_{r \to 0} \frac{F_{rx}}{F_{xt}} = \lim_{r \to 0} \frac{G_{yt}}{G_{ry}} = \lim_{r \to 0} \frac{G_{xt}}{G_{rx}} = \frac{1}{e^{2} \widetilde{\sigma}(\omega)}.$$
 (2.220)

We have used isotropy in the second-to-last equality. We have written $\tilde{\sigma}(\omega)$ to denote the conductivity of the dual theory, defined in terms of G rather than F. However, electromagnetic duality (??) means that G satisfies the same equations of motion as F. Therefore, we must have

$$\sigma(\omega) = \tilde{\sigma}(\omega) = \frac{1}{e^2}$$
. (2.221)

To paraphrase the above argument: from the bulk point of view, the conductivity is a magnetic field divided by an electric field. Electromagnetic duality means we have to get the same answer when we exchange electric and magnetic fields. This fixes the conductivity to be constant.

The argument of the previous paragraph can be extended to include the spatial momentum k dependence and recover (??) from bulk electromagnetic duality (??), allowing for the duality map to exchange the longitudinal and transverse modes satisfying (??) and (??) above [?]. Furthermore, an explicit mapping between electromagnetic duality in the bulk and particle-vortex duality in the boundary theory can be shown at the level of the path integrals for each theory. See for instance [?, ?, ?].

The inversion of conductivities (??) under the duality map (??) is useful even when the theory is not self-dual. We noted above that for small deformations γ , the theory (??) is mapped back to itself with $\gamma \to -\gamma$ under (??). We can see the corresponding inversion of the conductivity clearly in figure ??.

Quasinormal modes replace quasiparticles

Physics and computation of quasinormal modes

We have emphasized around equation (??) above that zero temperature quantum critical correlation functions are typically characterized by branch cut singularities. These branch cuts smear out the spectral weight that in weakly interacting theories is carried by dispersing quasiparticle poles, at $\omega = \epsilon(k)$, on or very close to the real frequency axis. Holographic methods of course reproduce this fact, as in equation (??) above. In contrast, at T > 0, all strongly interacting holographic computations have found that the retarded Green's function is characterized purely by poles in the lower half complex frequency plane (causality requires the retarded Green's function to be analytic in the upper half plane):

$$G_{\mathcal{O}\mathcal{O}}^{R}(\omega) = \sum_{\omega_{\perp}} \frac{c_{\star}}{\omega - \omega_{\star}}.$$
 (2.222)

The poles ω_{\star} are known as quasinormal modes. They are the basic 'on shell' excitations of the system. Taking the Fourier transform of (??), we see that the (imaginary part of the) quasinormal modes determine the rates at which the system equilibrates [?].

Quasinormal modes do not indicate the re-emergence of quasiparticles at T > 0. Instead, the imaginary and real parts of ω_{\star} are typically comparable, so that each modes does not represent a stable excitations. Long-lived quasinormal modes, close to the real axis, can generically only arise in special circumstances (as we shall see): as Goldstone bosons, Fermi surfaces and hydrodynamic modes. Occasionally, poles that are somewhat close to the real axis can produce features in spectral functions. More typically, the spectral density will be seen to receive contributions from a large number of quasinormal modes. Nonetheless, quasinormal modes have a rich and constrained mathematical structure and, in the bulk, capture essential features of gravitational physics. As $T \to 0$, the poles coalesce to form the branch cuts of (??). Some quasinormal modes can survive as poles in the T = 0 limit, as we shall see in our later descriptions of nonzero density states of holographic matter.

Perturbative computations at weak coupling lead to branch cuts in T > 0 correlation functions. It is an open question whether these are artifacts of perturbation theory – that the cuts break up nonpertubatively into finely spaced poles at arbitrarily weak nonzero coupling – or whether the cuts become poles at some finite intermediate coupling or perhaps only in the infinite coupling limit [?, ?]. In any case, in this section we elaborate on the description of strongly interacting T > 0 retarded Green's functions given holographically

⁹A large part of the first gravitational wave signal detected by the LIGO collaboration is the 'ringdown' of a quasinormal mode [?].

in the form (??).

The quasinormal frequencies can be computed, in principle, from the formula for the holographic retarded Green's function in (??) above. Specifically, poles of the retarded Green's function occur at frequencies ω_{\star} such that the corresponding perturbation $\delta\phi(r)$ of the bulk solution [?, ?]

- 1. Satisfies infalling boundary conditions (??) at the horizon.
- 2. Is normalizable at the asymptotic boundary, so that $\delta \phi^{(0)} = 0$ in (??).

Satisfying the two conditions above typically leads to an infinite discrete set of complex frequencies ω_{\star} . In particular, the infalling boundary conditions may be imposed for real or complex frequencies.

A technical challenge that arises in numerical studies is the following: in the lower half complex frequency plane, the infalling mode grows towards the horizon while the unphysical 'outfalling' mode goes to zero (this fact is seen immediately from (??)). This means that for frequencies with large imaginary parts, imposing infalling boundary conditions requires setting to zero a small correction to a large term, which can require high precision. This problem is especially severe for infalling boundary conditions at extremal horizons (as in e.g. (??)), where one must set to zero an exponentially small correction to an exponentially large term. To circumvent this problem, various numerical methods have been devised to directly obtain the quasinormal modes in asymptotically AdS spacetimes. These include the use of truncated high order power series expansions [?] and a method using continued fractions [?]. For extremal horizons, a more general method due to Leaver is necessary [?], as described in [?].

Analytic computations of quasinormal modes are possible using WKB methods, suitably adapted to deal with complex frequencies. These methods were pioneered in [?]. While formally capturing modes at large frequencies, the WKB formulae often give excellent approximations for ω_{\star} down to the lowest or second-lowest frequency. Comprehensive results for planar AdS black holes using this techniques can be found in e.g. [?, ?]. For example, for a scalar operator in a CFT3 with large scaling dimension $\Delta \gg 1$, cf. section ?? above, one has [?]

$$\omega_{\star}^{(n)} = \pi T \left(\pm \sqrt{3} - 3i \right) \left(n + \frac{1 - 2^{2/3}}{2} + \frac{2^{2/3}}{3} \Delta \right) + \mathcal{O}\left(\frac{1}{\Delta} \right). \tag{2.223}$$

These are results for zero momentum, k=0. One corollary of this result is that there are infinitely many quasinormal frequencies, extending down at an angle in the complex frequency plane. The poles exist in pairs related by reflection about the imaginary frequency axis. This follows from time reversal invariance, according to which $G^R(-\omega^*) = G^R(\omega)^*$.

The quasinormal modes of scalar operators in quantum critical theories with z > 1 have been studied in [?] as function of scaling dimension Δ of the operator and dimension d of space. The modes have momentum

k=0. When z < d, the quasinormal modes are qualitatively similar to those in CFTs (i.e. with z=1). That is, they extend down in the complex frequency plane similarly to (??). However, for $z \ge d$ all quasinormal frequencies are overdamped, with purely imaginary frequencies. This is illustrated in the following figure ??. The density of states in these quantum critical theories, on dimensional grounds, satisfies $\rho(\omega) \sim \omega^{(d-z)/z}$

Figure 18: Quasinormal poles as a function of z. Hollow dots denote quasinormal frequencies at z = 1. The arrows show the motion of the poles as z is increased. For $z \ge d$ the modes are all overdamped, lying along the negative imaginary axis. All modes have momentum k = 0. [Figure adapted with permission from [?]]

[?]. Therefore, d < z implies a large number of low energy excitations. Decay into these excitations may possibly be the cause of the overdamped nature of the modes. Precisely at z = d, the quasinormal frequencies may be found analytically [?]. They have a similar integrable structure to those of CFT2s [?, ?].

An example where a low-lying quasinormal mode imprints a feature on the conductivity along the real frequency axis is the theory (??), Maxwell theory modified by a coupling to the Weyl tensor, that we studied above. Figure ?? plots $|\sigma(\omega)|$ in the lower half complex frequency plane. This plot is obtained using the same Mathematica code that produced figure ?? above. A higher order series expansion has been used to set the initial conditions close to the horizon and a higher WorkingPrecision has been used in numerically solving the differential equation. In the figure we see that $\gamma = 1/12$ leads to a pole on the negative imaginary axis whereas $\gamma = -1/12$ leads to a zero on the negative imaginary axis. These are responsible for the peak and dip seen in figure ??, respectively. The poles and zeros are exchanged in the two plots of figure ??. This is consistent with the fact that electromagnetic duality inverts the conductivity (??), and also, for $\gamma \ll 1$, sends $\gamma \to -\gamma$. We thus learn that the zeros of the conductivity in the complex frequency plane are also important, as they become the poles of the particle-vortex dual theory. A similar zero-pole structure to that of figure ?? is seen in other cases where particle-vortex duality acts in nontrivial way, such as in a background

Figure 19: $|\sigma(\omega)|$ in the lower half plane, with $\gamma = 1/12$ (left) and $\gamma = -1/12$ (right). The dominant features are poles (blue) and zeros (red). The plot has been clipped at $e^2|\sigma| = 2$, the dark blue regions.

magnetic field [?]. We will discuss magnetic fields and particle-vortex duality further in section ?? below.

Beyond peaks or dips caused by specific poles or zeros, one can use the lowest few poles and zeros to construct a 'truncated conductivity' that accurately captures the low frequency behavior of the conductivity along the real frequency axis [?].

In the case of $\gamma=0$, pure Maxwell theory in the bulk, there are no quasinormal modes. Recall that the conductivity (??) is featureless in this case. It is instructive to see how the quasinormal modes plotted in the previous figure ?? annihilate in a 'zipper-like' fashion as $\gamma \to 0$. Figure ?? shows that, as γ is lowered, pairs of zero and poles move towards the imaginary frequency axis. Once the pair reaches the axis, one moves up and the other moves down the axis. The pole or zero that moves up then annihilates, as $\gamma \to 0$, with a zero or pole that is higher up the axis. The poles and zero annihilate precisely at the Matsubara frequencies $\omega_n^{\text{zip}} = -i2\pi nT$, with $n=1,2,3,\ldots$ [?].

A very important class of quasinormal poles are those associated with hydrodynamic modes. Hydrodynamic modes have the property that $\omega_{\star}(k) \to 0$ as $k \to 0$. These modes are forced to exist on general grounds due to conservation laws (we will discuss hydrodynamics in section ??) and can usually be found analytically. In fact, relativistic hydrodynamics can be derived in some generality from gravity using the 'fluid/gravity' correspondence [?]. We have already computed a hydrodynamic quasinormal mode in section ?? above. In equation (??) we found the diffusion mode

$$\omega_{\star}(k) = -iDk^2 + \cdots, \tag{2.224}$$

Figure 20: Motion of poles and zeros as γ is decreased. Crosses are poles and circles are zeros. Pais of poles and zeros move to the imaginary frequency axis, and then move up and down the axis to annihilate with a zero or pole. In these plots $w = \omega/(4\pi T)$. [Figure taken with permission from [?]]

together with a formula for D. Important early holographic studies of hydrodynamic modes in zero density systems include [?, ?, ?], for CFT4s, and [?, ?] for CFT3s. In addition to diffusive modes there are sound modes of the form

$$\omega_{\star}(k) = v_s k - i\Gamma k^2 + \cdots . \tag{2.225}$$

Finally, an interesting perspective on hydrodynamic quasinormal modes of black holes can be obtained by taking the number of spatial dimensions $d \to \infty$. In this limit aspects of the gravitational problem simply and, in particular, the influence of black hole horizons on the geometry becomes restricted to a thin shell around the horizon [?]. The hydrodynamic quasinormal modes become a decoupled set of modes existing in the thin shell around the horizon, and can be studied to high order in a derivative expansion [?].

In later parts of this review we shall come across other circumstances where $\omega_{\star} \to 0$: Goldstone modes, zero temperature sound modes and Fermi surface modes.

1/N corrections from quasinormal modes

We have said that quasinormal poles define the 'on-shell' excitations of the strongly interacting, dissipative finite temperature system. Virtual production of these excitations in the bulk should be expected to contribute to observables at subleading order in the large N expansion (which, we recall, is the semi-classical expansion in the bulk). Occasionally such a 'one-loop' effect in the bulk can give the leading contribution to interesting observables. In the boundary theory, these effects either correspond to non-equilibrium thermodynamic fluctuations or else to physics that is suppressed because it involves a number of modes that remains finite in the large N limit (e.g. there might only be one Goldstone boson).

The usual Euclidean determinant formulae for the one-loop correction to black hole backgrounds obscures the physical role of quasinormal modes. The determinant correction to the bulk partition function (??) takes the schematic form

$$Z = \det\left(-\nabla_{g_{\star}}^{2}\right)^{\pm 1} e^{-S_{E}[g_{\star}]}.$$
 (2.226)

Here g_{\star} denotes the (Euclidean) saddle point and det $\left(-\nabla_{g_{\star}}^{2}\right)$ schematically denotes the determinants corresponding to fluctuations about the background. Bosonic determinants are in the denominator and fermionic determinants in the numerator. In [?, ?] formulae for these determinants were derived in terms of the quasinormal modes of the fluctuations. For bosonic fields, for instance, the formula is

$$\frac{1}{\det\left(-\nabla_{g_{\star}}^{2}\right)} = e^{\text{Pol}} \prod_{\omega_{\star}} \frac{|\omega_{\star}|}{4\pi^{2}T} \left| \Gamma\left(\frac{i\omega_{\star}}{2\pi T}\right) \right|^{2}. \tag{2.227}$$

Here ω_{\star} are the quasinormal frequencies. Pol denotes a polynomial in the dimension Δ of the scalar field; this term is determined by short distance physics in the bulk and cannot contribute any interesting non-analyticities. One-loop effects are mainly interesting, of course, insofar as they can lead to non-analytic low energy ('universal') physics. This also simplifies the calculation – we do not wish to compute the whole determinant, but just to isolate the important part.

The formula (??) is useful for calculating the correction to thermodynamics quantities. One may also be interested in non-analytic corrections to Green's functions. Here quasinormal modes also play an essential role. We will sketch how this works, more details can be found in [?, ?, ?, ?]. A typical one-loop correction ΔG to a Green's function will be given by the convolution of two bulk propagators. The finite temperature calculation is set up by starting with periodic Euclidean time. Fourier transforming in the boundary directions, but working in position space for the radial direction, the bulk Euclidean propagators take the form

 $G(i\omega_n, k, r_1, r_2)$. Thus, schematically,

$$\Delta G(i\omega_n, k) \sim T \sum_m \int \frac{d^d q}{(2\pi)^d} \int dr dr' G_1(i\omega_m, q, r, r') G_2(i\omega_m + i\omega_n, q + k, r', r) + (1 \leftrightarrow 2). \tag{2.228}$$

The second step is to re-express the correction in terms of retarded Green's functions. This is achieved using standard representations of the sum over Matsubara frequencies as a contour integral. See the references above. For bosonic fields, this leads to, again schematically,

$$\Delta G(\omega) \sim \int \frac{d\Omega}{2\pi} \int \frac{d^dq}{(2\pi)^d} \int dr dr' \coth \frac{\Omega}{2T} \operatorname{Im} \left[G_1^R(\Omega, q, r, r') G_2^R(\Omega + \omega, q, r', r) \right] + (1 \leftrightarrow 2). \tag{2.229}$$

We analytically continued the external frequency $i\omega_n \to \omega$ and for simplicity set the external k=0. We are interested typically in small $\omega \ll T$. The objective now is to identify the most IR singular part of these integrals. This looks challenging, in particular because of the integrals over the radial direction. However, if there is a quasinormal frequency $\omega_{\star}(k)$ that goes to zero, say as the momentum goes to zero, then one can isolate the singular contribution of this mode to the Green's function [?]. Schematically,

$$G^{R}(\omega, k, r, r') \sim \frac{\overline{\phi_{\star}(r)}\phi_{\star}(r')}{\omega - \omega_{\star}(k)}$$
 (2.230)

Here $\phi_{\star}(r)$ is the radial profile of the quasinormal mode with frequency ω_{\star} . In the numerator k can be set to zero (in some cases the correct normalization of G^R may require overall factors of k). Hence, using the above formula in (??), the radial integrals simply lead to a numerical prefactor. The remaining integrals are then only in the field theory directions.

To illustrate how zooming in on the quasinormal mode (??) picks out the singular physics of interest, consider the case of long-time tails that appear in the electrical conductivity. Here one is looking for a one-loop correction to the propagator of the bulk Maxwell field (photon). The one-loop diagram is one in which a photon and a graviton run in the loop (there are no photon self-interactions in Einstein-Maxwell theory). The retarded Green's functions of these bulk field each have a diffusive quasinormal mode, corresponding to diffusion of charge and heat. Zooming in on these modes, and assuming that the relevant frequencies will have $\Omega \ll T$, the integrals in (??) become, without keeping track of the overall numerical prefactor,

$$\Delta G_{J^x J^x}(\omega) \sim \int \frac{d\Omega}{2\pi} \int \frac{d^d q}{(2\pi)^d} \frac{T}{\Omega} \operatorname{Im} \left[\frac{q^2}{\Omega + iD_1 q^2} \frac{q^2}{\Omega + \omega + iD_2 q^2} \right] + (1 \leftrightarrow 2)$$
 (2.231)

$$\sim \int \frac{d^d q}{(2\pi)^d} \frac{q^2 \omega}{\omega^2 + D_2^2 q^4} + (1 \leftrightarrow 2)$$
 (2.232)

$$\sim \begin{cases} \omega^{1/2} & d=1\\ \omega \log \omega & d=2 \end{cases} . \tag{2.233}$$

The results (??) are precisely the well-known singular 'late time tail' contributions to $G_{JxJx}^R(\omega)$ in one and two spatial dimensions. They lead to an infinite dc conductivity $\sigma_{dc} = \lim_{\omega \to 0} [G_{JxJx}^R(\omega)/i\omega]$. Because this effect has arisen from a quantum correction to the bulk, the singular late time tails are suppressed in holographic theories by factors of 1/N. This fact was first noted in [?]. The logarithmic divergence in two spatial dimensions should be negligible for most practical purposes.

The above outline is essentially enough to isolate the singular effect in many cases. To obtain the correct numerical prefactor, or to convince oneself that there are no other singular contributions, substantially more work is typically necessary [?, ?, ?, ?].

Compressible quantum matter

The condensed matter systems described in Section ?? had the common feature of being at some fixed density of electrons (or other quantum particles) commensurate with an underlying lattice: this was important in realizing a low energy description in terms of a conformal field theory. However, the majority of the experimental realizations of quantum matter without quasiparticle excitations are not at such special densities. Rather, they appear at generic densities in a phase diagram in which the density can be continuously varied.

More precisely stated, the present (and following) section will consider systems with a global U(1) symmetry, with an associated conserved charge density \mathcal{Q} which can be varied smoothly as a function of system parameters even at zero temperature. The simplest realization of such a system is the free electron gas, and (as is well known) many of its properties extend smoothly in the presence of interactions to a state of compressible quantum matter called the 'Fermi liquid'. The Fermi liquid has long-lived quasiparticle excitations, and almost all of its low temperature properties can be efficiently described using a model of a dilute gas of fermionic quasiparticles. Indeed, the term Fermi liquid is a misnomer, as the excitations do not interact strongly as in a liquid like water.

Our interest here will be in realizations of compressible quantum matter which do not have quasiparticle excitations. One can imagine reaching such a state by turning up the strength of the interactions between the quasiparticles until they reach a true liquid-like state in which the quasiparticles themselves lose their integrity.

Any compressible state has to be gapless, otherwise the density would not vary as a function of the chemical potential. The non-quasiparticle states of interest to us invariably have a scale-invariant structure

at low energies, and so it is useful work through some simple scaling arguments at the outset. As in (??), we write for the T dependence of the entropy density

$$S \sim T^{(d-\theta)/z} \tag{2.234}$$

where d is the spatial dimensionality, and θ is the violation of hyperscaling exponent [?]. In the presence of a global conserved \mathcal{Q} , it is useful to introduce a conjugate chemical potential μ , and consider the properties as a function of both μ and T.

Let us begin by reviewing the thermodynamics of QFTs at finite z and θ . Thermodynamics is controlled by a "master function", which we'll take to be the pressure $P(\mu, T)$ in the grand canonical ensemble. Scale invariance implies that up to dimensional analysis, P can only be a function of the dimensionless ratio μ/T :

$$P = T^{1+(d-\theta)/z} \mathcal{F}\left(\frac{\mu}{T}\right). \tag{2.235}$$

The charge density \mathcal{Q} and entropy density \mathcal{S} are defined as

$$Q = \frac{\partial P}{\partial \mu} = T^{(d-\theta)/z} \mathcal{F}'\left(\frac{\mu}{T}\right), \tag{2.236a}$$

$$S = \frac{\partial P}{\partial T} = T^{(d-\theta)/z} \left[\left(1 + \frac{d-\theta}{z} \right) \mathcal{F} \left(\frac{\mu}{T} \right) - \frac{\mu}{T} \mathcal{F}' \left(\frac{\mu}{T} \right) \right]. \tag{2.236b}$$

Using the thermodynamic identity

$$\epsilon + P = \mu \mathcal{Q} + T\mathcal{S},\tag{2.237}$$

where ϵ is the energy density, we obtain

$$\epsilon = \frac{d - \theta}{z} P. \tag{2.238}$$

We have only seen examples of theories with $\theta = 0$ or $\theta = d - 1$. A simple model for theories with more general θ consists of $N \gg 1$ species of free Dirac fermions with power-law mass distributions [?]. We do not know of any non-large N model which has other θ . $\theta < 0$ suggests that the effective theory "grows" in dimensionality, which seems to require $N \to \infty$ degrees of freedom. $d - 1 \neq \theta > 0$ suggests that (barring a "fractal Fermi surface") spatial isotropy has been lost. Isotropic holographic models of these values of θ are well-posed, as best we know.

The first subsection below describes various condensed matter realizations of compressible quantum matter. The subsequent subsections take a holographic approach by 'doping' a strongly-coupled conformal field theory. We will then propose interpretations of the holographic realizations of compressible matter by

comparing their properties to those of the condensed matter systems in Section ??.

Condensed matter systems

We begin with a review of some basic ideas from the Fermi liquid theory of interacting fermions in d dimensions. We consider spin-1/2 fermions $c_{k\alpha}$ with momentum k and spin $\alpha = \uparrow, \downarrow$ and dispersion ε_k . Thus the non-interacting fermions are described by the action

$$S_c = \int d\tau \int \frac{d^d k}{(2\pi)^d} c_{k\alpha}^{\dagger} \left(\frac{\partial}{\partial \tau} + \varepsilon_k \right) c_{k\alpha}, \qquad (2.239)$$

The fermion Green's function under the free fermion action S_c has the simple form

$$G_0(k,\omega) = \frac{1}{\omega - \varepsilon_k} \tag{2.240}$$

This Green's function has a pole at energy ε_k with residue 1. Thus there are quasiparticle excitations with residue Z=1, with both positive and negative energies, as ε_k can have either sign; the Fermi surface is the locus of points where ε_k changes sign. The positive energy quasiparticles are electron-like, while those with negative energy are hole-like *i.e.* they correspond to the absence of an electron. Numerous text books describe the effect of interactions on this simple free fermion description. A key result is that the pole survives on the Fermi surface: for small $|\varepsilon_k|$, the interacting fermion retarded Green's function take the form

$$G(k,\omega) = \frac{Z}{\omega - \tilde{\varepsilon}_k + i\,\alpha\,\tilde{\varepsilon}_k^2} + G_{\rm inc}$$
(2.241)

where $\tilde{\varepsilon}_k$ is the renormalized quasiparticle dispersion, α is a numerical constant, 0 < Z < 1 is the quasiparticle residue, and $G_{\rm inc}$ is the incoherent contribution which is regular as $\tilde{\varepsilon}_k \to 0$. The Fermi surface is now defined by the equation $\tilde{\varepsilon}_k = 0$, and we note that the lifetime of a quasiparticle with energy $\tilde{\varepsilon}_k$ diverges as $1/\tilde{\varepsilon}_k^2$, indicating that the quasiparticles are well-defined. Although the interactions can renormalize the shape of the Fermi surface, Luttinger's theorem states that the volume enclosed by the Fermi surface remains the same as in the free particle case:

$$\int_{\tilde{\varepsilon}_k < 0} \frac{d^d k}{(2\pi)^d} = \mathcal{Q}. \tag{2.242}$$

A universal description of the low energy properties of a Fermi liquid is obtained by focusing in on each point on the Fermi surface. For each direction \hat{n} , we define the position of the Fermi surface by the

wavevector $\vec{k}_F(\hat{n})$, so that $\hat{n} = \vec{k}_F(\hat{n})/|\vec{k}_F(\hat{n})|$. Then we identify wavevectors near the Fermi surface by

$$\vec{k} = \vec{k}_F(\hat{n}) + k_\perp \,\hat{n} \tag{2.243}$$

Now we should expand in small momenta k_{\perp} . For this, we define the infinite set of fields $\psi_{\hat{n}a}(k_{\perp})$, which are labeled by the spin a and the direction \hat{n} , related to the fermions c by

$$c_{\vec{k}\alpha} = \frac{1}{\sqrt{S_F}} \psi_{\hat{n}\alpha}(k_\perp), \tag{2.244}$$

where \vec{k} and k_{\perp} are related by (??), and S_F is the area of the Fermi surface. Inserting (??) into (??), expanding in k_{\perp} , and Fourier transforming to real space x_{\perp} , we obtain the low energy theory

$$S_{\rm FL} = \int d\Omega_{\hat{n}} \int dx_{\perp} \psi_{\hat{n}\alpha}^{\dagger}(x_{\perp}) \left(\frac{\partial}{\partial \tau} - i v_F(\hat{n}) \frac{\partial}{\partial x_{\perp}} \right) \psi_{\hat{n}\alpha}(x_{\perp}), \tag{2.245}$$

where the Fermi velocity is energy gradient on the Fermi surface $v_F(\hat{n}) = |\nabla_k \varepsilon_{\vec{k}_F(\hat{n})}|$. For each \hat{n} , (??) describes a fermions moving along the single dimension x_{\perp} with the Fermi velocity: this is a one-dimensional chiral fermion; the 'chiral' refers to the fact that the fermion only moves in the positive x_{\perp} direction, and not the negative x_{\perp} direction. In other words, the low energy theory of the Fermi liquid is an infinite set of one-dimensional chiral fermions, one chiral fermion for each point on the Fermi surface. Apart from the free Fermi term in (??), Landau's Fermi liquid theory also allows for contact interactions between chiral fermions along different directions [?]. These are labeled by the Landau parameters, and lead only to shifts in the quasiparticle energies which depend upon the densities of the other quasiparticles. Such shifts are important when computing the response of the Fermi liquid to external density or spin perturbations.

The chiral fermion theory in Eq. (??) allows to deduce the values of the exponents characterizing the low temperature thermodynamics of a Fermi liquid. We have

$$z = 1$$
 , $\theta = d - 1$ (2.246)

from the linear dispersion and the effective dimensionality $d - \theta = 1$ of the chiral fermions.

For d > 1, interactions are irrelevant at a Fermi liquid fixed point. Hence, most ordinary compressible matter (such as the electron gas in iron, or liquid helium) is a Fermi liquid. Nonetheless, it is possible to find routes to destabilize the Fermi liquid to obtain compressible states without quasiparticles, as we detail in the following subsections.

Figure 21: Fermionic excitations at the Ising-nematic critical point. We focus on an extended patch of the Fermi surface, and expand in momenta about the point \vec{k}_0 on the Fermi surface. This yields a theory of d-dimensional fermions ψ in (??). The co-ordinate y represents the d-1 dimensions parallel to the Fermi surface.

Ising-nematic transition

One route to non-Fermi liquid behavior is to study a quantum critical point associated with the breaking of a global symmetry in the presence of a Fermi surface. This is analogous to our study in Section ??, where we considered spin rotation symmetry breaking in the presence of massless Dirac fermions whose energy vanished at isolated points in the Brillouin zone. But here we have a (d-1)-dimensional surface of massless chiral fermions, and so they can have a more singular influence.

We describe here the field theory for the simplest (and experimentally relevant) example of an Ising order parameter, represented by the real scalar field ϕ , associated with the breaking of a point-group symmetry of the lattice. Other order parameters which carry zero momentum have similar critical theories; the case of non-zero momentum order parameters which break translational symmetry will be considered in the following subsection.

Unfortunately, in this case the field theory cannot be obtained by simply coupling the field theory of ϕ to the chiral fermion theory in (??), and keeping all terms consistent with symmetry. A shortcoming of the effective action (??) is that it only includes the dispersion of the fermions transverse to the Fermi surface. Thus, if we discretize the directions \hat{n} , and pick a given point on the Fermi surface, the Fermi surface is effectively flat at that point. The curvature of the Fermi surface turns out to be important at the Ising-nematic critical point [?]. So we have to take the continuum scaling limit in a manner which keeps the curvature of the Fermi surface fixed, and does not scale it to zero. For this, as shown in Fig. ??, we focus attention on a single arc of the Fermi surface in the vicinity of any chosen point \vec{k}_0 . With \vec{k}_0 chosen as Fig. ??, let us now define our low energy theory and scaling limit. Unlike the one-dimensional chiral fermions which appeared in (??), we will now use a d dimensional fermion $\psi_{\alpha}(x,y)$. Here x is the one dimensional co-ordinate orthogonal to the Fermi surface, and \vec{y} represents the (d-1)-dimensional transverse co-ordinates; expanding the dispersion in the vicinity of \vec{k}_0 (contrast to the expansion away from all points on the Fermi surface in (??)), we obtain the low energy theory [?]

$$S_{\psi} = \int d\tau \int dx \int d^{d-1}y \ \psi_{\alpha}^{\dagger} \left(\zeta_{1} \frac{\partial}{\partial \tau} - i v_{F} \frac{\partial}{\partial x} - \frac{\kappa}{2} \nabla_{y}^{2} \right) \psi_{\alpha}. \tag{2.247}$$

We have added a co-efficient ζ_1 to the temporal gradient term for convenience: we are interested in $\zeta_1 = 1$, but

the disappearance of quasiparticles in the ultimate theory is captured by the renormalization $\zeta_1 \to 0$. Notice the additional second-order gradients in y which were missing from (??): the co-efficient κ is proportional to the curvature of the Fermi surface at \vec{k}_0 . There are zero energy fermion excitations when

$$v_F k_x + \kappa \frac{k_y^2}{2} = 0, (2.248)$$

and so (??) defines the position of the Fermi surface, which is then part of the low energy theory including its curvature. Note that (??) now includes an extended portion of the Fermi surface; contrast that with (??), where the one-dimensional chiral fermion theory for each \hat{n} describes only a single point on the Fermi surface.

The field theory for the Ising-nematic critical point now follows the traditional symmetry-restricted route described also in Section ??. We restrict our subsequent attention to the important case of d=2, because this is the dimensionality in which quasiparticles are destroyed by the critical fluctuations. We combine a field theory like (??) for ϕ with a 'Yukawa' coupling λ between the fermions and bosons

$$S_{\rm IN} = S_{\psi} + \int dx dy d\tau \left[\zeta_2 \left(\partial_{\tau} \phi \right)^2 + \zeta_3 \left(\partial_x \phi \right)^2 + \left(\partial_y \phi \right)^2 + s \phi^2 + u \phi^4 + \lambda \phi \psi_{\alpha}^{\dagger} \psi_{\alpha} \right]. \tag{2.249}$$

As usual, the coupling s is a tuning parameter across the quantum critical point, and we are interested here in the quantum state at the critical value $s = s_c$. The theory S_{IN} has been much studied in the literature by a variety of sophisticated field-theoretic methods [?, ?, ?, ?]. For the single fermion patch theory as formulated above, exact results on the non-quasiparticle compressible state are available. In the scaling limit, all the $\zeta_i \to 0$, and the fermionic and bosonic excitations are both characterized by a common emergent dynamic critical exponent z. Their Green's functions do not have any quasiparticle poles (unlike (??)), and instead we have the following scaling forms describing the non-quasiparticle excitations:

$$G_{\psi}(k_{x}, k_{y}, \omega) \sim \frac{1}{(v_{F}q_{x} + (\kappa/2)q_{y}^{2})^{1-\eta}} \mathcal{F}_{\psi} \left(\frac{\omega}{(v_{F}q_{x} + (\kappa/2)q_{y}^{2})^{z}} \right)$$

$$G_{\phi}(k_{x}, k_{y}, \omega) \sim \frac{1}{q_{y}^{(2z-1)}} \mathcal{F}_{\phi} \left(\frac{\omega}{q_{y}^{2z}} \right), \qquad (2.250)$$

where η is the anomalous dimension of the fermion, the boson does not have an independent anomalous dimension, and $\mathcal{F}_{\psi,\phi}$ are scaling functions. Note that the curvature of the Fermi surface, κ/v_F , does not renormalize, and this follows from a Ward identity obeyed by \mathcal{S}_{IN} [?]. For the single-patch theory described

Figure 22: Fermi surfaces of ψ_1 and ψ_2 fermions in the plane defined by the Fermi velocities \vec{v}_1 and \vec{v}_2 . The gapless Fermi surfaces are one-dimensional, and are indicated by the full lines. The lines intersect at the hot spot, which is the filled circle at the origin.

so far, the exact values of the exponents in d=2 are [?]

$$z = 3/2$$
 , $\theta = 1$, $\eta = 0$. (2.251)

In the presence of additional symmetries in the problem, the single patch description is often not adequate. Many important cases have inversion symmetry, and then we have to include a pair of antipodal patches of the Fermi surface in the same critical theory [?, ?]. The resulting two-patch theory is more complicated, and exact results are not available. Up to three loop order, we find that $\eta \neq 0$, while the value z = 3/2 is preserved. There is also a potentially strong instability to superconductivity in the two patch theory [?].

Spin density wave transition

Now we consider the case of an order parameter at non-zero momentum leading to symmetry breaking in the presence of a Fermi surface. The experimentally most common case is a spin density wave transition, represented by a scalar field φ^a , with a=1,2,3, very similar to that found in Section ?? for the Gross-Neveu model. The order parameter carries momentum K, and so the condensation of φ^a breaks both spin rotation and translational symmetries. The scalar will couple to fermion bilinears which also carry momentum K; as we are interested only in low energy fermionic excitations near the Fermi surface, we need to look for "hot spots" on the Fermi surface which are separated by momentum K. If no such hot spots are found, then the Fermi surface can be largely ignored in the theory of the transition, as it is described by a conventional Wilson-Fisher theory for the scalar φ^a . Here we consider the case where the hot spots are present, and then there is a relevant Yukawa coupling between φ^a and fermion bilinears spanning the hot spots.

For simplicity, we describe the simplest case here of a single pair of hot spots, described by the fermion fields $\psi_{1\alpha}$ and $\psi_{2\alpha}$ representing points on the Fermi surface at wavevectors k_1 and k_2 . The low energy fermion action in (??) is now replaced by

$$S_{\psi} = \int d\tau \int d^2x \left[\psi_{1\alpha}^{\dagger} \left(\frac{\partial}{\partial \tau} - i\vec{v}_1 \cdot \nabla_x \right) \psi_{1\alpha} + \psi_{2\alpha}^{\dagger} \left(\frac{\partial}{\partial \tau} - i\vec{v}_2 \cdot \nabla_x \right) \psi_{2\alpha} \right]. \tag{2.252}$$

Here we are again restricting attention to the important case of spatial dimension d=2, $\vec{v}_1=\nabla_k \varepsilon_k|_{k_1}$ is the Fermi velocity at k_1 , and similarly for \vec{v}_2 . In the $\psi_{1,2}$ formulation, the configurations of the Fermi surfaces and hot spots are shown in Fig. ??. The Fermi surface of the ψ_1 fermions is defined by $\vec{v}_1 \cdot \vec{k} = 0$, and the

Fermi surface of the ψ_2 fermions is defined by $\vec{v}_2 \cdot \vec{k} = 0$, and the hot spot is at k = 0. We assume here and below that \vec{v}_1 and \vec{v}_2 are not collinear: the collinear case corresponds to the "nesting" of the Fermi surfaces, and has to be treated separately. Finally, as in Section ??, we can couple these fermions to the scalar field φ^a and obtain the field theory for the onset of spin density wave order in a metal [?]

$$S_{\text{sdw}} = S_{\psi} + \int d^2x \int d\tau \left[(\nabla_x \varphi^a)^2 + s (\varphi^a)^2 + u \left((\varphi^a)^2 \right)^2 + \lambda \varphi^a \sigma_{\alpha\beta}^a \left(\psi_{1\alpha}^{\dagger} \psi_{2\beta} + \psi_{2\alpha}^{\dagger} \psi_{1\beta} \right) \right].$$

$$(2.253)$$

Here σ^a are the Pauli matrices. Notice the similarity of S_{sdw} to the theory for the onset of antiferromagnetism in the honeycomb lattice in Section ??: the main difference is that the massless Dirac fermions (which are gapless only at the isolated point k=0) have been replaced by fermions with dispersion illustrated in Fig. ?? (which are gapless on two lines in the Brillouin zone).

The non-Fermi liquid physics associated with the theory S_{sdw} has been studied in great detail in the literature. The expansion in powers of λ is strongly coupled, and a variety of large N and dimensionality expansions have been employed [?, ?, ?]. We will not enter into the details of this analysis here, and only mention a few important points. The theory has a strong tendency to the appearance of d-wave superconductivity, and this has been confirmed in quantum Monte Carlo simulations [?, ?, ?, ?, ?]. The non-Fermi liquid behavior is characterized by a common dynamic critical exponent z > 1 for both the fermions and bosons, but with no violation of hyperscaling $\theta = 0$ [?, ?]. The preservation of hyperscaling indicates that the critical non-Fermi liquid behavior is dominated by the physics in the immediate vicinity of the hot spot; the gapless Fermi lines (responsible for violation of hyperscaling in a Fermi liquid) are subdominant in their non-Fermi liquid contributions.

Emergent gauge fields

Compressible quantum phases with emergent gauge fields are most directly realized by doping the insulating phases discussed in Section ?? by mobile charge carriers. We can dope the resonating valence bond state in Fig. ??a by removing a density p of electrons. We are then left with a density 1-p of electron on the square lattice. However, as long as the emergent gauge field of the parent resonating valence bond state remains deconfined, it is more appropriate to think of this system of have a density p of positively charged carriers [?, ?]. As illustrated in Fig. ??, these charge carriers can either remain as spinless fermionic holons h_q , or bind with the quanta of the neutral spin-1/2 scalars z_{α} in Fig. ??b to form fermions, d_{α} , with electromagnetic charge +e and spin S=1/2 [?].

Figure 23: Schematic of a component of a state obtained by doping the resonating valence bond state in Fig. ??a by a density p of holes. The orange circles represent spinless 'holons' h_q of electromagnetic charge +e, and emergent gauge charge $q=\pm 1$. The green dimers, d_{α} are bound states of holons and the z_{α} quanta: the d_{α} are neutral under the emergent gauge field, but carry electromagnetic charge +e and spin S=1/2. Finally, the resonance of the blue and green dimers is captured by the emergent gauge field A_{μ} .

So the final low energy description of this state is left with two kinds of fermions, both of which carry the Maxwell electromagnetic charge (which is a global U(1) symmetry, as is conventional in the non-relativistic condensed matter contexts). There are the 'fractionalized' fermions, h_q , which carry charges ± 1 under the emergent gauge field A_{μ} of (??). And we have the 'cohesive' fermions, d_{α} , which are neutral under A_{μ} . We will see below that holographic descriptions of compressible phases also lead naturally to such catergories of fermionic charge carriers. So we can write down an effective low energy theory for the fermions in the spirit of (??):

$$S_{hd} = \int d\tau \int \frac{d^2k}{4\pi^2} \left[d^{\dagger}_{k\alpha} \left(\frac{\partial}{\partial \tau} + E_d(k) \right) d_{k\alpha} + \sum_{q=\pm 1} h^{\dagger}_{kq} \left(\frac{\partial}{\partial \tau} - iA_{\tau} + E_h(\vec{k} - q\vec{A}) \right) h_{kq} \right]$$
(2.254)

where $E_d(k)$ and $E_h(k)$ are the dispersions of the cohesive and fractionalized fermions respectively. Note that the fractionalized fermions are minimally coupled to the emergent gauge field.

A modified version of the Luttinger relation (??) also applies here. As the fractionalized fermions can convert into cohesive fermions by binding with the z_{α} , the relation only applies to the sum of the volumes

enclosed by all the Fermi surfaces [?, ?]

$$\sum_{\alpha} \int_{E_d(k)<0} \frac{d^2k}{4\pi^2} + \sum_{q} \int_{E_h(k)<0} \frac{d^2k}{4\pi^2} = p.$$
 (2.255)

Note that this is expected to be an exact relationship, satisfied by the fully renormalized excitations in the presence of the gauge excitations, as long as the gauge field does not undergo a confinement transition.

Actually, there is an important feature we have glossed over in the discussion so far of (??). The h_q fermions are minimally coupled to a U(1) gauge field, and this coupling leads to a breakdown of the quasiparticle physics near the Fermi surface. Indeed, the theory of the Fermi surface coupled to a gauge field [?, ?] is nearly identical to that Ising-nematic transition discussed in Section ??. The field theory (??) applies also to the gauge field problem, with the scalar field ϕ representing the component of the gauge field normal to the Fermi surface (in the Coulomb gauge). Consequently, much of the analysis for the structure of the excitations near the Fermi surface can be adapted from the Ising-nematic analysis summarized in Section ??. Despite the absence of quasiparticles, however, the position of the Fermi surface in Brillouin zone can be defined precisely. Now, rather then the quasiparticle condition $E_h(k) = 0$ used naively in (??), we have the more general condition on the h_q fermion Green's function $G_h^{-1}(k,\omega=0) = 0$ [?]. With this modification, the Luttinger relation in (??) continues to apply to this realization of compressible quantum matter without quasiparticles (similar relations also apply to the examples discussed in Sections ?? and ??).

residual comments

COMMENT: moving zero sound discussion to probe brane section. i alray dislike this terminology and don't think RN black hole should be thought of as having zero sound... also going to move the discussion of sound waves (including RN at zero T) to after the discussion of hydrodynamics in Chapter 5...I guess this whole section could be moved earlier but I think it's more natural there for the moment

mention ahead of time that one recurring motivation for the chapter will be Fermi surfaces and whether they exist in holography (though without a sharp answer to the question by the end?)

"classification" of compressible phases without broken symmetries. known examples. role of z, theta.

Additional possibilities when you have emergent gauge fields. Luttinger theorem vs gauge symmetries. I.e. are the charge-carryng particles gauge-neutral ("cohesive") or not ("fractionalized").

Charged horizons

Let us now turn to the holographic realizations of low energy effective theories with various non-trivial scaling exponents. The major workhorse of these models will be the Einstein-Maxwell-dilaton (EMD) theory:

$$S = \int d^{d+2}x \sqrt{-g} \left[\frac{1}{2\kappa^2} \left(R - 2\Lambda - 2(\partial \Phi)^2 - \frac{V(\Phi)}{L^2} \right) - \frac{Z(\Phi)}{4e^2} F^2 \right], \tag{2.256}$$

with background fields $\Phi(r)$ (a scalar called the dilaton), A = p(r)dt, and metric

$$ds^{2} = \frac{L^{2}}{r^{2}} \left[\frac{a(r)}{b(r)} dr^{2} - a(r)b(r)dt^{2} + d\mathbf{x}^{2} \right].$$
 (2.257)

This ansatz [?] proves convenient as near a black hole horizon at $r = r_+$,

$$b(r) \approx 4\pi T(r_{+} - r),\tag{2.258}$$

regardless of other fields. The bulk equations of motion are also more transparent using this coordinate system. For simplicity, we assume that this space is asymptotically AdS, which simplifies the holographic dictionary to what we're familiar with. This implies that a(0) = b(0) = 1.

The form of (??) is inspired by top-down constructions from supergravity: indeed, recall the discussion of §??. In many of the models listed in that section, upon taking the analogue of the scalar field $\Phi \to \infty$, one finds an action of the form (??). In this section, we take the point of view that (??) is a consistent holographic model regardless of whether or not it can be derived from string theory. We will find it necessary to include the dilaton field Φ ; the solutions to (??) with $\Phi = 0$ are incredibly constrained. But adding only one more field Φ allows for a wealth of new solutions.

The relevant equations of motion are

$$-\frac{da'}{ra} = 2\Phi'^2, (2.259a)$$

$$r^d a \left(\frac{(ab)'}{ar^d}\right)' = \frac{2\kappa^2 r^2}{e^2 L^2} p'^2,$$
 (2.259b)

$$\left(\frac{Zp'}{ar^{d-2}}\right)' = 0, (2.259c)$$

$$4\left(\frac{b}{r^d}\Phi'\right)' = \frac{a}{r^{d+2}}\frac{\partial V}{\partial \Phi} - \frac{\kappa^2 p'^2}{e^2 L^2 a r^{d-2}}\frac{\partial Z}{\partial \Phi}.$$
 (2.259d)

In order, these equations come from the rr and tt components of Einstein's equation, the tt and ii components of Einstein's equation, the tt component of Maxwell's equation, and the dilaton equation. In fact, the Maxwell

equation above is simply Gauss' Law, and so after integrating this equation, we can interpret the integration constant as the charge density Q of the black hole horizon (and the dual field theory):

$$-\frac{e^2Q}{L^{d-2}} = \frac{Zp'}{ar^{d-2}}. (2.260)$$

a is directly determined by the dilaton profile; and then the gauge field p is determined from a and Φ . The coefficient b is related to the gauge field – in the case where the black hole is uncharged, then we find that the computation of b(r) for a black hole geometry reduces to a first order differential equation.

Although (??) can be derived analytically, in practice it is helpful to use numerical differential geometry packages to evaluate the Ricci tensor in Einstein's equations. For convenience, we provide below the Mathematica code necessary to analytically compute (??), employing the RGTC package. The code below will only solve the equations in a specific spacetime dimension d = 2, but is easily changed for any d of interest:

```
\% define the coordinate labels
coords = \{r,t,x,y\};
% define the metric ansatz
g = Diagonal Matrix[{a[r]*L^2/(r^2*b[r]), -a[r]*b[r]*L^2/r^2, L^2/r^2, L^2/r^2}];
% generate R_{MN}, R_{MNRS} etc.
RGtensors[g, coords, {0, 0}];
% define the ansatz for \Phi
Phi := phi[r];
% define the 1-form \nabla_M \Phi.
dPhid := covD[Phi];
% define the ansatz for A_M; the d label reminds us that the index is down
Ad := \{0, p[r], 0, 0\};
\% define F_{MN}
Fdd := Transpose[covD[Ad]] - covD[Ad];
\% define F^{MN}; raise indices
FUU := Raise[Fdd, 1, 2];
```

% \varPhi contributions to the right hand side of Einstein's equations; multiplying tensors together

PhiTdd := 2*Outer[Times,dPhid,dPhid] - (Contract[Outer[Times,dPhid,gUU,dPhid], {1,2},{3,4}]
+ V[Phi])*gdd/2;

% F^2 contributions to the right hand side of Einstein's equations

F2scalar := Contract[Outer[Times, Fdd, FUU], {1, 3}, {2, 4}];

F2Tdd := Z[Phi]*(Contract[Outer[Times, Fdd, gUU, Fdd], {2, 3}, {4, 6}] - F2scalar*gdd/4);

% Einstein's equations; the output is a (0,2) tensor, and vanishes on-shell

EOM1 := Rdd - $R*gdd/2 - k^2/e^2 * F2Tdd - PhiTdd;$

% Maxwell's equations; the output is a (1,0) tensor

 $EOM2 := covDiv[Z[r]*FUU, {1, {2}}];$

% dilaton equation

 $EOM3 := 4*covDiv[Raise[dPhid,1],1] - V'[Phi]/L^2 - Z'[Phi] * F2scalar * k^2/(2*e^2);$

Given this code, one finds a very messy set of equations to then re-organize into (??). At this point, it is an art to pick the right gauge and arrange the equations.

Einstein-Maxwell models: $AdS_2 \times \mathbb{R}^d$

Let us begin with a simple example. We set Z=1 and V=-d(d+1), and assume for simplicity that d>1. (??) then reduces to the Einstein-Maxwell-AdS theory, the response of which we have extensively studied assuming $\mathcal{Q}=0$. So let us now construct the solutions to (??) when $\mathcal{Q}\neq 0$. The fact that $\Phi=0$ immediately implies that a(r)=1. Employing (??), we find that

$$p(r) = \mu - \frac{e^2 Q r^{d-1}}{(d-1)L^{d-2}}. (2.261)$$

If there is a black hole horizon at $r = r_+$, we must fix $p(r_+) = 0$. Indeed, the Killing vector ∂_t vanishes on the horizon, and so must A_t if A is to remain a well-defined 1-form. This immediately tells us that

$$\mu = \frac{e^2 \mathcal{Q} r_+^{d-1}}{(d-1)L^{d-2}}. (2.262)$$

Next, we study (??):

$$\left(\frac{b'}{r^d}\right)' = \frac{2\kappa^2 r^{2-d}}{e^2 L^2} \left(-\frac{e^2 \mathcal{Q} r^{d-2}}{L^{d-2}}\right)^2 = \frac{2\kappa^2 \mathcal{Q}^2 e^2}{L^{2d-2}} r^{d-2}. \tag{2.263}$$

Hence, we find that

$$b(r) = 1 - \left(1 + \frac{\kappa^2 \mathcal{Q}^2 e^2 r_+^{2d}}{d(d-1)L^{2d-2}}\right) \left(\frac{r}{r_+}\right)^{d+1} + \frac{\kappa^2 \mathcal{Q}^2 e^2 r^{2d}}{d(d-1)L^{2d-2}},$$

$$= 1 - \left(1 + \gamma \mu^2 r_+^2\right) \left(\frac{r}{r_+}\right)^{d+1} + \gamma \mu^2 r_+^2 \left(\frac{r}{r_+}\right)^{2d},$$
(2.264)

where we have fixed all integration constants via the boundary conditions b(0) = 1 and $b(r_{+}) = 0$, and defined

$$\gamma = \frac{d-1}{d} \frac{\kappa^2}{e^2 L^2}.\tag{2.265}$$

The resulting black hole is called the AdS-Reissner-Nördstrom (RN) black hole.

Next, we relate r_+ to the temperature T using (??):

$$r_{+} = \frac{\sqrt{(4\pi T)^{2} + 4(d+1)(d-1)\gamma\mu^{2} - 4\pi T}}{2(d-1)\gamma\mu^{2}}.$$
(2.266)

The limiting behavior of r_+ is given by

$$r_{+} \approx \begin{cases} \frac{d+1}{4\pi T} & \mu \ll T \\ \sqrt{\frac{d+1}{(d-1)\gamma}} \frac{1}{\mu} & \mu \gg T \end{cases}$$
 (2.267)

From this, we can read off the entropy density

$$S = \frac{2\pi L^d}{\kappa^2 r_+^d} \sim \max(\mu, T)^d. \tag{2.268}$$

Interestingly, we see that the entropy density is *finite* even at T=0. This is a violation of the third law of thermodynamics, and indeed mollifying this will be an important goal of the more general EMD models. Despite this rather curious feature, the RN black hole is a workhorse of holography, and exhibits many interesting features which do extend to other EMD models, which do not violate the third law of thermodynamics. For completeness, let us note that the energy density and pressure of the dual field theory are

$$\frac{\epsilon}{d} = P = \frac{L^d}{2\kappa^2 r_+^d} \left(1 + \gamma \mu^2 r_+^2 \right).$$
 (2.269)

When $T \gg \mu$, it is straightforward to see from (??) that the geometry is essentially the AdS-Schwarzchild black brane, with some gauge field "hair". However, the fact that $S \sim \mu^d$ when $\mu \gg T$ immediately tells us that the low temperature geometry is not AdS-Schwarzchild, and is something more interesting. Furthermore,

since it is the near-horizon limit of the geometry which controls many IR processes, it is worth determining exactly what this geometry is. To do so, let us switch to the new coordinate

$$\zeta = \frac{1}{r_* - r} \frac{r_*^2}{d(d+1)},\tag{2.270}$$

where we have defined

$$r_* = \sqrt{\frac{d+1}{(d-1)\gamma}} \frac{1}{\mu} \tag{2.271}$$

as the T=0 limit of the horizon location. Let us temporarily fix T=0 exactly. Then $\zeta \to \infty$ as we approach the horizon. Switching from the r coordinate to ζ , as $\zeta \to \infty$:

$$ds^{2} = \frac{L^{2}}{r_{*}^{2}} d\mathbf{x}^{2} + \frac{L^{2}}{d(d+1)} \left[\frac{d\zeta^{2}}{\zeta^{2}} - \frac{dt^{2}}{\zeta^{2}} \right].$$
 (2.272)

The near-horizon geometry is $\mathrm{AdS}_2 \times \mathbb{R}^d$ [?]. The radius of the emergent AdS_2 is

$$L_2 = \frac{L}{\sqrt{d(d+1)}} < L, \tag{2.273}$$

and we will see later that this has very interesting implications for possible instabilities of the near-horizon geometry. Furthermore, we see that this emergent scaling regime in the IR does not involve the spatial coordinates! Following (??), we obtain a dynamic critical exponent $z = \infty$; such a theory is called locally critical. Local criticality also leads to interesting physics, that we will return to later in this chapter.

Finally, let us add a small but finite temperature T. This will lead to the location of the horizon shifting to

$$r_{+} = r_{*} \left[1 - \frac{2\pi T}{(d-1)\gamma\mu^{2}r_{*}} \right] + \mathcal{O}\left(T^{2}\right) \equiv r_{*}(1-\delta).$$
 (2.274)

In this case, we change the definition of ζ slightly:

$$\zeta = \frac{1}{r_*(1 - \delta(d-1)/d) - r} \frac{r_*^2}{d(d+1)}.$$
(2.275)

The metric becomes

$$ds^{2} \approx \frac{L^{2}}{r_{*}^{2}} d\mathbf{x}^{2} + \frac{L^{2}}{d(d+1)} \left[\frac{d\zeta^{2}}{\zeta^{2}} \left(1 - \frac{\zeta^{2}}{\zeta_{+}^{2}} \right)^{-1} - \frac{dt^{2}}{\zeta^{2}} \left(1 - \frac{\zeta^{2}}{\zeta_{+}^{2}} \right) \right]$$
(2.276)

where

$$\zeta_{+} \equiv \frac{1}{2\pi T}.\tag{2.277}$$

Indeed, as one might have guessed, the emergent geometry is $\mathbb{R}^d \times$ an AdS₂-Schwarzschild black brane. Once $T \sim \mu$, this emergent scaling geometry disappears, and we transition back to the AdS_{d+2} black brane.

The zoo of z, θ

Let us now describe a simple family of models, which will have an emergent IR scaling region which can lead to "arbitrary" z and θ [?], up to some constraints which we will derive. These geometries will be supported by a finite charge density Q. Indeed, one finds that for $0 < r < r^*$ the geometry will be approximately AdS, and for $r^* < r$ the geometry will be hyperscaling-violating, where

$$r^* = \hat{\mathcal{Q}}^{-1/d},\tag{2.278}$$

with

$$\hat{\mathcal{Q}} \equiv \mathcal{Q} \frac{e\kappa}{L^{d-1}}.\tag{2.279}$$

As it must, we see that the charge density Q sets the UV cutoff for the emergent scaling region, as at T=0 it is the only dimensional quantity in the problem. In fact, if we rescale $p=(eL/\kappa)\tilde{p}$, and switch to the coordinate $\tilde{r}=r/r^*$, then all dimensional quantities drop out of (??), making it easier to construct scaling solutions.

To do so, plug in the ansatz

$$a = a_{\infty} r^{-(d(z-1)-\theta)/(d-\theta)},$$
 (2.280a)

$$b = b_{\infty} r^{-(d(z-1)+\theta)/(d-\theta)}$$
(2.280b)

into the equations of motion (??). This ansatz will be valid for zero temperature geometries, and we will discuss the extension to finite T shortly. Note that this ansatz is the same as the hyperscaling-violating metrics we have previously studied, albeit in a different coordinate system, which makes it easier to solve the bulk equations. From (??) we find that

$$\Phi = \sqrt{\frac{d[d(z-1) - \theta]}{2(d-\theta)}} \log \frac{r}{r_0} + \text{subleading}$$
(2.281)

with r_0 a constant related to the crossover to AdS. As $\Phi(r)$ must be real, we see that

$$\frac{d(z-1)-\theta}{d-\theta} \ge 0. \tag{2.282}$$

This condition is also sufficient for the geometry to obey the null energy condition [?]. One can now use the remainder of the equations of motion to show that as $\Phi \to \infty$,

$$V(\Phi) = -V_0 e^{-\beta \Phi}, \tag{2.283a}$$

$$Z(\Phi) = Z_0 e^{\alpha \Phi}, \tag{2.283b}$$

with

$$\alpha = (d(d-\theta) + \theta)\sqrt{\frac{8}{d(d-\theta)(dz - d - \theta)}},$$

$$\beta = \theta\sqrt{\frac{8}{d(d-\theta)(dz - d - \theta)}}.$$
(2.284a)

$$\beta = \theta \sqrt{\frac{8}{d(d-\theta)(dz-d-\theta)}}.$$
(2.284b)

The exact prefactors V_0 and Z_0 are not particularly important, but can be found in [?, ?]. Finally, one finds that

$$p \sim r^{-d-dz/(d-\theta)}; \tag{2.285}$$

the prefactor is fixed by (??).

In general, these geometries at T=0 have singularities in the IR at $r=\infty$. At finite θ , this singularity is generally a naked singularity [?]; otherwise if $z \neq 1$, there is a null curvature singularity [?]. And since $r \to \infty$, we see that these geometries do obey the second law of thermodynamics, since the entropy density $S \sim r^{-d} \to 0$ as $r \to \infty$. When $z = 1 + \theta/d$, the IR geometry is not singular [?].

We may also find a class of black hole solutions to (??). To do this, we notice that (??) is satisfied (in the IR scaling region) by

$$b(r) = b_{T=0}(r) + \text{constant} \times r^{d+1}.$$
 (2.286)

Hence, we can add a black hole horizon by modifying

$$b(r) = b_{\infty} r^{-(d(z-1)+\theta)/(d-\theta)} \left[1 - \left(\frac{r}{r_{+}}\right)^{d(1+z/(d-\theta))} \right]$$
(2.287)

Using (??),

$$r_{+} = \left[\frac{4\pi T}{db_{\infty}} \frac{d-\theta}{d-\theta+z}\right]^{-(1-\theta/d)/z},$$
(2.288)

and hence

$$S \sim T^{(d-\theta)/z}. (2.289)$$

As advertised, for general values of d, θ and z, $S \to 0$ as $T \to 0$. Adding any finite T > 0 hides geometric

singularities behind a black hole horizon, and so in this sense the singular nature of the IR geometry is "good" [?].

We can add probe scalars into the EMD background to compute correlation functions of scalar operators beyond the one sourced by the dilaton. This should generically be done through the action

$$S_{\phi} = -\frac{1}{2} \int d^{d+2}x \sqrt{-g} \left((\partial \varphi)^2 + B(\Phi) \varphi^2 \right)$$
 (2.290)

for a probe scalar φ . If the profile $B(\Phi) = m^2/L^2$, then for $\theta \neq 0$ these operators are gapped, with $G(x) \sim e^{-mx}$ [?]. However, if we make the choice [?]

$$B(\Phi(r)) = \frac{B_0 b(r)}{L^2 a(r)}, \quad (\Phi \to \infty), \tag{2.291}$$

then in the IR, this probe scalar has Green's functions of the form $G(x) \sim x^{-2\Delta'}$, with the dimension Δ' given by

$$B_0 = \left(\Delta' - \frac{d+z}{2}\right)^2 - \left(\frac{d-\theta+z}{2}\right)^2. \tag{2.292}$$

Note that $B(\Phi) \sim e^{-\beta \Phi}$.

We derived the thermodynamics of a theory with exponents z and θ in (??). If we apply the standard holographic dictionary at an asymptotically AdS boundary (assuming that the emergent scaling geometry connects to an asymptotically AdS space in the UV), the thermodynamics of this black hole need not obey (??). Indeed, let us take the example of the AdS-RN black hole, where $P(\mu, T)$ given in (??) is consistent with (??) when z = 1 and $\theta = 0$. (??) is not optional – in particular, (??) follows from a Ward identity in a Lifshitz theory [?]. The resolution to this puzzle is that there can be an "emergent stress tensor" $\mathcal{T}_{\mu\nu}$ (generally with $\mathcal{T}_{ti} \neq \mathcal{T}_{it}$), which deviates from the UV $T_{\mu\nu}$, and does obey Lifshitz Ward identities: see e.g. [?].

Anomalous scaling of charge density

The EMD models described in the previous subsection seem to exhibit a very curious effect: anomalous scaling of the charge density operator! This is quite surprising. Conventional wisdom is that J^{μ} can pick up no anomalous dimensions [?, ?]; indeed, the gauge invariant derivative in ordinary QFT is $\nabla_{\mu}-iA_{\mu}$, implying that A can pick up no anomalous dimensions. Nonetheless, let us explore the possibility, introducing an exponent Φ such that $[n] = d - \theta + \Phi$ [?]. We do not have any microscopic model (beyond a similar free fermion construction in the large N limit [?]) with $\Phi \neq 0$. Exotic theories with temperature-dependent fractionalization [?] could avoid the non-renormalization theorems on anomalous dimensions for J^{μ} .

The most common way that Φ is detected in holography is through the conductivity σ . In fact, this is also a slightly subtle issue, because as we will see in the next section, in charged matter it is not clear which conductivity one should be computing! Sweeping this issue aside for now, the conductivity is expected to scale as [?]

$$\sigma \sim T^{(d-2-\theta+2\Phi)/z}. (2.293)$$

For the EMD models we have just discussed, we find $\Phi = z$. If the charge density is irrelevant, one can find more general values of Φ [?]. Another interesting possibility for realizing the exponent Φ in holographic models involves the use of probe brane physics [?]. We will discuss probe brane models in §??. Probe brane realizations do not require violation of current conservation in the QFT. Additional models which exhibit this anomalous scaling include Proca bulk actions [?]. One should be cautious about the latter models – recall from (??) that broken gauge invariance in the bulk implies that in the boundary theory, $\partial_{\mu}J^{\mu} \neq 0$.

Rather surprisingly, it is still not known the extent to which Φ imprints itself on thermodynamic quantities, and if it does so in a manner consistent with the 3 emergent scaling exponents z, θ and Φ .

Hidden Fermi surfaces?

Many of the condensed matter models studied at the start of this chapter contained a Fermi surface. Now that we have constructed the holographic dual to quantum matter at finite density, we can ask whether or not our models contain such Fermi surfaces (or rather, a strongly coupled analogue of them). For the remainder of this chapter, we will present some of the proposals for how holography realizes a Fermi surface, though we *strongly* emphasize that this question is far from settled. Here, we begin by discussing the possibility for a "hidden Fermi surface".

Spectral weight: zero temperature

One of the most important signatures of a Fermi surface is the presence of non-vanishing spectral weight $\lim_{\omega\to 0} \omega^{-1} \operatorname{Im} G^{\mathbb{R}}$ at finite momentum. Let us begin by studying models at T=0. For non-interacting fermions, the spectral weight of certain operators will diverge on a finite momentum shell, which is (by definition) where the low energy excitations reside.

Let us now show that the AdS-RN black hole is dual to a field theory with spectral weight at finite momentum. More precisely, we will focus on a neutral scalar operator of UV dimension Δ , and will comment on other operators later. We need to solve the equations of motion for a massive scalar field in the AdS-RN background. Given our previous experience, we expect that the low energy spectral weight will be completely fixed, at least qualitatively, by the IR geometry $(AdS_2 \times \mathbb{R}^d)$. We will go ahead and make this assumption,

justifying it at the end of the calculation.

In the near-horizon $AdS_2 \times \mathbb{R}^d$ geometry, the equation of motion for a massive scalar field φ at spatial momentum k and frequency ω is

$$\frac{1}{\sqrt{-g}}\partial_M\left(\sqrt{-g}g^{MN}\partial_N\varphi\right) = \frac{\zeta^2}{L_2^2}\partial_\zeta^2\varphi + \frac{\zeta^2}{L_2^2}\omega^2\varphi - k^2\frac{r_*^2}{L^2}\varphi = \frac{\Delta(\Delta - d - 1)}{L^2}\varphi. \tag{2.294}$$

We begin by assuming $\omega = 0$. The two linearly independent solutions to (??) are power laws:

$$\varphi_0(\mathbf{k},\zeta) = A_1 \zeta^{\frac{1}{2} - \nu_k} + A_2 \zeta^{\frac{1}{2} + \nu_k}, \tag{2.295}$$

where ν_k is given by

$$\nu_k \equiv \sqrt{\frac{1}{4} + \Delta(\Delta - d - 1)\frac{L_2^2}{L^2} + \left(\frac{kr_*L_2}{L}\right)^2}.$$
 (2.296)

Once again, we see a remarkable feature of the emergent $AdS_2 \times \mathbb{R}^d$ geometry [?]. Each momentum k has decoupled from the others – we have a zoo of operators with a continuum of operator dimensions, signifying the large number of degrees of freedom at low energy. We will return to this point shortly once we have computed the actual Green's functions.

What happens at finite ω ?¹⁰ So long as $\omega \zeta \ll 1$, (??) is a good approximation to the solutions of (??), even at finite ω . But when $\omega \zeta \gtrsim 1$, we cannot use (??). Instead, imposing infalling boundary conditions at the horizon, we find that the approximate solution to (??) is

$$\varphi(\zeta \gg 1/\omega) \approx e^{-i\omega\zeta}$$
. (2.297)

We need to match this onto the solution (??). This can be done qualitatively (in very general circumstances) through the following line of logic. In the "transition region" $\zeta \sim \zeta_{\omega} \equiv 1/\omega$, continuity of φ and $\partial_{\zeta} \varphi$ demands that (without fine tuning)

$$A_1 \zeta_{\omega}^{\frac{1}{2} - \nu_k} \sim A_2 \zeta_{\omega}^{\frac{1}{2} + \nu_k}, \quad \text{and} \quad \partial_{\zeta} \left(A_1 \zeta^{\frac{1}{2} - \nu_k} \right) \Big|_{\zeta = \zeta_{\omega}} \sim \left. \partial_{\zeta} \left(A_2 \zeta^{\frac{1}{2} + \nu_k} \right) \right|_{\zeta = \zeta_{\omega}}.$$
 (2.298)

If this is not true, then we have to have a miracle: one term in (??) and its derivative smoothly connect with the solution in (??). This generically does not happen. Assuming $\nu_k = \mathcal{O}(1)$, then both conditions in (??) are qualitatively the same and we conclude that for $\zeta \omega \ll 1$:

$$\varphi(\mathbf{k},\omega,\zeta) = A_1 \zeta^{\frac{1}{2} - \nu_k} \left(1 + \mathcal{A}(\omega\zeta)^{2\nu_k} \right), \tag{2.299}$$

¹⁰ If we study charged bosons with bulk charge q, the low energy limit shifts from $\omega \to 0$ to $\omega_{\perp} \to 0$, where $\omega_{\perp} = \omega - \mu q$.

with \mathcal{A} a complex constant (as (??) is complex). By linearity, we may set $A_1 = 1$ without loss of generality. If we "assume" the holographic dictionary just relates $G_{\mathcal{O}\mathcal{O}}^{\mathbb{R}} \sim A_2/A_1$, then we estimate that the spectral weight is

$$\frac{\operatorname{Im}\left(G_{\mathcal{O}\mathcal{O}}^{\mathrm{R}}\right)}{\omega} \sim \omega^{2\nu_k - 1}.\tag{2.300}$$

Of course, this argument is a bit fast – we've only proven the holographic dictionary in the UV! Let us denote with $\varphi_{1,2}(\mathbf{k},\omega,r)$ the solutions to the full scalar equation of motion which asymptote to the $A_{1,2}$ terms in (??) in the near-horizon region. In the UV as $r \to 0$,

$$\varphi_1 = \frac{B_{1-}}{L^{d/2}} r^{d+1-\Delta} + \frac{B_{1+}}{(2\Delta - d - 1)L^{d/2}} r^{\Delta} + \cdots$$
 (2.301)

We define $B_{2\pm}$ analogously for φ_2 . All the B coefficients are real – the only factors of i emerge from (??). If (??) is the near-horizon solution to the equations of motion as $\omega \to 0$, then the solution to the full equations of motion must be

$$\varphi(\mathbf{k}, \omega, r) \approx \varphi_1(\mathbf{k}, \omega, r) + \mathcal{A}\omega^{2\nu_k}\varphi_2(\mathbf{k}, \omega, r). \tag{2.302}$$

We are still assuming that ω is small, and neglecting subleading contributions in ω/μ . We can now apply the holographic dictionary in the UV. The retarded Green's function is

$$G_{\mathcal{O}\mathcal{O}}^{R}(\mathbf{k},\omega) = \frac{B_{1+} + B_{2+}\mathcal{A}\omega^{2\nu_{k}}}{B_{1-} + B_{1-}\mathcal{A}\omega^{2\nu_{k}}}.$$
(2.303)

Evidently, $\mathcal{A}\omega^{2\nu_k}$ is not the full Green's function. However, \mathcal{A} is the only complex coefficient in the full Green's function. So we see that in fact, the spectral weight given in (??) is correct, despite completely ignoring the UV geometry!

For $|2\Delta - d - 1| < \sqrt{d+1}$, as $k \to 0$, (??) gives $2\nu_k < 1$. Hence,

$$\lim_{\omega \to 0} \frac{\operatorname{Im} \left(G_{\mathcal{O}\mathcal{O}}^{\mathbf{R}}(\omega, \mathbf{k}) \right)}{\omega} = \begin{cases} \infty & k < k_* \\ 0 & k > k^* \end{cases}, \tag{2.304}$$

where

$$k_* = \sqrt{\frac{\Delta(d+1-\Delta)}{r_*^2} - \left(\frac{L}{2L_2r_*}\right)^2}.$$
 (2.305)

Even at T = 0, there is a soup of low energy excitations present in the dual of the AdS-RN geometry. This is not the usual Fermi surface, but perhaps a signature of something similar. We will provide further discussion after we generalize this computation to finite temperature. In general, models with finite z and θ have exponentially suppressed (or strictly vanishing, in some cases) spectral weight as $\omega \to 0$ with k fixed [?]. These calculations are quite cumbersome in general, but a simple calculation can be done for a pure CFT. In this case, we have $G_{\mathcal{O}\mathcal{O}}^{\mathbb{R}} \sim (k^2 - \omega^2)^{2\Delta - d - 1}$, which is completely real for $\omega < k!$ In this case, the spectral weight trivially vanishes at low momenta.

Spectral weight: finite temperature

In this section, we will directly compute the spectral weight of a scalar operator at finite temperature T: $\lim_{\omega \to 0} \omega^{-1} G_{\mathcal{O}\mathcal{O}}^{\mathbb{R}}(\omega, \mathbf{k})$. We employ a "modern" Wronskian approach, developed in [?]. To begin, let us consider the equations of motion associated with a neutral scalar (with action (??)) in the background (??):

$$L^{2}B(\Phi)\varphi(\mathbf{k},\omega,r) + k^{2}r^{2}\varphi(\mathbf{k},\omega,r) - \omega^{2}\frac{r^{2}}{ab}\varphi(\mathbf{k},\omega,r) = ar^{d+2}\left(\frac{b}{r^{d}}\varphi(\mathbf{k},\omega,r)'\right)'. \tag{2.306}$$

The crucial observation is that this equation only depends on ω^2 , not ω . Hence, to linear order in ω , we may write

$$\varphi(\mathbf{k}, \omega, r) = \varphi_0(\mathbf{k}, r) + \omega \varphi_{\mathrm{I}}(\mathbf{k}, r) + \mathcal{O}(\omega^2). \tag{2.307}$$

At first glance, the zero of b(r) at the horizon means that we cannot ignore ω when solving (??). However, upon taking $r \to r_+$, infalling boundary conditions (??) amount to

$$\varphi(r \to r_+, \omega) = \text{constant} \times \left(1 - \frac{r}{r_+}\right)^{-i\omega/4\pi T}.$$
 (2.308)

So if we work at fixed $r_+ - r$, and take $\omega \to 0$, we may safely expand

$$\left(1 - \frac{r}{r_{+}}\right)^{-\mathrm{i}\omega/4\pi T} = 1 + \frac{\mathrm{i}\omega}{4\pi T}\log\frac{r_{+}}{r_{+} - r} + \mathcal{O}\left(\omega^{2}\right).$$
(2.309)

We only need to find a solution which has this precise logarithmic singularity near the horizon to capture the $\mathcal{O}(\omega)$ response.

Suppose now that we know the regular solution φ_0 to (??), and that we have normalized it so that $\varphi_0(\mathbf{k}, r \to 0) \sim r^{d+1-\Delta}/L^{d/2}$ (i.e. it is sourced by unity). We can construct the singular solution as an integral (we have conveniently normalized it):

$$\varphi_1(\mathbf{k}, r) = \frac{\varphi_0(\mathbf{k}, r)}{L^d} \int_0^r ds \frac{s^d}{b(s)\varphi_0(\mathbf{k}, r)^2}.$$
 (2.310)

Near r = 0,

$$\varphi_1(\mathbf{k}, r \to 0) \approx \frac{1}{2\Delta - d - 1} \frac{r^\Delta}{L^{d/2}}.$$
(2.311)

Near $r = r_+$, this solution is singular. The integral expression (??) makes clear that this singular behavior comes from the factor of b(s) in this integral:

$$\varphi_1(\mathbf{k}, r \to r_+) \approx \frac{r_+^d}{4\pi T L^d \varphi_0(\mathbf{k}, r_+)} \log \frac{r_+}{r_+ - r} + \text{regular}.$$
(2.312)

Using the same logic as before, if we wish to compute Green's functions of the operator \mathcal{O} dual to φ to linear order in ω , it will consist of a sum of two terms with (??) obeyed as $r \to r_+$. Hence

$$\varphi(\mathbf{k}, r, \omega) = \varphi_0(\mathbf{k}, r) + \frac{\mathrm{i}\omega L^d}{r_\perp^d} \varphi_0(\mathbf{k}, r_+)^2 \varphi_1(\mathbf{k}, r) + \mathcal{O}\left(\omega^2\right). \tag{2.313}$$

Combining (??), (??), (??), (??), and analyticity properties of Green's functions, we obtain

$$\lim_{\omega \to 0} \frac{\operatorname{Im} \left(G_{\mathcal{O}\mathcal{O}}^{\mathbb{R}}(\omega, \mathbf{k}) \right)}{\omega} = \frac{L^d}{r_+^d} \varphi_0(\mathbf{k}, r)^2. \tag{2.314}$$

The finite temperature spectral weight computed above plays a crucial role in the theory of transport in (almost) clean metals that we will develop in §??.

It is often quite easy to determine the scaling behavior of $\varphi_0(\mathbf{k}, r)$, and hence calculate the spectral weight, at least qualitatively. Let us return to the example of the spectral weight of an operator with $k \ll \mu$ in the AdS-RN background; however, now we will turn on a very small temperature $T \ll \mu$. Let us now construct (up to $\mathcal{O}(1)$ prefactors) the solution $\varphi_0(\mathbf{k}, r)$. We take $B(\Phi) = \Delta(\Delta - d - 1)/L^2$, as usual.

Extremely close to the horizon, we demand that $\varphi_0(\mathbf{k},r)$ is a regular function. Expanding φ_0 as

$$\varphi_0(\mathbf{k}, r) = C_0(\mathbf{k}) + C_1(\mathbf{k}) \frac{r_+ - r}{4\pi T} + \cdots,$$
 (2.315)

then regularity at the horizon imposes the Robin boundary condition¹¹

$$(L^2B(\Phi(r_+)) + k^2r_+^2)C_0(\mathbf{k}) = a(r_+)r_+^2C_1(\mathbf{k}).$$
(2.316)

Temporarily switching to the ζ coordinate defined in (??), we explore the evolution of $\varphi_0(\mathbf{k}, \zeta)$. For $\zeta \ll \zeta_+$ (the horizon), we may write φ a sum of two power laws, just as in (??). When $\zeta \sim \zeta_+$, we must connect

¹¹This is employed frequently when looking for numerical solutions to holographic problems, as it avoids any "shooting" or "peeling" method, and so can be applied directly to very complicated set-ups.

this function to a regular function which obeys the near horizon equations of motion. We fix $A_{1,2}$ identically to the previous computation, but with ζ_+ playing the role of $1/\omega$. Up to $\mathcal{O}(1)$ factors:

$$\varphi_0(\mathbf{k},\zeta) \approx A_1 \zeta^{\frac{1}{2} - \nu_k} \left[1 + \left(\frac{\zeta}{\zeta_+} \right)^{2\nu_k} \right]$$
(2.317)

Just as the ω -scaling of the spectral weight was unaltered at T=0, here the UV geometry will not alter the T-scaling of the spectral weight. We further emphasize that it is the *smaller* of the two terms in (??) which determined the overall scaling. Using (??), the spectral weight is

$$\lim_{\omega \to 0} \frac{\operatorname{Im} \left(G_{\mathcal{O}\mathcal{O}}^{\mathbb{R}}(\omega, \mathbf{k}) \right)}{\omega} = \frac{L^d}{r_+^d} A_1^2 \zeta_+^{1 - 2\nu_k} \sim T^{2\nu_k - 1}, \tag{2.318}$$

where we have employed the fact that r_+ is independent of T for the AdS-RN geometry. Just as in our finite ω computation, we see that there is a power law spectral weight at finite momentum in these locally critical theories.

The argument above immediately extends to EMD theories at finite z and θ . In this case, one solves (??) at $\omega = 0$ and find [?]

$$\varphi_0(\mathbf{k}, r) = r^{\frac{d}{2}(1 + \frac{z}{d-\theta})} \left(A_1 \mathbf{K}_a(|\mathbf{k}| r^{d/(d-\theta)}) + A_2 \mathbf{I}_a(|\mathbf{k}| r^{d/(d-\theta)}) \right). \tag{2.319}$$

where $a \equiv [2\Delta - \theta - d - z]/2$. The steps are identical to before. If $k \lesssim T^{1/z}$, then the Bessel functions can be approximated by two power laws, and after a bit more algebra we obtain, employing (??) to relate r_+ to T in an EMD background:

$$\lim_{\omega \to 0} \frac{\operatorname{Im} \left(G_{\mathcal{O}\mathcal{O}}^{R}(\omega, \mathbf{k}) \right)}{\omega} \sim T^{(2\Delta - 2z - d)/z}. \tag{2.320}$$

In contrast, when $k \gtrsim T^{1/z}$, then the Bessel functions are exponentially suppressed, and we obtain

$$\lim_{\omega \to 0} \frac{\operatorname{Im} \left(G_{\mathcal{O}\mathcal{O}}^{R}(\omega, \mathbf{k}) \right)}{\omega} \sim \exp \left[-C \frac{k}{T^{1/z}} \right], \tag{2.321}$$

with a constant C depending on the UV scale (typically charge density Q) which supports the emergent scaling geometry.

In particular, we see that for any finite z and θ , as $T \to 0$ all finite momentum spectral weight is exponentially suppressed. In contrast, the AdS-RN black hole has (power law) spectral weight supported at finite momentum. This led [?] to argue that only the latter geometries might have hidden "Fermi surfaces".

To explore this further, we can introduce a curious scaling limit where

$$z \to \infty$$
 with $-\frac{\theta}{z} \equiv \eta$ fixed. (2.322)

Note that $S \sim T^{\eta}$ will now vanish at T = 0, so long as $\eta > 0$. It is perfectly consistent to use our EMD geometries to study this limit. This limit preserves the power law spectral weight at finite momentum, up until momenta of order $Q^{1/d}$ [?]. The details of this computation are similar to, but more complicated than, what we have presented above. As $T \to 0$, we see from (??) that the spectral weight will diverge whenever $2\nu_k < 1$. When one looks at the spectral weight of the conserved current [?], in the AdS-RN background $2\nu_k \ge 1$, and so there is no diverging spectral weight at finite momentum. However, as ν_k is η dependent, at finite η , [?] found diverging spectral weight for $k < k_c$, a momentum scale of order μ (up to η -dependent prefactors).

As we have seen, for a non-interacting Fermi surface, we would expect spectral weight only on a (d-1)dimensional surface in momentum space. Hence, the finite η model above does not have a standard Fermi
surface. More carefully, one might argue that the finite η model does not have a *single* Fermi surface, but
may have many Fermi surfaces. We will come back to this question at the very end of this section.

Although the finite η limit above might seem a bit artificial, it does in fact occur in top-down holographic models: see e.g. [?], which has $\eta = 1$ (not explicitly stated).

Logarithmic violation of the area law of entanglement

Another test for the presence of Fermi surfaces relates to entanglement entropy. Consider a theory of free fermions which form a (d-1)-dimensional Fermi surface. It is known that the entanglement entropy of a spatial region of size R is [?, ?]

$$S = \left(\frac{R}{\epsilon}\right)^{d-1} \log \frac{R}{\epsilon}.$$
 (2.323)

This result can intuitively be understood by thinking of the low energy excitations near the Fermi surface as a collection of chiral fermions forming CFT2s at each point on the Fermi surface [?]. Hence, the logarithm is related to (??), and the area prefactor simply counts the number of these CFT2s.

[?] pointed out that this logarithmic area law violation may be a generic property of QFTs with hyperscaling violating exponent $\theta = d - 1$. For simplicity, let us employ the metric (??) in the calculation below. Using a holographic calculation similar to that presented in §??, we find that the entanglement entropy of

a sphere of radius R is given by

$$S = S_{\text{UV}} + \frac{L^d}{4G_{\text{N}}} \int \frac{\mathrm{d}r \, \rho^{d-1}}{R_*^{\theta} r^{d-\theta}} \sqrt{1 + \left(\frac{\mathrm{d}\rho}{\mathrm{d}r}\right)^2}.$$
 (2.324)

 $S_{\rm UV}$ is the contribution from the asymptotically AdS region, and has a characteristic area law: $S_{\rm UV} \sim (R/\epsilon)^{d-1}$. If $d-\theta > 1$, then we see that the integral in the hyperscaling violating region above is dominated by small r, leading to a further (finite) contribution to the area law. However, if $\theta = d-1$, then the integral scales as dr/r. This is just like the CFT2 case that we previously studied, which had a logarithmic area law violation. So we expect that in this case (schematically):

$$S \sim \left(\frac{R}{\epsilon}\right)^{d-1} + \left(\frac{R}{R_*}\right)^{d-1} \log \frac{R}{R_*} \tag{2.325}$$

A more careful calculation indeed confirms this [?]. Note that in the hyperscaling-violating EMD geometries supported by a finite charge density that we constructed earlier, $R_* \sim \mathcal{Q}^{-1/d}$. If $\theta > d-1$, then the integral (??) is dominated in the IR, and we find power law violations of the area law. In order to prevent this, we generically require that

$$\theta \le d - 1. \tag{2.326}$$

It seems natural to speculate that such logarithmic violations of the area law are signatures of a hidden Fermi surface. However, when $\theta = d-1$ and z are finite, then there is no spectral weight at finite momentum in any "canonical" operators (as we have discussed).

Fermions in the bulk I: classical effects

The holographic dictionary

We will now turn to the second possibility for realizing a Fermi surface in holography. Suppose that the boundary theory had fermionic operators whose correlation functions were of interest. Then the AdS/CFT dictionary tells us that the bulk theory itself must contain fermionic fields. So, we write down an action for Dirac fermions in the bulk

$$S_{\text{bulk fermions}} = -i \int d^{d+2}x \sqrt{-g} \left\{ \bar{\Psi} \Gamma^M \left(\partial_M + \frac{1}{4} \omega_{MAB} \Gamma^{AB} - iq A_M \right) \Psi - m \bar{\Psi} \Psi \right\}. \tag{2.327}$$

Here $\{\Gamma^M, \Gamma^N\} = 2\delta^{MN}$ are d+2 Gamma matrices in the bulk, and ω is the spin connection, necessary to describe fermions on curved spaces.

Unlike the scalar fields we have studied so far, this action is manifestly first order, and so we must revisit the basic holographic dictionary [?]. As the computations are similar to those for scalar fields, we will skip most details and outline the necessary changes. Crudely speaking, we think of writing down a second order equation for half of the components of the bulk spinor. It is this half of the bulk spinor which is dual to fermionic operators in the boundary theory. If d + 2 is odd, this is perfectly acceptable since the number of spacetime dimensions is odd and hence the bulk fermion lives in a higher dimensional spacetime. If d + 2 is even, then we must study "half" of a Dirac spinor in the boundary theory – namely, a Weyl spinor.

If the bulk metric depends only on r, we may make the change of variable [?]

$$\Psi = (-gg^{rr})^{-1/4}\mathcal{X},\tag{2.328}$$

in which case the equation of motion associated with (??) becomes

$$e_A^a \Gamma^A (\partial_a - iq A_a) \mathcal{X} = m \mathcal{X}. \tag{2.329}$$

The vielbein can be chosen as $e_A^a = \sqrt{|g^{aa}|}$. Near the asymptotically AdS boundary, this equation reads

$$\Gamma^r \frac{r}{L} \partial_r \mathcal{X} = m\mathcal{X} + \cdots \tag{2.330}$$

which is solved by

$$\Psi = \psi_{+}(x)r^{(d+1)/2+mL} + \psi_{-}(x)r^{(d+1)/2-mL}.$$
(2.331)

Here $\Gamma^r \psi_{\pm} = \pm \psi_{\pm}$ – this is the "splitting" of the bulk spinor in half, as advertised. One can further show that

$$mL = \Delta - \frac{d+1}{2},\tag{2.332}$$

with Δ the operator dimension of the fermionic boundary operator. To apply holographic renormalization to bulk fermions, a boundary counterterm proportional to $\bar{\Psi}\Psi$ is required. At the end of the day, one finds that ψ_+ is the source term for the boundary fermion, and ψ_- is proportional to the expectation value of the boundary fermionic operator.

Bulk fermions around charged black holes

Let us now discuss the two point functions of probe bulk fermions in the AdS-RN background [?, ?, ?, ?], at temperatures $T \ll \mu$. The computation is rather similar to bulk scalar fields, and so we simply quote the

generic form of the result:

$$G^{R}(\omega, k) = \frac{\mathcal{B}_{1}(\omega, k) + \omega^{2\nu_{k}} \mathcal{B}_{2}(\omega, k)}{\mathcal{B}_{3}(\omega, k) + \omega^{2\nu_{k}} \mathcal{B}_{4}(\omega, k)},$$
(2.333)

where now

$$\nu_k = \sqrt{m^2 L_2^2 + \frac{k^2 r_*^2 L_2^2}{L^2} - \frac{q^2 e^2}{2d(d-1)}}$$
 (2.334)

and all the \mathcal{B} functions are regular. Once again, the emergent AdS_2 geometry controls the scaling dimensions of operators with $k \lesssim \mu$, which become momentum dependent, and given by $\nu_k + 1/2$. Note that if q is large enough, ν_k can become complex. This demonstrates an instability of this black hole, which we will resolve at the end of §??.

We focus on the limit where $\omega \to 0$, and q = 0 (uncharged bulk fermions). In this case, we may generically find that $\mathcal{B}_3 = 0$ for some special value of k, which we will call $k_{\rm F}$. Denoting $k_{\perp} = k - k_{\rm F}$ to be the momentum transverse to this critical value (as the theory is isotropic), we then generically find

$$G^{\rm R}(\omega, k_{\perp}) \approx \frac{Z}{\omega - v_{\rm F} k_{\perp} + \omega^{2\nu_k} \tilde{\Sigma}} + \cdots,$$
 (2.335)

with $\tilde{\Sigma}$ generically complex, but approximately constant in the limit $k_{\perp}, \omega \to 0$. Indeed, (??) looks like the two point function of a fermionic particle, with a Fermi surface at momentum $k_{\rm F}$, and with self-energy $\Sigma(k_*,\omega) = \omega^{2\nu_k}\tilde{\Sigma}$. In particular, the imaginary part of Σ corresponds to the "decay rate" of this excitation. Let us now contrast this generic result with the Fermi liquid result (??):

- 1. If $2\nu_k > 1$, then as $\omega \to 0$, (??) may be approximated as $G^R = Z(\omega v_F k_\perp)^{-1}$. The fermion propagator genuinely resembles that of the Fermi liquid. In this case, there is a long-lived quasiparticle, but its decay occurs via interactions with a locally critical bath and is not governed by the standard Fermi liquid phenomenology.
- 2. When $2\nu_k = 1$, then (??) becomes

$$G^{\rm R}(\omega, k_{\perp}) \approx \frac{Z}{\omega - v_{\rm F} k_{\perp} - \tilde{\Sigma} \omega \log(\omega/\mu)} + \cdots$$
 (2.336)

Such a Green's function was postulated in 1989 [?] to explain curious experimental properties of the cuprates, and is coined the "marginal Fermi liquid". This possibility is finely tuned in the AdS-RN black hole, but it is interesting to see these connections with a much older model.

3. If $2\nu_k < 1$, then as $\omega \to 0$, (??) is $G^{\rm R} \approx Z(\tilde{\Sigma}\omega^{2\nu_k} - v_{\rm F}k_{\perp})^{-1}$, and does not look like a long lived quasiparticle.

Of course, we have not discussed what the actual value of $k_{\rm F}$ is for these uncharged fermions, if it even exists, and which of the three categories we fall into. The reason for this is because once we allow for $q \neq 0$, all three possibilities can be realized.

Whenever such Fermi surfaces appear, as $k \to 0$ ν_k becomes imaginary. This indicates an instability of the low energy $AdS_2 \times \mathbb{R}^d$ geometry. The resolution of such an instability is the electron star – the subject of the next section.

A natural question to ask is whether this "Fermi surface" phenomenology appears in genuine top-down holographic constructions. We simply refer the reader to the long literature on this, with some supergravity truncations forbidding Fermi surfaces [?] and others allowing them [?], including both $\mathcal{N}=4$ SYM [?] and ABJM theory [?].

Semi-holography

A very intuitive understanding of (??), coined "semi-holography", was put forth in [?]. Let us consider a generic quantum system with a "free fermion" ψ coupled to a strongly interacting sector, via the action

$$S = S_{\text{strong}}[\chi, \ldots] + \int d^{d+1}x \left[\psi^{\dagger} \left(i\partial_t - \varepsilon(\partial_i) \right) \psi + \lambda \psi^{\dagger} \chi + \lambda \chi^{\dagger} \psi \right]. \tag{2.337}$$

Now, let us suppose that the χ fermion has a holographic dual which can be described by the AdS-RN geometry. The fact that χ has a holographic dual implies that in the large N limit, the only propagator which is not suppressed by a power of N is the two point function $\langle \psi^{\dagger} \psi \rangle$ – this is because in the bulk, the action for the field Ψ dual to χ is quadratic up to 1/N corrections. Hence, employing the bare Green's functions

$$G_{\psi\psi}^0 = \frac{1}{\omega - \varepsilon(k)}, \quad G_{\chi\chi}^0 = c\omega^{2\nu_k}, \tag{2.338}$$

with the latter Green's function coming from holography, the Green's function may be computed exactly as a sum of ladder diagrams:

$$G_{\chi\chi} = \sum_{n=0}^{\infty} G_{\psi\psi}^{0} \left(\lambda G_{\chi\chi}^{0} G_{\psi\psi}^{0}\right)^{n} + \mathcal{O}\left(N^{-1}\right) = \frac{1}{\omega - \varepsilon_{k} - \lambda c\omega^{2\nu_{k}}}$$
(2.339)

which matches the qualitative form of (??) up to the normalization coefficient, and upon "zooming in" near a Fermi surface where $\varepsilon_k \approx v_{\rm F}(k-k_{\rm F})$.

The non-trivial input above comes from $G_{\chi\chi}^0$, and so the large N limit was still essential in suppressing higher order correlation functions. Also crucial is local criticality, which ensures that $G_{\chi\chi}^0$ is suppressed only as a power law in ω , even at finite momentum $k_{\rm F}$. One could imagine other strongly interacting large N

models which could be solved and provide similar phenomenology. So long as this new model maintains a sense of local criticality, the essential physics of (??) could be reproduced beyond holography.

A somewhat similar proposal has also been made for understanding the emergence of hydrodynamic modes in strongly coupled theories [?].

Fermions in the bulk II: quantum effects

So far, we have focused on the probe effects of bulk fermions. This realizes interesting physics, but maintains a serious drawback – a serious violation of Luttinger's theorem (??). Recall that all of the charge Q is carried by the fermions which form the Fermi surface in an ordinary Fermi liquid. When we have studied probe fermions in the AdS-RN background, all of the charge is hidden behind the horizon, as enforced by the bulk Gauss law. We have seen a condensed matter analogue of this physics in our discussion of emergent gauge fields. The fermions sitting above the horizon are the analogue of a $\mathcal{O}(1)$ number of cohesive fermions (we will have more to say on this shortly). But the microscopic theory could contain $\mathcal{O}(N^2)$ fractionalized fermions – if these objects are not neutral under deconfined gauge fields, they must remain hidden behind the horizon in the bulk.

Do these deconfined fermions also exhibit Fermi surfaces? It has been argued (see e.g. [?]) that the probe fermions will have the same behavior as fermionic matrix degrees of freedom (which would contain the $\mathcal{O}(N^2)$ fermions required to make up the charge on the horizon). More recently, methods have been proposed to realize finite fractions of the $\mathcal{O}(N^2)$ electric charge in floating "fermionic clouds" above the horizon, and we will focus on this approach below. Of course, fermions obey a Pauli exclusion principle, and so a treatment of "condensed" fermions is necessarily more complicated, and requires taking into account quantum mechanical effects in the bulk. We will outline some of the approaches to solve this problem below.

Luttinger's theorem in holography

Let us begin by studying a free bulk Dirac fermion in the bulk, of charge q, coupled to an EMD theory. For simplicity we assume zero temperature. We may integrate out the fermion, finding the bulk action

$$S = S_{\text{EMD}} - \operatorname{tr}\log\left(i\Gamma^{\mu}D_{\mu} + m\right). \tag{2.340}$$

Employing standard many-body manipulations (ignoring time derivatives)

$$S = S_{\text{EMD}} - V_d \sum_{l} \int \frac{\mathrm{d}^d \mathbf{k}}{(2\pi)^d} \epsilon_l(\mathbf{k}) \Theta(-\epsilon_l(\mathbf{k})), \qquad (2.341)$$

where V_d is the spatial volume of the boundary theory, $\epsilon_l(\mathbf{k})$ are the eigenvalues of the bulk Dirac equation, with eigenspinors $\chi_l(\mathbf{k}, r)$, subject to appropriate boundary conditions [?, ?]. (??) is the statement that the free energy is just the energy of all the occupied sites in the bulk Fermi sea. $\epsilon_l(\mathbf{k})$ is implicitly a function of the background EMD fields.

As advertised, we are seeing the Pauli exclusion principle at work in the effective action (??). Indeed, the bulk geometry we are studying contains fermionic matter placed into its lowest energy states. We will see shortly the physical consequences of this fermionic matter. But for now, purely from the gravitational perspective, let us note that this construction is very reminiscent of the standard theory of astrophysical stars. As the fermions floating in the EMD background are charged, we will call these "electron stars" [?]. We will shortly discuss the gravitational solutions corresponding to such stars, but first let us return to the question of fractionalization.

To do so we study the equation of motion of the bulk gauge field [?]. Assuming the ansatz A = p(r)dt, as usual, we obtain

$$\frac{1}{e^2} \partial_r \left(\sqrt{-g} g^{rr} g^{tt} \partial_r p \right) = q \sum_l \int \frac{\mathrm{d}^d \mathbf{k}}{(2\pi)^d} \Theta(-\epsilon_l(\mathbf{k})) \chi_l^{\dagger}(\mathbf{k}, r) \chi_l(\mathbf{k}, r)$$
 (2.342)

To obtain the right hand side, we use the Feynman-Hellmann theorem. Integrating over r from the AdS boundary to the horizon, we obtain

$$\frac{1}{e^2} \left(\sqrt{-g} g^{rr} g^{tt} \partial_r p \right) \Big|_0^{r_+} \equiv \mathcal{Q} - \mathcal{Q}_{\text{hor}} = q \sum_l \int \frac{\mathrm{d}^d \mathbf{k}}{(2\pi)^d} \Theta(-\epsilon_l(\mathbf{k})) \equiv q V_{\text{FS}}$$
 (2.343)

where we have used the AdS/CFT dictionary at the boundary, orthonormality of χ_l , defined \mathcal{Q}_{hor} as a (normalized) radial electric flux across the horizon, and defined V_{FS} as the total volume of the bulk Fermi surfaces. (??) is the holographic analogue of the Luttinger relation (??) in the presence of both cohesive and fractionalized charge carriers. qV_{FS} counts the cohesive charge which can detected by a gauge-neutral fermionic operator. \mathcal{Q}_{hor} counts the fractionalized charge which cannot be detected by such gauge-neutral operators, and remains hidden behind the horizon. (??) has a finite temperature generalization [?, ?]. In all models studied before this subsection, $\mathcal{Q} = \mathcal{Q}_{hor}$ – essentially all of the charge is fractionalized.

Let us finally comment that when all of the charge is cohesive, and the ordinary Luttinger relation is satisfied, we expect that the holographic dual to this gravity theory may be a ordinary Landau Fermi liquid [?]. In a hard wall model of AdS, the imaginary part of the self-energy vanishes [?] and one expects quantum bulk computations to follow standard many-body treatments, leading to $\text{Im}(G^{R}(\omega \to 0)) \sim \omega^{2}$. That a weakly coupled theory is dual to classical gravity is analogous to how hadrons and mesons are "simple"

massive particles that emerge from strongly interacting QCD at low energies [?].

The Thomas-Fermi approximation

In general, solving the backreacted gravity problem with the quantum nature of the fermions accounted for is incredibly hard, and limited progress has been made [?, ?]. In this review, we focus on a simple semiclassical approximation to the electron star, which amounts to a Thomas-Fermi approximation [?]. We wish to work in a limit where the fermions backreact on the geometry, but they are so dense that they may be treated as a classical fluid in a locally flat space.

For simplicity, we focus on bulk geometries dual to d = 2 metals, following most of the literature. If we couple a classical fluid of fermions to an EMD model, then the stress tensor in the Einstein's equations must be modified to include the effects of the fermions. This can be accounted for by writing down the action [?]

$$S = S_{\text{EMD}} + \int d^{d+2}x \sqrt{-g} P_{\text{f}}(\mu_{\text{f}}),$$
 (2.344)

where μ_f is the local chemical potential:

$$\mu_{\rm f} = \frac{A_t}{\sqrt{-g_{tt}}},\tag{2.345}$$

and $P_{\rm f}$ is the pressure of the fermions:

$$P_{\rm f} = \mu_{\rm f} \int_{0}^{\mu_{\rm f}} dE \ \nu(E) - \int_{0}^{\mu_{\rm f}} dE \ \nu(E)E, \tag{2.346}$$

where $\nu(E)$ is the density of states of the bulk fermions in flat space. The first integral is the local number density of fermions, and the latter integral is the energy density. (??) is the analogue of the statement that in a curved spacetime, in thermal equilibrium the chemical potential should be scaled so that $A_{\hat{t}} = \text{constant}$, where $d\hat{t} = \sqrt{-g_{tt}}dt$ (so that the metric looks locally flat). For the fermion fluid to be dense enough to be treated as classical, and locally on flat space, we need that the Compton wavelength of the fermions μ_f^{-1} to be much smaller than the AdS radius L [?].

One can write down the equations of motion due to these fermions – in general they must be solved numerically. A typical ansatz is that the bulk fermions are massive Dirac fermions of mass m. The requirement of small Compton wavelength becomes

$$mL \sim \Delta_{\rm f} \sim \mathcal{O}(N),$$
 (2.347)

with $\Delta_{\rm f}$ the operator dimension of the dual fermionic operator. Then, wherever $\mu_{\rm f} > m$, we expect a cloud of fermions to form, and wherever $\mu_{\rm f} < m$ the cloud of fermions is absence (until quantum corrections are

included). Near the asymptotically AdS boundary, since $g_{tt} \to \infty$, $\mu_f \to 0$. Hence, the fermions in the bulk can only condense towards the IR, if at all.

Of particular interest is the emergent IR behavior at T = 0. One finds the following possibilities within a simple example of EMD theory [?]:

- 1. If $Z(\Phi) \to 0$ in the IR, then the effective charge $e/\sqrt{Z} \to \infty$. In this case, the fermions carry all of the charge in the bulk. All the charge is carried by cohesive carriers.
- 2. If Z(Φ) → ∞ in the IR, then we generically find that some of the charge remains on the horizon (and hence fractionalized, in the dual theory). The EMD fields look similar to the theory we described in §?? in this case. In particular, note from (??) and (??) that μ_f → 0 as r → ∞ in the IR. So we expect that the chemical potential shrinks to zero and so if a fermion fluid forms at all in the bulk, it only forms at an intermediate scale in the bulk. A more careful calculation confirms this. In fact, depending on the details of the model, it is possible for μ_f to be so small that no fermions ever condense at all, meaning that all the charge is fractionalized.
- 3. If $Z(\Phi) \to \text{constant}$, then an emergent Lifshitz geometry can arise. The precise dynamical exponent z depends on the particular model, and its parameters. For simplicity, let us specialize to the $\text{AdS}_2 \times \mathbb{R}^2$ geometry [?]. A perturbative calculation reveals that, when the operator dimension of the fermions is not taken to be parametrically large as in (??), the emergent Lifshitz exponent $z \sim 1/N^2$. Still, the electron star does form, and removes the zero temperature entropy density of the extremal AdS-RN black hole. At T=0, all of the charge is contained within the bulk fermions, dual to the cohesive boundary fermions. In some models, this Lifshitz geometry is unstable, and the transition between the first and second possibilities listed above is first order.

If the bulk fermions are dual to a cohesive Fermi liquid in the boundary theory, then we should expect to see poles in fermionic Green's functions at finite momentum. Of course, using the AdS/CFT dictionary, this requires computing the fermionic response at the boundary, where the classical electron star does not persist. We must again account for quantum effects. In the $AdS_2 \times \mathbb{R}^2$ geometry, assuming that the fermions have charge q, we can use a semiclassical WKB approximation to find the poles of the fermionic Green's functions [?, ?]. One finds $\mathcal{O}(N^2)$ densely spaced Fermi surfaces, with Fermi momenta $0 \le k_F \le k_{\text{max}}$, with k_{max} the value of k where (??) becomes real.

At finite temperature, we expect a black hole to form in the bulk. As we have neglected Hawking radiation in the bulk, we still treat the bulk fermion gas at zero temperature, insofar as the equations of state. As $\mu_f \to 0$ near the horizon, ¹² the fermions will be pushed away from the horizon, and exist only

¹²This follows from the definition of $\mu_{\rm f}$ and $A_t \sim g_{tt} \sim r - r_{\rm h}$.

in an intermediate region in the bulk. It turns out that upon heating the dual theory beyond a critical temperature, there is a third order phase transition to a state with no bulk Fermi gas, and hence with fully fractionalized charge in the boundary theory.

Metallic transport without quasiparticles

We now wish to compute the electrical (and, as we will see, thermal) conductivities of the charged metals described in the previous section. In the first half of this section, we will detail the major developments in the theory of transport in strongly interacting metals with weak disorder. In particular, very deep connections have been made between old many-body approaches and holography, and we will provide full details of the calculations. The second half of the section consists of non-perturbative holographic approaches to transport, a problem for which results are more limited.

We postpone our review of non-holographic condensed matter models until after we have had a chance to lay out the formalisms which are relevant for the discussion.

Thermoelectric conductivity matrix

As we will see in this section repeatedly, electric and thermal transport generally couple together in charged quantum matter. Hence, we will want to compute not just the electrical conductivity σ , as in §??, but a more general matrix of thermal conductivities. As a result, we will need to compute the transport coefficients

$$\begin{pmatrix} J^{i} \\ Q^{i} \end{pmatrix} = \begin{pmatrix} \sigma^{ij} & T\alpha^{ij} \\ T\bar{\alpha}^{ij} & T\bar{\kappa}^{ij} \end{pmatrix} \begin{pmatrix} E_{j} \\ \zeta_{j} \end{pmatrix}$$

$$(2.348)$$

where we have defined the heat current

$$Q^i \equiv T^{ti} - \mu J^i. \tag{2.349}$$

The heat current naturally couples to a temperature gradient, as we will demonstrate below, following [?]. The matrix of thermoelectric conductivities defined above is guaranteed to be symmetric, assuming time-reversal symmetry – this is called Onsager reciprocity.

We want to impose a uniform electric field δE_i , and a uniform temperature gradient

$$\delta \zeta_i \equiv -\frac{\partial_i T}{T}.\tag{2.350}$$

(This notation will prove useful shortly.) For simplicity, we suppose that the field theory lives on flat space.

The natural way to impose an electric field is by imposing an external gauge field

$$\delta A = \frac{\delta E_i e^{-i\omega t}}{i\omega} dx_i. \tag{2.351}$$

Imposing a temperature gradient is more subtle. The best way to do this is to think about Euclidean time in the coordinate $\tilde{t}_{\rm E}$:

$$t_{\rm E} = \frac{\tilde{t}_{\rm E}}{T}.\tag{2.352}$$

In this coordinate, the metric is

$$g_{\tilde{t}\tilde{t}} = \frac{1}{T^2}. (2.353)$$

Imposing a constant ζ_i implies that

$$g_{\tilde{t}\tilde{t}} = \frac{1 + 2\delta\zeta_i x^i e^{-i\tilde{\omega}\tilde{t}}}{T^2}.$$
 (2.354)

with $\tilde{\omega} = \omega/T$. We now make a coordinate change to

$$\tilde{t} \to \tilde{t} + \xi^{\tilde{t}}, \quad \xi^{\tilde{t}} = ix^i \delta \zeta_i \frac{e^{-i\tilde{\omega}\tilde{t}}}{\tilde{\omega}T^2},$$
(2.355)

which changes

$$\delta g_{\mu\nu} \to \delta g_{\mu\nu} + \partial_{\mu} \xi_{\nu} + \partial_{\nu} \xi_{\mu}, \quad \delta A_{\mu} \to \delta A_{\mu} + \delta A_{\nu} \partial_{\mu} \xi^{\nu} + \xi^{\nu} \partial_{\nu} \delta A_{\mu}.$$
 (2.356)

This coordinate change leads to the following set of perturbations: $\delta g_{\tilde{t}\tilde{t}}=0$ as we have cancelled off the ζ_i dependence, and

$$\delta g_{\tilde{t}i} = -i\delta \zeta_i \frac{e^{-i\tilde{\omega}\tilde{t}}}{\tilde{\omega}T^2}, \quad \delta A_i = i\delta \zeta_i \frac{e^{-i\tilde{\omega}\tilde{t}}}{\tilde{\omega}T^2} A_{\tilde{t}}. \tag{2.357}$$

Let us now collect our results and rescale back to the usual time coordinate t. If we perturb the metric and gauge field, using (??) and (??) the action of the field theory has deformed to

$$\delta S = \int d^{d+1}x \left[T^{\mu\nu} \delta g_{\mu\nu} + J^{\mu} \delta A_{\mu} \right] = \int d^{d+1}x \left[\frac{\delta E_i J^i}{i\omega} + \frac{\delta \zeta_i Q^i}{i\omega} \right]$$
(2.358)

Hence, temperature gradients naturally couple to the heat current, and the natural thermoelectric transport coefficients to discuss are given by (??). In holography, we have also learned how to encode a thermal gradient by perturbing g_{ti} at the boundary. For simplicity assuming that the boundary is asymptotically AdS:

$$\delta g_{ti}(r=0) = \frac{L^2}{r^2} \frac{\delta \zeta_i e^{-i\omega t}}{i\omega}.$$
 (2.359)

There is a zoo of thermoelectric coefficients used in the condensed matter literature. All such coefficients

are related to the matrices defined in (??), and are defined by changing the "boundary conditions" (instead of measuring J_i and Q_i given E_i and ζ_i , we choose to fix J_i and ζ_i , for example). Let us note two famous ones for convenience. By far the most important is the thermal conductivity at vanishing electric current:

$$Q_i|_{J_i=0} \equiv T\kappa_{ij}\zeta_j, \quad \kappa_{ij} = \bar{\kappa}_{ij} - T\bar{\alpha}_{ik}\sigma_{kl}^{-1}\alpha_{lj}.$$
 (2.360)

The Seebeck coefficient \mathfrak{s}_{ij} is the ratio of the voltage drop to the temperature drop, again when $J_i = 0$:

$$E_i|_{J_i=0} \equiv -\mathfrak{s}_{ij}T\zeta_j, \quad \mathfrak{s}_{ij} = \sigma_{ik}^{-1}\alpha_{kj}. \tag{2.361}$$

Hydrodynamic transport (with momentum)

Before discussing holographic transport, it is important to understand what features of holography are genuinely novel, and which features are already expected on general field theoretic grounds. In fact, we will see that the transport problem is tightly constrained by hydrodynamics.

Hydrodynamics is the effective theory describing the relaxation of an interacting classical or quantum system towards thermal equilibrium. The key assumption of hydrodynamics is that the field theory has locally reached thermal equilibrium. In thermal equilibrium, we assign to a QFT with conserved charge and energy-momentum a chemical potential μ , and a temperature T and four-velocity u^{μ} , defined such that the local density matrix is "approximately"

$$\rho \sim \exp\left[\frac{u^{\mu}P_{\mu} + \mu N}{T}\right] \tag{2.362}$$

with P_{μ} the total energy-momentum in a volume of linear size $l_{\rm th}$, and N the charge. More precisely, (??) is true so long as we only ask for the expectation value of products of local operators. The equations of hydrodynamics describe the dissipative dynamics under which a theory with long wavelength inhomogeneity in μ , T and u^{μ} slowly relaxes to global equilibrium (or as close to it as boundary conditions allow).

We characterize the dynamics perturbatively in powers of $l_{\rm th}/\xi$, where $l_{\rm th}$ is the "thermalization length scale". We will focus on the case of relativistic dynamics, and so after trivial multiplication by the speed of light c the same considerations apply to time scales: the local thermalization time is fast compared to the scale of hydrodynamic phenomena. To do so, we will expand $T^{\mu\nu}$ and J^{μ} as functions of T, μ and u^{μ} , and their derivatives. We will perform this task explicitly in the next subsection. But beforehand let us emphasize that the hydrodynamic limit is parametrically opposite to the standard limit of quantum field theory computations – $\xi/l_{\rm th}$ crudely counts the "number of collisions" (in a quasiparticle framework), which

apparently must be large for the hydrodynamic limit to be sensible. Hence, recovery of hydrodynamics from quasiparticle approaches such as kinetic theory requires some conceptual care – though this can be done [?, ?].

Relativistic hydrodynamics near quantum criticality

The equations of motion of hydrodynamics read

$$\partial_{\mu}T^{\mu\nu} = F^{\mu\nu}J_{\mu},\tag{2.363a}$$

$$\partial_{\mu}J^{\mu} = 0, \tag{2.363b}$$

where $T^{\mu\nu}$ is the expectation value of the local stress tensor, J^{μ} is the charge current, and $F^{\mu\nu}$ is an external electromagnetic field tensor. Our goal is to construct $T^{\mu\nu}$ and J^{μ} for a relativistic theory, following [?].

To be a little bit more precise, our expansion in $l_{\rm th}/\xi$ will be an expansion in derivatives ∂_{μ} . So we begin by constructing $T^{\mu\nu}$ and J^{μ} at zeroth order in derivatives. The most general possible answer is

$$T^{\mu\nu} = (\epsilon + P)u^{\mu}u^{\nu} + P\eta^{\mu\nu}, \qquad (2.364a)$$

$$J^{\mu} = \mathcal{Q}u^{\mu}.\tag{2.364b}$$

We were only able to use $\eta^{\mu\nu}$ and u^{μ} to construct these tensors, since $F_{\mu\nu} = \partial_{\mu}A_{\nu} - \partial_{\nu}A_{\mu}$ is first order in derivatives. In the rest frame of the fluid, we readily interpret ϵ as the energy density, P as the pressure, and Q as the charge density.

We now assert that there is a further conservation law at this order in derivatives:

$$\partial_{\mu}s^{\mu} = 0, \tag{2.365}$$

where

$$s^{\mu} = \mathcal{S}u^{\mu} \tag{2.366}$$

and S is the entropy density. We can derive (??) by using that at leading order in derivatives:

$$-\partial^{\mu}P = u^{\mu}u^{\nu}\partial_{\nu}(\epsilon + P) + (\epsilon + P)u^{\mu}\partial_{\nu}u^{\nu} + (\epsilon + P)u^{\nu}\partial_{\nu}u^{\mu}. \tag{2.367}$$

Contracting with u_{μ} and employing $u_{\mu}u^{\mu} = -1$ and (??), we obtain:

$$\partial_{\mu} \left((\epsilon + P) u^{\mu} \right) = u^{\nu} \partial_{\nu} P = \mathcal{Q} u^{\nu} \partial_{\nu} \mu + \mathcal{S} u^{\nu} \partial_{\nu} T. \tag{2.368}$$

Further employing (??), (??), along with (??) to define S, we obtain (??). (??) asserts that entropy is conserved at leading order, and is the second law of thermodynamics for a non-dissipative system. At higher orders in hydrodynamics, we will require that

$$\partial_{\mu}s^{\mu} \ge 0, \tag{2.369}$$

so that the fluid is dissipative, and entropy increases over time locally.

Next, let us construct the first order derivative corrections to $T^{\mu\nu}$ and J^{μ} . A priori, we have to add a huge number of terms containing all possible combinations of $\partial_{\mu}\mu$, $\partial_{\mu}T$ and $\partial_{\mu}u_{\nu}$. However, we immediately run into an ambiguity with how to define the fluid variables in an inhomogeneous background. This is the issue of picking a "fluid frame": a simultaneous re-definition of u^{μ} , T and μ at first order in derivatives is allowed. We will work in the Landau frame, which chooses

$$0 = u_{\nu} T_{(1)}^{\mu\nu} = u_{\nu} J_{(1)}^{\nu}. \tag{2.370}$$

where $T_{(1)}^{\mu\nu}$ are the terms of the conserved currents at first order in the derivative expansion.

Now, we use the equations of motion to construct the most general $T_{(1)}^{\mu\nu}$ and $J_{(1)}^{\mu}$ consistent with (??) and the Landau frame conditions. We follow the steps we used above to derive (??), but now include first order corrections. We find

$$\partial_{\mu} \left(\mathcal{S} u^{\mu} \right) = \frac{\mu}{T} \partial_{\nu} J^{\nu}_{(1)} - \frac{1}{T} F^{\mu\nu} u_{\mu} J_{(1)\nu} - \frac{1}{T} T^{\mu\nu}_{(1)} \partial_{\mu} u_{\nu}, \tag{2.371}$$

$$\partial_{\mu} \left(\mathcal{S} u^{\mu} - \frac{\mu}{T} J^{\mu}_{(1)} \right) = -J^{\nu}_{(1)} \left[\partial_{\nu} \left(\frac{\mu}{T} \right) + \frac{1}{T} F^{\mu\nu} u_{\mu} \right] - \frac{1}{T} T^{\mu\nu}_{(1)} \partial_{\mu} u_{\nu}. \tag{2.372}$$

The most general form of $J^{\nu}_{(1)}$ and $T^{\mu\nu}_{(1)}$ consistent with the second law and the Landau frame is hence

$$J_{(1)}^{\mu} = -\sigma_{\mathcal{Q}} \mathcal{P}^{\mu\nu} \left(\partial_{\nu} \mu - \frac{\mu}{T} \partial_{\nu} T + F_{\rho\nu} u^{\rho} \right), \tag{2.373a}$$

$$T_{(1)}^{\mu\nu} = -\eta \mathcal{P}^{\mu\rho} \mathcal{P}^{\nu\sigma} \left[\partial_{\rho} u_{\sigma} + \partial_{\sigma} u_{\rho} - \frac{2}{d} \eta_{\rho\sigma} \partial_{\lambda} u^{\lambda} \right] - \zeta \mathcal{P}^{\mu\nu} \partial_{\rho} u^{\rho}$$
 (2.373b)

where σ_{Q} , η and ζ are all positive, and we have defined the projector

$$\mathcal{P}^{\mu\nu} = \eta^{\mu\nu} + u^{\mu}u^{\nu}. \tag{2.374}$$

 η and ζ are the shear and bulk viscosity of the fluid. $\sigma_{\rm Q}$ is a "quantum critical conductivity" which plays a very important role in transport, as we will see; in the zero density limit, $\sigma_{\rm Q}$ reduces to the "relativistic" conductivity described in Section ??. If we define the entropy current at first order as

$$s^{\mu} = Su^{\mu} - \frac{\mu}{T} J_{(1)}^{\mu} = \frac{(\epsilon + P)u^{\mu} - \mu J^{\mu}}{T}$$
 (2.375)

we see that it is nothing more than the heat current, up to a factor of T: $Q^{\mu} = Ts^{\mu}$.

As we have emphasized previously, the black hole geometries employed in holography are dual to field theories with consistent thermodynamics. One could ask – if we perturbed these black holes on very long wavelengths, could we see hydrodynamic behavior? The answer is yes – in fact there is a mapping between solutions of hydrodynamics and those of charged black branes, perturbed on very long length scales. Though we will not discuss it further, as this is a rather technical exercise, this famous result goes by the name "fluid-gravity correspondence": for original papers see [?, ?, ?], and for a review see [?].

Sound waves

Let us return to a question which we have already glimpsed in §??: what are the hydrodynamic modes of a charged fluid? To answer this question, we linearize the hydrodynamic equations about a fluid at rest:

$$u^{\mu} = (1, \delta v^{i}), \quad \mu = \mu_{0} + \delta \mu, \quad T = T_{0} + \delta T.$$
 (2.376)

To linear order in the perturbations, the stress tensor and charge current are

$$\delta J^t = \delta \mathcal{Q}, \quad \delta J^i = \mathcal{Q} \delta v^i,$$
 (2.377a)

$$\delta T^{tt} = \delta \epsilon, \quad \delta T^{ij} = \delta^{ij} \left[\partial_{\epsilon} P \delta \epsilon + \partial_{n} P \delta n \right], \quad \delta T^{ti} = (\epsilon + P) \delta v^{i}.$$
 (2.377b)

Following [?], we have used $\delta\epsilon$ and $\delta\mathcal{Q}$ as hydrodynamic variables instead of $\delta\mu$ and δT Assuming that δv^i , $\delta\epsilon$ and $\delta\mathcal{Q}$ have x and t dependence given by $e^{ik_x-i\omega t}$, it is straightforward to use the conservation laws to obtain a set of algebraic equations. The condition that these equations admit non-vanishing perturbations defines the hydrodynamic normal modes. One finds that the perpendicular components of the velocity field

obey a diffusion equation with dispersion relation

$$\omega = -i\frac{\eta}{\epsilon + P}k^2. \tag{2.378}$$

The longitudinal modes are as follows: there is a diffusive mode with $\delta P \approx 0$, with dispersion relation $\omega = -iDk^2$, with

$$D = \sigma_{\mathcal{Q}} \frac{(\partial_{\epsilon} P)_{\mathcal{Q}} [(\partial_{\mathcal{Q}} \mu)_{\epsilon} - (\mu/T)(\partial_{\mathcal{Q}} T)_{\epsilon}] - (\partial_{\mathcal{Q}} P)_{\epsilon} [(\partial_{\epsilon} \mu)_{\mathcal{Q}} - (\mu/T)(\partial_{\epsilon} T)_{\mathcal{Q}}]}{(\partial_{\epsilon} P)_{\mathcal{Q}/s}}.$$
 (2.379)

This is the generalization of the diffusive mode derived in §??. Finally, there is a sound mode

$$\omega = \pm v_{\rm s}k - i\Gamma_{\rm s}k^2 \tag{2.380}$$

with speed of sound

$$v_{\rm s} = \sqrt{(\partial_{\epsilon} P)_{\mathcal{Q}/s}} \tag{2.381}$$

and attenuation constant

$$\Gamma_{\rm s} = \frac{1}{\epsilon + P} \left(\frac{2d - 2}{d} \eta + \zeta \right) + \frac{\sigma_{\rm Q}(\partial_{\mathcal{Q}} P)_{\epsilon}}{v_{\rm s}^2} \left[(\partial_{\epsilon} \mu)_{\mathcal{Q}/s} - \frac{\mu}{T} (\partial_{\epsilon} T)_{\mathcal{Q}/s} \right]. \tag{2.382}$$

In various simple cases, these sound modes have explicitly been found by finding quasinormal modes of black holes. [?, ?, ?] demonstrated that the lowest lying quasinormal modes of the AdS₅-Schwarzchild black brane were precisely the hydrodynamic modes predicted for an uncharged fluid above, up to quadratic order in $\omega(k)$. The general computational strategy is identical to §?? – reduce the (much more complicated) coupled differential equations governing the bulk metric perturbations to a single gauge-invariant second order equation. For the diffusive momentum mode (??), one can solve for the bulk metric perturbations δg_{ty} and δg_{xy} , upon fixing the gauge $\delta g_{rM} = 0$ and $\delta A_r = 0$; for the remaining longitudinal modes one must couple δA_t , δA_x , δg_{ii} , δg_{xx} , δg_{tx} , δg_{tt} , and any further scalar modes such as a dilaton. By integrating this equation from the horizon to the boundary and demanding the absence of a source at the boundary, a perturbative expansion in $\omega, k \to 0$ with ω/k fixed reveals the presence of a pole in the Green's functions of the stress tensor precisely at the frequencies given by (??).

Perhaps more surprisingly, these sound modes exist even at T=0 in the AdS-RN black hole [?], and obey the expected dispersion relations. It is likely that this is a consequence of the finite entropy density at T=0. We expect that in more complicated EMD models, such sound modes will ultimately disappear at

T=0.

Transport coefficients

We are now almost ready to use hydrodynamics to compute transport coefficients defined in (??). However, there is an immediate problem which arises: at finite \mathcal{Q} and \mathcal{S} , the transport coefficients are all divergent as $\omega \to 0$ in any fluid with translation invariance! To see this, let us consider an easy way to generate a finite J_i and Q_i : start with a fluid at rest $(u^{\mu} = (1, 0, ...))$, and simply perform a small "Galilean" boost of velocity v_x . We now obtain a charge current $J_x = \mathcal{Q}v_x$ and $Q_x = T\mathcal{S}v_x$. But there is no temperature gradient, or no electric field. Evidently, all of the coefficients in (??) are divergent in any direction with translation invariance. This is not inconsistent with our results from §??, because for those systems $\mathcal{Q} = 0$.

Nonetheless, let us now compute $\sigma(\omega)$ at $\omega > 0$ from hydrodynamics; for simplicity, we assume the theory is isotropic. We apply a uniform electric field E, so $F^{xt} = -E$, which is infinitesimally small. This will induce a perturbatively small velocity field v, and a perturbatively small momentum current $T^{tx} = (\epsilon + P)v$. Integrating (??) over space, we find that

$$\partial_t T^{ti} = -i\omega(\epsilon + P)v = EQ, \tag{2.383}$$

since $J_t \approx -\mathcal{Q}$. Solving (??) for v and using that

$$J^x = Qv + \sigma_0 E \tag{2.384}$$

at leading order, we obtain

$$\sigma(\omega) = \sigma_{Q} + \frac{Q^{2}}{\epsilon + P} \frac{i}{\omega}.$$
 (2.385)

In fact, exactly at $\omega = 0$, analytic properties of σ demand that there be a δ function:

$$\sigma(\omega) = \sigma_{Q} + \frac{Q^{2}}{\epsilon + P} \left[\frac{i}{\omega} + \pi \delta(\omega) \right]. \tag{2.386}$$

We will see in the next section another way to see the emergence of this δ function. Using the constitutive relation for Q_x , we also obtain

$$\alpha(\omega) = -\frac{\mu}{T}\sigma_{Q} + \frac{\mathcal{QS}}{\epsilon + P} \left[\frac{\mathrm{i}}{\omega} + \pi\delta(\omega) \right]. \tag{2.387}$$

To compute $\bar{\kappa}$ we need an expression for the heat current. In the presence of a thermal "drive" sourced by

(??), one can show that (??) is replaced by

$$\partial_{\mu}T^{\mu i} = \mathcal{S}\zeta^{i},\tag{2.388}$$

and so

$$\bar{\kappa}(\omega) = \frac{\mu^2}{T} \sigma_{Q} + \frac{TS^2}{\epsilon + P} \left[\frac{i}{\omega} + \pi \delta(\omega) \right]. \tag{2.389}$$

In experiments, it is often convenient to measure κ , defined in (??). Unlike σ , α and $\bar{\kappa}$, there is no divergence in κ as $\omega \to 0$: one finds

$$\kappa = \frac{\sigma_{\mathcal{Q}}(\epsilon + P)^2}{T\mathcal{Q}^2}.$$
(2.390)

General linearized hydrodynamics

Let us briefly mention the extension of the (linearized) hydrodynamics derived above to models which are not Lorentz invariant. In the derivation above, we exploited the fact that $T^{ti} = T^{it}$ to conclude that both the energy current and the momentum density would not pick up any derivative corrections in the Landau frame. However, without Lorentz invariance, this condition must be relaxed. We choose to set the momentum density \mathfrak{g} to be unchanged by derivative corrections:¹³

$$\mathfrak{g}^i = \mathcal{M}v^i. \tag{2.391}$$

The parameter \mathcal{M} will be defined just above (??), and it is analogous to the "mass density". The spatial components of the stress tensor are identical to before:

$$T^{ij} = P\delta^{ij} - \eta \left(\partial^i v^j + \partial^j v^i\right) + \left(\zeta - \frac{2\eta}{d}\right) \partial_k v^k \delta^{ij}. \tag{2.392}$$

as are the charge density Q and energy density ϵ .

We find an energy current

$$J_i^{\rm E} = (\epsilon + P)v_i - (T\alpha_{\rm Q} - \mu\sigma_{\rm Q})(\partial_i\mu - E_i) - (\bar{\kappa}_{\rm Q} - \mu\bar{\alpha}_{\rm Q})\partial_iT + \cdots, \qquad (2.393)$$

with E the external electric field, and α_Q , $\bar{\alpha}_Q$ and $\bar{\kappa}_Q$ new dissipative coefficients. We will see that they play the same roles as σ_Q , as microscopic "quantum critical" thermoelectric conductivities. While the energy current looks similar to the (linearized when $v \ll 1$) relativistic energy current, for a non-relativistic fluid

 $^{13\}mathfrak{g}^i$ is T^{ti} in a relativistic theory. We think it is more physically sensible to use manifestly non-relativistic notation for such theories.

 $J_i^{\mathrm{E}}
eq \mathfrak{g}_i$, even when neglecting dissipative effects. The charge current is now

$$J_i = \mathcal{Q}v_i - \sigma_0(\partial_i \mu - E_i) - \bar{\alpha}_0 \partial_i T. \tag{2.394}$$

In terms of our new non-relativistic notation, the hydrodynamic equations read

$$\partial_t \mathcal{Q} + \partial_i J^i = 0, \tag{2.395a}$$

$$\partial_t \epsilon + \partial_i J_{\mathcal{E}}^i = E_i J^i, \tag{2.395b}$$

$$\partial_t \mathfrak{g}^i + \partial_j T^{ij} = \mathcal{Q}(E^i + v_k F^{ki}). \tag{2.395c}$$

One can compute α by either applying a temperature gradient and computing J_i , or applying an electric field and computing the heat current. Demanding Onsager reciprocity (that these two computations of α yield the same result) gives

$$\alpha_{\mathbf{Q}} = \bar{\alpha}_{\mathbf{Q}}.\tag{2.396}$$

Hence, the transport coefficients are

$$\sigma = \sigma_{Q} + \frac{Q^{2}}{\mathcal{M}} \left[\frac{i}{\omega} + \pi \delta(\omega) \right], \qquad (2.397a)$$

$$\alpha = \alpha_{Q} + \frac{\mathcal{QS}}{\mathcal{M}} \left[\frac{i}{\omega} + \pi \delta(\omega) \right], \qquad (2.397b)$$

$$\bar{\kappa} = \bar{\kappa}_{Q} + \frac{TS^{2}}{\mathcal{M}} \left[\frac{i}{\omega} + \pi \delta(\omega) \right].$$
 (2.397c)

Similarly, κ is finite:

$$\kappa = \bar{\kappa}_{Q} - \frac{2TS}{O}\alpha_{Q} + \frac{TS^{2}}{O^{2}}\sigma_{Q}. \tag{2.398}$$

In the special case of Galilean-invariant field theories, it follows from the Galilean Ward identities that the momentum density $\mathfrak g$ is

$$\mathfrak{g}^i = mJ^i. (2.399)$$

In this case, we find that

$$\sigma_{\mathcal{O}} = \alpha_{\mathcal{O}} = \bar{\alpha}_{\mathcal{O}} = 0. \tag{2.400}$$

In addition to the two viscosities, there is a single dissipative coefficient $\bar{\kappa}_{Q}$, and from (??) we see that $\kappa = \bar{\kappa}_{Q}$.

In the case where Lorentz invariance is restored, we have

$$\mathcal{M} = \epsilon + P, \quad \alpha_{Q} = -\mu \sigma_{Q}, \quad \bar{\kappa}_{Q} = \frac{\mu^{2}}{T} \sigma_{Q}.$$
 (2.401)

While at the linearized level the velocity v_i defined in this subsection is the same as δv_i defined in (??), further corrections are required at the nonlinear level to restore full Lorentz invariance. We do not have a systematic understanding of how this arises. Indeed, to the best of our knowledge, there has not been a systematic development of hydrodynamics for theories which are neither Galilean or Lorentz invariant. We encourage filling this gap in the literature.

Weak momentum relaxation I: inhomogeneous hydrodynamics

To obtain finite transport coefficients, which is necessary for making contact with "real" systems, we must break translation invariance. The simplest way to do this is in a "mean field" approximation, where we simply relax momentum at some constant (small) rate τ , and modify the spatial components of (??) to: [?]

$$\partial_t \mathfrak{g}^i + \partial_j T^{ij} = -\frac{\mathfrak{g}^i}{\tau_{\text{imp}}} + F^{i\nu} J_{\nu}. \tag{2.402}$$

Following the previous section, we may derive the electrical conductivity

$$\sigma(\omega) = \sigma_{Q} + \frac{Q^{2}}{\mathcal{M}} \frac{1}{\tau_{imp}^{-1} - i\omega}.$$
 (2.403)

Indeed, as is manifest from (??), we may simply set $-i\omega \to \tau_{\rm imp}^{-1} - i\omega$ in (??).

Let us make a few qualitative comments on these results. Up to the unknown parameter τ , every coefficient in the transport coefficients can be computed in the clean theory. Hence, this model predicts that a single parameter τ controls the scaling behavior of various transport coefficients. Remarkably, we have also managed to derive the "Drude model" directly from hydrodynamics, without any reference to quasiparticles! For in the non-relativistic "quasiparticle" limit, $Q \to ne$ and $\epsilon + P \to nm$, with n the number density of quasiparticles of charge e and mass m. Evidently, the Drude model is not sensitive to quasiparticles, and is valid for any model with a clean hydrodynamic limit of transport.

More careful calculations, which we will describe in more detail throughout this section, have shown that the formulas such as (??) for σ , α and $\bar{\kappa}$ are not correct in general. The reason for this is that $\tau_{\rm imp}^{-1}$ is a perturbatively small parameter, and so corrections to $\epsilon + P$ of order $\tau_{\rm imp}^{-1}$, e.g., are of the same size as $\sigma_{\rm Q}$. Holography gives a particularly convenient way to account for these corrections, as we will see.

To go further, we need a more "microscopic" way to derive an expression for τ . A physically transparent way to account for such corrections is to directly solve the hydrodynamic equations described above, but to explicitly break translational symmetry in the background fluid with long wavelength, hydrodynamic disorder. A particularly simple way this can be done is to source the fluid with charged disorder. Although the resulting equations must in general be numerically solved, this approach is non-perturbative in the amplitude of disorder [?, ?]. Similar ideas were put forth in [?] a few years earlier, albeit less rigorously, and so we follow the more modern papers.

Suppose that we have a translationally invariant fluid at finite temperature and density. The translation-invariant Hamiltonian H_0 is perturbed by a time-independent, spatially-varying source which linearly couples to a scalar operator O:

$$H = H_0 - \int d^d \mathbf{x} \ h_0(\mathbf{x}) O(\mathbf{x}). \tag{2.404}$$

Suppose further for simplicity that the local expressions for Q and S are only corrected at $O(h^2)$, as they are even in h. There is a Ward identity which states

$$\partial_{\mu}T^{\mu\nu} = \langle O \rangle \partial^{\nu} h_0. \tag{2.405}$$

with $\langle O \rangle$ the thermal expectation value of O; for simplicity henceforth we drop the angle brackets. Analogously to how we wrote down the pressure as a function of μ and T, we must also account for the dependence of pressure on h. Indeed, this is necessary for the hydrodynamic equations to be locally satisfied. Using the fact that ¹⁴

$$\frac{\partial P}{\partial h} = O, (2.406)$$

we find an exact static solution of the hydrodynamic equations with μ and T uniform, $u^{\mu} = (1, 0, ...)$, and $h = h_0$, since

$$\partial_i T^{ij} = \partial_j P = O \partial_j h = O \partial_j h_0. \tag{2.407}$$

Now, we linearly perturb this background. For simplicity, we an apply an electric field E_i , though a thermal gradient works similarly. The argument below is not long, but is somewhat subtle. We are performing a strict linear response calculation in E. After taking this limit, we then impose the perturbative limit $h_0 \to 0$. We also turn on a small frequency ω , which we treat as $\omega = \mathcal{O}(h_0^2)$ for the purposes of our perturbative calculation.¹⁵

¹⁴This can be understood as follows. The pressure is microscopically $P = W/V_d$, with W the generator of correlation functions in the QFT, and by definiton $\partial W/\partial h(\mathbf{k}) = O(\mathbf{k})$.

¹⁵More precisely, we introduce an artifical perturbative parameter λ , such that $h_0 = \lambda h'_0$, $\omega = \lambda^2 \omega'$, and compute the conductivity to leading order in λ . We will use the \sim notation as above throughout our discussion of transport in nearly clean

We make an ansatz that the only two fields which pick up corrections are a constant shift to the velocity: $v_i \sim h_0^{-2}$, and a perturbation to h, $\delta h \sim h_0^{-1}$; given the solution we construct below, it is straightforward to check that this ansatz is consistent, with all other perturbations $\sim h_0^0$. The momentum conservation equation reads

$$-i\omega \mathcal{M}v_j + \partial_j P = -i\omega \mathcal{M}v_j + (O + \delta O)\partial_j (h_0 + \delta h)$$
$$= \mathcal{Q}E_j + (O + \delta O)\partial_j h_0 + \text{subleading in } h_0.$$
(2.408)

At linear order in perturbations, we have

$$\frac{1}{L^d} \int d^d \mathbf{x} \ O \partial_j \delta h = \mathcal{Q} E_j. \tag{2.409}$$

It turns out to be easier to evaluate δO than δh . Happily, these can be related by a static susceptibility, or retarded Green's function, in Fourier space:

$$\delta O(\mathbf{k}) = \chi_{OO}(\mathbf{k})\delta h(\mathbf{k}) = G_{OO}^{R}(\mathbf{k}, \omega = 0)\delta h(\mathbf{k}). \tag{2.410}$$

Now, when we apply E_i and induce fluid flow, δO must be corrected because the rest frame in which the source is static is no longer the same as the fluid rest frame. In particular:

$$O(\mathbf{k}) + \delta O(\mathbf{k}) = G_{OO}^{R}(\mathbf{k}, -\mathbf{k} \cdot \mathbf{v}) h_{0}(\mathbf{k}) \approx \chi_{OO}(\mathbf{k}) h_{0}(\mathbf{k}) - \mathbf{k} \cdot \mathbf{v} \frac{\partial G_{OO}^{R}(\mathbf{k}, \omega = 0)}{\partial \omega} h_{0}(\mathbf{k})$$
(2.411)

where we have only kept terms to linear order in our perturbative expansion in E, as $v \sim E$. Hence, we obtain

$$i\omega \mathcal{M}v_{j} + \mathcal{Q}E_{j} = \sum_{\mathbf{k}} O(-\mathbf{k})ik_{j} \frac{\delta O(\mathbf{k})}{\chi_{OO}(\mathbf{k})} = \sum_{\mathbf{k}} \frac{O(-\mathbf{k})}{\chi_{OO}(-\mathbf{k})}ik_{j} \left(-k_{i}v_{i} \frac{\partial G_{OO}^{R}(\mathbf{k}, \omega = 0)}{\partial \omega}\right) h_{0}(\mathbf{k})$$
$$= \sum_{\mathbf{k}} |h_{0}(\mathbf{k})|^{2} k_{i}k_{j} \lim_{\omega \to 0} \frac{\operatorname{Im}\left(G_{OO}^{R}(\omega, \mathbf{k})\right)}{\omega} v_{i} \equiv \frac{\mathcal{M}}{\tau_{imp}} v_{j}$$
(2.412)

where we have used isotropy and (??) on the background in our manipulations, along with analyticity properties of Green's functions to re-write the answer. Assuming that the source h_0 is isotropic, then we fluids.

may replace $k_i k_j \to (k^2/d) \delta_{ij}$ above. Hence, we obtain an explicit formula for τ :

$$\frac{1}{\tau_{\text{imp}}} = \frac{1}{d\mathcal{M}} \sum_{\mathbf{k}} |h(\mathbf{k})|^2 k^2 \lim_{\omega \to 0} \frac{\text{Im} \left(G_{OO}^{\text{R}}(\omega, \mathbf{k})\right)}{\omega}.$$
 (2.413)

Now, using that

$$v_i = \frac{QE_i}{\mathcal{M}(\tau_{\text{imp}}^{-1} - i\omega)},\tag{2.414}$$

along with the constitutive relation $J_i \approx Qv_i$ at this order in perturbation theory, we obtain the Drude formula

$$\sigma(\omega) = \frac{Q^2 \tau_{\rm imp}}{\mathcal{M}(1 - i\omega \tau_{\rm imp})},\tag{2.415}$$

which is what we obtained from hydrodynamics, but without the σ_Q contribution, which is generically subleading at this order in perturbation theory.

Weak momentum relaxation II: the memory matrix formalism

Let us now re-derive these results with the memory matrix formalism [?]. Although this is a more abstract toolkit, it does not require the existence of quasiparticles, and extends beyond the hydrodynamic limit. We start with a rather formal definition of a correlation function between two Hermitian operators A and B:

$$C_{AB}(t) \equiv T \int_{0}^{1/T} d\lambda \left\langle A(t)^{\dagger} B(i\lambda) \right\rangle_{T} = T \int_{0}^{1/T} d\lambda \left\langle A e^{-iLt} B(i\lambda) \right\rangle_{T}$$
(2.416)

where $\langle \cdots \rangle_T$ denotes an average over quantum and thermal fluctuations, $\langle \cdots \rangle$ denotes just over quantum fluctuations, and $L = [H, \circ]$ is the Liouvillian operator. What is the usefulness of this object? We take a time derivative and perform some basic manipulations:

$$\partial_{t} \mathcal{C}_{AB} = -iT \int_{0}^{1/T} d\lambda \left\langle AL e^{-iLt} B(i\lambda) \right\rangle_{T} = -iT \int_{0}^{1/T} d\lambda \left\langle A e^{-iLt} L e^{-\lambda L} B e^{-H/T} \right\rangle$$

$$= iT \left\langle A e^{-iLt} \left(e^{-L/T} - 1 \right) B e^{-H/T} \right\rangle = iT \left\langle A \left(e^{-H/T} B(-t) e^{H/T} - B(-t) \right) e^{-H/T} \right\rangle$$

$$= -iT \left\langle [A(t), B] \right\rangle_{T}, \qquad (2.417)$$

where in the last step we have used time translation invariance. We now note that

$$\Theta(t)\partial_t \mathcal{C}_{AB}(t) = -TG_{AB}^{R}(t), \qquad (2.418)$$

and so integrating t from $-\infty$ to $+\infty$:

$$\frac{1}{T}C_{AB}(t=0) = G_{AB}^{R}(\omega=0) = \chi_{AB}.$$
(2.419)

We may also do the integral:

$$\int_{0}^{\infty} dt e^{izt} \Theta(t) \partial_{t} \mathcal{C}_{AB}(t) = -\mathcal{C}_{AB}(z=0) - iz \mathcal{C}_{AB}(z)$$

$$= -T \int_{-\infty}^{\infty} dt G_{AB}^{R}(t) e^{izt} = -T G_{AB}^{R}(z), \qquad (2.420)$$

and so we conclude

$$C_{AB}(z) = \frac{T}{iz} \left(G_{AB}^{R}(z) - G_{AB}^{R}(0) \right). \tag{2.421}$$

Suppose that we pick $A = B = J_x$, and that we have a metal with finite electrical conductivity. Then $G^{R}(z) \to iz\sigma$ as $z \to 0$, and we conclude that $C = T\sigma$. Up to the overall factor of T, C_{AB} is just computing a generalized conductivity.

As we have just seen, C_{AB} is parametrically large when translation symmetry breaking is weak. The goal of the memory matrix formalism is to re-organize the computation of C_{AB} so that we can instead compute parametrically small quantities, which can then be analyzed easily perturbatively. In order to do this, we will introduce a further abstraction: an inner product on an "operator Hilbert space"

$$(A(t)|B) \equiv \mathcal{C}_{AB}(t). \tag{2.422}$$

This inner product obeys all axioms of complex linear algebra, and further obeys

$$\frac{1}{T}(A(0)|B) = \frac{1}{T}(A|B) = \chi_{AB}, \tag{2.423}$$

which will soon come in handy. We can now readily perform the Laplace transform

$$C_{AB}(z) = \int_{0}^{\infty} dt \, e^{izt} \left(A \left| e^{-iLt} \right| B \right) = \left(A \left| i(z - L)^{-1} \right| B \right). \tag{2.424}$$

We now perform a series of manipulations on (??) in order to cleanly extract out the perturbatively small "denominator" to the conductivity C_{AB} . We pick a selective set of "long-lived" modes $AB\cdots$ (these will be the hydrodynamic degrees of freedom in a nearly clean fluid), which must include any operators whose

correlation functions we wish to compute, and define the operator

$$\mathfrak{q} \equiv 1 - \mathfrak{p} \equiv 1 - \frac{1}{T} \sum_{AB} |A\rangle \chi_{AB}^{-1}(B),$$
(2.425)

with χ the reduced susceptibility matrix, only including the long-lived modes. It is simple to check that $\mathfrak{q}^2 = \mathfrak{q}$, and hence \mathfrak{q} projects out the slow degrees of freedom. We strongly emphasize that we are free to choose any set of operators to call the "long-lived" modes, at this point, so long as we only compute correlation functions between this set of privileged operators. Only at the end of the calculation will it be clear why to choose the modes which are, in fact, long-lived to be privileged.

Our goal is now to separate z - L into the contributions from fast and slow modes. Note the exact operator identities

$$(z-L)^{-1} = (z-L\mathfrak{p} - L\mathfrak{q})^{-1} = (z-L\mathfrak{q})^{-1} \left(1 + L\mathfrak{p}(z-L)^{-1}\right)$$
(2.426)

Now, since by definition $\mathfrak{q}|B) = 0$:

$$(A|(z-L\mathfrak{q})^{-1}|B) = \left(A\left|\frac{1}{z} + \frac{L\mathfrak{q}}{z^2} + \cdots\right|B\right) = \frac{\chi_{AB}}{Tz},\tag{2.427}$$

and

$$i\mathfrak{p}(z-L)^{-1}|B) = \frac{i}{T} \sum_{CD} |C| \chi_{CD}^{-1}(D|(z-L)^{-1}|B) = \frac{1}{T} \sum_{CD} |C| \chi_{CD}^{-1} \mathcal{C}_{DB}, \tag{2.428}$$

we find that

$$\mathcal{C}_{AB} = \frac{i\chi_{AB}}{z} + \frac{1}{T} \sum_{CD} (A|(z - L\mathfrak{q})^{-1}L|C) \chi_{CD}^{-1} \mathcal{C}_{DB}
= \frac{i\chi_{AB}}{z} + \frac{1}{T} \sum_{CD} \left(A \left| \left(\frac{1}{z} + \frac{L\mathfrak{q}}{z} (z - L\mathfrak{q})^{-1} \right) L \right| C \right) \chi_{CD}^{-1} \mathcal{C}_{DB}.$$
(2.429)

Now, note that

$$(A|L\mathfrak{q}(z-L\mathfrak{q})^{-1}L|C) = \left(\dot{A}\left|\frac{\mathfrak{q}}{z} + \frac{\mathfrak{q}L\mathfrak{q}}{z^2} + \frac{\mathfrak{q}(L\mathfrak{q})^2}{z^3} + \cdots \right| \dot{C}\right)$$
$$= (\dot{A}|\mathfrak{q}(z-\mathfrak{q}L\mathfrak{q})^{-1}\mathfrak{q}|\dot{C}) \equiv -iTM_{AC}, \tag{2.430}$$

where we have defined the memory matrix M_{AC} in the last step, and used the property $\mathfrak{q}^2 = \mathfrak{q}$ in this chain

of equations. Let us further define

$$N_{AB} = \chi_{A\dot{B}} = \frac{1}{T}(A|\dot{B}) = \frac{\mathrm{i}}{T}(A|L|B).$$
 (2.431)

Note that M is a symmetric matrix, while N is antisymmetric; further, N=0 in a time-reversal symmetric theory (if the operators A transform identically under time reversal, as will often be the case). Then, (??) becomes

$$C = \frac{iT\chi - i(N+M)\chi^{-1}C}{z},$$
(2.432)

which can be further rearranged:

$$\frac{1}{T}\mathcal{C}_{AB} \equiv \sigma_{AB} = \chi_{AC}(M + N - i\omega\chi)_{CD}^{-1}\chi_{DB}, \qquad (2.433)$$

with σ_{AB} the generalized conductivity between operators A and B. Of particular relevance to us will be the thermoelectric conductivities:

$$\sigma_{J_i J_j} = \sigma_{ij}, \quad \sigma_{J_i Q_j} = T \alpha_{ij}, \quad \sigma_{Q_i Q_j} = T \bar{\kappa}_{ij}.$$
 (2.434)

The Drude conductivites

So far, the discussion has been quite abstract. Therefore, let us turn to a concrete application of the memory matrix formalism, and re-derive (??) and (??). We again consider a clean and isotropic fluid, weakly perturbed by an inhomogeneous field coupling to a scalar operator O, as in (??). If this breaking of translation invariance is small enough, then the longest-lived mode that will have substantial overlap with the (vector) current J_x is the momentum P_x . Hence, we will allow the long-lived modes in the memory matrix formalism to be J_x and P_x . These are both time-reversal odd, so we may set the matrix N = 0. The next key observation is that as $\omega \to 0$, M has a zero eigenvalue associated with M_{PP} in the clean limit. This follows from the definition of M_{PP} because in a clean metal $\dot{P} = 0$ as an operator equation. Indeed, in our model

$$\dot{P} = i[H, P] = -\int d^d \mathbf{x} \ h(\mathbf{x})(\partial_i O)(\mathbf{x}). \tag{2.435}$$

Now, let us evaluate the memory matrix. $|\dot{P}\rangle$ is a sum of finite momentum operators, and hence in the clean theory has no overlap with any zero momentum operator, such as J, \dot{J} , etc. Hence, $\mathfrak{q}|\dot{P}\rangle = |\dot{P}\rangle$. Comparing

(??) and (??), we see that

$$M_{PP} = (\dot{P}|\mathfrak{q}(\omega - L + L\mathfrak{p})^{-1}|\dot{P}) = (\dot{P}|(\omega - L)^{-1}[1 - L\mathfrak{p}(\omega - L)^{-1} + \cdots]|\dot{P})$$

$$= (\dot{P}|(\omega - L)^{-1}|\dot{P}) + \frac{1}{T} \sum_{A,B \in \{J,P\}} (\dot{P}|(\omega - L)^{-1}|\dot{A})\chi_{AB}^{-1}(B|(\omega - L)^{-1}|\dot{P}) + \cdots$$
(2.436)

The first term in (??) is $\mathcal{O}(h^2)$. The second term is the square of terms taking the form $(\dot{P}|(\omega-L)^{-1}|A)$ where |A| is a zero momentum operator. This cannot be non-zero unless we include $\mathcal{O}(h)$ corrections to L associated with the breaking of translation invariance. Accounting for $\dot{P} \sim h$, we obtain

$$(\dot{P}|(\omega - L)^{-1}|A) \sim h^2.$$
 (2.437)

Hence, the second term (and higher order terms) in (??) may be neglected. At leading order in h, we conclude:

$$M_{PP}(\omega = 0) \equiv \frac{\mathcal{M}}{\tau_{\text{imp}}} \equiv \lim_{\omega \to 0} \frac{\text{Im}\left(G_{\dot{P}\dot{P}}^{\text{R}}(\omega)\right)}{\omega} = \sum_{\mathbf{k}} |h(\mathbf{k})|^2 k_x^2 \lim_{\omega \to 0} \frac{\text{Im}\left(G_{OO}^{\text{R}}(\omega, \mathbf{k})\right)}{\omega}.$$
 (2.438)

The Green's functions in the above formula may be evaluated in the clean theory. The first step in this equation follows from the same logic that we used to argue that $C_{AB} \sim \sigma_{AB}$. We note that $M_{JP} \sim h^2$, with h a perturbatively small quantity. This follows from identical considerations to (??). Generically, we expect that $M_{J_xJ_x} \sim h^0$.

Next, the susceptibility $\chi_{J_x P_x}$ is the charge density \mathcal{Q} . To see this, recall that the velocity is thermodynamically conjugate to momentum, the same way that μ is conjugate to \mathcal{Q} . If we boost to a frame with infinitesimal velocity v_x , then $\chi_{JP} \equiv J_x/v_x = \mathcal{Q}$. We define further $\chi_{P_x P_x} \equiv \mathcal{M}$; in a relativistic fluid, $\mathcal{M} = \epsilon + P$, the enthalpy. In a Galilean-invariant fluid, \mathcal{M} is the mass density. At leading order in h, we may neglect M_{JP} and M_{JJ} when inverting $M - \mathrm{i}\omega\chi$. (??) becomes

$$\sigma(\omega) = \sigma_{JJ}(\omega) = \frac{\chi_{JP}^2}{M_{PP} - i\omega\chi_{PP}},$$
(2.439)

and upon plugging in for the parameters above, we see that we recover (??), with the same formula for τ_{imp} as in (??), but in more general circumstances:

$$\sigma(\omega) = \frac{Q^2}{\mathcal{M}(\tau_{\text{imp}}^{-1} - i\omega)}.$$
 (2.440)

This formula is only valid when we take $\omega \sim h^2$ to be perturbatively small.

It is also possible to account for σ_{Q} in the memory function formalism, with some care about which quantities are small or large in perturbation theory. This was first presented in [?]. Here we present a cleaner derivation, similar to [?]. If we temporarily focus on the case Q = 0, we expect that $\sigma = \sigma_{Q}$. Indeed, in this limit, as $\chi_{JP} = 0$, the memory matrix formalism immediately gives us

$$\sigma_{JJ} = \frac{\chi_{JJ}^2}{M_{JJ} - i\omega\chi_{JJ}}. (2.441)$$

In any appropriate scaling limit, $M_{JJ} \gg \omega \chi_{JJ}$. Hence, defining σ_Q via the relation

$$M_{JJ} \equiv \frac{\chi_{JJ}^2}{\sigma_{\rm o}} \tag{2.442}$$

we recover that $\sigma = \sigma_Q$. For simplicity here, we will take $\chi_{JJ} \sim 1/\omega$ and $\sigma_Q \sim 1/\omega$, though only the latter scaling is essential. Next, let us turn on a finite charge density Q. The conductivity is

$$\sigma(\omega) = \begin{pmatrix} \chi_{JJ} & \chi_{JP} \end{pmatrix} \begin{pmatrix} M_{JJ} - i\omega\chi_{JJ} & M_{JP} - i\omega\chi_{JP} \\ M_{JP} - i\omega\chi_{JP} & M_{PP} - i\omega\chi_{PP} \end{pmatrix}^{-1} \begin{pmatrix} \chi_{JJ} \\ \chi_{JP} \end{pmatrix}. \tag{2.443}$$

As $M_{JP} \sim h^2$, we conclude that at leading order in ω , we have schematically

$$\sigma \sim \left(\begin{array}{cc} \omega^{-1} & 1 \end{array}\right) \left(\begin{array}{cc} \omega^{-1} & \omega \\ \omega & \omega \end{array}\right)^{-1} \left(\begin{array}{cc} \omega \\ 1 \end{array}\right). \tag{2.444}$$

In the above formula, we have only kept track of the ω -scaling of each term. Hence, it is clear that upon taking the matrix inverse, the off-diagonal parts may be neglected in the determinant and so we may just invert the diagonal elements component wise. In the end we find

$$\sigma(\omega) = \frac{\chi_{JJ}^2}{M_{JJ}} + \frac{\chi_{JP}^2}{M_{JP} - i\omega\chi_{JP}} = \sigma_Q + \frac{Q^2 \tau_{imp}}{\mathcal{M}(1 - i\omega\tau_{imp})}.$$
 (2.445)

The crucial thing about the above derivation is that we see that to perturbatively recover σ_{Q} in an exact formalism, we have to treat σ_{Q} as anomalously large in perturbation theory. In general this will not be the case, and we will observe corrections to (??) at the order of σ_{Q} : see §??.

To account for α_Q and $\bar{\kappa}_Q$, we must add the heat current Q as an index to the memory matrix. We assume that $\chi_{JQ} \sim M_{QQ} \sim \omega^{-1}$, etc., as before. Analogous to (??), we define σ_Q , α_Q and $\bar{\kappa}_Q$ within the

memory matrix formalism via

$$\begin{pmatrix}
\sigma_{Q} & T\alpha_{Q} \\
T\alpha_{Q} & T\bar{\kappa}_{Q}
\end{pmatrix} = \begin{pmatrix}
\chi_{JJ} & \chi_{JQ} \\
\chi_{JQ} & \chi_{QQ}
\end{pmatrix} \begin{pmatrix}
M_{JJ} & M_{JQ} \\
M_{JQ} & M_{QQ}
\end{pmatrix}^{-1} \begin{pmatrix}
\chi_{JJ} & \chi_{JQ} \\
\chi_{JQ} & \chi_{QQ}
\end{pmatrix}$$
(2.446)

The net σ , α and $\bar{\kappa}$ are then found using the net matrices (third row/column in matrix corresponds to the momentum P index):

$$\chi = \begin{pmatrix} \chi_{JJ} & \chi_{JQ} & \mathcal{Q} \\ \chi_{JQ} & \chi_{QQ} & T\mathcal{S} \\ \mathcal{Q} & T\mathcal{S} & \mathcal{M} \end{pmatrix},$$

$$M \approx \begin{pmatrix} M_{JJ} & M_{JQ} & 0 \\ M_{JQ} & M_{QQ} & 0 \\ 0 & 0 & \mathcal{M}\tau^{-1} \end{pmatrix}.$$
(2.447a)

$$M \approx \begin{pmatrix} M_{JJ} & M_{JQ} & 0 \\ M_{JQ} & M_{QQ} & 0 \\ 0 & 0 & \mathcal{M}\tau_{\rm imp}^{-1} \end{pmatrix}.$$
 (2.447b)

 $\chi_{QP} \equiv TS$ defines the entropy density in terms of microscopic Green's functions. We have only included leading order contributions to the memory matrix M.

Accounting for slow momentum relaxation as before, we recover the thermoelectric conductivities from $\sigma = \chi (M - i\omega \chi)^{-1} \chi$, and keeping only the leading order contributions as $\omega \to 0$:

$$\sigma = \sigma_{JJ} = \sigma_{Q} + \frac{Q^{2}}{\mathcal{M}(\tau_{imp}^{-1} - i\omega)},$$
(2.448a)

$$\alpha = \frac{\sigma_{JQ}}{T} = \alpha_{Q} + \frac{QS}{\mathcal{M}(\tau_{imp}^{-1} - i\omega)},$$
(2.448b)

$$\alpha = \frac{\sigma_{JQ}}{T} = \alpha_{Q} + \frac{QS}{\mathcal{M}(\tau_{\rm imp}^{-1} - i\omega)},$$

$$\bar{\kappa} = \frac{\sigma_{QQ}}{T} = \bar{\kappa}_{Q} + \frac{TS^{2}}{\mathcal{M}(\tau_{\rm imp}^{-1} - i\omega)}.$$
(2.448b)

This is exactly (??), upon setting $i\omega \to i\omega - \tau_{\rm imp}^{-1}$, as discussed in the previous section.

Note that M_{JJ} changes (but σ_Q does not) depending on whether or not Q is included as an index in the memory matrix or not, due to the change in the projection operator \mathfrak{q} . In general, computing χ_{JJ} , M_{JJ} etc. will require a microscopic computation more complicated than the perturbative computation of $\tau_{\rm imp}$, which is readily expressed in terms of microscopic Green's functions as in (??).

Finally, it is worth noting that in a relativistic theory, $Q = P - \mu J$ holds as an operator equation. In this case, Q should not be a separate index in the memory matrix, and instead one computes $\sigma_{JQ} = \sigma_{JP} - \mu \sigma_{JJ}$, e.g. Similarly, in a Galilean invariant fluid, the momentum P = mJ, and hence J should be removed as an independent index in the memory matrix.

Transport co-efficients in condensed matter

With general form of the thermoelectric transport response functions at hand in (??) via hydrodynamics, and also in (??) via memory matrices, we now return to the condensed matter models of compressible quantum matter in Sections ??-??, and discuss the frequency and temperature dependence of their transport properties.

First, we have the "diffusive components", σ_{Q} , α_{Q} , and $\bar{\kappa}_{Q}$. These are not expected to experience special constraints from total momentum conservations, and so should be finite at finite ω and T, in the scaling limit of their respective quantum-critical theories. Applying a naive scaling dimensional analysis to these terms, we can expect that they obey scaling forms similar to those discussed in Section ??:

$$\sigma_{\rm Q} \sim \alpha_{\rm Q} \sim \frac{\bar{\kappa}_{\rm Q}}{T} \sim T^{(d-2)/z} \Upsilon(\omega/T),$$
 (2.449)

with different scaling functions Υ for each of the transport co-efficients. As discussed at the beginning of Section ??, thermodynamic quantities related to the free energy density typically violated hyperscaling, and this amounted to a replacement $d \to d - \theta$ in scaling forms. So we might similarly expect that (??) is replaced more generally by

$$\sigma_{\rm Q} \sim \alpha_{\rm Q} \sim \frac{\bar{\kappa}_{\rm Q}}{T} \sim T^{(d-2-\theta)/z} \Upsilon(\omega/T).$$
 (2.450)

This issue has been investigated in recent works in the models of non-Fermi liquids described in Section ?? for the case of σ_{Q} , and it has been found that (??) is indeed obeyed. The Ising-nematic transition of Section ?? was investigated in Ref. [?], and σ_{Q} obeyed (??) in d=2 with $\theta=1$. Similarly, for the spin-density-wave transition of Section ??, the expected value, $\theta=0$, appeared also in σ_{Q} in d=2 [?, ?]. Note that these computations do not show evidence for the separate anomalous dimension for the charge density discussed in Section ??.

Next, let us consider the "momentum drag" terms in $(\ref{eq:constraint})$ and $(\ref{eq:constraint})$. The parameters \mathcal{Q} and \mathcal{M} are invariably dominated by non-critical 'background' contributions of the compressible state. So we can take them to be non-singular T- and ω -independent constants. The singular behavior of the entropy density, \mathcal{S} , was discussed already at the beginning of Section $\ref{eq:constraint}$. So it only remains to discuss the singular behavior of τ_{imp} .

The memory matrix result for τ_{imp} in (??) (and in (??)) was expressed in terms of the two-point correlator of the operator O coupling to a space-dependent source, $h(\mathbf{x})$, in (??). If we assume that average of $|h(\mathbf{k})|^2$ is \mathbf{k} -independent (this is the case for a Gaussian random source which is uncorrelated at different spatial points), and the scaling dimension $\dim[O] = \Delta$ in the theory without the random source, then a scaling

analysis applied to (??) yields [?]

$$\frac{1}{\tau_{\rm imp}} \sim h^2 T^{2(1+\Delta-z)/z}$$
 (2.451)

at small disorder.

The expression (??) has been evaluated for specific models of disorder in the non-Fermi liquids discussed above. For the Ising-nematic critical point, Ref. [?] argued that the most relevant disorder was a 'random field' term that coupled linearly to the Ising-nematic order parameter ϕ in Section ??. However, it was found that the order parameter susceptibility, *i.e.* $G_{\phi\phi}$, violated the expected scaling form because of an emergent gauge-invariance in the underlying critical theory. Consequently, (??) is not obeyed in this specific model. It was found that, in d = 2, $1/\tau_{\rm imp} \sim T^{-1/2}$ (up to logarithms).

For the spin-density-wave transition of Section ??, (??) was evaluated in Ref. [?]. Here, the disorder was assumed to be associated with local variations in the position of the critical point, and so coupled linearly to $(\varphi^a)^2$. In this case, the scaling law (??) was found to apply, and yields $1/\tau_{imp} \sim T$ (up to logarithms), implying a resistivity linear in T.

From holography to memory matrices

Remarkably, (??) and (??) can be derived entirely from holography [?]. The discussion below is a bit technical, but we believe it is useful. Firstly, this confirms that the truncation of the memory matrix to a single momentum mode is correct, at least when disorder is perturbatively weak. Secondly, the holographic calculation in [?] contains new computational tricks which we believe are useful and physically instructive. We will thus provide more or less a complete derivation, closely mimicking [?].

Let us consider the following rather general set-up. Consider a background EMD geometry, analogous to that of §??. We add disorder in a fourth bulk scalar field φ , via the action (??). We choose φ to be dual to an operator of dimension $\Delta > (d+1)/2$, and choose boundary conditions

$$\varphi = r^{d+1-\Delta} \sum_{\mathbf{k}} h(\mathbf{k}) e^{i\mathbf{k} \cdot \mathbf{x}} + \cdots$$
 (2.452)

Then at leading (linear) order in h, the bulk φ is

$$\varphi = \sum_{\mathbf{k}} h(\mathbf{k}) \varphi_0(\mathbf{k}, r) e^{i\mathbf{k} \cdot \mathbf{x}}, \qquad (2.453)$$

with φ_0 regular at the black hole horizon, along with $\varphi_0(\mathbf{k}, r \to 0) = r^{d+1-\Delta} L^{-d/2} + \cdots$. Our goal is to show that the conductivity $\sigma(\omega)$ contains a Drude peak so long as h is perturbatively small, and to recover

(??). We will assume for simplicity that the modes $h(\mathbf{k})$ are effectively chosen so that $\sigma_{ij} = \sigma \delta_{ij}$ – i.e., the theory is microscopically disordered but macroscopically isotropic.

The Drude peak is a perturbative limit of a double expansion in small ω and small h. From (??), $\sigma_{\rm dc} \sim \tau \sim h^{-2}$; evidently we must treat h^{-2} and ω as small parameters on the same footing. Now, the original EMD fields are altered at order h^2 , but only as perturbative corrections to the background. These cannot lead to a singular conductivity as $h, \omega \to 0$. Leading order effects are caused by the smearing out the δ function in $\sigma(\omega)$ that would have existed with translation invariance. We may thus treat the EMD fields as uniform, and only consider the finite momentum response in the φ field [?]. We further need only compute the holographic linear response problem to linear order in ω [?].

We first identify the perturbations which we will excite when we apply an infinitesimal uniform electric field. Since the electric field is uniform, the lowest order processes in h occur when a linear perturbation $\delta\varphi(\mathbf{q})$ scatters off of the background $\varphi(-\mathbf{q})$. Hence the perturbations of interest will be $\delta\varphi(\mathbf{q})$, as well as spin 1 perturbations under the spatial SO(d) group – these will be δA_x and $\delta \tilde{g}_{tx} \equiv r^2 \delta g_{tx}/L^2$ (these perturbations both tend to constants at r=0). We use the "axial" gauge $\delta g_{rx}=0$ as before. The linearized equations of motion read:¹⁶

$$\frac{L^d \delta \tilde{g}_{tx}'}{2\kappa^2 a r^d} = \mathcal{Q} \delta A_x - \frac{L^d b}{r^d \omega} \sum_{\mathbf{k}} k_x |h(\mathbf{k})|^2 \varphi_0(\mathbf{k}, r)^2 \left(\frac{\delta \varphi(\mathbf{k}, r)}{\varphi_0(\mathbf{k}, r)} \right)', \tag{2.454a}$$

$$\frac{e^2 \mathcal{Q} \delta \tilde{g}'_{tx}}{L^{d-2}} = \left(br^{2-d} Z \delta A'_x\right)' + \frac{r^{2-d} Z \omega^2}{b} \delta A_x, \tag{2.454b}$$

$$-\frac{k_x\omega\varphi_0(\mathbf{k},r)^2\delta\tilde{g}'_{tx}}{br^d} = \left(\frac{b\varphi_0(\mathbf{k},r)^2}{r^d}\left(\frac{\delta\varphi(\mathbf{k},r)}{\varphi_0(\mathbf{k},r)}\right)'\right)' + \frac{\omega^2}{br^d}\varphi_0(\mathbf{k},r)\delta\varphi(\mathbf{k},r). \tag{2.454c}$$

Terms $\sim \omega^2$ are beyond the order in perturbation theory to which we work, so we may drop them. Now (??) collapses to a set of 3 differential equations:

$$\frac{L^d \delta \tilde{g}_{tx}'}{2\kappa^2 a r^d} = \mathcal{Q} \delta A_x - L^d \delta \mathcal{P}_x, \tag{2.455a}$$

$$\frac{e^2 \mathcal{Q} \delta \tilde{g}'_{tx}}{L^{d-2}} = \left(br^{2-d} Z \delta A'_x\right)', \tag{2.455b}$$

$$\delta \mathcal{P}_{x}' = -\delta \tilde{g}_{tx} \sum_{\mathbf{k}} \frac{k^{2} |h(\mathbf{k})|^{2} \varphi_{0}(\mathbf{k}, r)^{2}}{db r^{d}}$$
(2.455c)

where in the last line above, we have used the isotropy approximation to replace $k_x^2 \to k^2/d$, and defined the new field

$$\delta \mathcal{P}_x \equiv \frac{b}{r^d \omega} \sum_{\mathbf{k}} k_x |h(\mathbf{k})|^2 \varphi_0(\mathbf{k}, r)^2 \left(\frac{\delta \varphi(\mathbf{k}, r)}{\varphi_0(\mathbf{k}, r)} \right)'. \tag{2.456}$$

¹⁶We highly recommend the use of symbolic manipulations such as Mathematica, along with a differential geometry/general relativity package, to perform many tedious steps in such computations.

We now proceed to directly construct (at leading order) the bulk response to the applied electric field. Counting derivatives in (??) shows there are 4 linearly independent modes. With the benefit of hindsight, none are singular in h, and so we may look for these modes assuming h = 0. The first such mode – and the only one containing $\delta \mathcal{P}_x$, is:

$$Q\delta A_x = L^d \delta \mathcal{P}_x = \text{constant}, \quad \delta \tilde{g}_{tx} = 0. \tag{2.457}$$

The remaining three are the modes of the translation invariant black hole, and so have $\delta \mathcal{P}_x = 0$. There is a "diffeomorphism mode" $\delta \tilde{g}_{tx} = 1$, a "Galilean boost" mode:

$$\delta \tilde{g}_{tx} = 1 - ab, \quad \delta A_x = p + \frac{Ts}{\mathcal{Q}},$$

$$(2.458)$$

and a third mode (explicitly given in [?]) which is the "Wronskian" partner to this Galilean boost mode; it is logarithmically divergent at the horizon. (??) near $r = r_+$ allows us to fix the constant term in δA_x in (??).

What is the bulk response if we impose the boundary condition that $\delta A_x(\omega, r=0)=1$, and infalling boundary conditions? We will see that the response is not singular, and so we need only compute the response at $\mathcal{O}(\omega^0)$. However, we will see that this is subtle: the response contains terms proportional to ω/h^2 . $\delta \tilde{g}_{tx}(r=0)=0$ since we do not source a heat current, and so the diffeomorphism mode is not sourced. At $\omega=0$, $\sigma(\omega)$ remains finite, and so there can be no current sourced; we source only (??). Next, we need the $\mathcal{O}(\omega)$ correction to this response. We follow the discussion in §??, and by keeping the bulk radius fixed while taking the limit $\omega \to 0$, imposing infalling boundary conditions is equivalent to forcing a fixed ratio between coefficients of the regular and singular modes of the linear response equations. For $\delta \mathcal{P}_x$, we find that (??) becomes singular near the horizon unless

$$\delta \tilde{g}_{tx}(r=r_{+}) = -\frac{\mathrm{i}\omega \mathcal{Q}\tau}{\epsilon + P},\tag{2.459}$$

where

$$\frac{\epsilon + P}{\tau} \equiv \frac{L^d}{r_+^d} \sum_{\mathbf{k}} \frac{k^2}{d} |h(\mathbf{k})|^2 \varphi_0(\mathbf{k}, r)^2.$$
 (2.460)

Note at this order $\delta \tilde{g}_{tx}$ is not singular near the horizon, but it is actually $\mathcal{O}(\omega^0)$ in perturbation theory. Infalling boundary conditions for δA_x will lead to $\mathcal{O}(\omega)$ corrections can be neglected. Further, since δA_x must be regular at leading order near the horizon, we conclude that the only mode sourced is the Galilean boost mode (??). Hence,

$$\delta A_x(\omega, r) \approx 1 - \frac{\mathrm{i}\omega \mathcal{Q}\tau}{\epsilon + P} \left(p + \frac{Ts}{\mathcal{Q}} \right).$$
 (2.461)

A straightforward computation using (??) (with z = 1), (??) to relate subleading behavior in p to Q (recall $p(0) = \mu$), and the thermodynamic identity (??), shows that the conductivity is given by the Drude formula (??).

To show that τ is given by (??), we employ the Wronskian method discussed in §??. Comparing (??) with (??), we can obtain (??) directly from holography [?].

Let us now take a step back and analyze this result. Firstly, the bulk response is dominated by a "Galilean boost". This is the holographic analogue of our derivation of (??) from hydrodynamics. Secondly, this derivation provides a rigorous justification for the approximations used in the memory matrix formalism, in a class of strongly interacting theories without quasiparticles. Finally, we have revealed a deep connection between transport computations in holography, hydrodynamics and the memory matrix formalism. To some extent, we will see that holography allows us to extend a "hydrodynamic" formalism beyond perturbative limits.

Holographic examples

Let us now go through a few examples of the holographic application of (??). We have really done the hard work in §?? by computing the spectral weight of scalar operators in various holographic examples.

1. As we found previously in (??), a scalar operator in the $AdS_2 \times \mathbb{R}^d$ with momentum $k \ll \mu$ will have power law spectral weight as $T \to 0$. Hence, a single "lattice" deformation of the UV theory by $\varepsilon \mathcal{O}(k_L) \cos(k_L x)$ will lead to [?]

$$\frac{1}{\sigma} \sim \varepsilon^2 k_{\rm L}^2 T^{2\nu_{k_{\rm L}} - 1}.\tag{2.462}$$

2. We can also consider "random-field" disorder [?, ?], where the $h(\mathbf{k})$ defined in the previous section are random variables, with average $\overline{h(\mathbf{k})} = 0$ and variance (assuming the system is in a finite size box of volume V_d):

$$\overline{h(\mathbf{k})h(\mathbf{q})} = \delta_{\mathbf{k},-\mathbf{q}} \frac{\varepsilon^2}{V_d}.$$
(2.463)

We assume that the bulk geometry is an EMD geometry has finite z and θ . We found in §?? that only modes with $k \lesssim T^{1/z}$ do not have exponentially suppressed spectral weight. Hence using (??) and (??), we obtain (at the level of scaling):

$$\frac{1}{\sigma} \sim \varepsilon^2 T^{(d+2)/z} \times \lim_{\omega \to 0} \frac{\operatorname{Im} \left(G_{\mathcal{O}\mathcal{O}}^{R}(k=T,\omega) \right)}{\omega} \sim \varepsilon^2 T^{(2+2\Delta-2z)/z}. \tag{2.464}$$

The extra factor of $T^{(d+2)/z}$ comes from the number of non-exponentially suppressed modes, as well as the factor of k^2 in (??). This result agrees with our general scaling theory for the resistivity in

condensed matter models, as discussed earlier.

3. Finally, we can consider random field disorder in the $T \ll \mu$ limit of the AdS-RN theory. We take $\Delta = 0$ for a scalar operator; the analysis then becomes quite similar to the analysis for charged disorder (where the operator $\mathcal{O} = J^t$) [?]:

$$\frac{1}{\sigma} \sim \varepsilon^2 \int_0^{\mu} dk \ k^{d+1} T^{2\nu_k - 1}. \tag{2.465}$$

Employing (??), we find

$$2\nu_k - 1 \approx \sqrt{1 + c\left(\frac{k}{\mu}\right)^2} - 1 \approx \frac{c}{2} \left(\frac{k}{\mu}\right)^2 \tag{2.466}$$

for an $\mathcal{O}(1)$ constant c, we find

$$\frac{1}{\sigma} \sim \varepsilon^2 \int_0^{\mu} dk \ k^{d+1} \exp\left[-\frac{c}{2} \log \frac{\mu}{T} \times \left(\frac{k}{\mu}\right)^2\right] \sim \varepsilon^2 \left[\log \frac{\mu}{T}\right]^{-1-d/2}. \tag{2.467}$$

The conductivity logarithmically diverges as $T \to 0$. The power of the logarithm is sensitive to the operator being studied, and its presence is a consequence of the k-dependent operator dimensions (??). Similar logarithmic corrections occur in scaling theories of σ in $z = \infty$ holographic models at finite θ/z [?], and/or if $\Delta \neq 0$.

Magnetotransport

We now turn to the question of transport in a magnetic field. For simplicity in this section, we restrict to d=2; in higher dimensions, adding a magnetic field breaks isotropy. As previously, let us begin with a discussion of the results of the predictions of hydrodynamics.

The discussion is very similar to what was done before, and we consider the same set-up: a fluid with translational symmetry broken weakly by an inhomogeneous field $h(\mathbf{x})$ coupled to a scalar operator \mathcal{O} , in a uniform magnetic field B.¹⁷ Again, we focus on the momentum conservation equation, which now reads

$$\partial_t \mathfrak{g}^i + \partial_j T^{ij} = O\partial^i h_0 + F^{i\mu} J_\mu, \tag{2.468}$$

with $F_{\mu\nu}$ the (externally imposed) gauge flux; in our case, we will have $F_{xy} = B$, as well as $F^{it} = -E$. We assume that $B \sim \omega \sim \mathcal{O}(h_0^2)$, as before. We now generalize (??) to

$$-i\omega \mathcal{M}v_j + (O + \delta O)\partial_j(h_0 + \delta h) = \mathcal{Q}E_j + (O + \delta O)\partial_j h_0 + B\varepsilon_{jk}J_k.$$
 (2.469)

 $^{^{17}}$ The uniformity of the magnetic field is required by Maxwell's equations.

The treatment of δh is identical to before – B-dependent corrections to τ are subleading, just as ω -dependent corrections were. So we find

$$-i\omega \mathcal{M}v_j = \mathcal{Q}E_j + \mathcal{Q}B\varepsilon_{jk}v_k - \frac{\mathcal{M}}{\tau_{imp}}v_j, \qquad (2.470)$$

with an *identical* τ to (??). Hence,

$$\sigma_{xx} = \sigma_{yy} = \frac{\mathcal{Q}^2 \mathcal{M}(\tau_{\text{imp}}^{-1} - i\omega)}{(\mathcal{Q}B)^2 + \mathcal{M}^2(\tau_{\text{imp}}^{-1} - i\omega)^2}$$
(2.471a)

$$\sigma_{xy} = -\sigma_{yx} = \frac{Q^3 B}{(QB)^2 + \mathcal{M}^2 (\tau_{\text{imp}}^{-1} - i\omega)^2}.$$
 (2.471b)

Following [?], we can modify our above derivation by using $J_i = \sigma_Q E_i + Qv_i$, instead of only including the latter term. One finds:

$$\sigma_{xx} = \frac{(\tau_{\text{imp}}^{-1} - i\omega)\mathcal{M}\sigma_{Q} + \mathcal{Q}^{2} + B^{2}\sigma_{Q}^{2}}{\mathcal{Q}^{2}B^{2} + ((\tau_{\text{imp}}^{-1} - i\omega)\mathcal{M} + B^{2}\sigma_{Q})^{2}}\mathcal{M}\left(\frac{1}{\tau_{\text{imp}}} - i\omega\right),$$
(2.472a)

$$\sigma_{xy} = \frac{2(\tau_{\text{imp}}^{-1} - i\omega)\mathcal{M}\sigma_{Q} + \mathcal{Q}^{2} + B^{2}\sigma_{Q}^{2}}{\mathcal{Q}^{2}B^{2} + ((\tau_{\text{imp}}^{-1} - i\omega)\mathcal{M} + B^{2}\sigma_{Q})^{2}}B\mathcal{Q}.$$
(2.472b)

It is instructive to derive (??) from the memory matrix formalism. To do so, we employ the generalized (??) including the matrix N which breaks time reversal symmetry. By symmetries, N is an antisymmetric matrix, and since the long lived quantities A that we maintain are P_x and P_y , the new quantity to compute is

$$N_{P_x P_y} = \chi_{P_x \dot{P}_y}. (2.473)$$

Now, employing the equations of motion of hydrodynamics, the total momentum loss is a sum of contributons from translation symmetry breaking, and the external B field. Since $\chi_{P_x\dot{P}_y}$ is a two-point Green's function,

$$\chi_{P_x \dot{P}_y} = -\frac{1}{\tau} \chi_{P_x P_y} - B \chi_{P_x J_x} = 0 - B \mathcal{Q}. \tag{2.474}$$

We have used linearity properties of Green's functions to simplify the above, as well as the isotropy and parity-even nature of the clean thermal state. (??) then gives

$$\begin{pmatrix}
\sigma_{xx} & \sigma_{xy} \\
\sigma_{yx} & \sigma_{yy}
\end{pmatrix} = \begin{pmatrix}
\mathcal{Q} & 0 \\
0 & \mathcal{Q}
\end{pmatrix} \begin{pmatrix}
\mathcal{M}(\tau^{-1} - i\omega) & -B\mathcal{Q} \\
B\mathcal{Q} & \mathcal{M}(\tau^{-1} - i\omega)
\end{pmatrix}^{-1} \begin{pmatrix}
\mathcal{Q} & 0 \\
0 & \mathcal{Q}
\end{pmatrix}, (2.475)$$

which recovers (??).

Recovering (??) more generally requires the same scaling limit as before, where $\sigma_Q \sim 1/\omega$. It may be

found straightforwardly from (??), employing the matrices (indices are ordered as J_x , J_y , P_x and P_y)

$$\chi = \begin{pmatrix}
\chi_{JJ} & 0 & Q & 0 \\
0 & \chi_{JJ} & 0 & Q \\
Q & 0 & \mathcal{M} & 0 \\
0 & Q & 0 & \mathcal{M}
\end{pmatrix},$$
(2.476a)

$$N = \begin{pmatrix} 0 & 0 & 0 & -B\chi_{JJ} \\ 0 & 0 & B\chi_{JJ} & 0 \\ 0 & -B\chi_{JJ} & 0 & -BQ \\ B\chi_{JJ} & 0 & BQ & 0 \end{pmatrix},$$
(2.476b)

$$\chi = \begin{pmatrix} \chi_{JJ} & 0 & Q & 0 \\ 0 & \chi_{JJ} & 0 & Q \\ Q & 0 & \mathcal{M} & 0 \\ 0 & Q & 0 & \mathcal{M} \end{pmatrix},$$

$$N = \begin{pmatrix} 0 & 0 & 0 & -B\chi_{JJ} \\ 0 & 0 & B\chi_{JJ} & 0 \\ 0 & -B\chi_{JJ} & 0 & -BQ \\ B\chi_{JJ} & 0 & BQ & 0 \end{pmatrix},$$

$$M = \begin{pmatrix} \chi_{J}J^{2}/\sigma_{Q} & 0 & 0 & 0 \\ 0 & \chi_{JJ}^{2}/\sigma_{Q} & 0 & 0 & 0 \\ 0 & 0 & \mathcal{M}(\tau_{\text{imp}}^{-1} - i\omega) & 0 \\ 0 & 0 & 0 & \mathcal{M}(\tau_{\text{imp}}^{-1} - i\omega) \end{pmatrix},$$
(2.476b)

One can check that the subleading contributions to this matrix do not affect the conductivities until $\mathcal{O}(\omega, B, h^2)^0$. The only new components of the matrices above are $N_{J_x P_y}$, e.g., which follow immediately along the lines of (??).

One of the interesting features of (??) is a violation of Kohn's theorem. Suppose we take a translationally invariant fluid with $\sigma_{\rm Q} = 0$. Then if we set

$$\pm \omega = \omega_{\rm c} \equiv \frac{QB}{\mathcal{M}},\tag{2.477}$$

the conductivities given by (??) diverge. This is called the cyclotron resonance, and is associated with exciting a collective mode which uniformly rotates the momentum of the fluid. Kohn's theorem states that this cyclotron resonance frequency is robust against electron-electron interactions in a Galilean-invariant fluid [?]. In a quantum critical fluid with $\sigma_Q \neq 0$, but $\tau = \infty$, we see that this cyclotron resonance disappears - there is no longer any infinite resonance, as it is damped by the particle-hole "friction". The loophole in Kohn's theorem that we exploit is that we have both electrons and holes, and that a generic quantum critical system does not conserve the number of electrons (due to electron-hole creation/annihilation processes).

Another interesting feature of (??) is the possibility for anomalous scaling in the Hall angle, defined as

$$\tan \theta_{\rm H} = \frac{\sigma_{xy}}{\sigma_{xx}}.\tag{2.478}$$

We work at $\omega = 0$. If $\sigma_Q = 0$, then we obtain

$$\tan \theta_{\rm H} \sim \frac{BQ\tau_{\rm imp}}{\mathcal{M}} \sim \sigma_{xx}.$$
(2.479)

In particular, as $B \to 0$, $\theta_{\rm H} \sim \sigma_{xx}$. It has been known for some time that this is violated in the cuprates [?]. [?] pointed out that (??) provides a natural mechanism for this: suppose that $\sigma_{xx}(B=0) \approx \sigma_{\rm Q}$ (recall from (??) that σ_{xx} is a sum of two terms). Using (??), the scaling $\tan \theta_{\rm H} \sim \tau$ is unchanged, meaning that if $\tau_{\rm imp}$ and $\sigma_{\rm Q}$ have unrelated T-scaling, then the scaling $\tan \theta_{\rm H} \sim \sigma_{xx}$ need not hold.¹⁸

As we discussed near (??), at higher orders in perturbation theory in $1/\tau_{\rm imp}$, corrections appear to the theory of [?], and to these equations. And so if $\sigma_{\rm Q} \sim \tau_{\rm imp}^0$, corrections arise to (??) [?]. Nonetheless, if we set $\omega = 0$, and replace $\sigma_{\rm Q}$ and τ with appropriately defined holographic quantities as in (??), in the mean-field models discussed previously, (??) is exact [?]. If we study α_{ij} and $\bar{\kappa}_{ij}$ in holography, we see discrepancies with the theory of [?] even at $\omega = 0$ [?, ?, ?]. One holographic subtlety that arises in the derivation of (??) is the presence of magnetization currents in the bulk – these are present even when $E = \zeta = 0$ and must be subtracted off to compute the transport coefficients [?].

Finally, we can gain further insight between the relationship between particle-vortex duality in the boundary theory, and Maxwell self-duality in the bulk. For simplicity, set $\tau_{\rm imp} = \infty$. Under the transformations

$$Q \leftrightarrow B \text{ and } \sigma_0 \leftrightarrow 1/\sigma_0$$
 (2.480)

then

$$\sigma_{xx} \leftrightarrow \rho_{xx} \text{ and } \sigma_{xy} \leftrightarrow -\rho_{xy}$$
 (2.481)

where $\rho = \sigma^{-1}$ is the resistivity matrix. We can understand these results as a consequence of Maxwell self-duality [?]. Firstly, $F_{tr}(r=0) \sim \mathcal{Q}$ and $F_{xy}(r=0) = B$; employing (??) leads to the first half of (??). The duality of $F_{tx} \sim E$ and $F_{ry} \sim J$, along with σ_{Q} as a proportionality coefficient, leads to the second half of (??).

Hydrodynamic transport (without momentum)

So far, we have discussed hydrodynamic transport assuming that (up to weak disorder) energy, momentum and charge are all good conserved quantities. If translational symmetry is very strongly broken – for example, the amplitude of short wavelength disorder is large – then there is no reason to expect that the dynamics

¹⁸In principle, an ultra-clean sample should always have $Q^2\tau_{\rm imp}/\mathcal{M}\gg\sigma_{\rm Q}$, as $\tau=\infty$ if translation invariance is restored, and so in the cleanest samples $\tan\theta_{\rm H}\sim\sigma_{xx}$ should hold. This may provide an interesting experimental test of this theory.

associated with momentum relaxation are slower than other microscopic processes. In this limit, the only conserved quantities are charge (and possibly energy, if inelastic phonon scattering is not important) [?], and so our hydrodynamic description should only include the chemical potential μ and temperature T. We coin such a system an "incoherent metal". Symmetries constrain the first order hydrodynamic equations to be simple diffusion equations:

$$\partial_t \begin{pmatrix} \mathcal{Q} \\ \epsilon \end{pmatrix} = \partial_j \begin{pmatrix} \sigma_0 & \alpha_0 \\ T\alpha_0 & \bar{\kappa}_0 \end{pmatrix} \partial_j \begin{pmatrix} \mu \\ T \end{pmatrix}. \tag{2.482}$$

Note that these equations are generically nonlinear, as Q, σ_0 , etc. can depend on μ and T. The matrix of coefficients above is nothing more than the local thermoelectric conductivity matrix, which explains the suggestive notation. The loss of Lorentz invariance means that we can proceed no further on symmetries alone – unlike the hydrodynamics described previously. There are few non-trivial constraints beyond the second law of thermodynamics, which enforces that the matrix above is positive definite.

Until recently, most understanding of hydrodynamic transport in this limit is phenomenological and non-rigorous. A common approximation is that the only good conserved quantity is charge, in which case (??) reduces to a single diffusion equation. Assuming knowledge of the coefficients of (??), there is a large literature on the resulting "phases". Various methods for tackling such problems have been developed, including effective medium theory (EMT) [?] and analogies with resistor networks [?]. For simple models of inhomogeneous metals, EMT can work quite well. A simple model of the metal-insulator transition beyond EMT consists of a resistor network with a random fraction p of resistors deleted (so the resistance $R = \infty$ for that link); the classical percolation transition of these deleted links then becomes the metal-insulator transition [?]. Some of these techniques generalize to (??), and to hydrodynamic transport with momentum [?].

Ultimately to use these approaches, we need knowledge of the coefficients of (??), and in this regard progress has been much more limited. A simple argument [?] leads to the so-called Mott-Ioffe-Regel bound in quasiparticle theories of transport, in the presence of a sharp Fermi surface. A well-defined quasiparticle must have a mean free path $l_{\rm mfp}$ larger than its Compton wavelength $\sim k_{\rm F}^{-1}$. Along with the definition of quasiparticle mass $m = \hbar k_{\rm F}/v_{\rm F}$, we obtain from the Drude formula

$$\sigma = \frac{ne^2\tau}{m} = \frac{e^2}{\hbar} \frac{k_{\rm F}^{d-1} v_{\rm F} \tau}{\hbar k_{\rm F}} = k_{\rm F} l_{\rm mfp} \times \frac{e^2}{\hbar} k_{\rm F}^{d-2} \gtrsim \frac{e^2}{\hbar} k_{\rm F}^{d-2}. \tag{2.483}$$

This bound is violated in many strange metals [?], and if these systems lack quasiparticles this is not

surprising. Nonetheless, these compounds do seem to saturate the bound [?]

$$\sigma = \frac{ne^2\tau}{m} \sim \frac{\tau E_{\rm F}}{\hbar} \frac{e^2}{\hbar} k_{\rm F}^{d-2} \gtrsim \frac{e^2}{\hbar} k_{\rm F}^{d-2} \frac{E_{\rm F}}{k_{\rm B}T},\tag{2.484}$$

where we have used the Heisenberg uncertainty principle to bound the scattering lifetime: $\tau \gtrsim \hbar/k_{\rm B}T$. It was proposed in [?] that (??) may be re-cast using the Einstein relation $\sigma = D\chi$ into the form

$$D \gtrsim \frac{\hbar v_{\rm F}^2}{k_{\rm B}T},$$
 (2.485)

under plausible assumptions about the charge susceptibility χ . We have finally arrived at a bound which makes no reference to quasiparticles, and provides a simple explanation for the ubiquitous scaling $\sigma \sim 1/T$. (??) is also appealingly similar to holographic viscosity bounds [?].

Let us now raise immediate and important questions, along with the partial resolutions that exist in the literature. These themes will be important to keep in mind as we review the recent holographic progress on this problem. All of these points do remain important open problems:

- 1. (??) is violated in clean conformal field theories as $T \to 0$: as we have shown in (??), σ is T-independent. So is σ , D, or neither the quantity which is fundamentally bounded, and if so under what conditions does a tight bound exist?
- 2. How do insulators avoid (??) and/or (??)? Non-interacting electrons placed in a strongly disordered background become localized, and as a consequence are an insulator; this effect can persist in some interacting theories [?]. Does some mechanism prevent (many-body) localization in incoherent metals? One possibility is that we perturb our metal with a long wavelength (but large amplitude) perturbation. It is then possible to apply hydrodynamics (with momentum) locally [?]. Holographic models often realize bounds on conductivities, without the assumption of "hydrodynamic" disorder, but we do not have a physical understanding of why.
- 3. Can we derive explicit formulae for the coefficients of (??) from a more microscopic perspective? How should this computation proceed?

Strong momentum relaxation I: "mean field" methods

The simplest way to holographically model an incoherent metal is through a "mean field" approach, where translational symmetry has been broken, but the geometry is homogeneous. Although this might seem contradictory, this is not so. The first mean field model of translational symmetry breaking was to use holographic massive gravity [?, ?]. Other mean field approaches include holographic "Q-lattices" [?], and "helical lattices" [?] based on the Bianchi classification of homogeneous spacetimes [?].

The simplest mean field model, however, turns out to be a model with the following general action [?]:

$$S = S_{\text{EMD}} - \frac{1}{2} \sum_{I=1}^{d} \int d^{d+2}x \sqrt{-g} Y(\Phi) (\partial \chi^{I})^{2}$$
 (2.486)

with the ansatz that the EMD fields depend only on the radial direction, while

$$\chi^{I} = \frac{mx^{I}}{\sqrt{2}\kappa}, \quad (I = 1, \dots, d). \tag{2.487}$$

The χ field is often called the axion, as it has a shift symmetry, just like an axion in particle physics. In a homogeneous background, it is easy to see that (??) solves the χ equation of motion. Now, note that the dilaton and graviton equations of motion depend only on derivatives of χ^I , and that the derivatives of χ^I are constants, and thus homogeneous in the spatial directions. Hence, the assumption that the EMD fields are homogeneous is justified.

To compute σ in these models, or any other type of mean field model, we can proceed using a variety of methods. Here, let us short-cut the "membrane paradigm" technique developed in [?]. We have essentially computed the equations of motion in §??: in particular, (??) is valid for any homogeneous geometry, and if we rewrite (??) in position space, and use (??), we obtain

$$\delta \mathcal{P}_x' = \frac{-\delta \tilde{g}_{tx}}{b} \sum_{I} \frac{|\nabla \chi^I|^2}{dr^d} = -\frac{Ym^2}{2\kappa^2 br^d} \delta \tilde{g}_{tx}$$
 (2.488)

with

$$\delta \mathcal{P}_x = \frac{\mathrm{i}bm}{\sqrt{2}\kappa\omega r^d} Y(\Phi)\delta\chi_x'. \tag{2.489}$$

Now, we can essentially carry through the same calculation as before, but taking $\omega \to 0$ while not taking a perturbative limit $m \to 0$. (??) is equivalent to

$$-i\omega\sigma_{\rm dc}\frac{e^2}{L^{d-2}} = br^{2-d}Z\delta A_x' - \frac{e^2Q}{L^{d-2}}\delta \tilde{g}_{tx}.$$
 (2.490)

The equation itself only gives that the right hand side is constant – we fix this constant to be related to the dc conductivity using the near-boundary asymptotics of δA_x , Z, b and $\delta \tilde{g}_{tx}$, and concluding that as $r \to 0$

only the first term contributes. Near $r = r_h$,

$$\delta A_x' \approx -\frac{\mathrm{i}\omega}{b} \delta A_x,$$
 (2.491)

and similarly for other fields. (??) implies that near the horizon $Q\delta A_x = L^d\delta \mathcal{P}_x$, and combining this fact, (??) and (??) we obtain

$$\sigma_{\rm dc} = \frac{Z_{\rm h} L^{d-2}}{e^2 r_{\rm h}^{d-2}} + \frac{2\kappa^2 \mathcal{Q}^2 r_{\rm h}^d}{m^2 L^d Y_{\rm h}} = \frac{Z_{\rm h} L^{d-2}}{e^2 r_{\rm h}^{d-2}} + \frac{4\pi \mathcal{Q}^2}{\mathcal{S} m^2 Y_{\rm h}}$$
(2.492)

where Z_h and Y_h are the values of $Z(\Phi)$ and $Y(\Phi)$ on the horizon, respectively. (??) was found in very similar models by [?, ?]. Many models lead to results similar to (??), where the conductivity is a sum of two terms. There is an obvious comparison to make with the hydrodynamic prediction (??), with the zeroth order term in Q analogous to " σ_Q ", and the quadratic term in Q the analogue of the Drude term. We will see shortly that this is not quite right. Let us point out three further important points:

- 1. As $m \to 0$, the regime where translational symmetry is broken, we recover the perturbative memory matrix regime [?, ?].
- 2. As $m \to \infty$, the conductivity is limited not by the "strength" m of translation symmetry breaking, but only by the first term in (??). This is quite surprising from a condensed matter perspective, where normally transport coefficients get smaller at stronger disorder strengths. We will see that this is a generic prediction of many holographic models in d = 2.
- 3. σ_{dc} is a sum of two contributions, which can have different T-scalings, due to Z_h and Y_h . This suggests a richness of possible scaling laws in quantum critical systems, while at the same time a lack of unambiguous predictions.

Metal-insulator transitions

A frequently studied aspect of these holographic models is a metal-insulator transition. Metal-insulator transitions driven by interactions are quite challenging to study using traditional methods in condensed matter.

The most common mechanism for realizing an interaction-driven metal-insulator transitions is described in [?, ?]. Suppose that the dilaton coupling to F^2 , $Z(\Phi) = \exp[\gamma \Phi]$. For simplicity, we also temporarily set Q = 0. Depending on the value of $\gamma \Phi$ in the IR – in an isotropic model – one either has a metal in d = 2 if $\gamma \Phi \to +\infty$, versus an insulator if $\gamma \Phi \to -\infty$. This follows immediately from the scaling of (??). In anisotropic models one must be a bit more careful, due to the presence of additional metric factors

associated with anisotropy, but qualitatively the same idea holds. Crucially, we see that the metal-insulator transition in cases such as [?, ?] is driven entirely by γ (and other parameters in the *action*) and not m (the "disorder strength"). This is therefore not a metal-insulator transition of a single QFT. The conductivity in the insulating phase is also not sensitive to the "disorder" strength—if we set $m \to \infty$, (??) is still finite.

A slightly different approach involves the use of helical lattices [?]. In this case, we study the holographic duals of metals in d = 3. One constructs a solution to the Einstein equations where the metric is built up of the following three 1-forms:

$$\omega_1 = \mathrm{d}x, \quad \omega_2 + \mathrm{i}\omega_3 = \mathrm{e}^{\mathrm{i}px}(\mathrm{d}y + \mathrm{i}\mathrm{d}z),$$
 (2.493)

and measures the conductivity along the x-direction. Although translational symmetry has been broken in this direction, it is done so in a special way – the prefactors of the coefficients $\omega_i \otimes \omega_j$ in the metric are independent of x. In this case, through a change in the parameter p, implemented only through the boundary conditions in the field theory, one may realize a metal-insulator transition. This is associated with a change in the scaling behavor of the IR geometry; for lack of a better phrase, this transition is called "localization-driven". This transition is clearly distinct from the previous case, as the same bulk action describes both phases. Unfortunately, we do not have a clear understanding of the interpretation of this helical lattice in the boundary theory. One might anticipate that the parameter p models the disorder strength, but this is not likely. Depending on the particular model, increasing p may either lead to a metal-to-insulator transition or an insulator-to-metal transition [?].

ac transport

Although these mean field methods give nothing more than (??) at $\omega = 0$, in reality holographic models are a bit more subtle, as " σ_{Q} " and " τ " need not admit their naive interpretations. [?, ?] computed $\sigma(\omega)$ (in particular) at next-to-leading order in the "mass" parameter m^2 , in a simple axion model for d = 2, and found

$$\sigma(\omega) = \sigma_{Q} + \frac{1}{1 - i\omega\tau} \left(\frac{1}{e^{2}} - \sigma_{Q} + \frac{\mu^{2}}{m^{2}} \right) + \mathcal{O}\left(\omega, \frac{1}{\tau}\right), \tag{2.494}$$

with $m^2 \sim 1/\tau$ a perturbatively small parameter, and

$$\frac{1}{\tau} = \frac{Sm^2}{4\pi(\epsilon + P)} \left(1 + \lambda m^2 + \cdots \right), \quad \sigma_{Q} = \frac{1}{e^2} \left(\frac{ST}{\epsilon + P} \right)^2. \tag{2.495}$$

The expression for σ_{Q} was known earlier [?].

(??) tells us that (??) does not hold at $\mathcal{O}(\tau^0)$. This should not be particularly surprising. As we made clear in our more formal derivations of (??) at weak disorder, the σ_Q contribution was generically a subleading

term in perturbation theory. Hence, disorder-induced corrections to both " τ " (though this may lose a sharp definition) and the equations of state, lead to corrections as relevant as σ_{Q} .

At higher orders in perturbation theory, [?] has demonstrated the loss of a Drude peak in $\bar{\kappa}(\omega)$ once $m \sim T$ in this same axion model, in agreement with the qualitative predictions of [?].

Demystifying massive gravity

(Sean???)

Thermoelectric conductivities

So far, we have focused on computing σ . Computations of α and $\bar{\kappa}$ can be a bit more involved, but let us sketch out the procedure [?, ?, ?]. We follow a similar approach to that used in §??; again, we assume d=2 for simplicity, and use the axion model from before. This time, we study perturbations of the form

$$\delta A_x = t(A_t \zeta - E) + \delta \tilde{A}_x(r), \qquad (2.496a)$$

$$\delta g_{tx} = t g_{tt} \zeta + \delta \tilde{g}_{tx}(r), \tag{2.496b}$$

along with time-independent perturbations $\delta \chi^x$ and δg_{rx} . The time-dependent parts of the perturbations above are chosen by employing the tx component of the linearized Einstein's equations and the x-component of the Maxwell equations, and showing the t-linear piece only vanishes when the above choices are made. Asymptotic analysis near r=0 confirms that these perturbations encode electric field E and thermal "drive" ζ . The linearized Maxwell equations imply that $\partial_r J=0$, where

$$e^{2}J = \sqrt{-g}Z(\Phi)F^{rx} = \sqrt{-\frac{g_{tt}}{g_{rr}}}Z(\Phi)\left[\partial_{r}\delta\tilde{A}_{x} + |g^{tt}|(\partial_{r}A_{t})\delta\tilde{g}_{tx}\right]$$
(2.497)

The asymptotic behavior as $r \to 0$ that J is nothing more than the expectation value of the electric current in the dual field theory. Next, the t-independent part of the tx-Einstein equation implies that $\partial_r Q = 0$, where

$$Q = \frac{1}{2\kappa^2} \sqrt{-\frac{g_{tt}^3}{g_{rr}}} \partial_r \left(\frac{\delta \tilde{g}_{tx}}{g_{tt}}\right) - JA_t, \tag{2.498}$$

and again boundary asymptotics imply Q is the boundary heat current. Demanding regularity near the horizon, we find that

$$Q = \frac{1}{2\kappa^2} \sqrt{-\frac{g_{tt}^3}{g_{rr}}} \partial_r \frac{\delta g_{rx}}{\sqrt{-g_{rr}g_{tt}}} \bigg|_{r=r_{\rm h}} . \tag{2.499}$$

The linearized rx-Einstein equation, along with the background equations of motion, enforces

$$\delta g_{rx} = \frac{\zeta}{2(r_h - r)} \frac{\kappa^2 \mathcal{S}}{\pi Y_h m^2} + E \sqrt{-\frac{g_{rr}}{g_{tt}}} \frac{2\kappa^2 \mathcal{Q}}{m^2 Y_h}$$
(2.500)

and using the definitions of $T\alpha$ and $T\bar{\kappa}$ as the coefficients of $\partial_{\zeta} J$ and $\partial_{\zeta} Q$, one finds:

$$\alpha = \frac{4\pi \mathcal{Q}}{Y_{\rm h} m^2},\tag{2.501a}$$

$$\bar{\kappa} = \frac{4\pi T \mathcal{S}}{Y_{\rm h} m^2}.\tag{2.501b}$$

Using the expression for J, we can independently compute σ , as given in (??), and confirm that Onsager reciprocity holds by an independent computation of α .

When $m \to 0$, we recover the Drude predictions for thermoelectric conductivities as derived from hydrodynamics. As m gets larger, we see deviations from the hydrodynamic predictions – there seems to be no $\sigma_{\mathcal{Q}}$ dependence in α or $\bar{\kappa}$, in contrast to (??) and (??). This is the same issue that we discovered in §?? – namely, the transport theory of [?] is not correct beyond leading order in perturbation theory in m.

Strong momentum relaxation II: exact methods

Analytic methods

Let us now move beyond the mean field strong disorder limit, and study holographic models with explicitly broken translational symmetry analytically. Remarkably, it has recently been shown that for a large class of EMD holographic models [?, ?], the dc transport problem reduces to the solution of some "hydrodynamic" PDEs on the black hole horizon. The derivation of these results is a much more souped up version of the membrane paradigm calculation of thermoelectric conductivities that we just reviewed for the axion model, and so we simply state the results. We assume that the black hole horizon is at constant temperature T > 0 and admits a connected horizon with the topology of a torus. The answer is simplest if we employ Gaussian normal coordinates near the horizon [?], in which case the EMD fields have near-horizon expansion (switching to coordinates \tilde{r} where the horizon is at $\tilde{r} = 0$):

$$ds^{2} = d\tilde{r}^{2} - \left(2\pi T\tilde{r} + \frac{F(\mathbf{x})}{6}\tilde{r}^{3} + \cdots\right)^{2}dt^{2} + \left(\gamma_{ij}(\mathbf{x}) + \frac{h_{ij}(\mathbf{x})}{2}\tilde{r}^{2} + \cdots\right)dx^{i}dx^{j},$$
(2.502a)

$$A = (\pi T p(\mathbf{x})\tilde{r}^2 + \cdots) dt, \tag{2.502b}$$

$$\Phi = \phi(\mathbf{x}) + \cdots \tag{2.502c}$$

 γ_{ij} is the induced metric on the black hole horizon. Then, by solving the following sourced linear partial differential equations on the black hole horizon:

$$0 = \nabla_i \left(\mathcal{S}_h T v^i \right), \tag{2.503a}$$

$$0 = \nabla_i \left(\mathcal{Q}_h v^i + \Sigma_h \left(E^i - \nabla^i \mu \right) \right), \tag{2.503b}$$

$$-\nabla_i \phi \nabla_j \phi v^j = \mathcal{Q}_h(\nabla_i \mu - E_i) + \mathcal{S}_h(\nabla_i \Theta - T\zeta_i) - 2\eta_h \nabla^j \nabla_{(j} v_{i)}$$
 (2.503c)

where covariant derivatives are taken with the induced horizon metric, E_i and ζ_i are constants and

$$\eta_{\rm h} = \frac{\mathcal{S}_{\rm h}}{4\pi} = 1,\tag{2.504a}$$

$$\Sigma_{\rm h} = Z(\phi),\tag{2.504b}$$

$$Q_{\rm h} = Z(\phi)p, \tag{2.504c}$$

one can show that the spatially averaged charge and heat currents in the boundary theory are given by

$$J^{i} = \frac{1}{L^{d}} \int d^{d}\mathbf{x} \sqrt{\gamma} \left(\mathcal{Q}_{h} v^{i} + \Sigma_{h} \left(E^{i} - \nabla^{i} \mu \right) \right)$$
 (2.505a)

$$Q^{i} = \frac{1}{L^{d}} \int d^{d}\mathbf{x} \sqrt{\gamma} T \mathcal{S}_{h} v^{i}. \tag{2.505b}$$

Given expressions for J and Q linear in E and ζ it is straightforward to use (??) to obtain the conductivities.

(??) look like the equations describing transport in a relativistic fluid on a curved space, with disorder imposed via an external chemical potential [?], but with strange equations of state. In particular, the thermodynamic Maxwell relations are not obeyed for any sensible equation of state.¹⁹ In a simple axion model, [?, ?] has perturbatively shown that these equations of state can be understood from a hydrodynamic perspective, choosing a curious fluid frame where the fluid velocity is proportional to the heat current, which seems to be a convenient frame in holography. One can gain further intuition by sprinkling factors of $\sqrt{\gamma}$ in front of each term in (??) – then \mathcal{S}_h follows from the Bekenstein-Hawking formula, and \mathcal{Q}_h is the local charge density on the horizon [?].

In general, these horizon fluid equations are a dramatic simplification from a numerical point of view – given a complicated black hole geometry, one can solve a lower dimensional PDE to compute the dc transport coefficients. Remarkably, there are some powerful statements that can also be made analytically. For example, Onsager reciprocity immediately follows from the hydrodynamic form of these equations [?].

One can analytically solve the transport equations if translational symmetry is only broken in a single

¹⁹Thermodynamic Maxwell relations can only be obeyed by (??) if the pressure is a separable function of μ and T.

direction. In fact this, was noted earlier [?, ?]. To understand why this is so, consider the following simple limit. If we have a charge-neutral system, then the hydrodynamic equations reduce to a simple diffusion equation. Discrete diffusion equations are resistor networks. The resistance of a 1d resistor network is just the sum of all the individual resistances. We can compute this resistance by just computing the net power dissipated in the network, which is a sum of a local quantity. This latter perspective readily generalizes to the full equations (??). One finds using this approach that the inverse conductivity matrix is expressed as a single integral over *local* quantities on the horizon [?], just as the power dissipated in the resistor network is the sum of local Joule heating:

$$\frac{T\bar{\kappa}}{T\sigma\bar{\kappa} - (\alpha T)^2} = \frac{1}{L} \int dx \, \frac{\gamma_{xx}}{\sqrt{\gamma}Z(\phi)},\tag{2.506a}$$

$$-\frac{T\alpha}{T\sigma\bar{\kappa} - (\alpha T)^2} = -\frac{1}{4\pi TL} \int dx \, \frac{\gamma_{xx}p}{\sqrt{\gamma}},\tag{2.506b}$$

$$\frac{\sigma}{T\sigma\bar{\kappa} - (\alpha T)^2} = \frac{1}{(4\pi T)^2 L} \int dx \left[\frac{(\partial_x \phi)^2}{\sqrt{\gamma}} + \frac{g_{xx} Z(\phi) p^2}{\sqrt{\gamma}} + \frac{(\partial_x \log \sqrt{\gamma \gamma^{xx}})^2 + \gamma^{ik} \gamma^{jl} \partial_x \gamma_{ij} \partial_x \gamma_{kl}}{2\sqrt{\gamma}} \right]$$
(2.506c)

where we have assumed that translation invariance is broken in the x-direction, and assumed that $\gamma_{xj} = 0$ for $x \neq j$, for simplicity.

One can prove non-trivial lower bounds on conductivities for bulk theories dual to d = 2 metals for flows with translational symmetry broken in all directions. For simplicity, we assume that the metal is isotropic. The intuition behind this approach again follows from resistor network tricks [?]. The calculations are a bit technically involved, so let us state without proof the results, which hold for any isotropic theory with a connected black hole horizon. The first is a bound on the electrical conductivity in the Einstein-Maxwell system [?]:

$$\sigma \ge \frac{1}{e^2}.\tag{2.507}$$

The second is a bound on the thermal conductivity κ in any EMD theory [?]:

$$\kappa = \bar{\kappa} - \frac{T\alpha^2}{\sigma} \ge \frac{L^2}{16\pi G_N} \frac{8\pi^2 T}{|\min(V(\Phi))|}.$$
(2.508)

For theories with bounded potentials (which can generally occur for models with $\theta \geq 0$ in the clean limit) we hence find a strictly finite thermal conductivity at finite T (the factor of T is trivially necessary by dimensional analysis).

Remarkably, both of these bounds are essentially saturated in some of the simplest mean field models,

implying that these mean field approaches to breaking translational symmetry are – at least in part – quantitatively sensible. In particular, in a simple Einstein-Maxwell model with massive gravity [?] or axions [?], one finds (??) with $Z_h = Y_h = 1$, which we readily see saturates (??) either when $m \to \infty$ or $Q \to 0$. In this same model, the thermal conductivity is given by [?]

$$\kappa = \frac{L^2}{16\pi G_N} \frac{4\pi T S}{m^2 + \mu^2} \ge \frac{L^2}{16\pi G_N} \frac{4\pi^2 T}{3},\tag{2.509}$$

where the second inequality follows from bounding the entropy density by S(T=0). This again agrees with (??) upon using that V=-6 for the Einstein-Maxwell system.

Both of these results provide a strict no-go theorem on the possibility of realizing a many-body localized state in holographic models. Such a state is non-ergodic, with the absence of thermalization and transport coefficients vanishing at finite energy density [?]. This is in contrast with (??) and (??) – hence we conclude that holographic models with connected black hole horizons do not realize such many-body localization. Whether or not the absence of localization is a robust feature of other higher-dimensional strongly interacting continuum quantum field theories without the holographic large N limit is an important open question.

It has recently been shown that the dc magnetotransport problem in EMD models reduces once again to solving fluid-like equations on a black hole horizon [?]. Interestingly, particle-vortex duality in holography is robust to disorder [?, ?], and (??) can partially be understood as a consequence of this duality [?]. It will be interesting whether universal results, like those discussed in the previous section, once again emerge.

Numerical methods

The main drawback to the physics discussed above is that, of course, to employ (??) in general, one needs to first construct an inhomogeneous black hole background. In essentially all cases, this must be done numerically [?]. Furthermore, to compute conductivities at finite frequency, we need to linearize around the inhomogeneous black hole background. Because both of these procedures are computationally intensive (the latter more so), most work in this direction has been restricted to models which only break homogeneity in a single (x) direction.

One of the simplest things to do is to break translation invariance in a single direction – this can be done by sourcing a bulk field with an inhomogeneous chemical potential of the form [?, ?]

$$\mu = \mu_0 + V \cos(kx). \tag{2.510}$$

This can also be done with scalar fields [?]. These potentials often go by the name "holographic lattices" in

the high energy literature.²⁰ One of the main lessons of numerical work is that – in all known cases so far – for such a single lattice, the IR geometry is homogeneous as $T \to 0$, though possibly deformed from the V = 0 geometry. Most work has been done for d = 2, but we expect these qualitative results are independent of d. At finite μ_0 , the IR geometry is $AdS_2 \times \mathbb{R}^d$ [?]; when $\mu_0 = 0$, the IR geometry is a rescaled AdS_{d+2} [?]. We will discuss the IR geometry of disordered black holes in §??.

As we have discussed analytically above, the low T dc conductivities should be described by the memory matrix formalism at $\mu_0 \neq 0$. This was confirmed [?], and the analytic predictions of [?] were numerically found. Numerically one can also compute ac conductivities at all frequencies. A qualitative sketch of typical results for d=2 is shown in Figure ??. At $\omega \lesssim 1/\tau$, the conductivity is governed by a Drude peak (??). For "monochromatic lattices" of the form (??), additional structure may be found at $\omega \sim k$, associated with resonances with the modulating potential [?, ?]. At high frequencies ω , which are much larger than all other scales in the problem, one finds that $\sigma(\omega) \to 1$, in agreement with (??).

Figure 24: A sketch of $\text{Re}(\sigma(\omega))$ in a holographic model deformed by chemical potential (??), with $\mu_0 \gg k \gg 1/\tau$. In accordance with the memory matrix formalism, $1/\tau \sim V^2$.

Finally, in an EMD model, [?] has shown a metal insulator transition driven by the wavelength of a periodic potential source for the dilaton. This is analogous to the original metal-insulator transition of [?] and confirms its presence in a more rigorous setting.

Further topics

Probe branes

As we discussed in §??, much of the early work in holography focused on finding "top-down" models. This is because such theories are known to be consistent quantum theories of gravity, and so it makes sense that a duality should exist. Nonetheless, one immediately runs into severe limitations – for example, in modeling QCD with $\mathcal{N}=4$ SYM (dual to Einstein gravity on $AdS_5 \times S^5$) we find a model of gluons, but without any quarks. This led to the historical development of "probe brane" holographic models [?], though as we will see they are also interesting objects in their own right for AdS/CMT. For now, we digress from condensed matter physics temporarily.

Recall that d = 3 $\mathcal{N} = 4$ SYM with gauge group SU(N) is in fact the effective theory describing a coincident stack of N D3-branes (neglecting gravitational backreaction), and that the massless degrees of

²⁰This name is not entirely appropriate because there is no relation between the lattice spacing and the charge density, the way that there is for an ionic lattice in traditional condensed matter models. We will return to this point later in the review.

freedom come from open strings stretching between the branes (double "flavor" indices correspond to strings beginning and ending on different branes). Such open strings carry two indices (one for each brane they end on) and hence are in the adjoint representation of SU(N). If we want to construct quarks, which transform in (anti-)fundamental representations of the gauge group, we need to place an object on which an open string can end, leaving a single endpoint on the D3 stack. Hence, we just need to place another Dp brane somewhere – wherever the new Dp brane intersects the D3 stack, massless "quarks" exist due to strings stretching between D3 and Dp branes. The choice of where to place these Dp branes, as well as how to wrap them on internal cycles of S^5 in order to preserve $\mathcal{N}=2$ supersymmetry, is discussed in [?]. Here we present two of the most useful examples:

- 1. To obtain quarks living in d = 3 spatial dimensions, we place a D7 brane on $AdS_5 \times S^3$. The choice of $S^3 \subset S^5$ plays a physical role that we will elucidate below.
- 2. To obtain quarks living in d=2 spatial dimensions, we place a D5 brane on $AdS_4 \subset AdS_5$, wrapping two dimensions along an $S^2 \subset S^5$. This charged matter lives on a defect in the $\mathcal{N}=4$ SYM theory, and hence can exchange energy and momentum with a higher dimensional bath.

The effective action for the U(1) component of the gauge theory on the Dp brane (neglecting any higher form background gauge fields) can be shown to be the Dirac-Born-Infeld (DBI) action:

$$S_{\mathrm{D}p} = -T_{\mathrm{D}p} \int \mathrm{d}^{p+1} x \sqrt{X} \tag{2.511}$$

where

$$X \equiv -\det\left(g_{\alpha\beta} + 2\pi\alpha' F_{\alpha\beta}\right) \tag{2.512}$$

where $\alpha\beta$ denote worldvolume indices on the Dp brane, and $2\pi\alpha'$ is the fundamental string tension. Also recall (??) and (??), and note that $T_{\mathrm{D}p} \sim (2\pi\alpha')^{-(p+1)/2} g_{\mathrm{s}}^{-1}$.

Such models are called "probe brane" models for the following reason: a single²¹ probe brane will negligibly backreact on the geometry. One simple way to see this is to recall that the free energy of the D3 branes scales as N^2 , compared to N for the fundamental quarks on the probe brane. We also note for future reference that other thermodynamic and hydrodynamic quantities for the quark matter will also scale $\sim N$.

Hence, we may place the Dp brane on top of the AdS₅ (Schwarzschild) geometry, treating $g_{\alpha\beta}$ as fixed in (??). Assuming spacetime translation symmetry in the boundary directions, $g_{\alpha\beta}$ is immediately found by

²¹Or more generally, a stack of $N_{\rm f} \ll N$ Dp branes (though we will set $N_{\rm f} = 1$ to avoid clutter).

using (??) and (??) to obtain

$$\frac{g_{\alpha\beta}\mathrm{d}x^{\alpha}\mathrm{d}x^{\beta}}{L^{2}} = \left(\frac{1}{r^{2}f(r)} + \theta'(r)^{2}\right)\mathrm{d}r^{2} - \frac{f(r)}{r^{2}}\mathrm{d}t^{2} + \frac{\mathrm{d}x_{i}\mathrm{d}x^{i}}{r^{2}} + \cos^{k}\theta(z)\mathrm{d}\Omega_{k}^{2}.$$
 (2.513)

where k is defined as the dimension of the sphere which the brane wraps, and $L\cos\theta$ is the radius of the S^k . Upon integrating out the internal directions, we obtain

$$S = -T_{\mathrm{D}p}V_{\mathrm{S}^k} \int \mathrm{d}^{d+2}x (L\cos\theta)^k \sqrt{-\det(g_{ab}^{\mathrm{induced}} + 2\pi\alpha' F_{ab})}$$
 (2.514)

where V_{S^k} is the volume of a unit-radius S^k , and g^{induced} the first three terms of (??). Upon Taylor expanding (??) in the limit of small $F_{\alpha\beta}$, we readily recover the Einstein-Maxwell action, with

$$\frac{1}{e^2} = T_{Dp} V_{S^k} (L \cos \theta)^k (2\pi \alpha')^2, \tag{2.515}$$

When the background charge density is large, nonlinear corrections to the Maxwell action become important, and play a noticable role in the properties of probe brane models. We will give a few examples below. Also note that if the brane is not static on the internal sphere, then the effective charge e is radially dependent, analogous to a $Z(\Phi)$ factor in an EMD model such as (??).

We will assume in the computations below that the Dp brane wraps a finite size sphere (i.e. $|\theta| < \pi/2$) for all z. This is true at finite charge density [?], which will be the case of most interest, or when $\theta(z) = 0$ exactly, corresponding to massless quarks. For massive quarks, there is a critical temperature below which the Dp brane "caps off" – namely, $\theta(z_{\text{crit}}) = \pi/2$, and the brane does not extend below this radius [?, ?]. In this case, the quark matter becomes confined.

Conductivity

Here we compute the electrical conductivity in these probe brane models [?]. Before presenting the computation, however, we should note a curious feature of the result. Recall (??) and the scalings discussed in the previous section:

$$\sigma = \sigma_{\rm Q} + \frac{\mathcal{Q}^2}{\epsilon + P} \left(\frac{\mathrm{i}}{\omega} + \pi \delta(\omega) \right) \sim N + \frac{N^2}{N^2} \left(\frac{\mathrm{i}}{\omega} + \pi \delta(\omega) \right). \tag{2.516}$$

Hence, at leading order in the large N limit, we will only compute σ_{Q} . This is naturally understood from the fact that in the probe brane approximation, the backreaction of the geometry is neglected. We hence cannot recover the "boost" perturbation in the bulk corresponding to the δ function in (??), as we did in §??. This lack of backreaction on the geometry does come with an interesting "advantage" – we may compute σ

beyond linear response without worrying about the heating of the black hole at nonlinear orders. So below, we will compute the conductivity $\sigma \equiv J/E$, but with J a non-linear function of the electric field E.

The DBI equations of motion imply radially conserved currents, assuming that all bulk fields are spatially homogeneous:

$$J^{\mu} = \frac{1}{2e^2(2\pi\alpha')} \left(\sqrt{X} (g + 2\pi\alpha' F)^{\mu r} - \sqrt{X} (g + 2\pi\alpha' F)^{r\mu} \right). \tag{2.517}$$

These are, in fact, equal to the expectation value of the charge current operator in the boundary theory. Let us focus on the two examples of top-down probe brane theories described above – in both cases, the background geometry is the AdS₅-Schwarzschild geometry given in (??) and (??) (in real time, with z=1and $\theta = 0$). Upon applying the electric field $A_x = -Et + a_x(r)$, and assuming a background gauge field $A_t(r)$, we obtain the set of equations

$$J^{t} = \frac{L^{d-2}}{e^{2}} \frac{-r^{2-d} A'_{t}}{\sqrt{1 - (2\pi\alpha')^{2} \frac{r^{4}}{L^{4}} (A'_{t}\prime^{2} + f^{-1}(E^{2} - f^{2}a'_{x}^{2}))}},$$
 (2.518a)

$$J^{t} = \frac{L^{d-2}}{e^{2}} \frac{-r^{2-d}A'_{t}}{\sqrt{1 - (2\pi\alpha')^{2} \frac{r^{4}}{L^{4}} (A'_{t}\prime 2 + f^{-1}(E^{2} - f^{2}a'_{x}^{2}))}},$$

$$J^{x} = \frac{L^{d-2}}{e^{2}} \frac{r^{2-d}fa'_{x}}{\sqrt{1 - (2\pi\alpha')^{2} \frac{r^{4}}{L^{4}} (A'_{t}\prime 2 + f^{-1}(E^{2} - f^{2}a'_{x}^{2}))}}.$$
(2.518a)

After a bit of algebra, we may rearrange these equations into the following useful forms:

$$\left(\frac{J^t}{J^x}\right)^2 = \left(\frac{A_t'}{fa_x'}\right)^2,\tag{2.519a}$$

$$\left(\frac{J^x e^2}{L^{d-2}}\right)^2 \left[1 - \frac{r^4}{L^4} \frac{(2\pi\alpha' E)^2}{f}\right] = \left[(r^{2-d})^2 + \left(\frac{J^x e^2}{L^{d-2}} 2\pi\alpha'\right)^2 \frac{r^4}{L^4} \left[\left(\frac{J^t}{J^x}\right)^2 - \frac{1}{f}\right]\right] (fa_x')^2.$$
(2.519b)

We focus on the second equation. As $f \rightarrow r_+ = 1/\pi T$ where there is a black hole horizon, the objects in square brackets on both sides are negative. However, as $r \to 0$ near the boundary, both brackets are positive. Since they multiply manifestly positive quantities, one can show that these square brackets must both vanish at the same radius $r = r_*$. The left hand side implies the simple equation

$$\frac{1}{r_*^4} = (\pi T)^4 + \left(\frac{2\pi\alpha' E}{L^2}\right)^2. \tag{2.520}$$

Using the right hand side, we obtain a simple equation for the conductivity:

$$\sigma = \frac{L^{d-2}}{e^2} \sqrt{r_*^{2(2-d)} + \left(J^t \frac{2\pi\alpha' e^2}{L^d}\right)^2 r_*^4}.$$
 (2.521)

Similar formulas hold for probe brane models in a background magnetic field [?] and in Lifshitz backgrounds [?]. In the latter theories, when the second term of (??) dominates, one finds $\sigma \sim J^t/T$ in d=2, giving one of the earliest holographic mechanisms for linear-in-T resistivity.

Rather surprisingly, in linear response, one finds that the optical conductivity at low temperatures contains a "Drude-like" peak [?]. Given that we are computing the ω -dependence of σ_Q alone in the probe brane limit, this is not the physical Drude peak observed in coherent metallic states, related to a parametrically long-lived momentum mode.

For the most part, using these probe brane models to compute transport in AdS/CMT has fallen out of favor, due to the more "realistic" set-ups described previously. However, due to the lack of backreaction of the probe branes, some computations (which are very hard in the full gravity theory) may be carried out more readily in probe brane models. An example of such a calculation are the thermal fluctuations of the current operator. For simplicity considering d=2 and $J^t=0$, an explicit calculation [?] reveals that this thermal noise is related by an "equilibrium" fluctuation-dissipation relation at temperature T_* , related to T_* in (??) by $T_*=1/\pi r_*$.

"Zero sound" modes

In an ordinary Fermi liquid, there exist linearly dispersing modes called zero sound modes. Such modes essentially correspond to the "sloshing" of the Fermi surface at fixed density. In contrast, in an ordinary sound mode, the charge density (along with the pressure) will oscillate at finite density. Rather surprisingly, it turns out that the fundamental matter on probe branes admits a strange new type of quasinormal mode in this limit. Assuming that the chemical potential for the fundamental matter is μ , the dispersion relation is [?]

$$\omega = \pm \frac{q}{\sqrt{d}} - \frac{\mathrm{i}q^2}{2d\mu}.\tag{2.522}$$

Unlike the zero temperature sound in the AdS-RN black hole, this should not be thought of as ordinary (first) sound, despite the suggestive propagation velocity. To see this, we recall that in the probe limit, the geometry is pure AdS at T=0 and hence there is no positive entropy density to support a sound mode. These modes have been coined holographic "zero sound", though we will retain quotes as there is no evidence that these modes are related to the dynamics of an emergent Fermi surface.

It is instructive to track the quasinormal modes in the complex plane upon increasing the temperature [?]. What one finds is that the pair of "zero sound" modes has a decreasing propagation speed and increasing attenuation constant. At a critical temperature, the propagation speed vanishes, and the two poles begin moving in opposite directions along the imaginary axis. At high temperatures, one such pole becomes the ordinary hydrodynamic charge diffusion mode (recall that in the probe brane limit the ordinary hydrodynamic sound is absent, as the metric is fixed). Hence, these "zero sound" modes cannot be attributed to

classical hydrodynamics.

These "zero sound" modes persist in other probe brane models, including models with a mass for the charge carriers in the hypermultiplet [?]. In probe brane models with $z \geq 2$, this "zero sound" mode disappears [?].

Defects and impurities

So far, we have assumed that all physics of interest is associated with brane degrees of freedom. But in some field theories, physical defects and impurities do play important roles, and probe branes can be interpreted as corresponding to actual defects in the field theory. A classic model of such a system is the Kondo model, which couples a single impurity spin to a Fermi liquid. Various holographic methods have been proposed to model the coupling of a single impurity to strongly coupled field theories, and certain phenomena admit very natural holographic descriptions. It is argued in [?] that the screening of the impurity spin at low temperatures in the Kondo model is analogous to a holographic superconductor on the defect (i.e., the condensation of charged scalars, which then reduce the net charge as seen in the UV vs. IR). A top down model for such impurities consists of D5 branes intersecting D3 branes at a point in the worldvolume [?]: when the number of D5 branes becomes large, the backreaction of the branes on the holographically dual geometry can be understood as a geometric transition [?, ?] where various higher-form fluxes thread new cycles that emerge in the geometry. This geometric transition is also reminiscent of screening in the Kondo model.

An interesting new phenomenon occurs when probe branes and anti-branes are placed a finite distance R apart [?]. This is analogous to two "opposite" impurities spatially separated in the field theory description. When $TR \gg 1$, each brane extends into the horizon. However, when $TR \ll 1$, the minimal free energy solution corresponds to a single brane which begins and ends on the AdS boundary, only extending a finite distance into the bulk. This "dimerization" transition may lead to interesting observable phenomena in the boundary theory, but has not been well-explored (though see [?, ?] for possible directions).

Rather than treating the probe branes themselves as defects, one can also consider probe brane actions (such as DBI) with inhomogeneous boundary conditions. The discussion turns out to be very similar to that in §??, and similar phenomenology holds: see e.g. [?, ?].

Disordered fixed points

It is possible that upon adding marginal or relevant disorder to a quantum field theory, there is an RG flow to a "disordered fixed point" where the disorder strength is either finite or infinite [?]. Unfortunately, standard

tricks (the replica method and perturbative field theory) are not amenable to such disordered fixed points in higher dimensions. Upon writing down the RG equations, one finds that [?]

$$\beta(\bar{V}) = (d - d_{\text{u.c.}})\bar{V} - c\bar{V}^2$$
 (2.523)

where \bar{V} is a coupling constant related to disorder strength, defined in (??), and c > 0. Hence below the critical dimension, $\bar{V} \to 0$, and the fixed point has no disorder. In contrast, we will see that holography is a natural tool for these fixed points.

When dealing with disorder, one must be careful to revisit the notion of relevant vs. irrelevant operators. We can see this simply in holography. Let us consider Einstein gravity coupled to a massive scalar field. Neglecting the backreaction of scalar fields on the geometry, a disordered bulk scalar field takes the form

$$\phi(\mathbf{x}, r) = \int \frac{\mathrm{d}^d \mathbf{k}}{(2\pi)^d} h(\mathbf{k}) e^{i\mathbf{k} \cdot \mathbf{x}} \mathcal{F}_{\Delta}(kr) r^{d+1-\Delta}, \qquad (2.524)$$

where $h(\mathbf{k})$ are Gaussian quenched random variables obeying

$$\overline{h(\mathbf{k})} = 0, \tag{2.525a}$$

$$\overline{h(\mathbf{k})h(\mathbf{q})} = \bar{V}^2 \delta(\mathbf{k} + \mathbf{q}) \tag{2.525b}$$

and $\mathcal{F}_{\Delta}(kr)$ can be expressed in terms of modified Bessel functions. Its precise form is tangential to our discussion. Even before averaging over disorder realizations, we immediately know that the metric will feel the first perturbative corrections due to this scalar hair at $\mathcal{O}(\bar{V}^2)$. Of course, it may be the case that the perturbation is large compared to the background, in which case perturbation theory has failed. Let us diagnose whether or not such a perturbative treatment about AdS is consistent in the UV $(r \to 0)$ [?]. This can be done quite simply. Einstein's equations read

$$G_{ab} \sim \frac{1}{r^2} \sim \overline{T_{ab}[\phi]} \sim \frac{1}{r^2} \times \bar{V}^2 r^{d+2-2\Delta}.$$
 (2.526)

We have assumed that we may average over disorder realizations to extract the long wavelength behavior of the metric. The final step follows from straightforward scaling arguments – importantly, the power of r multiplying \bar{V}^2 is not $2(d+1-\Delta)$ (as it would be for a single cosine) but is $d+2-2\Delta$. This is a consequence of the fact that \bar{V}^2 has a reduced dimension. Evidently, as $r \to 0$, the right hand side of (??) is small

compared to the left hand side – and hence perturbation theory is sensible – so long as

$$2\Delta < d + 2. \tag{2.527}$$

(??) is known as the Harris criterion for the relevance of disorder. In the case of more general hyperscaling-violating theories, (??) generalizes to [?]

$$2\Delta < d - \theta + 2z. \tag{2.528}$$

What happens when Δ is (Harris) marginal? In this case \bar{V}^2 is a dimensionless number. This system was studied in [?], where an emergent Lifshitz scaling in the IR was discovered; here we present a cleaner derivation of this result. For simplicity, we focus on the case d=1. Consider the following convenient ansatz for the metric (in units where $L=\kappa=1$):

$$ds^{2} = A(r) (dr^{2} + dx^{2}) - B(r)dt^{2}.$$
(2.529)

The assumption that the metric is homogeneous is sensible – averaging over disorder at leading order, Einstein's equations now read

$$\frac{A}{\sqrt{B}}\partial_r\left(\frac{\partial_r B}{\sqrt{B}A}\right) = \overline{(\partial_x \phi)^2 - (\partial_r \phi)^2},\tag{2.530a}$$

$$\frac{1}{\sqrt{B}}\partial_r\left(\frac{\partial_r B}{\sqrt{B}}\right) = 4A + \frac{3A}{4}\overline{\phi^2}.$$
 (2.530b)

At leading order in perturbation theory, we may treat the right hand side of (??) as a small source, using $A = 1/r^2$ as for AdS, which is manifestly homogeneous. Employing scale invariance and the precise form of \mathcal{F}_{Δ} we find that at second order in perturbation theory:

$$\overline{\phi^2} = \overline{V}^2 \int \frac{\mathrm{d}k}{2\pi} r \mathcal{F}_\Delta(kr)^2 = \overline{V}^2, \qquad (2.531a)$$

$$\overline{(\partial_x \phi)^2 - (\partial_r \phi)^2} = \frac{\overline{V}^2}{4}.$$
(2.531b)

It is simple to check that a consistent solution to (??) is

$$A = \frac{a_0}{r^2}, \quad B = \frac{b_0}{r^{2+\bar{V}^2/4}},$$
 (2.532)

implying a non-trivial Lifshitz exponent $z = 1 + \bar{V}^2/8$. Note that our normalization of \bar{V} is different from [?] due to different bulk scalar normalizations.

One can construct the finite temperature generalizations of these black holes [?] and check that the entropy density $S \sim T^{1/z}$ with the \bar{V} dependent z. More interestingly, the thermal conductivity $\bar{\kappa}$ has log-periodic oscillations [?], suggesting the possibility that scalar operators pick up complex scaling dimensions in the emergent IR geometry. This may suggest an instability of the emergent Lifshitz geometry.

So far, disorder has made black holes "bumpy." It is also possible for disorder to do something even more extreme – split a black hole horizon into disconnected pieces [?]. This effect is quite challenging to find numerically, but it can be understood heuristically as the statement that some black hole spacetimes admit static geodesics. It is natural to imagine placing a point particle of charge q and mass m at such a geodesic, and "growing it" into a tiny black hole. More extreme scenarios, with many such black holes with such disconnected horizons, may avoid the "no-go theorems" on many-body localization discussed in [?, ?].

Out of equilibrium I: quenches

The focus of this review so far has been on entirely "static" properties of quantum matter: we have asked about the nature of the ground state, and about what happens when we perturb it a little bit (this gives us transport coefficients like the electrical conductivity). In this section, we will briefly mention what happens when you "kick" quantum matter a lot. One of the simplest (but most important) questions that we can ask is: given an interacting quantum system far from equilibrium, will it relax to a steady state (equilibrium)? What is the mechanism through which equilibrium is reached – especially as the dynamics "passes through" a phase transition? We will focus in this section on quenches in field theories in $d \ge 2$ spatial dimensions, where there are almost no techniques from field theory that can answer these questions.

The simplest way to probe this question is through a quantum quench. The idea is as follows: consider a time dependent Hamiltonian

$$H(t) = H_0 + H'f(t), (2.533)$$

with f(t) a function which varies over time scales τ which are often quite fast. For simplicity, most research focuses on the case where f(t) either interpolates between $f(-\infty) = 0$ and $f(\infty) = 1$ (quench from one state to another), or where $f(\pm \infty) = 0$ but f(0) = 1 (pulsed quench). We will see examples of both in this section.

The case where $f(t) = \sin(\omega t)\Theta(t)$ is also interesting, though we will have little to say on it in this review. Such a drive generically does work on a system, possibly until it reaches infinite temperature. In holographic models, this periodic driving leads to the creation and growth of a black hole with time [?]. At late times, this model is pathological and reaches infinite temperature. On the other hand, let us also note the possibility for curious states in field theory which do not thermalize despite oscillating with non-vanishing energy density. This possibility was discovered holographically by curious solutions of Einstein's equations which oscillate: for example, gravitational analogues of standing waves which are nonlinearly stabilized [?, ?].

Uniform quenches

Let us begin with the case where H_0 describes a conformal field theory, and

$$H' = \lambda \mathcal{O}, \quad f(t) \sim \operatorname{sech} \frac{t}{\tau},$$
 (2.534)

where \mathcal{O} is the zero momentum mode of a relevant operator of dimension $0 < \Delta < d+1$, λ is a small parameter, and we take the quench time scale $\tau \to 0$ as well. The exact behavior of f(t) is not relevant. This setup was considered in a series of papers [?, ?, ?, ?], and we summarize the main conclusions. The most interesting observation is that the energy density added to the CFT scales as

$$\epsilon = \frac{\lambda^2}{\tau^{2\Delta - d - 1}} \mathcal{E} \left(\tau^{d + 1 - \Delta} \lambda \right), \tag{2.535}$$

with $\mathcal{E}(x)$ a dimensionless function of its parameter. In the limit $\tau \to 0$, this parameter is *small*, and so all quenches have a universal behavior up to $\mathcal{E}(0)$.

Holographically, the universality of this result follows from the fact that for a fast quench, the "information" about the quench cannot propagate very deep into the bulk before the quench has ended. Therefore, the quench dynamics is characterized by the fast dynamics of a scalar field in AdS, and the resulting slow dynamics of black hole formation (but with properties like ϵ already fixed on the fast time scale). In the end, (??) can be understood from essentially dimensional grounds when $\Delta > (d+1)/2$. The leading order coefficient in ϵ must scale as λ^2 , since following a "hydrodynamic" Ward identity (c.f. (??))

$$\epsilon = -\int_{-\infty}^{\infty} dt \, \langle \mathcal{O}(t) \rangle \partial_t (\lambda f(t))$$
 (2.536)

and $\langle \mathcal{O} \rangle \sim \lambda$ to leading order in λ , since $\langle \mathcal{O} \rangle_{\text{CFT}} = 0$ as it is relevant. Indeed (??) is valid for both free theories and strongly interacting theories [?].

Another example of a spatially homogeneous quench is as follows. Consider a holographic superfluid at an initial temperature $T < T_c$ with a source for the superfluid order parameter which is pulsed analogously to above [?]. The pulse injects energy into the superfluid and the late time dynamics of the order parameter are described by

$$|\langle \mathcal{O}_{SF}(t)\rangle| \approx |B + Ae^{-i\omega t - \gamma t}|$$
 (2.537)

Three possible behaviors were found, depending on the strength " λ " of the quench, as shown in Figure ??. When $0 < \lambda < \lambda_1$, both γ and ω are positive, and $\langle \mathcal{O}_{SF}(\infty) \rangle > 0$; when $\lambda_1 < \lambda < \lambda_2$, $\omega = 0$ but B > 0; when $\lambda > \lambda_2$, $\omega = 0$ and B = 0. Hence, for $\lambda < \lambda_2$, the final state is a superfluid, while for $\lambda > \lambda_2$ it is a normal fluid.

Figure 25: A sketch of the dynamics of the order parameter in a holographic superfluid quench. Top row: $\langle \mathcal{O} \rangle$ as a function of t. Bottom row: location of the lowest lying QNMs, and their motion upon increasing λ . Columns left to right: $0 < \lambda < \lambda_1$; $\lambda_1 < \lambda < \lambda_2$; $\lambda > \lambda_2$.

As we have seen repeatedly in this review, this late time dynamics is naturally understood by studying the lowest lying QNMs of the bulk geometry. In the superfluid phase, the existence of a Goldstone mode is manifested as a mode with $\gamma = \omega = 0$, and so the relaxation in (??) is governed by the QNM with next smallest imaginary part. The "motion" of these QNMs with increasing λ is shown in Figure ??. This reveals the holographic origin of the dynamical transition at $\lambda = \lambda_1$. When the purely damped ($\omega = 0$) mode collides with the Goldstone mode, these modes separate off the $\omega = 0$ axis and γ is increasing with increasing λ . This corresponds to a quench which has injected enough energy so that the final state is in the normal phase. These holographic dynamics reproduce the expectations of weakly interacting field theories [?], but it is instructive to see how the QNMs of "superfluid" black holes recover this dynamics even at strong coupling.

Spatial quenches

Let us now consider a slightly more complicated set-up: suppose we take two copies of a conformal field theory in d spatial dimensions, one (L) defined for x < 0 and the other (R) defined for x > 0. Now, suppose that we prepare L in a thermal state at temperature $T_{\rm L}$, and R in a thermal state at $T_{\rm R}$. Without loss of generality,²² we suppose that $T_{\rm L} > T_{\rm R}$. At time t = 0 we allow these theories to couple. The set-up is depicted in Figure ??.

Figure 26: Left: two CFTs placed next to each other at different temperature. Right: a NESS forms as energy flows from the left to right bath.

This set-up is very well studied in one spatial dimension in non-conformal but integrable spin chains [] . What is often found is that the theory reaches a non-equilibrium steady state (NESS), where the local density matrix near x = 0 is given by $\exp[-\sum \lambda_i H_i]$, for all conserved quantities H_i . For the case of a conformal field theory, the answer is known exactly [?]. For |x| < t, the local density matrix takes the

 $^{^{22}}$ So long as the theory is not chiral in d=1.

remarkably simple form

$$\rho_{\text{NESS}} = e^{-\beta(\cosh\theta H - \sinh\theta P)}, \qquad (2.538)$$

with

$$\beta = (T_{\rm L}T_{\rm R})^{-1/2}, \quad e^{2\theta} = \frac{T_{\rm L}}{T_{\rm R}}.$$
 (2.539)

 ρ_{NESS} only contains two conserved quantities, despite the existence of an infinite number. There is a very simple explanation: CFT2s consist of decoupled left and right moving theories, and so at the speed of light the left movers at T_{R} from the right bath and right movers at T_{L} from the left bath "mix" near the interface. This argument is rigorous and can be shown using CFT technology [?]; see [?] for a holographic derivation.

It was pointed out using hydrodynamic arguments in [?, ?] that the NESS could exist in any dimension. Let us consider a CFT for simplicity, but our argument generalizes naturally, and focus on the case where $T_{\rm L} \approx T_{\rm R}$ to simplify the mathematics. In this limit the system is almost in equilibrium and we can linearize the equations of hydrodynamics. These equations lead to elementary sound waves and we conclude that a NESS forms for $|x| < t/\sqrt{d}$ between a pair of sound waves propagating away from the interface. The basic dynamics is depicted in Figure ??. The nonlinear calculation is more subtle but a NESS can be shown to form within hydrodynamics [?, ?].

At early times, the dynamics is complicated and possibly non-universal near the interface. Holographic approaches [?] allow us to access both the early and late time dynamics in a unified approach. One immediate consideration is that if a NESS exists, it is thermal (c.f. (??)) in a holographic model: this follows from black hole uniqueness theorems [?]. It is further proposed that knowledge of the heat current in the NESS allows one to determine fluctuations of the heat current, giving the first solvable model of "current noise" in higher dimensions [?].

Kibble-Zurek mechanism and beyond

An even more complicated quench set-up is as follows. Consider a Hamiltonian H with a thermal phase transition at finite temperature T_c . As an explicit example, we will keep in mind a normal-to-superfluid transition in d = 3. The effective action for the order parameter φ dynamics is an O(2) model:

$$\mathcal{L} = -|\partial\varphi|^2 + \epsilon|\varphi|^2 - \frac{\lambda}{2}|\varphi|^4. \tag{2.540}$$

Suppose that we perform a thermal quench on the system in between times $-a_1\tau_Q \le t \le a_2\tau_Q$, for $a_{1,2} \sim \mathcal{O}(1)$, such that the "reduced temperature"

$$\epsilon(t) \equiv 1 - \frac{T(t)}{T_{\rm c}} = \frac{t}{\tau_{\rm Q}}.\tag{2.541}$$

A priori, a superfluid condensate forms, with $|\varphi|^2 = \epsilon/\lambda$, and nothing interesting happens. But what is the phase of the complex number φ ? Some thermal fluctuation will lead to the local orientation of φ , but these thermal fluctuations will kick $\arg(\varphi)$ to different values at different points. We will now argue that this dynamics leads to the formation of vortex lines (or more general topological defects in more general models).

The canonical description of the resulting dynamics is due to Kibble [?] and Zurek [?], and so is called the Kibble-Zurek mechanism (KZM). In a theory of dynamical critical exponent z and correlation length exponent ν , the time scale associated with the dynamics is

$$\tau(\epsilon) = \tau_0 |\epsilon|^{-z\nu}. \tag{2.542}$$

If $\tau(\epsilon) \ll |t|$, then we expect that the dynamics this far from the quench is adiabatic – the system is in equilibrium (or as close to it as possible). But when $\tau(\epsilon) \gg t$, then the system cannot reach equilibrium during the quench. Hence, we define a freeze-out time when $\tau(\epsilon(t_f)) \sim t_f$:

$$t_{\rm f} \sim \tau_0 \left(\frac{\tau_{\rm Q}}{\tau_0}\right)^{z\nu/(z\nu+1)}. \tag{2.543}$$

On this short time scale the system is far from equilibrium. In particular, in the superfluid phase the early time dynamics (0 < $t \ll t_{\rm f}$) will be in response to the thermal fluctuations imprinted on the system just above $T_{\rm c}$, which are of a characteristic size

$$\xi_{\rm f} \sim \xi_0 \left(\frac{t_{\rm f}}{\tau_0}\right)^{1/z} \sim \xi_0 \left(\frac{\tau_{\rm Q}}{\tau_0}\right)^{\nu/(z\nu+1)}$$
 (2.544)

The number density of vortices in the superfluid at T=0 should be approximately set by this length scale:

$$n_{\text{vort}} \sim \frac{1}{\xi_{\text{f}}^{d-d_{\text{top}}}},\tag{2.545}$$

where d_{top} is the dimension of topological defects; for a superfluid, $d_{\text{top}} = d - 2$.

Recent holographic studies have shown that this argument holds for slow thermal quenches [?, ?]. To recover this effect in holography is slightly subtle – thermal fluctuations are suppressed by a factor of $1/N^2$ which vanishes in the classical gravity limit. So [?, ?] simply added (small) random external forcing as a boundary condition to mimic these fluctuations – the resulting dynamics will lead to defect formation across the phase transition. Holographic models recover the KZM in its regime of validity when τ_Q is long. As [?] also emphasized, holographic methods are well suited to model defect formation for rapid quenches, beyond the regime of validity of KZM. The KZM argument fails once the condensate amplitude $|\varphi(t_{eq})|^2 \sim \epsilon(t_{eq})^{2\beta}$

for a critical exponent β ; in the example (??) above, $\beta = 1/2$. The amplitude of fluctuations, however, may be parametrically suppressed – as in holography, where they are suppressed by $1/N^2$ corrections. Hence the defects are frozen not at $t_{\rm f}$, but at $t_{\rm eq}$, which is generally much longer (since it takes longer for the exponentially growing $|\varphi(t_{\rm eq})|^2$ to reach $\epsilon^{2\beta}$. It is then $t_{\rm eq}$ that controls the density of defects, and this can lead to (possibly parametrically small) prefactors in front of (??).

When $t_{\rm eq} \gg \tau_{\rm Q} \gg t_{\rm f}$, the system may always be treated in linear response during the quench as the condensate is far from well-formed. Hence, the final density of defects is governed only by the most unstable modes of the condensate at the final quench temperature. This dynamics is also associated with a characteristic length scale $\xi_{\rm f} \sim \epsilon_{\rm f}^{-\nu}$, which is independent of $\tau_{\rm Q}$. Thus, the density of vortices is expected to scale as (using $\beta = \nu = 1/2$, z = 2 for the holographic model of [?])

$$n \sim \begin{cases} \text{const.} & \tau_{\text{Q}} \ll \tau_{\text{f}} \\ \tau_{\text{Q}}^{-1/2} & \tau_{\text{Q}} \gg t_{\text{f}} \end{cases}$$
 (2.546)

This result was recovered in holographic numerical simulations, although it should hold more generally.

Out of equilibrium II: turbulence

One of the most fascinating open problems in all of physics is the nonlinear and chaotic dynamics of turbulent fluids, a problem which has important practical and theoretical applications for classical fluids like water and air [?]. It has been appreciated more recently that strongly interacting quantum fluids will share many of the same dynamical phenomena. Indeed, given the fluid-gravity correspondence previously discussed, it is natural to expect that dynamical black holes can generically behave turbulently. This has indeed been shown numerically [?, ?] for 3+1 dimensional asymptotically-AdS black holes. The numerical methods necessary to study such dynamical problems are reviewed in [?].

As many of the phenomena associated with such turbulent black holes are familiar from classical turbulence, let us focus on interesting geometrical properties of a "turbulent horizon".²³ A purely gravitational calculation [?] shows that the horizon of such a black hole looks "fractal" over the inertial range (the length scales over which turbulent phenomena appear self-similar). This is reminiscent of the fact that turbulent fluids are more effective at dissipating energy than non-turbulent fluids. Indeed, the rapidly growing horizon is a signature of the fast growth of the entropy in the dual theory.

Although holography has not taught us anything about classical turbulence, it has proven to be more

 $^{^{23}}$ We neglect subtleties with defining the black hole horizon in a dynamical spacetime – such issues are less relevant in the fluid-gravity limit.

useful in the study of superfluid turbulence. Superfluid turbulence is often called "quantum" turbulence, though this is a lousy name. Although vortices are quantized in a superfluid, most turbulent phenomena are entirely classical in nature and insensitive to vortex quantization: if we place $M \gg 1$ vortices with circulation Ω next to one another, they will behave much like a classical vortex of circulation $M\Omega$, and create a superfluid velocity field just like a large classical vortex. Interestingly, the important difference between superfluid and classical turbulence actually arises at *finite temperature*.²⁴ At finite temperature, the normal fluid and superfluid can exchange energy and momentum, complicating the description of superfluid turbulence.

The major difficulty with studying superfluid turbulence theoretically is the treatment of dissipation at finite temperature. The standard approach is to use a damped Gross-Pitaevskii equation (see e.g. [?]), but this approach is formally unjustified. As we have seen repeatedly throughout this review, holographic methods are naturally adapted to study dynamics at finite temperature. In [?], the dynamics of superfluid vortices was studied in a probe limit. In addition to seeing some signatures of turbulence including Kolmogorov scaling laws, [?] was also able to give a "microscopic" description of vortex pair annihilation, a process in which a vortex of winding number +1 collides with a vortex of winding number -1, releasing a nonlinear burst of sound which ultimately dissipates away. By keeping track of the energy flux across the black hole horizon, they were able to show that dissipative processes during superfluid turbulence are essentially localized near vortex cores, over the "healing length" defining the vortex core size. This corresponds to the length scale over which superfluid hydrodynamics breaks down. Finally, in classical turbulence in two spatial dimensions, vortices of like sign tend to clump together. This signature was not strongly seen in holography, suggesting a different type of dissipative vortex dynamics which maintains signatures of turbulence.

The localized nature of dissipation in an manifestly finite temperature, dissipative theory of superfluid turbulence suggested the emergence of a simple effective description of superfluid turbulence, independent of holography. [?] emphasized this description, which is remarkably simple, as well as its practical consequences. Let $X_n(t)$ denote the spatial position of vortex n at time t; one can argue on very general principles that the dynamics of a dilute mixture of vortices is essentially given by

$$\rho_{\rm s}\Omega W_n \varepsilon^{ij} \left(\dot{X}_n^j - V_n^j \right) = -\eta \dot{X}_n^i \tag{2.547}$$

with V_n^i the superfluid velocity flowing through the core of vortex n:

$$V_n^i = -\frac{\Omega}{2\pi} \varepsilon^{ij} \sum_{m \neq n} W_m \frac{X_n^j - X_m^j}{|\mathbf{X}_n - \mathbf{X}_m|^2},\tag{2.548}$$

 $^{^{24}}$ This is quite surprising, since most quantum phenomena are most pronounced at zero temperature.

 $W_n = \pm 1$ the winding number of each vortex,²⁵ ρ_s the superfluid density, Ω the quantum of circulation, and η a dissipative coefficient whose determination requires a microscopic calculation, such as holography. The dynamics is described by a single dimensionless parameter

$$\hat{\eta} = \frac{\eta}{\rho_{\rm s}\Omega}.\tag{2.549}$$

Classical turbulence is recovered in the limit $\hat{\eta} \lesssim 10^{-2}$; in contrast, holographic simulations appear consistent with vortex dynamics with $\hat{\eta} \gtrsim 10^{-2}$. This provides a simple explanation for the new behavior observed in [?]. Furthermore, the vortex pair annihilation process, which plays a non-trivial role in holographic vortex dynamics, is described by

$$\dot{N} \sim -\hat{\eta}N^2,\tag{2.550}$$

with N(t) the number of vortices (of both W_n) at time t. A different exponent (5/3) is proposed for turbulent flows as $\hat{\eta} \to 0$ [?].

(??) is a remarkably simple prediction with ramifications for holographic and non-holographic theories, as well as experiments. Two-dimensional cold atomic gases have allowed us to study superfluid turbulence in two dimensions experimentally [?, ?]. In fact, the effective description advocated in [?] – inspired by the holographic description of vortex annihilation – may help lead to the first experimental detection of a turbulent superfluid flow in two spatial dimensions. While it is easy to experimentally measure the vortex annihilation rate, no other experimentally accessible probe of turbulence is known. Current holographic simulations of vortex annihilation "experiments" [?] may not be at low enough T/T_c to be relevant for cold atomic gases.

 $^{^{25}}$ Higher winding number vortices are unstable and will rapidly break apart – see e.g. [?]

Part II

Transport in weakly disordered metals

Chapter 3

Holographic strange metals with random-field disorder

Below we present the original text of [?]. Reprinted with permission from A. Lucas, S. Sachdev, and K. Schalm. "Scale-invariant hyperscaling-violating holographic theories and the resistivity of strange metals with random-field disorder", Physical Review **D89** 066018 (2014). Copyright (2014) by the American Physical Society.

Introduction

One of the remarkable puzzles in quantum critical phases is the universality of the resistivity across widely different systems. In particular strange metals exhibit almost exclusively a dc-resistivity that scales linear in temperature. This is in contrast to the array of models that exist for quantum critical systems. A wide class of such quantum critical models can be characterized by non-trivial dynamic critical ("Lifshitz") exponent z associated with the relative scaling of time and space ($t \sim x^z$), and a hyperscaling-violating exponent θ corresponding to the deviation of the scaling of the low-energy critical degrees of freedom from pure dimensional arguments: *i.e.* the degrees of freedom "effectively live in" (spatial) dimension $d - \theta$ [?].²⁶

At the same time the intimate tie-in of the dc-resistivity with translational symmetry breaking allows for a universal mechanism to emerge *if* there is a dominant such mechanism at low energies. One such mechanism is random-field disorder acting on a scalar order parameter, which has recently been shown to relax momentum much more rapidly than disorder coupled to charged fermionic excitations near the Fermi surface [?]. In

²⁶For example, in a theory with a Fermi surface, with low energy excitations described by chiral fermions, $\theta = d - 1$.

this paper, we will study its effects on the resistivity in a hyperscaling violating Lifshitz quantum critical system. The difficulty is that most such theories are thought to be (strongly) interacting in the regime of interest. We resort to two well-established techniques that can address the charge dynamics nevertheless: the memory matrix method [?] and gauge-gravity duality [?, ?, ?], with generalizations to Lifshitz [?] and hyperscaling-violating [?, ?, ?, ?, ?] geometries. Despite the fact that most systems of interest have explicit Fermi surfaces, and there are no explicit Fermi surfaces in the holographic computation, corrections due to fermion scattering near the Fermi surface are subleading [?]. The latter gives us an explicit description of a strongly coupled hyperscaling violating Lifshitz quantum critical system in terms of a dual Einstein-Maxwell-Dilaton (EMD) system. Strictly put this gravity-dual only describes the large N-matrix limit of the quantum critical theory, but arguably the scaling behavior we are interested does not depend strongly on this. This is confirmed by the memory matrix computation, which works universally when translational symmetry is only weakly broken.²⁷ With a necessary refinement of EMD holography that we explain below, we show that these two approaches agree. Our holographic computation shows that for random fields of typical size ε , which couple to a random field of dimension Δ , the leading-order perturbative contribution to the d.c. resistivity is given by

$$\rho_{\rm dc} \sim \varepsilon^2 T^{2(1+\Delta-z)/z} + O\left(\varepsilon^4\right).$$
 (3.1)

Interestingly, this result is independent of the hyperscaling-violation exponent θ . Some limiting cases of this result have been obtained earlier [?, ?] by memory matrix methods.

From Eq. (??), we conclude that random-field disorder has an extremely strong effect on the resistivity in hyperscaling violating Lifshitz quantum critical systems. This is in contrast to the recent result [?] which studied the same question in the locally critical limit $z \to \infty$ of some holographic models and found the enticing identity $\rho_{\rm dc} \sim s$ (where s is the thermal entropy density). This scaling suggests a possible universal explanation for the linear-in-temperature resistivity of the strange metals. However, we found that for finite Lifshitz scaling $z \neq \infty$ this identity does not hold. Even at $z = \infty$, we recover this result in a rather curious way — although this identity does not appear to follow from Eq. (??), we will see that $\rho_{\rm dc} \sim s$ precisely at the onset of the regime where disorder must be treated non-perturbatively.

Our refinement of EMD theory is to include non-trivial dilaton coupling into the action of the disordered scalar. From the perspective of supergravity truncations, this is a natural coupling to include. This nontrivial dilaton coupling allows us to construct a strongly coupled hyperscaling-violating theory via holography which maintains scale invariant correlation functions, a simple but important result which has been noted

²⁷In principle the memory matrix method always works for a clean separation of fast and slow modes. In practice one needs to know the correlation functions of the slow modes, which are not always universal. If translational symmetry is weakly broken, however, then the universality of the energy-momentum current as a slow mode allows one to obtain universal analytic answers.

in [?, ?]. We expand on this result by explicitly deriving correlation functions, as well as criteria for the relevance of operators in terms of their boundary dimension Δ , both with and without disorder, in a hyperscaling-violating background.

Scale-Invariant Hyperscaling-Violating Holography

The Einstein-Maxwell-Dilaton models that can capture through gauge-gravity duality the physics of hyperscalingviolating quantum critical field theories are described by the action

$$S_{\text{EMD}} = \int d^{d+2}x \sqrt{-g} \left(\frac{R - 2(\partial \Phi)^2 - V(\Phi)}{2\kappa^2} - \frac{Z(\Phi)}{4e^2} F^2 \right)$$
 (3.2)

The deep infrared (IR) of these theories is controlled by the leading exponent of the arbitrary functions $V(\Phi) = -V_0 e^{-\beta \Phi} + \dots$ and $Z(\Phi) = Z_0 e^{\alpha \Phi} + \dots$ Truncating these functions to this exponent, the theory has black brane solutions dual to the hyperscaling violating quantum critical ground states supported by a charge density Q [?, ?, ?]. These solutions have a metric

$$ds^{2} = \frac{L^{2}}{r^{2}} \left[\frac{G(r)}{f(r)} dr^{2} - f(r)H(r)dt^{2} + d\mathbf{x}^{2} \right].$$
(3.3)

with non-vanishing Maxwell flux

$$F = \frac{eL}{\kappa} h'(r) dr \wedge dt \tag{3.4}$$

which sources a constant charge density Q, which can be determined from Gauss' Law:

$$\frac{e\kappa}{L^{d-1}}Q \equiv \hat{Q} = -Z\sqrt{-g}g^{tt}g^{rr}h', \tag{3.5}$$

and a running dilaton

$$\Phi = \frac{2}{\alpha} \left(d + \frac{\theta}{d - \theta} \right) \log \frac{r}{r_0}.$$
 (3.6)

The functions G, H, h' scale with r as follows:

$$G(r) = G_0 r^{2\theta/(d-\theta)} \tag{3.7a}$$

$$H(r) = H_0 r^{-2d(z-1)/(d-\theta)}$$
 (3.7b)

$$h'(r) = h_0 r^{-1 - d - dz/(d - \theta)}$$
 (3.7c)

The choice of the coefficients α, β in $Z(\Phi), V(\Phi)$ determine the dynamical critical exponent z and hyperscaling violation as

$$\theta = \frac{d^2\beta}{\alpha + (d-1)\beta},\tag{3.8a}$$

$$z = 1 + \frac{\theta}{d} + \frac{8(d(d-\theta) + \theta)^2}{d^2(d-\theta)\alpha^2}$$
(3.8b)

The emblackening factor

$$f(r) = 1 - \left(\frac{r}{r_{\rm h}}\right)^{d(1+z/(d-\theta))}$$
 (3.9)

places the system at a small but finite temperature T, related to the horizon radius $r_{\rm h}$ as

$$r_{\rm h} \sim T^{-(1-\theta/d)/z} \mathcal{Q}^{-1/d}$$
. (3.10)

The entropy density of this black hole manifestly exhibits hyperscaling violation:

$$s \sim r_{\rm h}^{-d} \sim T^{(d-\theta)/z}.\tag{3.11}$$

In these coordinates $r \to r_h$ captures the low energy regime of the dual QFT. At the opposite high energy end $r \to 0$, this IR solution can be connected to a complete asymptotically AdS_{d+2} EMD solution; see, e.g., [?]. We will not do so explicitly here. Based on the insight that the radial direction corresponds to the Wilsonian scale of the theory, we shall cut-off the metric beyond this IR region and apply the holographic dictionary at this cut-off. Recalling that the IR geometry is completely controlled by the charge density Q: it sets the ultraviolet (UV) cut-off. As we will show later, ρ_{dc} is quantitatively controlled by the IR geometry, and therefore a precise characterization of a UV completion is not necessary to understand scaling. For more on matching procedures to asymptotically AdS spaces (in the UV), see [?]. For completeness let us mention that the ratio L^d/κ^2 roughly counts the degrees of freedom in the holographic theory, and must be large for classical gravity to be valid; e is the unit of charge.

Via the holographic dictionary, additional fields in the bulk correspond to additional operators in the boundary theory. For simplicity, we focus on bulk scalar fields. To quadratic order the action of an additional bulk scalar field ψ will be of the form

$$S_{\psi} = -\int d^{d+2}x \sqrt{-g} \left(\frac{1}{2} (\partial \psi)^2 + \frac{B(\Phi)}{2} \psi^2 \right).$$
 (3.12)

The function $B(\Phi)$ will be fine-tuned such that the correlation functions of ψ exhibit manifest scaling

behavior.

To compute the Green's functions of the operator \mathcal{O} dual to ψ , we solve the equation of motion for the bulk field ψ in the background of Eq. (??):

$$\partial_M \left(\sqrt{-g} g^{MN} \partial_N \psi \right) = \sqrt{-g} B(\Phi) \psi. \tag{3.13}$$

To do this, we look for a simple choice of $B(\Phi)$. In [?], the choice $B(\Phi) = m^2$ was used, and the result was a non-scale invariant quantum field theory, with a length scale set by the AdS radius L. We make a different choice: it is easy to see that choosing

$$B(\Phi(r)) \equiv \frac{B_0}{L^2 G(r)} = \frac{B_0}{L^2 G_0} r^{-2\theta/(d-\theta)} , \qquad (3.14)$$

equivalent to the choice $B(\Phi) \sim e^{\gamma \Phi}$ with

$$\gamma = -\frac{\alpha\theta}{d(d-\theta) + \theta} = -\beta \tag{3.15}$$

leads to a field theory which has both hyperscaling violation and scale invariance. Generating scale invariance by adding dilaton couplings has been noted in [?, ?]. Below we elaborate on the consequences. At T = 0, the zero-frequency solutions to the scalar equation of motion are now the usual Bessel functions

$$\psi(k,r) = r^{\frac{1}{2}(d + \frac{dz}{(d-\theta)})} \left(\alpha K_{\frac{(d-\theta)}{2d}(\nu_{+} - \nu_{-})} \left(C_{d,\theta} |k| r^{d/(d-\theta)} \right) \right. \\ \left. + \beta I_{\frac{(d-\theta)}{2d}(\nu_{+} - \nu_{-})} \left(C_{d,\theta} |k| r^{d/(d-\theta)} \right) \right)$$
(3.16)

with $C_{d,\theta} = \frac{(d-\theta)\sqrt{G_0}}{d}$. $\nu_- < \nu_+$ correspond to the power laws of the two solutions to the equations of motion at zero momentum and frequency: $\psi(\mathbf{k} = \mathbf{0}, \omega = 0, r) \sim r^{\nu_{\pm}}$ with

$$2\nu_{\pm} \equiv d + \frac{dz}{d-\theta} \pm \sqrt{\left(d + \frac{dz}{d-\theta}\right)^2 + 4B_0}.$$
 (3.17)

Following the usual dictionary of gauge-gravity duality, the ratio of the subleading solution ($\alpha = 0$) in Eq. (??) to the leading solution ($\beta = 0$) in the limit $r \to 0$ gives the scaling behavior of the zero-frequency Green's functions of the operator \mathcal{O} in the dual field theory.²⁸ By construction the choice of $B(\Phi)$ gives the scaling solution:

$$G(k,\omega=0) \sim k^{(1-\theta/d)(\nu_+-\nu_-)}$$
. (3.18)

We denote by Δ the scaling dimension of the \mathcal{O} operator. Then, in position space $G(x, t = 0) \sim x^{-2\Delta}$, and

²⁸We ignore subtleties between Euclidean and Lorentzian signature. For the scaling argument, this does not matter.

we find

$$\frac{d-\theta}{d}\nu_{+} = \Delta - \frac{\theta}{2},\tag{3.19a}$$

$$\frac{d-\theta}{d}\nu_{+} = \Delta - \frac{\theta}{2},$$

$$\frac{d-\theta}{d}\nu_{-} = d + z - \Delta - \frac{\theta}{2}.$$
(3.19a)

The corresponding value of B_0 for any Δ can be straightforwardly found. The requirement that a operator not be described by "alternate quantization" (i.e. the requirement that $\nu_+ > \nu_-$) is $\Delta > (d+z)/2$. The condition that an insertion of the operator \mathcal{O} in the boundary theory is a relevant perturbation, i.e. the scaling dimension of the uniform field h_0 is positive (where the insertion is $h_0 \int d^{d+1}x \, \mathcal{O}(x)$) is the same as the requirement that $\nu_{-} > 0$, which corresponds to

$$\Delta < d + z - \frac{\theta}{2}.\tag{3.20}$$

We do not allow such uniform field insertions in the present paper.

Conductivity with Random Field Disorder.

We now discuss the impact of random field disorder on the resistivity at zero frequency and momentum, $\rho_{\rm dc}$, in the field theory dual to the EMD black brane at finite T and Q, in two spatial dimensions. In a translation invariant background, the symmetry enforces that $\rho_{\rm dc} = 0$ [?]. However, no realistic condensed matter system has true translational invariance. One source of translational symmetry breaking is an underlying lattice, or any other periodic potential, whose effects on transport coefficients have been intensively studied recently with holography [?, ?, ?, ?, ?, ?, ?, ?, ?, ?]. The other noted source of translational symmetry breaking is disorder [?, ?, ?, ?, ?]. Because disorder preserves translation symmetry on average, it is likely a much more tractable approach analytically. Indeed there are arguments that holographically the phenomology of disorder can be simply captured by a theory with massive gravity [?, ?], even non-perturbatively.²⁹

Below we will consider the limit of weak random-field disorder explicitly and compute the leading order temperature scaling of $\rho_{\rm dc}$ with two independent calculations: first, using EMD holography, and second using memory matrix methods. In the holographic calculation, we will exploit recent weak-field results [?, ?, ?] to compute ρ_{dc} , though we will use some of the language of massive gravity. The disorder is made manifest

²⁹However, it may be the case that non-perturbative disorder causes horizon fragmentation, which certainly is not captured by massive gravity. It is known that this is possible in d=1 [?]. This is an important open question in higher dimensions. We thank Sho Yaida for bringing up this possibility to us.

through the addition in the field theory side, of a random-field term to the Hamiltonian:

$$H_{\rm rf} = \int d^d \mathbf{x} \ g(\mathbf{x}) \mathcal{O}(\mathbf{x}), \tag{3.21}$$

where $g(\mathbf{x})$ is a (t-independent) Gaussian random variable:

$$\mathbb{E}[g(\mathbf{k})] = 0, \tag{3.22a}$$

$$\mathbb{E}[g(\mathbf{k})g(\mathbf{q})] = \varepsilon^2 \delta(\mathbf{k} + \mathbf{q}). \tag{3.22b}$$

Here \mathcal{O} is the operator dual to the scalar field ψ introduced above and ε is a small dimensionful number characterizing the scale of the disorder. Note that this disorder will locally, but not globally, violate the \mathbb{Z}_2 symmetry $\psi \to -\psi$ (corresponding to $\mathcal{O} \to -\mathcal{O}$ in the field theory). We choose \mathcal{O} to be a relevant operator even with random field disorder. As we derive shortly, this leads to a hyperscaling-violating generalization of the Harris criterion [?]:

$$\Delta < \frac{d-\theta}{2} + z. \tag{3.23}$$

Disorder may thus be treated perturbatively in the UV; disorder is relevant in the IR, but we use finite temperature to serve as an IR regulator, allowing us to treat disorder perturbatively everywhere. We will discuss the IR as $T \to 0$ in more detail below. Due to scattering off of the random field disorder, we expect that $\rho_{\rm dc} \sim \varepsilon^2$.

Holography

We now discuss our holographic computations related to the computation of ρ_{dc} . We proceed in three steps: first, we use holography to derive the Harris criterion, as advertised. Then, we compute ρ_{dc} using the massive gravity analogy. Finally, we discuss the breakdown of perturbation theory.

The Harris Criterion and a Dirty Black Hole

From standard holography, we immediately see that the Gaussian variable $g(\mathbf{x})$ can be directly translated to the source of $\psi(\mathbf{x})$. In order to compute ρ_{dc} , we therefore perturbatively construct a statistical ensemble of EMD black holes with sourced scalar hair, one for each value of the source $\psi(\mathbf{x})$, and then take the statistical average. From this black hole with "dirty" scalar hair, we then compute ρ_{dc} using the technique of [?, ?]. Before beginning, we must ensure that the scalar hair is perturbative in both the UV and the IR, and so we must find a generalization of the Harris criterion to hyperscaling-violating theories. This can be seen by

an elegant holographic argument: the contribution to the stress tensor T_{MN} from the scalar fields must be small compared to R_{MN} (e.g.) in the UV. For a hyperscaling-violating geometry we have $R_{rr} \sim r^{-2}$; the contribution from the scalar fields will be $r^{2\nu_--d^2/(d-\theta)-2}$. We conclude when $\nu_- > d^2/2(d-\theta)$ the disorder will be perturbative. This results in the generalized Harris criterion, Eq. (??).

If the disordered hair is perturbative, to leading order in ε , we can simply solve Eq. (??) to determine the ψ background. The correct solution is the one which is regular in the interior deep IR of the geometry. E.g. at T=0 the solution is

$$\psi_0 = g(\mathbf{k})r^{\nu_-} + \dots = Cr^{\frac{d}{2}(1 + \frac{z}{d-\theta})} K_{(1-\theta/d)(\nu_+ - \nu_-)/2} \left(C_{d,\theta} |k| r^{d/(d-\theta)} \right)$$
(3.24)

 \mathcal{C} is dependent on k and $g(\mathbf{k})$ and is chosen to ensure the correct UV scaling. At finite T, the solution will be modified slightly, although this description is quantitatively accurate for large momentum modes. To leading order in ε this is a complete solution [?]; corrections to EMD fields are $\sim \varepsilon^2$. Although this is the same order as ρ_{dc} , the inhomogeneous corrections cannot affect ρ_{dc} , and the homogeneous corrections are subleading to the background, so for the purposes of computing ρ_{dc} , we can treat the EMD background as unchanged [?].

DC conductivity

The analytic computation of ρ_{dc} due to a scalar perturbation at a single fixed momentum k_L has been shown in [?]. We will generalize their formalism to an infinite number of random momentum modes with the distribution Eq. (??). It is not entirely obvious that this generalization is possible. A calculation of the conductivity naively requires considering coupling a spatial component of the gauge field δA_x to all spin 1 moments of the distribution $\int d^d \mathbf{k} k_x k^{2n} \delta \psi$. We will see that a judicious choice of scalar perturbations effectively reduces the number of spin 1 perturbations to three as before. We will also find that we can compute ρ_{dc} before averaging over the disorder.

We proceed. The conductivity follows from the response to a finite frequency, zero-momentum perturbation $\delta A_x(\omega, \mathbf{k} = 0, r)$. As in [?] this perturbation couples to $\delta \tilde{g}_{tx}(\omega, r) = \delta g_{tx} r^2 / L^2$, $\delta \tilde{g}_{rx}(\omega, r)$, and

$$\delta\psi(\omega, \mathbf{k} \neq 0, r) = \psi_0(\mathbf{k}, r)\delta P(\omega, \mathbf{k}, r). \tag{3.25}$$

where $\psi_0(\mathbf{k}, r)$ is the perturbative solution in Eq. (??). To lowest order none of these couple to dilaton perturbation, despite the nontrivial functions $Z(\Phi), V(\Phi), B(\Phi)$, because the dilaton is a spin zero mode,

³⁰Note that this infinite tower automatically collapses for a single momentum mode, as $\partial^2 \cos(kx) = -k^2 \cos(kx)$, so all of these modes are proportional. This is not true when we have modes at different momentum.

and the dilaton background is at zero spatial momentum.

Following [?] we can set $\delta \tilde{g}_{rx} = 0$ by a gauge choice. Its corresponding equation of motion —the rxcomponent of Einstein's equations— is a constraint. Projecting on the zero-momentum mode one finds

$$\hat{\mathcal{Q}}\delta A_x - L\kappa e \delta \mathcal{P}_x = \frac{eL\delta \tilde{g}'_{tx}}{r^d \kappa \sqrt{GH}}$$
(3.26)

where we have defined

$$\frac{f}{\omega r^d} \sqrt{\frac{H}{G}} \int \frac{\mathrm{d}^d \mathbf{k}}{(2\pi)^d} k_x \psi_0(\mathbf{k}, r)^2 \delta P(\omega, \mathbf{k}, r)' \equiv \delta \mathcal{P}_x(\omega, r). \tag{3.27}$$

In deriving Eq. (??) the contribution proportional to $\psi_0\psi'_0\delta P$ which survives if δP is a constant has been ignored. It should be considered as an ϵ^2 contribution to the background, whereas we only keep terms up to ϵ . The other equations are the x component of Maxwell's equation:

$$\left(\frac{eL}{\kappa}\delta\tilde{g}_{tx}\hat{Q} - r^{2-d}\sqrt{\frac{H}{G}}fZ\delta A_x'\right)' + r^{2-d}Z\sqrt{\frac{G}{H}}\frac{\omega^2}{f}\delta A_x = 0,$$
(3.28)

and the scalar equation

$$-\sqrt{\frac{G}{H}}\frac{\psi_0(\mathbf{k})^2 k_x \omega \delta \tilde{g}_{tx}}{fr^d} = \left(\frac{f\psi_0(\mathbf{k})^2 \delta P(\mathbf{k})'}{r^d} \sqrt{\frac{H}{G}}\right)' + \frac{\omega^2}{fr^d} \sqrt{\frac{G}{H}} \psi_0(\mathbf{k})^2 \delta P(\mathbf{k})$$
(3.29)

The rt-component of Einstein's equations is not independent and follows from the previous equations.

The key observation is as follows: "averaging" the scalar equation over its momentum distribution with weight $k_x \int \frac{\mathrm{d}^d \mathbf{k}}{(2\pi)^d} k_x$, we can turn it into

$$\delta \mathcal{P}_{x}' = -\frac{\delta \tilde{g}_{tx}}{df r^{d}} \sqrt{\frac{G}{H}} \int \frac{\mathrm{d}^{d} \mathbf{k}}{(2\pi)^{d}} k^{2} \psi_{0}(\mathbf{k})^{2} - \frac{\omega}{f r^{d}} \sqrt{\frac{G}{H}} \int \frac{\mathrm{d}^{d} \mathbf{k}}{(2\pi)^{d}} k_{x} \psi_{0}(\mathbf{k})^{2} \delta P(\mathbf{k})$$
(3.30)

In the first term on the right-hand side we have used isotropy of the random disorder to substitute k^2/d for k_x^2 .

For the dc-conductivity we wish to know the $\omega \to 0$ solution to these equations. This limit is subtle, due to the presence of the horizon where $f(r_h) = 0$. Note, however, that away from the horizon, where in the $\omega \to 0$ limit we can ignore the higher order ω contributions in (??) and (??), the system of equations closes to a finite set of differential equations for δA_x , $\delta \mathcal{P}_x$, and $\delta \tilde{g}_{tx}$.

We now proceed to compute the conductivity following the steps in [?], generalized to higher dimensions.

Integrating once, Eq. (??) is equal to

$$\left(r^{2-d}\sqrt{\frac{H}{G}}fZ\delta A_x' - \delta \tilde{g}_{tx}\frac{eL\hat{Q}}{\kappa}\right) = C - \int dr \ r^{2-d}Z\sqrt{\frac{G}{H}}\frac{\omega^2}{f}\delta A_x \tag{3.31}$$

in terms of an unknown integration constant C. We eliminate $\delta \tilde{g}_{tx}$ using the scalar equation of motion Eq. (\ref{eq}) and obtain

$$C = \sqrt{\frac{H}{G}} f \left[r^{2-d} Z \delta A_x' + \delta \mathcal{P}_x' \frac{eL\hat{\mathcal{Q}}}{\kappa} dr^d \left(\int \frac{d^d \mathbf{k}}{(2\pi)^d} k^2 \psi_0(\mathbf{k}, r)^2 \right)^{-1} \right]$$

$$+ \omega^2 \sqrt{\frac{G}{H}} \frac{1}{fr^d} \left[\int_0^r r^2 Z \delta A_x + \frac{eL\hat{\mathcal{Q}}}{\omega \kappa} \int \frac{d^d \mathbf{k}}{(2\pi)^d} \psi_0(\mathbf{k}, r)^2 \delta P(\mathbf{k}) \right].$$
(3.32)

We now show that the constant $C(\omega, \mathbf{k})$ is proportional to the dc-conductivity. Note that in the derivation of Eq. (??) and (??) we have only used the form of the metric and the background solution, but not any specific expressions. In particular, a full solution interpreting from an asymptotically AdS boundary to an hyperscaling violating quantum critical IR will have solution that is of exactly the same form. For the background we now take such a fully asymptotically AdS completed solution, and evaluate the solution near the AdS-boundary. There $f \approx G \approx H \approx Z \approx 1$ as $r \to 0$. Consider first Eq. (??). As ψ_0 by construction corresponds to a relevant operator, ψ_0 behaves as $\psi_0 = g(\mathbf{k})r^{\Delta_{\text{UV}}} + \dots$ with $\Delta_{\text{UV}} > 0$, it follows that $\delta \tilde{g}_{tx} \sim r^{d+1}$, as $\delta A_x \sim r^{0.31}$ Consider then Eq. (??). It means that $\delta \tilde{g}_{tx}$ is always subleading near $r \to 0$ and we can solve for the AdS-boundary behavior of the fluctuation $\delta A_x = C_0 + \frac{1}{d-1}Cr^{d-1} + \dots$ The AdS/CFT dictionary tells us that the dc-conductivity is equal to

$$\sigma_{\rm dc} = \frac{1}{e^2} \lim_{\omega \to 0} \frac{-1}{i\omega} \lim_{r \to 0} r^{2-d} \frac{\delta A_x'(r)}{\delta A_x(r)} = \frac{1}{e^2} \lim_{\omega \to 0} \frac{-1}{i\omega} \frac{C}{C_0},\tag{3.33}$$

and therefore

$$C = -i\omega \sigma_{\rm dc} e^2 \delta A_x(r=0). \tag{3.34}$$

The coefficient C can be evaluated at the horizon, as follows. We know that, near the horizon, where $f(r)\sqrt{H/G} \sim T(r-r_{\rm h}) + \dots$:

$$\delta A_x, \ \delta \mathcal{P}_x, \ \frac{\delta \tilde{g}_{tx}}{f(r)} \sim \left(f \sqrt{\frac{H}{G}} \right)^{-i\omega/4\pi T} \sim \left(T(r_h - r) \right)^{-i\omega/4\pi T}.$$
 (3.35)

For $\delta A_x \sim O(1)$, it then follows that near the horizon $\delta A_x'$, $\delta \tilde{g}_{tx}$, $\delta \mathcal{P}_x' \sim \omega$. Therefore, to leading order in ω , as $\omega \to 0$, only the first line of Eq. (??) contributes. Now taking the limit $\omega \to 0$ the near-horizon limit of

³¹Note that this is precisely the expected scaling for $\delta \tilde{g}_{tx}$ in the absence of a source.

Eq. (??) reduces to

$$\hat{\mathcal{Q}}\delta A_x(r=r_h,\omega=0) = Le\kappa \,\delta \mathcal{P}_x(r=r_h,\omega=0). \tag{3.36}$$

Thus

$$C = \lim_{r \to r_{\rm h}} \sqrt{\frac{H}{G}} f \left[r^{2-d} Z + \frac{\hat{\mathcal{Q}}^2}{\kappa^2} dr^d \left(\int \frac{\mathrm{d}^d \mathbf{k}}{(2\pi)^d} k^2 \psi_0(\mathbf{k}, r)^2 \right)^{-1} \right] \delta A_x'(r = r_{\rm h}, \omega = 0).$$
 (3.37)

Substituting for the asymptotic behavior of $\delta A'_r$ near the horizon given in Eq. (??), we find

$$C = -i\omega \left[r_{\rm h}^{2-d} Z + \frac{\hat{\mathcal{Q}}^2}{\kappa^2} dr_{\rm h}^d \left(\int \frac{\mathrm{d}^d \mathbf{k}}{(2\pi)^d} k^2 \psi(\mathbf{k}, r_{\rm h})^2 \right)^{-1} \right] \delta A_x(r_h). \tag{3.38}$$

We conclude that, as ε is small, to leading order in ε :

$$\rho_{\rm dc} = \frac{1}{\sigma_{\rm dc}} \sim \left(\int d^d \mathbf{k} \ k^2 \psi(k, r_{\rm h})^2 \right) r_{\rm h}^{-d} \frac{\delta A_x(r = 0, \omega = 0)}{\delta A_x(r = r_{\rm h}, \omega = 0)}.$$
(3.39)

Now, the fact that $C \sim \omega$ implies that, $\delta A_x' \sim \omega$, or that δA_x is, to leading order in ω , independent of r.³² Noting that $s \sim r_h^{-d}$, we obtain

$$\rho_{\rm dc} \sim s \int d^d \mathbf{k} \ k^2 \psi(k, r_{\rm h})^2 \equiv s \, m^2(r_{\rm h}).$$
 (3.40)

In analogy with [?], we have noted this is an effective graviton mass.

Note that because $\rho_{\rm dc} \sim m^2 \sim \varepsilon^2$, as $\varepsilon \to 0$, the resistivity vanishes. This is consistent with the fact that ${\rm Re}(\sigma(\omega)) \sim \delta(\omega) + \cdots$ at small ω when there is translational symmetry and finite charge density. Holography can be used to compute $\sigma_{\rm dc}(\omega)$ at finite ω as well – however, the massive gravity analogy will require modifications: we can see from Eq. (??) that the scalar equation does not close to an equation for $\delta \mathcal{P}_x$ unless $\omega \to 0$.

The remaining task is to determine $m^2(r_h)$. To do so we need to evaluate $\psi_0(\mathbf{k}, r)$ at the horizon $r = r_h$. For momenta where $k \gg r_h^{-d/(d-\theta)}$, i.e. $k \gg T^{1/z} \mathcal{Q}^{1/(d-\theta)}$, we may neglect the effect of temperature and approximate $\psi_0(\mathbf{k}, r)$ with its T = 0 Bessel function solution Eq. (??). For these momenta the Bessel function is exponentially small at $r = r_h$, and we can ignore their contribution. $T^{1/z}$ thus serves as an effective UV cut-off in the momentum integral in m^2 . The integral over k will give us an overall factor of $T^{(d+2)/z}$ – as we will see, the scaling due to ψ^2 is approximately independent of k in this regime.

³²This assumes that, generically in the bulk, $\delta A'_x$ and $\delta \mathcal{P}'_x$ do not cancel each other. See [?, ?] for more.

For the remaining modes $k \ll T^{1/z} \mathcal{Q}^{1/(d-\theta)}$ we evaluate $\psi_0(\mathbf{k}, r)$ by a matching procedure. For these solutions the presence of the horizon is relevant. Near the horizon, the equation of motion for the background ψ_0 becomes

$$\partial_r^2 \psi + \frac{1}{r - r_h} \partial_r \psi - \frac{M^2}{(1 - r/r_h)} = 0 ,$$
 (3.41)

$$M^{2} \equiv \frac{k^{2}G(r_{\rm h}) + B_{0}/r_{\rm h}^{2}}{d(1 + z/(d - \theta))}.$$
(3.42)

The solution regular at the horizon is the Bessel function

$$\psi_{\text{near-hor}}(\mathbf{k}, r) = \beta I_0 \left(2Mr_h \sqrt{1 - \frac{r}{r_h}} \right). \tag{3.43}$$

For the small momenta range of interest $k \lesssim r_{\rm h}^{-d/(d-\theta)}$, $Mr_{\rm h}$ is essentially a number independent of temperature. Therefore at a matching point $r \sim r_{\rm h}$, the Bessel function has no non-trivial scaling. Knowing that $\psi_{\rm far} \sim r^{\nu_-}$, we determine $\beta \sim r_{\rm h}^{\nu_-}$. Note that this estimate is independent of $k \lesssim T^{1/z}$. It is straightforward from here to recover the full temperature dependence of the graviton mass:

$$m^2 \sim \frac{\rho_{\rm dc}}{s} \sim T^{(d+2-2(1-\theta/d)\nu_-)/z} \sim T^{(2-d+2\Delta-2z+\theta)/z}$$
. (3.44)

Evidently, $\rho_{\rm dc}/s$ generically carries temperature dependence, showing that a conjecture of [?] only holds in special cases. Studying $\rho_{\rm dc}$ directly, we find

$$\rho_{\rm dc} \sim \varepsilon^2 T^{2(1+\Delta-z)/z} + \mathcal{O}\left(\varepsilon^4\right),$$
(3.45)

as we quoted in Eq. (??).

It is useful to express our main result in Eq. (??) in a condensed matter notation. It is conventional to determine the scaling dimension, Δ , of the "order parameter" \mathcal{O} coupling to the random field by its "anomalous" dimension η . For a theory with dynamic scaling exponent z, the relationship between Δ and η is [?]

$$\Delta = \frac{d+z-2+\eta}{2}.\tag{3.46}$$

Then Eq. (??) becomes

$$\rho_{\rm dc} \sim \varepsilon^2 T^{(d-z+\eta)/z},$$
(3.47)

a result quoted in Ref. [?].

Breakdown of Perturbation Theory

It is also worth asking for what value of ε we expect perturbation theory to break down. To do this, we check when the scalar hair non-perturbatively back-reacts on the geometry: i.e., when is the ψ contribution to Einstein's equations of the same order as the contributions of the solution we are perturbing around. A quick check at $r \sim r_h$ reveals that all components of Einstein's equations break down at the same scale, if the disorder strength is strong enough. For example, using the xx component of Einstein's equations at $r \sim r_h$, the scalar backreaction becomes nonperturbative when

$$R_{xx} \sim r_{\rm h}^{-2d/(d-\theta)} \sim T^{2/z} \sim \int d^d k \ k^2 \psi^2 \sim m^2,$$
 (3.48)

or when the temperature falls below

$$T^{(z-\Delta+(d-\theta)/2)/z} \lesssim \varepsilon$$
 (3.49)

Because the dilaton couples in a universal, exponential manner to each term in the matter stress tensor in the IR, the dilaton equation of motion will break at the same scale.

It is easy to check, given this result, that it is impossible to have a regime where we can trust the calculation where $\rho_{\rm dc} \to \infty$ (i.e., the strange metal becomes an insulator) as $T \to 0$, without the perturbative approximation breaking down. When perturbation theory breaks down, at $\varepsilon \sim T^{(z-\Delta+(d-\theta)/2)/z}$ we universally find

$$\rho_{\rm dc} \sim T^{(2+d-\theta)/z} \sim T^{2/z} s,$$
(3.50)

independent of the choice of Δ . This is in fact the scaling one finds for ε fixed and $\Delta = \frac{d-\theta}{2} + z$ saturating the Harris bound. It self-consistently shows that the effect of random-field disorder from operators with dimensions that violate the Harris criterion is always non-perturbative. Comparing to the conjecture of [?] we find agreement in the limit $z \to \infty$, up to a possible logarithmic correction, despite the fact that Eq. (??) appears to badly violate $\rho_{\rm dc} \sim s$.

Interestingly, this result also qualitatively agrees with a memory matrix based argument for the AdS₄-Reissner-Nördstrom geometry ($z = \infty$, $\theta = 0$), which found that $\rho_{\rm dc} \sim (\log T^{-1})^{-1}$ due to random-field disorder [?].³³ Due to the presence of 1/z corrections, it is natural to expect such logarithmic correction factors to appear in Eq. (??) as well.

One might ask why we could ignore the first term in Eq. (??) in this argument. It is straightforward to

³³This agreement is especially interesting, as [?] used irrelevant operators to add disorder, whereas we used relevant operators.

check that the first term is comparable to the second term precisely at the same scale as perturbation theory breaks down; thus, in the regime of validity of the perturbative massive gravity analogy, we can ignore this contribution to ρ_{dc} .

Memory Matrix Method

We will now confirm our holographic computation with an independent calculation via the memory matrix method [?], which is especially suited to the computation of transport quantities in the absence of long-lived quasiparticles [?, ?, ?]. The basic procedure was reviewed recently in [?], and the main result for the resistivity is

$$\rho_{\rm dc} \sim \varepsilon^2 \int_0^{T^{1/z}} d^d k \ k^2 \lim_{\omega \to 0} \operatorname{Im} \frac{G_{\mathcal{O}\mathcal{O}}^{\rm R}(\omega, k)}{\omega}. \tag{3.51}$$

The integral over k, and the k^2 factor, give $T^{(d+2)/z}$. Using the fact that for $k \sim T^{1/z}$ [?, ?]

$$\lim_{\omega \to 0} \operatorname{Im} \frac{G_{\mathcal{O}\mathcal{O}}^{R}(\omega, k)}{\omega} \sim T^{(2\Delta - 2z - d)/z}, \tag{3.52}$$

we arrive at Eq. (??).

Conclusions

In conjunction with the recent result [?], our findings show that random-field disorder can have an extremely strong effect on the low-temperature dc-conductivity. Unless there is a mechanism which protects transport from random-field scattering, at low-temperatures random-field disorder must always be taken into account. In particular, regardless of disorder strength, at low enough temperatures disorder due to relevant operators leads to non-perturbative effects in the IR [?, ?, ?, ?].

We noted that at the breakdown of perturbation theory $\rho_{\rm dc} \sim T^{2/z}s$. For $z=\infty$ this reduces to a linear relation between the dc-resistivity and the entropy density. It would be interesting if there is a deep reason why this must be the case.

The qualitative agreement in T-scaling between the effective graviton mass calculation, and the memory matrix formalism, has been shown for a single momentum mode in [?]. Quantitatively we have shown that the agreement between the effective graviton mass calculation, and the memory matrix formalism remains for a generic scaling theory with finite values of z and θ and for disorder, and when the memory matrix calculation is completely independent of holography. Note that the agreement of these two calculations is

not a trivial consequence of dimensional analysis – $\mathcal{Q}/T^{d/z}$ is a dimensionless quantity.

Although the memory matrix method appeared substantially faster, the holographic method contains its own advantages. In particular, we are able to determine the disorder strength at which perturbation theory breaks down. Holographic methods also allow, in principle, a determination of results to all orders in the disorder strength [?].

Looking forward, it would be interesting to extend these results to a quantum field theory which is manifestly UV-completed to a conformal field theory, or by duality, studying a geometry which is UV-completed to AdS. As [?] recently noted, such a UV-completion may provide another universal mechanism for $\rho_{\rm dc} \sim T$ at high temperatures, without the requirement of local criticality. In addition, it would be interesting to determine the optical (finite frequency) resistivity due to random-field disorder.

Chapter 4

From holography to memory matrices

Below we present the original text of [?]. Reprinted as published (open access) by Springer.

Introduction

Holographic duality has provided condensed matter physicists with a novel way to study the properties of strongly correlated transport and dynamics in theories without quasiparticles [?, ?, ?]. Charged black holes become dual to states of matter at finite charge density and temperature. At finite density, however, it becomes crucial to include the effects of momentum relaxation in order to obtain a finite direct electrical conductivity, σ_{dc} , at zero frequency and momentum.³⁴ These momentum relaxing effects may either be studied by numerically constructing a charged black hole which breaks translational invariance [?, ?, ?], or analytically, so long as the black hole breaks translation invariance only weakly [?, ?, ?, ?], translational invariance is broken via massive gravity [?, ?, ?, ?], "helical lattices" [?, ?] or "Q-lattices" [?, ?, ?].

In this paper we show, through a direct holographic computation, that the low-frequency conductivity is given by a Drude peak in a wide class of holographic metals where translational symmetry is weakly broken:

$$\sigma(\omega) = \frac{\sigma_{\rm dc}}{1 - i\omega\tau}.\tag{4.1}$$

These metals have coherent transport without quasiparticles, in the language of [?]. Furthermore, σ_{dc} and τ are identical to the results computed – independently of holography – through the memory function formalism [?, ?, ?]. Memory functions have been used, in conjunction with holographic methods, to evaluate conductivities in the past [?, ?], as well as in non-holographic condensed matter models for strange metals

³⁴This follows directly from the fact that at finite density, one can generate an electrical current without any energy in a translationally invariant theory by simply boosting to a reference frame with a relative velocity to the rest frame of the metal.

as well [?, ?, ?, ?]. More recently it has been noted that exact computations of σ_{dc} – the direct current conductivity at zero momentum and frequency – admit temperature scaling in agreement with results found through memory functions [?, ?]. In fact, the correspondence hinted at in these works is exact, including all other prefactors. A short computation within the memory function framework necessitates the emergence of a Drude peak (though with complications when magnetic fields and/or strong charge diffusion is present [?]). It is not obvious from a purely holographic computation why this Drude peak should be universal, and how it should arise – other than resorting to the argument that these metals should be describable by the memory function formalism. We will address these points in this paper.

We begin with a review of why the Drude peak is universal, via hydrodynamic arguments, in Section ??. We then describe how to the Drude peak arises within the memory function formalism in Section ??. Section ?? describes the holographic computation of $\sigma(\omega)$, and a proof of equivalence with the results of Section ??.

Hydrodynamics and the Drude Peak

Drude peaks generically emerge from quantum field theories described by hydrodynamics with a small amount of momentum relaxation. Unlike the historical model of Drude physics (electrons scattering off of a lattice or impurities), quasiparticles need not exist to observe (??). Consider the long-time equation for momentum relaxation in a charged fluid, placed in an electric field in the x-direction:

$$\partial_t \Pi_x + \partial_x P = -\frac{\Pi_x}{\tau} + \mathcal{Q}E_x. \tag{4.2}$$

Here Π_x is the x-momentum density, P is the pressure, τ is the momentum relaxation time, and Q is the charge density (at rest) of the fluid. As we are interested in zero-momentum transport, at frequency ω this equation simplifies to

$$\left(\frac{1}{\tau} - i\omega\right) \Pi_x = \mathcal{Q}E_x. \tag{4.3}$$

To compute

$$\sigma_{\rm dc} = \frac{J_x}{E_x},\tag{4.4}$$

we need to relate J_x to Π_x .

At this point, let us specialize further to a relativistic quantum field theory, and work in units where $\hbar = c = 1.35$ All holographic models we will study will fall into this class of theories. In such a theory, we

 $^{^{35}}$ Note that, from the perspective of condensed matter physics, "c" here is the effective emergent speed of light in the low energy Lorentz-invariant theory.

find that at small velocities v_x , the momentum density is given by

$$\Pi_x = (\epsilon + P)v_x,\tag{4.5}$$

where ϵ is the energy density of the fluid at rest and P is the pressure, and

$$J_x = Qv_x. (4.6)$$

Combining these equations we can relate J_x to Π_x , and find a Drude conductivity of the form (??) with

$$\sigma_{\rm dc} = \frac{Q^2 \tau}{\epsilon + P}.\tag{4.7}$$

This is a special limiting case of more general hydrodynamic results found in [?]. It is valid when charge diffusion is negligible, and there is no magnetic field.

Memory Functions

Hydrodynamics does not give us an explicit expression for any thermodynamic quantities, or τ . The thermodynamic functions such as ϵ and P are "intrinsic" to the quantum field theory, and are approximately independent to the precise mechanism of momentum relaxation (so long as τ^{-1} is small). On the other hand, τ is "extrinsic" and sensitive to the precise way in which momentum can relax. The memory function analysis provides us with a way of computing τ , given that we know the microscopic method by which momentum can relax.

More precisely, in a time-reversal symmetric theory in which momentum is the only almost conserved quantity, the memory matrix framework tells us that

$$\sigma(\omega) = \frac{\chi_{JP}^2}{M_{PP}(\omega) - i\omega\chi_{PP}},\tag{4.8}$$

where χ_{PP} is the momentum-momentum susceptibility, χ_{JP} is the current-momentum susceptibility, and $M_{PP}(\omega)$ is the momentum-momentum component of the memory matrix. If there are other long-lived conserved quantities, then a matrix generalization of this equation applies [?]. For us, $M_{PP}(\omega)$ is a small quantity and may thus be computed perturbatively. In our relativistic field theories, one finds

$$\chi_{PP} = \epsilon + P,\tag{4.9a}$$

$$\chi_{JP} = \mathcal{Q}.\tag{4.9b}$$

To derive these results, we note that the conjugate thermodynamic variable to momentum P_x is velocity v_x . The susceptibility $\chi_{\alpha P_x}$ is equal to $\langle \alpha \rangle / v_x$ as $v_x \to 0$. (??) then follows from (??) and (??). As $\omega \to 0$, one finds [?]

$$M_{PP}(0) = \lim_{\omega \to 0} \frac{\operatorname{Im} \left(G_{\dot{P}_x \dot{P}_x}^{R}(\omega) \right)}{\omega} \equiv \frac{\epsilon + P}{\tau}, \tag{4.10}$$

where \dot{P}_x is the time derivative of the total x-momentum. We will argue in the course of our holographic discussion that finite frequency corrections to the memory matrix will be extremely small in the regime we are interested in. τ may thus be computed from this memory matrix component at $\omega = 0$, and a simple calculation verifies that (??) and (??) are recovered.

Now, let us specialize further to a quantum field theory with a translationally invariant Hamiltonian H_0 , perturbed to

$$H = H_0 - \int d^d \mathbf{x} \ h(\mathbf{x}) \mathcal{O}(\mathbf{x}), \tag{4.11}$$

where \mathcal{O} is a Lorentz scalar operator in the original theory, and $h(\mathbf{x})$ is a (real-valued) static, spatially varying field. The quantum operator

$$\dot{P}_x = i[P_x, H] = -i \int d^d \mathbf{x} \ h(\mathbf{x})[P_x, \mathcal{O}(\mathbf{x})] = \int d^d \mathbf{x} \ h(\mathbf{x})(\partial_x \mathcal{O})(\mathbf{x})$$
(4.12)

We then employ

$$G_{\dot{P}_{x}\dot{P}_{x}}^{R}(\omega) = \int d^{d}\mathbf{k}d^{d}\mathbf{q} \ h(\mathbf{k})\overline{h(\mathbf{q})}G_{\partial_{x}\mathcal{O}\partial_{x}\mathcal{O}}^{R}(\mathbf{k},\mathbf{q},\omega)$$
(4.13)

The perturbative parameter that makes M_{PP} small is $\tau^{-1} \sim h^2$. At leading order in h, $G^{\rm R}$ is the Green's function of a translationally invariant theory and so the integral identically vanishes when $\mathbf{k} + \mathbf{q} \neq \mathbf{0}$.

If we have a "lattice" or periodic potential where

$$h(\mathbf{x}) = h_0 \cos(\mathbf{k}_0 \cdot \mathbf{x}),\tag{4.14}$$

then we obtain

$$G_{\dot{P}_{x}\dot{P}_{x}}^{R}(\omega) = \frac{h_{0}^{2}}{2}k_{0}^{2}G_{\mathcal{O}\mathcal{O}}^{R}(\mathbf{k}_{0},\omega).$$
 (4.15)

In the case of disorder, the function $h(\mathbf{x})$ will be random. It is common to take $h(\mathbf{x})$ to be a zero-mean

Gaussian random function with mean and variance given by $(\mathbb{E}[\cdots]]$ denotes disorder averaging)

$$\mathbb{E}[h(\mathbf{x})] = 0,\tag{4.16a}$$

$$\mathbb{E}[h(\mathbf{x})h(\mathbf{y})] = \varepsilon^2 \ 1 \ 0 - .18 \ \delta(\mathbf{x} - \mathbf{y}). \tag{4.16b}$$

We obtain [?]

$$G_{\dot{P}_{x}\dot{P}_{x}}^{R}(\omega) = \int d^{d}\mathbf{k}d^{d}\mathbf{q} \,\mathbb{E}[h(\mathbf{k})h(\mathbf{q})]k_{x}^{2}G_{\mathcal{O}\mathcal{O}}^{R}(\mathbf{k},\mathbf{q},\omega) = \int d^{d}\mathbf{k}d^{d}\mathbf{q} \,\varepsilon^{2}k_{x}^{2} \,1 \,0 \,\text{-.}18 \,\delta(\mathbf{k}+\mathbf{q})G_{\mathcal{O}\mathcal{O}}^{R}(\mathbf{k},\mathbf{q},\omega)$$

$$= \int d^{d}\mathbf{k} \,\varepsilon^{2}k_{x}^{2}G_{\mathcal{O}\mathcal{O}}^{R}(\mathbf{k},\omega). \tag{4.17}$$

We approximate $G_{\dot{P}_x\dot{P}_x}^{\rm R}$ by its average as fluctuations are suppressed in the large volume limit [?]. More generally, if we assume that $h(\mathbf{x})$ and its derivatives are non-vanishing (almost) everywhere in space, we will find

$$G_{\dot{P}_x\dot{P}_x}^{\mathrm{R}}(\omega) = \int \mathrm{d}^d \mathbf{k} |h(\mathbf{k})|^2 k_x^2 G_{\mathcal{O}\mathcal{O}}^{\mathrm{R}}(\mathbf{k},\omega).$$
 (4.18)

We have belabored this rather trivial discussion to emphasize the following – in the last equation, the quotes around the equals sign arise because technically, we have neglected a 10-.18 δ function enforcing momentum conservation in $|h(\mathbf{k})|^2$.³⁶ However, writing the equation in the form (??) is convenient: we will see a similar equation with a "missing" 10-.18 δ function arise holographically. Thus

$$\frac{\epsilon + P}{\tau} \equiv \int d^d \mathbf{k} |h(\mathbf{k})|^2 k_x^2 \times \lim_{\omega \to 0} \frac{\operatorname{Im} \left(G_{\mathcal{O}\mathcal{O}}^{\mathbf{R}}(\mathbf{k}, \omega) \right)}{\omega}. \tag{4.19}$$

Holography

Now let us turn to holography. We assume that d > 1. We consider solutions of the Einstein-Maxwell-dilaton (EMD) system with action

$$S = \int d^{d+2}x \sqrt{-g} \left(\frac{1}{2\kappa^2} \left(R - 2(\partial_M \Phi)^2 - \frac{V(\Phi)}{L^2} \right) - \frac{Z(\Phi)}{4e^2} F_{RS} F^{RS} \right), \tag{4.20}$$

where g_{MN} is the bulk metric (dual to the stress tensor of the boundary theory), A_M is a U(1) gauge field (dual to the electric current of the boundary theory), and Φ is a dilaton field. These holographic models are known to give rise to rich families of boundary theories; we focus on metallic phases in this paper.

Let us now, without proof, state some results about static, isotropic geometries that solve the equations

of motion associated with this EMD action. We use the conventions and results of [?] in what follows. These solutions have metric

$$ds^{2} = \frac{L^{2}}{r^{2}} \left[\frac{a(r)}{b(r)} dr^{2} - a(r)b(r)dt^{2} + d\mathbf{x}^{2} \right], \tag{4.21}$$

where b(r) plays the role of an "emblackening factor": in particular, near the black hole horizon (of planar topology), located at finite $r = r_h$, we find

$$b(r) \approx 4 \cdot 10 - .18 \, t T(r_{\rm h} - r),$$
 (4.22)

where T is the Hawking temperature of the black hole, which also equals the dual field theory's temperature; a is finite near the horizon. Near the boundary (r=0), a(0)=b(0)=1; $\Phi(r=0)=0$, Z(0)=1 and V(0)=-d(d+1); the asymptotic geometry is that of AdS. The UV of the continuum field theory is thus approximately conformal. The profile of the gauge field is

$$A = p(r)dt (4.23)$$

where $p(r_h) = 0$, and the asymptotic behavior near the boundary is

$$p(r) \approx \mu - \frac{r^{d-1}}{d-1} \frac{e^2 \mathcal{Q}}{L^{d-2}} + \cdots$$
 (4.24)

 μ is the chemical potential associated with the conserved charge. One finds that the object \mathcal{C} , defined as

$$C \equiv \frac{(ab)'}{ar^d} + \frac{2Q\kappa^2}{L^d}p \tag{4.25}$$

is independent of r, where here and henceforth, primes denote r-derivatives. There is, of course, much more that can be said about these geometries, but this is all we will need for the present paper. Although we have assumed (for technical ease) that the UV geometry is AdS, the remainder of the geometry may be completely arbitrary, so long as it may be constructed as a solution of EMD theory.

Now, we will add to this geometry a fourth field: a neutral scalar ψ , dual to the operator \mathcal{O} sourced by the translation symmetry breaking field $h(\mathbf{x})$. The action of ψ is

$$S_{\psi} = -\frac{1}{2} \int d^{d+2}x \sqrt{-g} \left((\partial_M \psi)^2 + B(\Phi) \psi^2 \right), \qquad (4.26)$$

If the operator \mathcal{O} has (UV) dimension $\Delta > (d+1)/2$ (we choose this so that the operator \mathcal{O} is described by

standard quantization in holography), then the near-boundary asymptotic expansion of \mathcal{O} is

$$\psi(r) = r^{d+1-\Delta} \frac{\psi^{(0)}(\mathbf{x})}{L^{d/2}} + \dots + r^{\Delta} \frac{\psi^{(1)}(\mathbf{x})}{L^{d/2}} + \dots$$
(4.27)

and $B(0) = \Delta(\Delta - d - 1)/L^2$. In general, B should be chosen non-trivially in order to obtain results which match boundary theory expectations [?]. The boundary conditions which imply that the Hamiltonian of the boundary theory is given by (??) are imposed by setting

$$\psi^{(0)}(\mathbf{x}) = h(\mathbf{x}). \tag{4.28}$$

This will induce a small backreaction on the original EMD system, as the bulk stress tensor of ψ is a source in Einstein's equations. However, this source is $O(h^2)$, and following [?, ?] we may treat the geometry at O(h) (thus the background metric is unperturbed) in order to compute the conductivity at leading order in h (as will be clear in the derivation shortly). We may thus take

$$\psi = \int d^d \mathbf{k} \ h(\mathbf{k}) \psi_0(\mathbf{k}, r) e^{i\mathbf{k} \cdot \mathbf{x}}, \tag{4.29}$$

with $\psi_0(\mathbf{k}, r \to 0) \sim L^{-d/2} r^{d+1-\Delta}$, and ψ_0 obeying the linear equation of motion associated with the action (??), subject to a regularity condition at $r = r_h$, and the boundary condition (??). A holographic calculation can explicitly determine the scale of h at which this approximation breaks down [?].

The expectation value of $\mathcal{O}(\mathbf{x})$ in our state at finite density and temperature, and in the background field h, is given by [?]

$$\langle \mathcal{O}(\mathbf{x}) \rangle = (2\Delta - d - 1)\psi^{(1)}(\mathbf{x}).$$
 (4.30)

If the asymptotic expansion of δA_x near r=0 is

$$\delta A_x = \delta A_x^{(0)} + \frac{r^{d-1}}{d-1} \delta A_x^{(1)} + \cdots, \tag{4.31}$$

then

$$\sigma(\omega) = \frac{L^{d-2}}{\mathrm{i}\omega e^2} \frac{\delta A_x^{(1)}}{\delta A_x^{(0)}}.$$
(4.32)

We will use these facts to compute Green's functions and conductivities in this section.

Drude Peak

To compute the conductivity, we need to compute the response of our background EMD-scalar solution to a perturbation $\delta A_x e^{-i\omega t}$ (at zero momentum) – equivalent in the boundary theory to imposing a small electric field. The solution need only be found within linear response theory, as is standard, but the computation below will proceed a bit different than that in [?, ?], as we must explicitly consider finite ω effects. δA_x can only consider spin 1 perturbations under the spatial SO(d) isometry of the metric. These perturbations are (in axial gauge $\delta g_{rx} = 0$):

$$\delta A_x, \ \delta \tilde{g}_{tx} \equiv \frac{r^2}{L^2} \delta g_{tx}, \ \partial_x \delta \psi, \ \partial^2 \partial_x \delta \psi, \dots$$

By computing the full linear response problem (we discuss the remainder of the necessary boundary conditions later), we can find the near boundary asymptotic behavior of $\delta A_x(r)$ and compute $\sigma(\omega)$ from (??).

Linearizing the EMD system, one finds the equations of motion:

$$\frac{L^d}{2\kappa^2 a r^d} \delta \tilde{g}'_{tx} = \mathcal{Q} \delta A_x - L^d \delta \mathcal{P}_x, \tag{4.33a}$$

$$\frac{e^2 \mathcal{Q}}{L^{d-2}} \delta \tilde{g}'_{tx} = \left(br^{2-d} Z \delta A'_x\right)' + \frac{r^{2-d} Z \omega^2}{b} \delta A_x, \tag{4.33b}$$

$$-\frac{k_x \omega \psi_0(\mathbf{k}, r)^2}{br^d} \delta \tilde{g}_{tx} = \left(\frac{b}{r^d} \psi_0(\mathbf{k}, r)^2 \left(\frac{\delta \psi(\mathbf{k}, r)}{\psi_0(\mathbf{k}, r)}\right)'\right)' + \frac{\omega^2}{br^d} \psi_0(\mathbf{k}, r) \delta \psi(\mathbf{k}, r), \tag{4.33c}$$

where we have defined

$$\delta \mathcal{P}_x \equiv \frac{b}{r^d \omega} \int d^d \mathbf{k} \ k_x |h(\mathbf{k})|^2 \psi_0(\mathbf{k}, r)^2 \left(\frac{\delta \psi(\omega, \mathbf{k}, r)}{\psi_0(\mathbf{k}, r)} \right)'. \tag{4.34}$$

In these equations, δA_x , $\delta \tilde{g}_{tx}$ and $\delta \mathcal{P}_x$ are Fourier components at zero momentum and finite (but small) ω ; they are functions of r only. The equations of (??) are in order: the rx-component of Einstein's equations, the x-component of Maxwell's equations, and the ψ wave equation at momentum \mathbf{k} ; all of these equations have been integrated over all of space. Up to the $O(\omega^2)$ terms in the scalar EOM, the equations close to a finite set of equations for δA_x , $\delta \mathcal{P}_x$, and $\delta \tilde{g}_{tx}$. Since we want to work at finite frequencies $\omega \ll T$, but $\omega \tau$ possibly $\gg 1$, it requires some care to argue that we need only consider these three perturbations.

We wrote coefficients of the form $\int d^d \mathbf{k} |h(\mathbf{k})|^2 \psi_0(\mathbf{k}, r)^2$ above. This is analogous to (??) – there is a "missing" 10-.18 δ function. The reason this arises is that we have integrated over all of space in order to isolate the zero momentum mode $\delta \mathcal{P}_x$ – this induces an "infinity" factor analogous to 10-.18 δ (0) in any term which does not vary in space: for example, the other two terms in (??). Properly regulating this infinity, we recover the equations above – provided that $|h(\mathbf{k})|^2$ is understood to be "missing" a factor 10-.18 δ (0), as in Section ??.

Our strategy is to show that the linearized fluctuations need only be computed to $O(\omega)$ in order to compute the linear response problem to all orders in $\omega\tau$. This will imply that we can focus on the $\omega \to 0$ limit of the equations of motion, where we need only solve a linear response problem in three variables, instead of an infinite number.

Let us begin by studying the linearized equations of motion when $\omega = 0$ exactly – we will not worry about computing the conductivity just yet. In this case, the equations of motion reduce exactly to

$$\frac{L^d}{2\kappa^2 a r^d} \delta \tilde{g}'_{tx} = \mathcal{Q} \delta A_x - L^d \delta \mathcal{P}_x, \tag{4.35a}$$

$$\frac{e^2 \mathcal{Q}}{I_{d-2}} \delta \tilde{g}'_{tx} = \left(br^{2-d} Z \delta A'_x \right)', \tag{4.35b}$$

$$\delta \mathcal{P}_x' = -\delta \tilde{g}_{tx} \left[\frac{1}{br^d} \int d^d \mathbf{k} |h(\mathbf{k})|^2 k_x^2 \psi_0(\mathbf{k}, r)^2 \right], \tag{4.35c}$$

These equations are identical to those of massive gravity [?] in the limit $\omega \to 0$, with the object in brackets in (??) playing the role of the graviton mass. It is important to remember that it is $\delta \mathcal{P}_x$ which stays O(1) as $\omega \to 0$, and not $\delta \psi(\omega, \mathbf{k}, r)$, which is O(ω). Let us exactly find – at leading order in h – all of the solutions of these equations; counting derivatives we find there must be 4 linearly independent solutions. The first is spotted by inspection (we will not normalize any of these linearly independent solutions with the correct dimensions):

$$\delta A_x = 1, \quad \delta \mathcal{P}_x = \frac{\mathcal{Q}}{L^d}, \quad \delta \tilde{g}_{tx} = 0.$$
 (4.36)

In fact, this is the only perturbation that, at leading order in h, couples to the ψ sector. All modes will couple to this sector, but only at $O(h^2)$, which will prove to be subleading in our computation of the conductivity. The remaining three modes are, at leading order, modes of the translationally invariant theory with $\psi = 0$, and may also be written down exactly. First there is a "diffeomorphism" mode

$$\delta \tilde{g}_{tx} = 1, \quad \delta A_x = 0, \quad \delta \mathcal{P}_x = 0.$$
 (4.37)

The next mode may be found by performing a Galilean boost to the static solution:

$$\delta A_x = p + p_h, \quad \delta \tilde{g}_{tx} = 1 - ab, \quad \delta \mathcal{P}_x = 0.$$
 (4.38)

where p_h is a constant, and we have conveniently chosen that $\delta \tilde{g}_{tx}(r=0) = 0$. We may fix the value of p_h by requiring that (??) be satisfied at $r = r_h$, and we find, using (??) and (??) (along with the fact that $\mathcal{C} = 0$

is fixed by the linearized equations of motion):

$$p_{\rm h} = \frac{2 \cdot 1 \cdot 0 - .18 \, \text{t} T L^d}{\kappa^2 r_{\rm h}^d \mathcal{Q}} = \frac{T s}{\mathcal{Q}},\tag{4.39}$$

where s is the entropy density (we have converted between the area of the black hole horizon and the entropy density of the dual field theory using the Bekenstein-Hawking formula). We may use the reduction of order method³⁷ [?] to compute the final solution, by using the fact that both (??), and the mode we are looking for, solve (at leading order) the differential equation

$$\frac{2e^2\kappa^2 Q^2 a r^d}{L^{2d-2}} \delta A_x = \left(br^{2-d} Z \delta A_x'\right)'. \tag{4.40}$$

and we find

$$\delta A_x = (p(r) + p_h) \int_0^r ds \frac{s^{d-2}}{b(s)Z(s)(p(s) + p_h)^2}, \quad \delta \tilde{g}_{tx} = \int_0^r ds \frac{2\kappa^2 Q a(s)s^d}{L^d} \delta A_x(s), \quad \delta \mathcal{P}_x = 0.$$
 (4.41)

Note that, at leading order in h, this mode has a logarithmic divergence at $r = r_h$ in δA_x alone.

As $\sigma_{\rm dc}$ must be finite, and we must have $\delta \tilde{g}_{tx}(r=0)=0$ (we are not sourcing any temperature gradients), at $\omega=0$ the solution to the linearized equations of motion obeying all boundary conditions turns out to be simply

$$\delta A_x = \delta A_x^0, \quad \delta \mathcal{P}_x = \frac{\mathcal{Q}}{L^d} \delta A_x^0, \quad \delta \tilde{g}_{tx} = 0.$$
 (4.42)

We now wish to include corrections when $\omega \ll T$, μ , but work to all orders in $\omega \tau$. More precisely, we set all subleading corrections in ω/T or ω/μ to vanish, and then to all orders in $\omega \tau$. First, we need to discuss the boundary conditions at the black hole horizon. Both $\delta \mathcal{P}_x$ and δA_x obey infalling boundary conditions:

$$\delta A_x, \ \delta \mathcal{P}_x \sim (r_{\rm h} - r)^{-i\omega/4} \ ^{1\ 0} \cdot ^{.18\ \text{#}T}.$$
 (4.43)

These boundary conditions arise from including the $O(\omega^2)$ terms in the equations of motion, and demanding that perturbations fall into the black hole horizon (in the boundary theory: energy is dissipated). They are, at first glance, non-perturbative in ω , which is frustrating for our purposes. However, things are not so bad. Let us fix $r_h - r$ to be arbitrarily small, but send $\omega \to 0$. We may then Taylor expand

$$(r_{\rm h} - r)^{-i\omega/4} {}^{1}{}^{0} {}^{-.18} {}^{\pm}T = 1 + \frac{i\omega}{4} {}^{1}{}^{0} {}^{-.18} {}^{\pm}T \log \frac{r_{\rm h}}{r_{\rm h} - r} + \cdots$$
 (4.44)

³⁷Suppose we have a differential equation $f_0y + (f_1y')' = 0$, and $y_0(r)$ is an exact solution of this differential equation. One can show that a linearly independent solution is $y_1(r) = y_0(r) \int_0^r ds f_1(s)^{-1} y_0(s)^{-2}$.

In a neighborhood of this fixed r, the Taylor expansion in ω must be a solution of the equations of motion, but the ω -dependence of the equations of motions themselves only comes in at $O(\omega^2)$. We therefore conclude that the $O(\omega)$ coefficient must be a solution to the equations of motion evaluated at $\omega = 0$. As we are going to argue later that it is sufficient to only compute δA_x , $\delta \tilde{g}_{tx}$ and $\delta \mathcal{P}_x$ to $O(\omega)$, this is a great simplification – as far as our computation is concerned, (??) is exact. Imposing infalling boundary conditions becomes equivalent to imposing the boundary conditions (up to $O(\omega)$ terms finite at the horizon):

$$\delta A_x(r \to r_{\rm h}) = \delta A_x^0 \left[1 + \frac{i\omega}{4 \cdot 1 \cdot 0 - .18 \, \text{tT}} \log \frac{r_{\rm h}}{r_{\rm h} - r} \right] + \cdots, \quad \delta \mathcal{P}_x(r \to r_{\rm h}) = \frac{\mathcal{Q}}{L^d} \delta A_x^0 \left[1 + \frac{i\omega}{4 \cdot 1 \cdot 0 - .18 \, \text{tT}} \log \frac{r_{\rm h}}{r_{\rm h} - r} \right] + \cdots.$$

$$(4.45)$$

We impose no specific boundary condition on $\delta \tilde{g}_{tx}$ at $r=r_{\rm h}$, other than no logarithmic divergences.

Let us now go ahead and compute the $O(\omega)$ corrections to the linearized modes, at leading order in h. Imposing infalling boundary conditions on $\delta \mathcal{P}_x$, (??) implies

$$\frac{\mathrm{i}\omega}{4 + 10 - .18 \, \text{ft}} \frac{\mathcal{Q}}{L^d} \delta A_x^0 \frac{1}{r_\mathrm{h} - r} \approx -\frac{\delta \tilde{g}_{tx}}{4 + 10 - .18 \, \text{ft}} T r_\mathrm{h}^d(r_\mathrm{h} - r) \int \mathrm{d}^d \mathbf{k} |h(\mathbf{k})|^2 k_x^2 \psi_0(\mathbf{k}, r_\mathrm{h})^2. \tag{4.46}$$

Evidently, this equation is only consistent if $\delta \tilde{g}_{tx}(r=r_h) \sim \omega h^{-2}$ is a finite number. Since our boundary conditions are that $\delta \tilde{g}_{tx}(r=0)=0$, we conclude that $\delta \tilde{g}_{tx}$ is not a constant at leading order. (??) then implies that δA_x must have a component at $O(h^{-2})$ as well. It is consistent in every equation, at $O(\omega)$, to take $\delta \mathcal{P}_x$ to be $O(h^0)$, so long as the $O(\omega h^{-2})$ coefficients in δA_x and $\delta \tilde{g}_{tx}$ obey the equations of motion associated with the translationally invariant black hole. In fact, at $O(\omega h^{-2})$, we find that the boost mode (??) is the only mode consistent with all of our boundary conditions: (??) is ruled out by $\delta \tilde{g}_{tx}(r=0)=0$, and (??) by the fact that the logarithmic divergence in δA_x occurs at $O(h^0)$. Using (??) we in fact find that the coefficient of the Galilean boost mode in δA_x is:

$$\delta A_x = \delta A_x^0 - \frac{i\omega Q\tau}{\epsilon + P} (p + p_h) \delta A_x^0 + O(\varepsilon^0), \qquad (4.47)$$

where we have defined

$$\frac{\epsilon + P}{\tau} \equiv \frac{L^d}{r_h^d} \int d^d \mathbf{k} |h(\mathbf{k})|^2 k_x^2 \psi_0(\mathbf{k}, r_h)^2. \tag{4.48}$$

In the next subsection, we show that this τ is equivalent to that defined via the memory matrix; for now this is simply a definition of τ . Note that the logarithmic divergence in δA_x is not included, as it is $O(h^0)$.

Now, let us explain why we do not have to worry about any further terms, in so far as computing the conductivity at leading order in our limit. Firstly, let us consider the term that arises from the logarithmic divergence at $O(h^0)$ in δA_x . This will indeed lead to subleading corrections to the Galilean mode described

above; however, these corrections, by dimensional analysis, will scale as $(\omega/T)\mathcal{F}(T/\mu)\delta A_x^0$ for some scaling function \mathcal{F} , and are subleading in our limit. A similar argument holds for the $O(\omega^2 h^{-2})$ term which arises from the fact that when $\omega\tau\gg 1$, the Galilean mode dominates the constant contribution δA_x^0 : the correction due to infalling boundary conditions on this term $\sim \omega^2 \tau/T$, and this can be neglected in our limit. Similar arguments will hold for all further corrections at higher orders in ω . In a nutshell, the linearized equations contain perturbations at most $\sim h^{-2}$, which implies that only the ωh^{-2} terms need to be included at leading order. The fact that the boost mode is the only important $O(\omega)$ contribution to δA_x is suggestive of the fact that this is "hydrodynamic" transport.

To compute $\sigma(\omega)$ we simply employ (??) to find the near boundary behavior of p(r). We thus find

$$\delta A_x^{(0)}(\omega) = \delta A_x^0 \left[1 - \frac{i\omega Q\tau}{\epsilon + P} \left(\mu + \frac{Ts}{Q} \right) \right] = \delta A_x^0 \left[1 - \frac{i\omega \tau (\mu Q + Ts)}{\epsilon + P} \right] = \delta A_x^0 (1 - i\omega \tau), \tag{4.49a}$$

$$\delta A_x^{(1)}(\omega) = -\frac{e^2 \mathcal{Q}}{L^{d-2}} \left(-\frac{i\omega \mathcal{Q}\tau}{\epsilon + P} \right) \delta A_x^0, \tag{4.49b}$$

where we have used the thermodynamic identity

$$\epsilon + P = \mu \mathcal{Q} + Ts \tag{4.50}$$

in the last step of (??). Recall that $\delta A_x^{(1)}/\delta A_x^{(0)}$ is related to $\sigma(\omega)$ by (??). It is straightforward from here to obtain (??), $\sigma(\omega) = \sigma_{\rm dc}/(1-{\rm i}\omega\tau)$, and the expression (??) for $\sigma_{\rm dc}$ in the limit where $\omega/T \to 0$ first, and $\omega\tau$ is held finite.

That Drude physics arises is not particularly surprising for a few reasons. Intuitively, we expect via the fluid-gravity correspondence [?] that a holographic system, weakly perturbed by translational symmetry breaking, behaves in the same way as a fluid with momentum relaxation would: see also [?]. Additionally, it was shown via matched asymptotic expansions in [?] that certain massive gravity theories contain Drude peaks in the limit of weak graviton mass, at T = 0. Due to the equivalence between the holographic set-ups above and massive gravity as $\omega \to 0$ [?] (with the caveat that the graviton mass becomes a function of r), this result makes sense. It is pleasing nonetheless to see the Drude peak emerge from a direct calculation for a wide range of holographic theories at finite T.

Equivalence with the Memory Function Approach

Our only remaining task is to show that the τ defined above is equivalent to the τ defined in (??), defined in terms of the leading order imaginary behavior of $G_{\mathcal{O}\mathcal{O}}^{\mathbb{R}}(\omega \to 0)$. By the holographic dictionary for retarded Green's functions, we impose infalling boundary conditions at the black hole horizon $r = r_h$, as before. Near

the black hole horizon:

$$\psi(\mathbf{k}, r, \omega \to 0) \approx \psi(\mathbf{k}, r, \omega = 0) \left[1 + \frac{i\omega}{4 \cdot 10 \cdot .18 \, \text{ft} T} \log \frac{r_{\text{h}}}{r_{\text{h}} - r} \right]. \tag{4.51}$$

As before, at $O(\omega)$, ψ solves its $\omega = 0$ equation of motion. Also note $\psi(\mathbf{k}, r, \omega = 0) = \psi_0(\mathbf{k}, r)$, with ψ_0 the finite scalar profile we defined previously. We wish to "propagate" this small imaginary piece from the horizon to the AdS boundary. This directly allows us to compute $\text{Im}(G^R(\omega))/\omega$ by using the AdS/CFT dictionary at r = 0. We compute the linearly independent solution to ψ 's equation of motion with the reduction of order technique:

$$\psi_1(\mathbf{k}, r) \equiv \frac{\psi_0(\mathbf{k}, r)}{L^d} \int_0^r \mathrm{d}s \frac{s^d}{b(s)\psi_0(\mathbf{k}, s)^2}$$
(4.52)

We assume that ψ_0 has the same asymptotics as before: $\psi_0(\mathbf{k}, r \to 0) \approx L^{-d/2} r^{d+1-\Delta}$, and have normalized ψ_1 conveniently. The integral as written above is convergent so long as $\Delta > (d+1)/2$, and we have assumed this property previously. In fact, this solution also has the $r \to 0$ asymptotics we wish: as $b \approx 1$ near the AdS boundary, we find that

$$\psi_1(\mathbf{k}, r) \approx L^{-d/2} \frac{r^{\Delta}}{2\Delta - d - 1}, \quad (r \to 0).$$
 (4.53)

Near the black hole horizon, ψ_1 is divergent – this divergence implies that the imaginary contribution to ψ is (for the purposes of our calculation) proportional to ψ_1 . As this divergence is associated with near-horizon physics, its coefficient is completely independent of the UV or intermediate scales in the geometry:

$$\psi_1(\mathbf{k}, r) \approx \frac{r_{\rm h}^d}{4 \cdot 1 \cdot 0 - .18 \, \pi T \psi_0(\mathbf{k}, r_{\rm h}) L^d} \log \frac{r_{\rm h}}{r_{\rm h} - r} + \text{finite}, \quad (r \to r_{\rm h}).$$
(4.54)

Comparing (??) and (??) we conclude that to order ω ,

$$\psi(\mathbf{k}, r, \omega) \approx \psi_0(\mathbf{k}, r) + i\omega \frac{L^d \psi_0(\mathbf{k}, r_h)^2}{r_h^d} \psi_1(\mathbf{k}, r) + O(\omega^2), \qquad (4.55)$$

The function ψ_0 is real. Therefore using (??), it is easy to conclude that

$$\lim_{\omega \to 0} \frac{\operatorname{Im} \left(G_{\mathcal{O}\mathcal{O}}^{\mathbb{R}}(\mathbf{k}, \omega) \right)}{\omega} = \frac{L^d \psi_0(\mathbf{k}, r_h)^2}{r_h^d} \tag{4.56}$$

Comparing (??), (??) and (??), we see that the conductivity of this metal, computed directly via holography, is identical to the result computed with the memory function formalism, without using any holography. These results are valid in the limit when ω , τ^{-1} are vanishingly small compared to T and μ , the regime of validity

where the approximation (??) holds.

Seebeck Coefficient

Let us briefly discuss thermoelectric transport coefficients [?, ?, ?, ?, ?]. One such coefficient is immediately computable given our discussion of the conductivity: the Seebeck coefficient α , defined by

$$q_x = \alpha T E_x,\tag{4.57}$$

where q_x is the heat flow density in the x direction. Using

$$q_x = \langle T^{tx} \rangle - \mu \langle J^x \rangle, \tag{4.58}$$

and reading off the expectation value of $\langle T^{tx} \rangle$ in the linearized modes computed in this section, it is straightforward to recover

$$\alpha(\omega) = \frac{sQ\tau}{\epsilon + P} \frac{1}{1 - i\omega\tau},\tag{4.59}$$

in agreement with hydrodynamics [?] and the memory function formalism (use that the heat-momentum susceptibility $\chi_{QP} = sT$). We also expect that a calculation of the thermal conductance $\bar{\kappa}$, defined by

$$q_x = -\bar{\kappa} \partial_x T|_{E_x = 0}, \tag{4.60}$$

would find, in agreement with hydrodynamics and the memory function formalism,

$$\bar{\kappa}(\omega) = \frac{s^2 T \tau}{\epsilon + P} \frac{1}{1 - i\omega \tau}.$$
(4.61)

Computations of $\bar{\kappa}(\omega)$ are a bit more involved [?, ?, ?, ?] and we will not pursue them further.

Conclusion

In this work, we have demonstrated an exact correspondence between the memory function approach and a holographic approach to transport in a strongly correlated "strange" metallic phase of matter without quasiparticles, in the limit of finite density and slow momentum relaxation. This result crispens the qualitative scaling agreements noted in special cases earlier [?, ?]. We have also pointed out the emergence of a universal Drude peak in these holographic models. These results are to be expected on physical grounds,

but it is nonetheless instructive to see them explicitly verified.

The reason that we add a fourth scalar field ψ , instead of say adding perturbations to the dilaton, is that the EMD background is only corrected at $O(h^2)$; it would receive corrections at O(h) if the dilaton had a component which breaks translational symmetry. As in [?, ?], adding a new scalar simplifies the resulting computation of $\sigma(\omega)$. It would be worthwhile to explicitly show that the correspondence with the memory matrix survives even if we break translational symmetry through one of the EMD fields: for example, using results of [?], it should be possible to do this for spatially-dependent chemical potentials.

One of the advantages to a holographic computation is that we are formally not restricted to the limit of weak momentum relaxation. Approaches including massive gravity and Q-lattices, which produce translation invariant geometries, allow for analytic control in this limit. Perhaps techniques similar to ours can remain valid even in this limit of strong momentum dissipation. While it is now clear that such approaches mimic more conventional "lattices" or disorder when momentum relaxation is weak, it is less clear whether this analogy remains when momentum relaxation is strong. It is possible that more exotic phases of holographic matter, analogous to a quantum glass or many-body localized phase [?], will arise when translational symmetry is explicitly broken strongly. Alternately, efficient momentum relaxation without "glassy" physics may be responsible for scaling properties of cuprate strange metals [?]; perhaps massive gravity/Q-lattice approaches are powerful tools for these problems. More work in this direction is warranted.

Chapter 5

Memory matrix theory of

magnetotransport

Below we present the original text of [?]. Reprinted with permission from A. Lucas and S. Sachdev, "Memory matrix theory of magnetotransport in strange metals", Physical Review **B91** 195122 (2015). Copyright (2015) by the American Physical Society.

Since this paper was written, a simpler derivation of σ_{Q} in the memory matrix formalism has been found, as we discussed in Part I. The crucial point is that it is possible to remove the regulator k_x introduced below. However, we believe that the physics of this derivation is more or less the same, although the original derivation is (in retrospect) more complicated than necessary.

Introduction

The strange metal phase of the hole-doped cuprate superconductors is the most important realization of quantum matter not amenable to a quasiparticle description [?, ?]. Apart from the well-known linear in temperature (T) resistivity, the strange metal has a Hall angle $\tan(\theta_{\rm H}) \sim 1/T^2$ [?, ?]. This combination cannot be reproduced in a Boltzmann theory of charge-carrying quasiparticles with a long lifetime; such a theory yields a $\tan(\theta_{\rm H})$ inversely proportional to the resistivity, and so these observations rule out the transport of charge by any fermionic quasiparticle, and not just those with the same quantum numbers as the electron.

A general hydrodynamic approach to magnetotransport in strange metals was introduced by Hartnoll et al. in [?], and compared to Nernst measurements in the strange metal of the cuprates. The main

assumption of their theory, apart from the absence of any quasiparticle excitations, was that there was a slow mode associated with the decay of the total momentum. Such a slow mode is indeed invariably present in proposed field-theoretic models of strange metals [?, ?], and the decay arises from perturbations which break the continuous translational symmetry of the field theory (umklapp scattering or impurities). Combining this momentum mode with reasonable assumptions on the diffusion of the conserved U(1) charge and energy densities, general results were obtained by Hartnoll et al. [?] for the charge and thermoelectric transport coefficients of a two-dimensional strange metal in the presence of a static magnetic field, B. Note that we are using the phrase "charge density" here to refer to the conserved density of a global U(1) symmetry. In the application to the cuprates, there are also long-range Coulomb interactions associated with such a conserved density, and we will briefly discuss this in Section ??.

Blake and Donos [?] have recently argued that the magnetotransport framework of Hartnoll *et al.* is compatible with the measurements of the longitudinal and Hall conductivities in the cuprates, and also provided a solvable holographic model for magnetotransport in the presence of momentum relaxation.

However, an important concern is that the present derivations of the above results for strange metals rely on models which are rather far removed from the microscopic situation in the cuprates. One approach [?] begins from a quantum critical point with a relativistic structure, and then breaks Lorentz invariance weakly by a chemical potential, the temperature, and the applied magnetic field; the equations were then derived using a hydrodynamic gradient expansion restricted by the requirements of the positivity of entropy production. The other approach [?, ?] uses holographic models of strange metals represented by gravitational theories in a spacetime with an extra dimension, whose field theory duals are not well understood.

In the present paper, we will provide a derivation for the equations for magnetotransport in a normal-state metal using the memory matrix approach [?, ?, ?]. Although the memory matrix framework has typically been applied to systems where the slow relaxation of momentum dominates magnetotransport and the diffusion of conserved quantities is negligible, we generalize and study the case where the diffusive dynamics is not negligible and must be consistently included in the memory matrix. In particular, we will focus on the consequences of the diffusion of exactly conserved heat, as well as an exactly conserved U(1) charge. Our main results may be found in (??) and (??), though there is a large amount of notation that must be explained, and so we defer their presentation. Our assumptions on the momentum mode, and the charge and energy diffusion will be the same as those in [?], but we will not assume any relativistic structure on the underlying theory. Using certain assumptions, our results agree with those of [?], and with the recent holographic papers [?, ?, ?], and shed light into a discrepancy between the two. Furthermore, our results can, in principle, be applied directly to microscopic models appropriate for the cuprates [?, ?, ?, ?], as we will describe more completely in Section ??.

Figure 27: An illustration of the connections between hydrodynamics, memory matrices, and holography.

Transport Without Quasiparticles

Let us briefly review our current understanding of theoretical frameworks for describing transport in strongly correlated systems without quasiparticles in two (or more) spatial dimensions. An overview is also provided in Fig. ??.

The simplest way of describing transport without reference to quasiparticles is, in fact, a very old framework – hydrodynamics. The modern understanding of hydrodynamics is that it describes the long wavelength, long time dynamics of a system close to thermal equilibrium, when there are a small number of conserved quantities [?]. We will be liberal, and also allow for some of these conserved quantities to decay on long time scales, while still maintaining the name "hydrodynamics". All we insist upon is that this list of conserved quantities is finite; this is in contrast to the typical condensed matter paradigm of a Fermi liquid, where occupation numbers at every single wave number are long lived quantities. For non-Fermi liquids, it is believed that generic higher dimensional theories do not admit infinite families of (nearly) conserved quantities at strong coupling.

Hydrodynamics proves to be a very powerful framework for describing the dynamics of systems without reference to quasiparticles. However, we must emphasize that hydrodynamics is an incomplete description. It provides a set of constraints that any (to date) reasonable (2+1)-dimensional quantum field theory at finite density and temperature, which is approximately translation invariant, must obey, and a universal framework within which we can interpret a microscopic calculation. But it does not give us particular values or temperature dependence for any microscopic coefficients.

So now we need a way of obtaining microscopic coefficients. A traditional framework for doing this is the memory matrix framework [?, ?]; see [?] for a thorough review. We will review it in this paper, but for now we emphasize that it is in principle an exact, microscopic calculation. Its usefulness is that it can be efficiently approximated in a hydrodynamic regime where there are only a few quantities which do not quickly relax to thermal equilibrium.

The main purpose of this paper is to clarify and sharpen the connections between the memory matrix framework for transport, and hydrodynamic descriptions of transport. In particular, we will not need to add a phenomenological momentum relaxation time in hydrodynamics, and compute this coefficient separately using the memory matrix formalism. We will also point out the microscopic computations which allow us to compute all phenomenological coefficients within hydrodynamics.

There has also been, in recent years, a third framework which allows for transport computations: gauge-gravity duality. This allows one to study a strongly coupled "large N matrix" quantum field theory, directly at finite temperature and density, in real time, by studying a classical gravity theory in one higher dimension, in particular black hole backgrounds. Ref. [?] has recently shown the equivalence between holographic and memory function calculations in zero magnetic field, in the regime where momentum relaxation is slow (this provides the bottom arrow in Fig. ??). One advantage of holographic methods is that the calculations are formally valid beyond the regimes of validity of hydrodynamics or memory functions. However, we point out in this paper that a wide variety of holographic results for transport, computed in regimes where hydrodynamics need not be valid, can nonetheless be understood within the framework we derive.

Outline of the Paper

We will begin in Section ?? by recalling the main hydrodynamic results of [?] for electrical transport in a simple manner, and using notation suitable for our memory matrix approach. The basic memory matrix formalism will be introduced in Section ??, along with its physical interpretation. Section ?? contains our main new results on magnetotransport in the memory matrix formalism under the simplifying assumption that the diffusion of heat has decoupled from the diffusion of charge and relaxation of momentum: this simplification will help us to elucidate many of the subtleties that arise in the memory matrix framework when describing magnetotransport. Section ?? relaxes the assumption that heat diffusion decouples, and Section ?? describes thermal and thermoelectric transport.

Hydrodynamics

Let us begin by computing electrical transport in a generic quantum field theory without quasiparticles, describable by hydrodynamics, following the approach of [?]. More precisely, we focus on a theory with exactly conserved energy and U(1) charge, and approximately conserved momentum, where the only dynamics on long time scales are momentum relaxation on the time scale τ , and charge/energy diffusion on the time scales λ^2/D , with λ the wavelength of the fluctuation and D an eigenvalue of the generalized diffusion matrix coupling heat and charge diffusion.³⁸

We wish to compute the electrical conductivity matrix, defined as

$$J_i = \sigma_{ij} E_j. (5.1)$$

³⁸Note that with momentum relaxation, there is no longer a propagating sound mode as $k \to 0$, so indeed the dynamics of charge and energy become governed by diffusion.

We assume that we have an isotropic, parity-symmetric theory in two spatial dimensions, which constrains

$$\sigma_{xx} = \sigma_{yy},\tag{5.2a}$$

$$\sigma_{xy} = -\sigma_{yx}. ag{5.2b}$$

Momentum conservation within a hydrodynamic framework – accounting for momentum relaxation – gives us the equation

$$\partial_t \Pi_x + \partial_x P = -\frac{\Pi_x}{\tau} + \mathcal{Q}E_x + B\epsilon_{ij}J^j \tag{5.3}$$

where Q is the background "charge" density, τ is the momentum relaxation time, B is the external magnetic field, P is the pressure and Π_x is the x-momentum density; a precise definition of Q, applicable to lattice models, appears later in (??). We have assumed that the velocities relevant for hydrodynamics are small and may be treated non-relativistically. As we are interested in perturbing the system with a spatially homogeneous electric field, oscillating at frequency ω , momentum conservation simplifies to

$$\left(-\mathrm{i}\omega + \frac{1}{\tau}\right)\mathcal{M}\delta v_i = \mathcal{Q}\delta E_i + B\epsilon_{ij}\delta J_j \tag{5.4}$$

where \mathcal{M} is the analogue of "mass density" (namely, the momentum density at small velocities is $\mathcal{M}\delta v_i$). The memory matrix definition of \mathcal{M} is in (??). The momentum relaxation time, τ , is – like all thermodynamic coefficients – undetermined within hydrodynamics. Unlike thermodynamic coefficients like \mathcal{M} and \mathcal{Q} , however, τ is extrinsic and sensitive to the precise mechanism by which momentum relaxes, as we will see explicitly within the memory matrix formalism.

(??) gives us an equation relating δv_i , δJ_i and δE_i – our perturbatively small quantities within linear response. δJ_i may be expressed in terms of δv_i and δE_i , in an isotropic and parity-symmetric (up to magnetic fields) theory, as

$$\delta J_i = \mathcal{Q}\delta v_i + \sigma_{\mathcal{Q}} \left(\delta E_i + B \epsilon_{ij} \delta v_i \right). \tag{5.5}$$

Here σ_{Q} is an intrinsic "quantum critical" conductivity which measures charge transport independent of the momentum mode; a precise definition relating it to the charge diffusivity appears later. Combining (??) and (??) we may relate δJ_{i} to δE_{i} , and we find

$$\sigma_{xx} = \frac{(\tau^{-1} - i\omega)\mathcal{M}\sigma_Q + \mathcal{Q}^2 + B^2\sigma_Q^2}{\mathcal{Q}^2 B^2 + ((\tau^{-1} - i\omega)\mathcal{M} + B^2\sigma_Q)^2} \mathcal{M}\left(\frac{1}{\tau} - i\omega\right),\tag{5.6a}$$

$$\sigma_{xy} = \frac{2(\tau^{-1} - i\omega)\mathcal{M}\sigma_{Q} + \mathcal{Q}^{2} + B^{2}\sigma_{Q}^{2}}{\mathcal{Q}^{2}B^{2} + ((\tau^{-1} - i\omega)\mathcal{M} + B^{2}\sigma_{Q})^{2}}B\mathcal{Q}.$$
 (5.6b)

The answer simplifies when B=0 to the form $\sigma_{xy}=0$ (by parity symmetry) and

$$\sigma_{xx} = \sigma_{Q} + \frac{Q^{2}\tau}{\mathcal{M}(1 - i\omega\tau)}.$$
(5.7)

Though in a system without Galilean invariance one might be concerned that the Qs in (??) and (??) need not be the same, we will carefully define Q via the memory matrix framework and show that (??) is indeed (at leading order) correct.

These results were first derived in [?], for the case of a quantum critical theory, and were argued in [?] to be compatible with Hall angle measurements in the strange metal of the cuprates. In fact, the structure here is identical, and is valid for any isotropic theory, whether or not it is Lorentz invariant. We even need not assume that diffusive charge and heat fluctuations are decoupled (as would be the case when the underlying theory has charge conjugation symmetry) – heat transport could only alter the equations above if temperature gradients were non-vanishing, which (by assumption) does not happen. It is a simple task to compute additional thermal and thermoelectric coefficients, but we will not do so using hydrodynamics.

We remarked previously that the dynamics which governs σ_{ij} is the only dynamics in the system occurring on long time scales. However, the expressions for σ_{ij} are rather complex! This is because there are four slow time scales in the problem: the slow driving time scale $1/\omega$, and the three time scales associated with the specific quantum field theory, and its realization: τ , $1/\omega_c$, and $1/\omega_Q$, where ω_c is the cyclotron frequency

$$\omega_{\rm c} = \frac{QB}{\mathcal{M}},\tag{5.8}$$

and $\omega_{\rm Q}$ is a "quantum frequency" given by

$$\omega_{\mathcal{Q}} = \frac{\mathcal{Q}^2}{\mathcal{M}\sigma_{\mathcal{Q}}}.\tag{5.9}$$

Within hydrodynamics, and the memory function formalism, we only work to leading order in ω – but to all orders in the dimensionless numbers $\omega \tau$, $\omega/\omega_{\rm q}$.

As τ^{-1} scales with the strength of the coupling to the operator which breaks translational symmetry (as we will explicitly see later), and $\omega_{\rm c} \sim B$, it is evident in what physical limit these two quantities would be perturbatively small. It is less clear how $\omega_{\rm q}$ would generically be perturbatively small. One mechanism is that the densities of the theory (\mathcal{Q} and \mathcal{M}) are small (with \mathcal{Q}/\mathcal{M} , the strong-coupling analogoue of the fixed charge-to-mass ratio of the electron, fixed). Another is that $\sigma_{\rm q}$ is anomalously large – though this should not be a consequence of weak coupling (i.e., long-lived quasiparticles), for our framework to be valid.

We should also comment that recently, this result has been obtained holographically at $\omega = 0$ [?] (though it is not expressed in terms of thermo/hydrodynamic quantities) in a set-up which is formally valid even

when τ is comparable to $\tau_{\rm m}$ – the time scale associated with microscopic dynamics, and the breakdown of hydrodynamics. The limiting case (??), also at $\omega = 0$, is found in various holographic set-ups in [?, ?, ?]. It is an interesting question whether or not this is a pathological feature of the holographic mechanism of strong momentum relaxation, or a signature that the "hydrodynamic" regime of strongly coupled transport persists far beyond our first expectations.

Memory Function Formalism

Let us now briefly review the memory function framework. As we emphasized in the introduction, the method works best when quasiparticles are not long-lived, and the only conserved (or approximately conserved) quantities are charge, energy and momentum. In recent years this has become a method of choice for studying transport in condensed matter systems without quasiparticles [?, ?, ?, ?], including using gauge-gravity duality [?, ?, ?, ?, ?]. We work in units with $\hbar = 1$.

Let us consider the set of operators A, B, C, \ldots in a time-translation invariant theory, and correlation functions of the form

$$C_{AB}(t - t') = (A(t)|B(0)) \equiv T \int_{0}^{1/T} d\lambda \left\langle A(t)^{\dagger} B(i\lambda) \right\rangle$$
 (5.10)

with averages over thermal and quantum fluctuations denoted in $\langle \cdots \rangle$. The Laplace transform of this expression can be shown to be

$$C_{AB}(z) = \frac{T}{iz} \left[G_{AB}^{R}(z) - G_{AB}^{R}(i0) \right].$$
 (5.11)

The retarded Green's function (in real space) is defined as:

$$G_{AB}^{R}(\mathbf{x},t) \equiv i\Theta(t)\langle [A(\mathbf{x},t),B(\mathbf{0},0)]\rangle$$
 (5.12)

where Θ is the Heaviside step function. The momentum dependence of the Green's functions have been suppressed in (??) as we will only be interested in the conductivities, evaluated at zero momentum. As standard, we take z to lie in the upper half of the complex plane. We are only computing thermoelectric transport coefficients, for which $G_{AB}^{\rm R}(\omega \to 0) \sim i\omega \sigma_{AB}$, with σ_{AB} strictly finite; thus for us, $G_{AB}^{\rm R}(i0) = 0$ and can be neglected. Up to the overall factor of temperature, we recognize $C_{AB}(z)$ in (??) as a generalized conductivity between the operators A and B, σ_{AB} . Some formal manipulations on a Hilbert space of operators using the inner product (??) give

$$\sigma_{AB}(z) \equiv \frac{1}{T} C_{AB}(z) = \chi_{AC} [M(z) + N - iz\chi]_{CD}^{-1} \chi_{DB},$$
 (5.13)

where χ_{AB} is the static susceptibility between the operators A and B:³⁹

$$\chi_{AB} \equiv G_{AB}^{R}(\omega = 0) = \frac{1}{T}(A|B),$$
(5.14)

the memory matrix M_{AB} is defined as

$$M_{AB}(z) = \frac{\mathrm{i}}{T} \left(\dot{A} \left| \mathfrak{q}(z - \mathfrak{q}L\mathfrak{q})^{-1} \mathfrak{q} \right| \dot{B} \right) , \qquad (5.15)$$

 $L = [H, \circ]$ is the Liouvillian operator with H the Hamiltonian, \mathfrak{q} is the projection operator

$$\mathfrak{q} = 1 - \frac{1}{T} \sum_{AB} \chi_{AB}^{-1} |A| (B|,$$
 (5.16)

and

$$N_{AB} \equiv \chi_{A\dot{B}} = -\chi_{\dot{A}B}.\tag{5.17}$$

Note that N_{AB} vanishes identically in a time-reversal invariant theory.

We will show that for the magnetotransport problem of interest in this paper, the memory matrix effectively truncates to a 6×6 matrix, given as $\mathfrak{m} = M + N - \mathrm{i}\omega\chi$ in (??).

Hydrodynamic Interpretation

The usefulness of the memory function formalism arises when the infinite dimensional matrix M has a finite number of parametrically small eigenvalues. This allows us to truncate the matrix to a small, finite dimensional object.

To give some physical intuition into (??), let us consider the dynamics of long-lived conserved quantities from the viewpoint of hydrodynamics. Let X_A denote quantities which are conserved on very long time scales, and let U_A be the conjugate thermodynamic variable. For simplicity, we define X_A by shifting X_A by a constant so that in equilibrium, $\langle X_A \rangle = 0$. In thermodynamics, we can then relate

$$X_A = \chi_{AB} U_B, \tag{5.18}$$

where χ is the same static susceptibility matrix as before, and we drop expectation values within hydrody-

³⁹Differing conventions appear in the literature [?]. This definition of the (overall sign of the) retarded Green's function is much more standard [?, ?] and is the common choice in condensed matter physics.

namics. The transport equations read

$$\dot{X}_A = -M_{AB}U_B - N_{AB}U_B + F_A, (5.19)$$

where N_{AB} , as before, is the static susceptibility between \dot{A} and B, M_{AB} is a (for now arbitrary, but symmetric) matrix which denotes the weak relaxation of X_A into an external bath, and F_A is an external driving force. Now, we relate F_A to the "thermodynamic field" E_A which drives X_A by

$$F_A = \chi_{AB} E_B. \tag{5.20}$$

 E_A should be interpreted as "the net \dot{U}_A " imposed on the system. Combining these equations together at frequency ω , we obtain

$$X_A = \sigma_{AB} E_B \tag{5.21}$$

where σ_{AB} is given by (??).

One aspect of the memory function framework that is now much clearer is the physical role of the memory matrix. Defining the memory matrix as

$$M_{AB} \equiv \tau_{AC}^{-1} \chi_{CB},\tag{5.22}$$

in an undriven, time reversal invariant theory (where N=0), we find

$$\dot{X}_A = -\tau_{AB}^{-1} X_B. (5.23)$$

Evidently, the memory matrix encodes relaxation times for the average values of the operators A of interest. It is now evident why we choose the operators A, B, \ldots to be almost conserved quantities. In this case, the matrix τ^{-1} will have parametrically small eigenvalues, and as the memory matrix enters the conductivity via an inverse, these quantities will dominate the conductivity.

This derivation is rather abstract, so let us give a simple example to clarify the thermodynamic structure of these equations: the dynamics of a point particle of mass m on a one dimensional line, subject to weak friction, but no potential energy. In this case, the momentum p is long lived. The thermodynamic conjugate variable is the velocity v, and so the susceptibility is simply the mass. $N_{pp} = 0$, as there is no generic proportionality coefficient between p and \dot{v} , and so we are left with $\dot{p} = F - M_{pp}v$. Of course if $M_{pp} = 0$ we simply have Newton's Law, $F = \dot{p} = m\dot{v}$; otherwise, $M_{pp} \neq 0$ provides a frictional force which dissipates momentum into an external bath.

It is also important to understand the role played by F in this equation. To compute the "momentum

conductivity" σ_{pp} of this particle, we can interpret the external driving by the force F as actually external "shaking" of the line with acceleration $a_{\text{ext}} = F/m$. The conductivity relates the response of p to an external source of the time derivative of its conjugate variable. We find at zero frequency:

$$\frac{p}{a_{\text{ext}}} = \frac{mv}{a_{\text{ext}}} = \frac{mF}{M_{pp}a_{\text{ext}}} = \frac{m^2}{M_{pp}},\tag{5.24}$$

in accordance with (??).

Of course, we are probably more familiar with electrical conductivity. In this case, the thermodynamic conjugate variable to \mathbf{J} is a gauge potential $-\mathbf{A}$. And as $-\mathrm{d}\mathbf{A}/\mathrm{d}t = \mathbf{E}$, the electrical conductivity $\sigma_{\mathbf{J}\mathbf{J}}$ relates the response of \mathbf{J} to an external electric field \mathbf{E} . In this case, as we will see in the next section, the analogue of (??) become the hydrodynamic equations which describe the dynamics of charge and momentum, which are a bit more cumbersome.

The usefulness of the memory function formalism beyond the hydrodynamic reasoning described above is that we now have explicit expressions for the matrices M, N and χ . In particular, this will allow us to explicitly compute τ , the momentum relaxation time. We will describe more in the following section what the components of this matrix actually look like.

Dynamics of Charge and Momentum

Let us now discuss how the memory function framework produces the magnetohydrodynamic electrical transport described earlier. For simplicity, we assume that charge and heat diffusion are decoupled processes at zero charge density – we relax this assumption in Section ??. There are two slow time scales in the problem: the time scale over which momentum relaxes $t_{\text{mom}} \sim \tau$, and the time scale over which charge fluctuations diffuse away, $t_{\text{diff}} \sim \lambda^2/D$, with λ the wavelength of the fluctuation; on the longest length scales, $t_{\text{diff}} \to \infty$. Note that at finite charge density, there will be heat diffusion; however, the slow diffusion of heat will not be linearly independent from the dynamics of charge or momentum. Our goal is to compute the electrical conductivity matrix σ_{ij} at zero momentum, and small but finite frequency ω . There are four operators associated with the long lived quantities above which have spin 1 under the SO(2) isotropy of the system: the momentum vector \mathbf{P} , and charge density fluctuations ∇n . This suggests that our memory matrix should be a 4×4 matrix, as we should only keep track of the (zero wave vector components) of these operators. Using the notation of the previous section, our goal is to compute the conductivities $\sigma_{J_x J_x} \equiv \sigma_{xx}$ and $\sigma_{J_x J_y} \equiv \sigma_{xy}$.

Diffusive Transport

Let us begin with the case when the charge density Q = 0, and the magnetic field B = 0. As B = 0, the time reversal symmetry breaking matrix N will vanish. In this case, hydrodynamics tells us that the conductivity is governed solely by diffusive processes. Let us see how this arises in the memory function framework. In this case, using the isotropy of the system, in order to compute σ_{xx} , we need only keep track of operators with long time dynamics which are spin 1, and oriented in the x direction: these are $\partial_x n$ and P_x – both evaluated at zero wave vector.

To get started, let us compute the susceptibility matrices. Formally, we introduce a velocity v, as a source term conjugate to the conserved momentum, so that Hamiltonian maps as

$$H_0 \to H_0 - v_x P_x,\tag{5.25}$$

where H_0 is translationally invariant, and thus commutes with P_x , the total momentum in the x-direction (we will add terms responsible for momentum decay later). We may compute the susceptibilities χ_{AP_x} by studying $\langle A \rangle_{v_x}$ – the response of the average value of A to a small external source of velocity [?]:

$$\chi_{P_x P_x} = \frac{\langle P_x \rangle_{v_x}}{v_x V} \equiv \mathcal{M},\tag{5.26}$$

where V is the spatial volume of the sample. This formally defines the value of \mathcal{M} ; alternatively, \mathcal{M} is related to $G_{P_xP_x}^{\mathbb{R}}$ via (??). Note that in the earlier relativistic formalism, \mathcal{M} was equal to the sum of the energy density and pressure, up to coefficients proportional to the (effective) speed of light. Analogously,

$$\chi_{P_x J_x} = \frac{\langle J_x \rangle_{v_x}}{v_x V} \equiv \mathcal{Q},\tag{5.27}$$

defines the charge density Q. As the perturbation (??) does not break translation invariance in $n(\mathbf{x})$:

$$\chi_{P_x \partial_x n} = 0. ag{5.28}$$

Identical results hold for the yy susceptibility matrices. By spatial parity symmetry, when B=0, we find

$$\chi_{P_x P_y} = \chi_{\partial_x n \partial_y n} = \chi_{P_x \partial_y n} = \chi_{P_y \partial_x n} = 0. \tag{5.29}$$

In fact, we now see there is a great simplification when Q = 0, because the **P** indices of the memory matrix can play no role in the computation of σ_{xx} , as $\chi_{P_xJ_x} = 0$. This is a bit fast; we will see explicitly

later that the necessary components of the memory matrix M_{P_xA} do not vanish fast enough as $Q \to 0$ to spoil this argument.

Next, let us compute $\chi_{J_x\partial_x n}$. The simplest way to proceed here is to choose a finite momentum regulator, and then show that the transport coefficients are independent of the choice of regulator, k_x . We choose $n(x) = -n(k_x)\sin(k_x x)$, ⁴⁰ and this implies that the overlap with the current operator $J_x(k_x)\cos(k_x x)$, is given by

$$\langle \mathbf{J} \rangle = -\sigma_{\mathcal{Q}} \nabla \mu, \tag{5.30}$$

as the conjugate field to n is the chemical potential μ (in the presence of long-range Coulomb interactions, μ should be replaced by the electrochemical potential [?, ?]). We conclude

$$\chi_{J_x \partial_x n} = \sigma_0 k_x. \tag{5.31}$$

Crudely speaking, we think of fixing x and sending $k_x \to 0$ – one then finds that $n(x) \to -n(k_x)k_xx$ and $J_x \to J_x(k_x)$, so that we have a linear density fluctuation sourcing a constant, diffusive current. But it is easiest to compute the memory matrix with the regulator explicitly finite.

It is a standard result that [?]

$$G_{nn}^{R}(\mathbf{k},\omega) = \frac{\sigma_{Q}k^{2}}{Dk^{2} - i\omega},$$
(5.32)

for any quantum field theory which has a hydrodynamic limit, where n will obey a simple diffusion equation at long wavelengths with diffusion constant D: $\partial_t n = D\nabla^2 n$ (recall we have assumed charge and heat fluctuations decouple at Q = B = 0); for the case with long-range Coulomb interactions, (??) refers to the irreducible density correlator i.e. the polarizability [?, ?]. We may now use (??) to obtain $M_{\partial_x n \partial_x n}$. By time reversal symmetry when B = 0, $(\partial_x \dot{n} | \partial_x n) = (\partial_x \dot{n} | P_x) = 0$; thus we take the abstract projection operator $\mathfrak{q} = 1$ in (??). Using that [?]

$$M_{AB}(z) = \frac{1}{\pi i} \int_{-\infty}^{\infty} d\omega \, \frac{\operatorname{Im}\left(G_{\dot{A}\dot{B}}^{R}(\omega)\right)}{\omega(\omega - z)},\tag{5.33}$$

and regulating this integral, we obtain

$$M_{\partial_x n \partial_x n}(\omega) = \frac{\sigma_Q D k_x^4}{D k_x^2 - i\omega} \approx \sigma_Q k_x^2 + i\omega \chi_{nn} + \cdots, \qquad (5.34)$$

⁴⁰The choice of sine waves instead of plane waves keeps things manifestly real, and so is a bit simpler.

where we have expanded to lowest non-trivial order in ω , and

$$\chi_{nn} = \frac{\sigma_{\mathcal{Q}}}{D} = \lim_{k \to 0} \lim_{\omega \to 0} \operatorname{Re} \left[G_{nn}^{\mathcal{R}}(\mathbf{k}, \omega) \right]$$
 (5.35)

is the static density-density susceptibility. The memory matrix formalism now gives

$$\sigma_{xx} = \frac{\chi_{J_x \partial_x n}^2}{M_{\partial_x n \partial_x n} - i\omega \chi_{nn}} = \frac{\sigma_Q^2 k_x^2}{\sigma_Q k_x^2} = \sigma_Q + \mathcal{O}\left(\omega^2\right). \tag{5.36}$$

This is exactly what we should expect – the diffusive hydrodynamic coefficient σ_{Q} is well-known to be the electrical conductivity at Q = B = 0. And importantly, the regulator k_x has decoupled from the answer. We may thus safely take the limit $k_x \to 0$. By spatial isotropy, $\chi_{J_x\partial_x n} = \chi_{J_y\partial_y n}$, etc., and $\chi_{J_x\partial_y n} = 0$, etc.

Momentum Relaxation

Next, let us consider the case where $Q \neq 0$, and B = 0. We have already computed all relevant static susceptibilities, so only the memory matrix M remains. Spatial isotropy implies that $M_{P_xP_y} = M_{P_x\partial_y n} = 0$, etc., and so we only need to compute $M_{\partial_x n P_x}$ and $M_{P_xP_x}$. Note that the diffusive form of $M_{\partial_x n \partial_x n}$ and $\chi_{J_x\partial_x n}$ from the previous subsection remains valid even with $Q \neq 0$, as momentum relaxation kills sound propagation at the longest wavelengths, and charge is still conserved, though the value of σ_Q may change.

We begin with $M_{P_xP_x}$. Let us consider for simplicity the case where the Hamiltonian of the system is given in d spatial dimensions by

$$H = H_0 - \int d^d \mathbf{x} \ h(\mathbf{x}) \mathcal{O}(\mathbf{x}), \tag{5.37}$$

where H_0 is a translationally invariant Hamiltonian, and $\mathcal{O}(\mathbf{x})$ is an arbitrary operator in the quantum field theory. $h(\mathbf{x})$ is an arbitrary function which should depend on space, and be non-trivial in (almost) all of the plane. We assume that $h(\mathbf{x})$ is small, so that translational symmetry breaking is weak – we will see that this is equivalent to the momentum relaxation time τ being large. The operator \dot{P}_i is easily computed to be

$$\dot{P}_x = i[H, P_x] = -\int d^d \mathbf{x} \ h(\mathbf{x})(\partial_i \mathcal{O})(\mathbf{x})$$
 (5.38)

The generalization to the case where multiple operators couple to \mathbf{x} -dependent fields is straightforward. We find

$$M_{P_x P_x}(z) = \frac{1}{\pi i} \int_{-\infty}^{\infty} d\omega \frac{\operatorname{Im} \left(G_{\dot{P}_x \dot{P}_x}^{R}(z) \right)}{\omega(\omega - z)}$$

$$= \frac{1}{\pi i} \int_{-\infty}^{\infty} d\omega \int d^{d}\mathbf{k}_{1} d^{d}\mathbf{k}_{2} \frac{\operatorname{Im}\left(G_{\mathcal{O}\mathcal{O}}^{R}(\mathbf{k}_{1}, \mathbf{k}_{2}, \omega)\right)}{\omega(\omega - z)} h(\mathbf{k}_{1}) h(\mathbf{k}_{2}) k_{1x} k_{2x}.$$
 (5.39)

As before, we have set $\mathfrak{q}=1$ in this equation: we assume the operator \mathcal{O} is independent of $\partial_x n$ or P_x . As h is a small parameter, we may safely take $G_{\mathcal{O}\mathcal{O}}^{\mathbb{R}}$ to be the Green's functions associated with H_0 ; translation invariance then implies that it vanishes unless $\mathbf{k}_1 + \mathbf{k}_2 = \mathbf{0}$. One finds [?, ?, ?, ?]

$$M_{P_x P_x}(0) \equiv \frac{\mathcal{M}}{\tau} = \lim_{\omega \to 0} \int d^d \mathbf{q} |h(\mathbf{q})|^2 q_x^2 \frac{\operatorname{Im} \left(G_{\mathcal{O}\mathcal{O}}^{\mathbf{R}}(\mathbf{q}, \omega)\right)}{\omega}, \tag{5.40}$$

up to a re-scaling of $h(\mathbf{q})$ to absorb a factor of the spatial volume [?]. We will shortly see that the τ defined here is equal to the τ defined within hydrodynamics; with the memory function framework, however, we now have an explicit expression for τ in terms of the fields h. A similar formula holds for $M_{P_yP_y}$. For simplicity, we will assume that the system is isotropic and so $M_{P_xP_x} = M_{P_yP_y}$.

We have focused on the $\omega = 0$ limit of $M_{P_x P_x}(\omega)$. This can be justified on very general grounds. Suppose that $\tau_{\rm m}$ is the microscopic time scale associated with the quantum dynamics of the system – for example, in many quantum critical theories, we have $\tau_{\rm m} = 1/T$. The Green's function $G_{\mathcal{O}\mathcal{O}}^{\rm R}$ is associated with the quantum dynamics of the Hamiltonian H_0 , and thus we obtain

$$G_{\mathcal{O}\mathcal{O}}^{\mathrm{R}}(\omega) = A_{\mathcal{O}\mathcal{O}}^{(0)} + (\omega \tau_{\mathrm{m}}) A_{\mathcal{O}\mathcal{O}}^{(1)} + (\omega \tau_{\mathrm{m}})^2 A_{\mathcal{O}\mathcal{O}}^{(2)} + \cdots$$

$$(5.41)$$

where, for a generic quantum field theory, the coefficients $A_{\mathcal{O}\mathcal{O}}^{(1)}$, etc., have no anomalously large coefficients, relative to any others. This implies that

$$M_{P_x P_x}(\omega) = \frac{\mathcal{M}}{\tau} \left[1 + \mathcal{C}\omega \tau_{\rm m} + \cdots \right], \tag{5.42}$$

with C an O(1) constant, and thus the finite frequency corrections to $M_{P_xP_x}$ are higher order in perturbation theory. At $\omega \tau_{\rm m} \sim 1$, hydrodynamics and the memory function formalism (when truncated to a finite set of operators) both cease to be good approximations for generic theories.

Next, let us discuss $M_{P_x\partial_x n}$. In the case where the operator \mathcal{O} is charge conjugation symmetric, this matrix element vanishes by charge conjugation symmetry. We discuss the more general case in Appendix ??.

Putting everything together, we obtain $\sigma_{xy} = 0$ (by parity symmetry) and, since the memory matrix is

diagonal up to this point:

$$\sigma_{xx} = \frac{\chi_{J_x \partial_x n}^2}{M_{\partial_x n \partial_x n} - i\omega \chi_{nn}} + \frac{\chi_{J_x P_x}^2}{M_{P_x P_x} - i\omega \chi_{P_x P_x}} = \sigma_Q + \frac{Q^2 \tau}{\mathcal{M}(1 - i\omega \tau)}$$
(5.43)

In a theory without momentum relaxation, we have $\tau \to \infty$; then the real part of the second term in (??) is proportional to $\delta(\omega)$. In such a theory we define $\sigma_{\mathcal{Q}}$ to be equal to σ_{xx} minus the delta function contribution, and this definition can be used to compute $\sigma_{\mathcal{Q}}$ in a particular model of a strange metal.

Magnetic Fields

Finally, we allow for $B \neq 0$. We still demand that B is perturbatively small, so that ω_c is a perturbative parameter. As each component of the memory matrix is first order within perturbation theory (we will see this does not change when $B \neq 0$), it will suffice to consider only the B-dependent corrections to the memory matrix – considering B-dependent corrections to the static susceptibilities is a higher order correction. Furthermore, within the memory matrix, any B-dependent correction to a parity even coefficient such as $M_{P_x P_x}$ must be $\mathcal{O}(B^2)$, which is second order in perturbation theory. The only matrix which may admit first order corrections within perturbation theory that are linear in B is the time-reversal non-invariant matrix N.

Let us consider the consequences of $B \neq 0$ on the matrix N, which relates to static susceptibilities. The consequences of an external magnetic field are that

$$\dot{P}_i = B\epsilon_{ij}J_i^{\text{tot}} + \cdots, \tag{5.44}$$

with \mathbf{J}^{tot} the spatially integrated momentum current, where \cdots includes effects such as momentum relaxation, that we have previously accounted for. The expression (??) represents the Lorentz force law, and follows similarly to (??), though with some subtleties. The (zero momentum component of the) canonical momentum operator $\mathcal{P}_i(\mathbf{x})$ which generates translations is no longer equivalent to the physical momentum:

$$\mathcal{P}_i = P_i + \int d^2 \mathbf{x} \, n A_{B,i}, \tag{5.45}$$

where \mathbf{A}_B is the gauge potential due to the externally imposed magnetic field. Note that only P_i is gauge invariant. In addition, the Hamiltonian is altered to $H \to H + H_B$, with

$$H_B = -\int \mathrm{d}^2 \mathbf{x} \, \mathbf{J} \cdot \mathbf{A}_B. \tag{5.46}$$

Now we evaluate \dot{P}_x using the convenient gauge choice $\mathbf{A}_B = -By\hat{\mathbf{x}}$:

$$\dot{P}_{x} = i[H_{0} + H_{B}, P_{x}] = i\left[H_{0} + H_{B}, \mathcal{P}_{x} + \int d^{2}\mathbf{x} \, nBy\right] = i[H_{B}, \mathcal{P}_{x}] + \int d^{2}\mathbf{x} \, \dot{n}By + \mathcal{O}(B^{2})$$

$$= -\int d^{2}\mathbf{x} \left(-\partial_{x}J_{x} - \dot{n}\right)By = -\int d^{2}\mathbf{x} \, \partial_{y}J_{y}By = \int d^{2}\mathbf{x} \, BJ_{y} = BJ_{y}^{\text{tot}}.$$
(5.47)

As B is a constant, this relates the total current in the y direction to \dot{P}_x , as claimed in (??). A similar argument works for \dot{P}_y , with the gauge $\mathbf{A}_B = Bx\hat{\mathbf{y}}$.

We can use (??) to find that the B dependent corrections to the matrix N, as $\chi_{\dot{P}_xA} = B\chi_{J_yA}$ for any operator A, as an example. Using this logic, we find

$$N_{P_x P_y} = -N_{P_y P_x} = \chi_{P_x \dot{P}_y} = -B\chi_{J_x P_x} = -B\mathcal{Q},$$
 (5.48a)

$$N_{\partial_x n P_y} = -N_{\partial_y n P_x} = -B\chi_{\partial_y n J_y} = -Bk_x \sigma_{\mathbf{Q}}.$$
 (5.48b)

In writing down these results we have used that $\chi_{P_x\partial_x n} = \chi_{P_y\partial_y n} = 0$, which follows from translation invariance of the thermodynamic state.

To recap: the "full memory matrix" $\mathfrak{m}(\omega)$ at this order in perturbation theory is

$$\mathfrak{m}(\omega) \equiv M(\omega) + N - i\omega\chi \approx \begin{pmatrix} k_x^2 \sigma_Q & 0 & 0 & -Bk_x \sigma_Q \\ 0 & k_x^2 \sigma_Q & Bk_x \sigma_Q & 0 \\ 0 & -Bk_x \sigma_Q & \mathcal{M}\left(\frac{1}{\tau} - i\omega\right) & -B\mathcal{Q} \\ Bk_x \sigma_Q & 0 & B\mathcal{Q} & \mathcal{M}\left(\frac{1}{\tau} - i\omega\right) \end{pmatrix}.$$
(5.49)

Along with $\chi_{J_x P_x} = \chi_{J_y P_y} = \mathcal{Q}$, $\chi_{J_x \partial_x n} = \chi_{J_y \partial_y n} = \sigma_Q k_x$, being the only non-vanishing static susceptibilities, it is straightforward to invert \mathfrak{m} and obtain the main results displayed in (??), using (??).

Dynamics of Charge, Heat and Momentum

Let us now relax the assumption that heat transport has decoupled from the problem, and compute the electrical conductivity using the memory matrix formalism. In fact, regardless of how many other long lived scalar quantities we have – governed by diffusive transport – we will see that (??) continues to hold.⁴¹ In practice, the only additional conserved quantity is heat.

Let us suppose that we have currents \mathbf{J}_R associated with long lived densities $n_R(\mathbf{x})$; the chemical poten-

⁴¹Indeed, such conserved quantities cannot at zero momentum have any overlap with the electrical current, as the latter is a vector and we have assumed rotational invariance in this paper.

tials associated to these long lived densities are μ_R ; the indices $RS\cdots$ will refer to the conserved charges, and indices $ij\cdots$ will refer to spatial indices as usual. Analogous to (??) we find

$$\mathbf{J}_R = -\Sigma_{RS} \nabla \mu_S, \tag{5.50}$$

with Σ a conductivity matrix. One finds analogously a susceptibility matrix χ_{RS} , and a diffusion matrix D_{RS} , with $\mathbf{J}_R = -D_{RS} \nabla n_S$, obeying the Einstein relation

$$\Sigma = D\chi. \tag{5.51}$$

Here we are multiplying together matrices with RS indices. These results are reviewed in [?]. The analogous Green's function to G_{nn}^{R} is

$$G_{n_R n_S}^{\mathrm{R}} = \left(k_x^2 D - \mathrm{i}\omega\right)_{RT}^{-1} k_x^2 \Sigma_{TS},\tag{5.52}$$

and so an analogous computation to before gives us

$$M_{\partial_x n_R \partial_x n_S} = k_x^2 \Sigma_{RS} \tag{5.53}$$

Let the index Q denotes the conserved charge; thus

$$\sigma_{\mathcal{Q}} \equiv \Sigma_{QQ}. \tag{5.54}$$

Denote with \mathbb{P} the projection operator onto the Q index: i.e.,

$$\sigma_{\mathcal{O}}\mathbb{P} = \mathbb{P}\Sigma\mathbb{P}.\tag{5.55}$$

m generalizes to

$$\mathfrak{m} \approx \begin{pmatrix} k_x^2 \Sigma_{RS} & 0 & 0 & -Bk_x \Sigma_{RQ} \\ 0 & k_x^2 \Sigma_{RS} & Bk_x \Sigma_{RQ} & 0 \\ 0 & -Bk_x \Sigma_{QR} & \mathcal{M}\left(\frac{1}{\tau} - i\omega\right) & -B\mathcal{Q} \\ Bk_x \Sigma_{QR} & 0 & B\mathcal{Q} & \mathcal{M}\left(\frac{1}{\tau} - i\omega\right) \end{pmatrix}.$$
 (5.56)

Our goal is to compute

$$\sigma_{J_i J_j} = \chi_{J_i A} \mathfrak{m}_{AB}^{-1} \chi_{B J_j}, \tag{5.57}$$

and to simply prove that this matrix product is independent of any additional conserved quantities. (It is straightforward to carry out the remainder of the algebra and explicitly recover the conductivities.)

A rather generic and useful result for us will be following formula from linear algebra. Suppose that we have a block matrix

$$U = \begin{pmatrix} X & Y \\ Z & W \end{pmatrix}, \tag{5.58}$$

with X an $m \times m$ matrix, Y an $m \times n$ matrix, Z an $n \times m$ matrix, and W an $n \times n$ matrix. Then

$$U^{-1} = \begin{pmatrix} (X - YW^{-1}Z)^{-1} & -X^{-1}Y(W - ZX^{-1}Y)^{-1} \\ -W^{-1}Z(X - YW^{-1}Z)^{-1} & (W - ZX^{-1}Y)^{-1} \end{pmatrix}$$

$$= \begin{pmatrix} (X - YW^{-1}Z)^{-1} & -(X - YW^{-1}Z)^{-1}YW^{-1} \\ -(W - ZX^{-1}Y)^{-1}ZX^{-1} & (W - ZX^{-1}Y)^{-1} \end{pmatrix}.$$
 (5.59)

A tedious set of calculations, repeatedly imploying the identities above, leads to the following block matrices in \mathfrak{m}^{-1} :

$$\mathfrak{m}_{P_i P_i}^{-1} = \mathcal{N} \left(B^2 \sigma_{\mathcal{Q}} + \mathcal{M}(\tau^{-1} - i\omega) \right) \delta_{ij} + \mathcal{N} B \mathcal{Q} \epsilon_{ij}, \tag{5.60a}$$

$$\mathfrak{m}_{P_i\partial_j n_R}^{-1} = \frac{B}{k_x} \delta_{RQ} \mathfrak{m}_{P_i P_k}^{-1} \epsilon_{kj}, \tag{5.60b}$$

$$\mathfrak{m}_{\partial_i n_R P_j}^{-1} = \frac{B}{k_x} \delta_{RQ} \epsilon_{ik} \mathfrak{m}_{P_k P_j}^{-1}, \tag{5.60c}$$

$$\mathfrak{m}_{\partial_{i}n_{R}\partial_{j}n_{S}}^{-1} = \frac{1}{k_{x}^{2}} \left[\left(\Sigma_{RS}^{-1} - \mathcal{N}B^{2} (\mathcal{M}(\tau^{-1} - i\omega) + B^{2}\sigma_{Q}) \mathbb{P}_{RS} \right) \delta_{ij} - \mathcal{N}B^{3} \mathcal{Q} \mathbb{P}_{RS} \epsilon_{ij} \right]. \tag{5.60d}$$

where

$$\mathcal{N} = \frac{1}{\mathcal{Q}^2 B^2 + (B^2 \sigma_0 + \mathcal{M}(\tau^{-1} - i\omega))^2}.$$
 (5.61)

To obtain (??), the following identity, along with (??), is helpful (below c is any constant):

$$(\Sigma + c\Sigma \mathbb{P}\Sigma)^{-1} = \Sigma^{-1} - \frac{c}{1 + c\sigma_0} \mathbb{P}.$$
 (5.62)

Using (??), we find the electric current - conserved density susceptibilities to be

$$\chi_{J_i \partial_i n_B} = \delta_{ij} \Sigma_{OR} k_x. \tag{5.63}$$

It is now a simple matter to see from (??) that the only component of Σ_{RS} that enters the final answer is $\Sigma_{QQ} = \sigma_{Q}$; thus the magnetohydrodynamic result for the electrical conductivity matrix, given in (??), is

unaltered by the presence of additional conserved scalar charges.

Thermal and Thermoelectric Transport

It is now clear how to extend our work to study thermoelectric transport. When describing thermoelectric transport, one must specify a set of three matrices: σ_{ij} from before, the Seebeck coefficient(s) α_{ij} , and $\bar{\kappa}_{ij}$, defined by:

$$\begin{pmatrix} J_i \\ Q_i \end{pmatrix} = \begin{pmatrix} \sigma_{ij} & \alpha_{ij} \\ T\alpha_{ij} & \bar{\kappa}_{ij} \end{pmatrix} \begin{pmatrix} E_j \\ -\partial_j T \end{pmatrix}$$

$$(5.64)$$

with Q_i the heat current. We follow the notation of [?], where $\bar{\kappa}$ is defined as the linear response coefficient between the heat current and the temperature gradient at vanishing electric field; often in experiments one measures the thermal conductivity κ_{ij} , the coefficient between the heat current and temperature gradient at vanishing electric current, $J_i = 0$. The two are related via

$$\kappa = \bar{\kappa} - T\alpha\sigma^{-1}\alpha. \tag{5.65}$$

In the memory matrix framework, we have:

$$\alpha_{ij}T = \chi_{J_iA} \mathfrak{m}_{AB}^{-1} \chi_{BQ_i}, \tag{5.66a}$$

$$\bar{\kappa}_{ij}T = \chi_{Q_iA} \mathfrak{m}_{AB}^{-1} \chi_{BQ_j}. \tag{5.66b}$$

The new susceptibilities we need relate to the heat current. Letting the index H (in the notation of Section ??) denote the diffusive scalar quantity heat, we obtain

$$\chi_{Q_i \partial_i n_R} = \delta_{ij} \Sigma_{HR} k_x. \tag{5.67}$$

There is also a new susceptibility:

$$\chi_{Q_i P_j} \equiv \delta_{ij} T \mathcal{S}. \tag{5.68}$$

This serves as a definition of the new quantity, S, which plays a role of "entropy density". Using the results of (??) thermoelectric transport coefficients may now be computed. Denoting

$$\Sigma_{HO} \equiv \alpha_{\rm o} T,$$
 (5.69a)

$$\Sigma_{HH} \equiv \bar{\kappa}_{Q} T,$$
 (5.69b)

we obtain

$$\alpha_{xx} = \alpha_{yy} = \frac{(\mathcal{M}(\tau^{-1} - i\omega) + B^2 \sigma_Q) \alpha_Q + \mathcal{S} \mathcal{Q}}{\mathcal{Q}^2 B^2 + (B^2 \sigma_Q + \mathcal{M}(\tau^{-1} - i\omega))^2} \mathcal{M}\left(\frac{1}{\tau} - i\omega\right), \tag{5.70a}$$

$$\alpha_{xy} = -\alpha_{yx} = \frac{\alpha_{Q} \mathcal{Q} \mathcal{M}(\tau^{-1} - i\omega) + \mathcal{S}(\mathcal{Q}^{2} + B^{2} \sigma_{Q}^{2} + \sigma_{Q} \mathcal{M}(\tau^{-1} - i\omega))}{\mathcal{Q}^{2} B^{2} + (B^{2} \sigma_{Q} + \mathcal{M}(\tau^{-1} - i\omega))^{2}} B,$$

$$(5.70b)$$

$$\alpha_{xy} = -\alpha_{yx} = \frac{\alpha_{Q} \mathcal{Q} \mathcal{M}(\tau^{-1} - i\omega) + \mathcal{S}(\mathcal{Q}^{2} + B^{2} \sigma_{Q}^{2} + \sigma_{Q} \mathcal{M}(\tau^{-1} - i\omega))}{\mathcal{Q}^{2} B^{2} + (B^{2} \sigma_{Q} + \mathcal{M}(\tau^{-1} - i\omega))^{2}} B,$$

$$\bar{\kappa}_{xx} = \bar{\kappa}_{yy} = \bar{\kappa}_{Q} + \frac{(B^{2} \sigma_{Q} + \mathcal{M}(\tau^{-1} - i\omega))(\mathcal{S}^{2} - B^{2} \alpha_{Q}^{2}) - 2\mathcal{S} \mathcal{Q} \alpha_{Q} B^{2}}{\mathcal{Q}^{2} B^{2} + (B^{2} \sigma_{Q} + \mathcal{M}(\tau^{-1} - i\omega))^{2}} T,$$
(5.70c)

$$\bar{\kappa}_{xy} = -\bar{\kappa}_{yx} = \frac{\mathcal{Q}\mathcal{S}^2 - B^2 \mathcal{Q}\alpha_Q^2 + 2\mathcal{S}\alpha_Q (B^2 \sigma_Q + \mathcal{M}(\tau^{-1} - i\omega))}{\mathcal{Q}^2 B^2 + (B^2 \sigma_Q + \mathcal{M}(\tau^{-1} - i\omega))^2} BT.$$
(5.70d)

Together with (??), this forms the main result of this paper, and is the most general framework for magnetotransport to date, applicable both to relativistic and non-relativistic systems.

If we specialize to a Lorentz-invariant quantum critical system deformed by a chemical potential (for charge) μ , we may compare to the results found in [?] using hydrodynamics. Using (note that we are setting the effective speed of light to be 1)

$$T\alpha_{Q} = -\mu\sigma_{Q},\tag{5.71a}$$

$$T\bar{\kappa}_{Q} = \mu^{2}\sigma_{Q},\tag{5.71b}$$

$$TS = \mathcal{M} - \mu \mathcal{Q},\tag{5.71c}$$

we find agreement with the results of [?]. On the other hand, if we set $\alpha_Q = \bar{\kappa}_Q = 0$, then these results agree with recent holographic calculations performed at $\omega = 0$ [?, ?, ?] – see also [?, ?]. This sheds light into the differences between these papers and hydrodynamics, and suggests how one might go about resolving this issue.

It can be helpful to study κ_{ij} instead of $\bar{\kappa}_{ij}$ – in the limit $B=0,\ \mathcal{Q}\neq 0,\ \tau\rightarrow \infty$, the former is not singular while the latter is (see, e.g., [?]). κ_{ij} can easily be computed using (??), given our main results (??) and (??):

$$\kappa_{xx} = \kappa_{yy} = \bar{\kappa}_{Q} + \frac{Q^{2}S^{2}\sigma_{Q} - 2SQ^{3}\alpha_{Q} - B^{2}Q^{2}\sigma_{Q}\alpha_{Q}^{2}}{Q^{2}B^{2}\sigma_{Q}^{2} + (Q^{2} + \mathcal{M}(\tau^{-1} - i\omega)\sigma_{Q})^{2}}T + \frac{\mathcal{M}(\tau^{-1} - i\omega)(\sigma_{Q}^{2}S^{2} - 2QS\alpha_{Q}\sigma_{Q} - \alpha_{Q}^{2}Q^{2}) - \sigma_{Q}\alpha_{Q}^{2}\mathcal{M}^{2}(\tau^{-1} - i\omega)^{2}}{Q^{2}B^{2}\sigma_{Q}^{2} + (Q^{2} + \mathcal{M}(\tau^{-1} - i\omega)\sigma_{Q})^{2}}T$$
(5.72a)

$$\kappa_{xy} = -\kappa_{yx} = \frac{(\alpha_{Q}Q - \sigma_{Q}S)^{2}}{Q^{2}B^{2}\sigma_{Q}^{2} + (Q^{2} + \mathcal{M}(\tau^{-1} - i\omega)\sigma_{Q})^{2}}BQT$$
(5.72b)

Indeed in the $\tau \to \infty$ limit, κ_{xx} is finite (only the first line contributes) so long as $\mathcal{Q} \neq 0$. Note that if we

first set Q = 0, then κ_{xx} does become singular when $\tau \to \infty$.

Conclusions

This paper has developed a model of electric, thermal and thermoelectric transport in strange metals which focuses on the influence of a long-lived momentum mode, along with the diffusion of charge and heat. Such a long-lived momentum mode is found in essentially all condensed matter models of non-Fermi liquids, including those obtained from lattice models appropriate for the cuprates [?, ?]. The influence of an external magnetic field on such a mode is universally determined by a few thermodynamic susceptibilities: this was established here by the memory matrix formalism, which can be applied to realistic models of the cuprates.

Our results are not valid for systems with spontaneously broken global or gauge symmetries, such as superfluids or superconductors. In this case, the Goldstone modes associated with the broken symmetry must be consistently included within hydrodynamics, so we expect that they must also be included within the memory matrix. Undertaking such task would be an interesting generalization of the present work.

The resulting B and T dependence of σ_{ij} , α_{ij} and $\bar{\kappa}_{ij}$ was then reduced to the T dependence of the momentum relaxation time τ , thermodynamic susceptibilities, and diffusive transport coefficients derived via Einstein relations: $\sigma_{\rm Q}$, $\alpha_{\rm Q}$ and $\bar{\kappa}_{\rm Q}$. An important feature of this approach is that very different physical processes control the values of τ and $\sigma_{\rm Q}$, $\alpha_{\rm Q}$ and $\bar{\kappa}_{\rm Q}$. Blake and Donos [?] argued that reasonable assumptions for the T dependence of τ and $\sigma_{\rm Q}$ (in particular, $\tau \sim 1/T^2$ and $\sigma_{\rm Q} \sim 1/T$) lead to an appealing explanation of the data on the Hall angle on the cuprates [?].

The B dependence of σ_{ij} , α_{ij} and $\bar{\kappa}_{ij}$ is explicit, as B is a perturbatively small parameter in this framework. Their and our discussions have implicitly ignored the B dependence of σ_{Q} , but this could be important for understanding experimental thermo-electric data [?, ?].

In combination with other recent studies [?, ?, ?, ?], our results now provide a route to the computation of transport properties of strange metals using microscopically realistic models.

- (i) For the theory of the onset of spin-density wave order in metals, there is a clear separation of the degrees freedom responsible for the two terms in (??). The "lukewarm" regions of the Fermi surface far from the "hot spots" contribute to the second term in (??), associated with the slow decay of the momentum mode: a computations of the values of \mathcal{Q} , \mathcal{M} , and τ in this framework was provided in Ref. [?]. In contrast, the "intrinsic" quantum critical conductivity, $\sigma_{\mathcal{Q}}$, in the first term of (??) is a property of the particle-hole symmetric hot spot theory; the scaling limit of this theory has $\mathcal{Q} = 0$, and so it provides a direct computation of $\sigma_{\mathcal{Q}}$ [?].
- (ii) The same separation between the lukewarm and hot regions of the Fermi surface applies also to the

Higgs critical theory of Ref. [?], with their respective contributions leading to the two terms in (??).

(iii) For the case of the nematic critical point in two-dimensional metals, the crucial role of the total momentum mode was discussed in Ref. [?]. The field theory of this critical point was employed to compute Q, \mathcal{M} , and τ , with weak disorder providing the source for momentum relaxation. There is not yet a complete understanding of the value of σ_Q in such models.

With these B=0 computations of \mathcal{Q} , \mathcal{M} , τ , and $\sigma_{\mathcal{Q}}$ in hand, then our present analysis shows that the extension to weak $B\neq 0$ in $(\ref{eq:proposition})$ follows immediately, and can be made on quite general grounds.

Part III

Transport in strongly disordered metals

Chapter 6

Lower bound on electrical conductivity

Below we present the original text of [?]. Reprinted with permission from S. Grozdanov, A. Lucas, S. Sachdev and K. Schalm, "Absence of disorder-driven metal-insulator transitions in simple holographic models", Physical Review Letters 115 221601 (2014). Copyright (2014) by the American Physical Society.

Introduction

Novel condensed matter systems such as graphene near half-filling [?], cold atomic gases [?], and the ever elusive strange metal phase of the high- T_c superconductors [?, ?, ?], are experimentally realizable strongly interacting many-body quantum systems. In many of these systems, macroscopic observables are governed by quantum critical physics. One such observable is the electrical conductance at finite temperature, density and disorder. Unfortunately, there are few reliable theoretical methods for such strongly coupled regimes. Some recent work has advocated the memory matrix formalism [?, ?, ?, ?], in combination with hydrodynamic insight [?]. These methods may be used directly in microscopic models [?, ?, ?]. However, this approach is perturbative in disorder, and may not be adequate for understanding non-Drude physics in strange metals [?].

The advent of gauge-gravity duality [?, ?, ?] has allowed for controlled, non-perturbative transport computations in a strongly interacting quantum system. The quantum dynamics is holographically encoded in the classical response of a black hole in an asymptotically anti-de Sitter space time in one higher dimension. These systems have large N matrix degrees of freedom, but we focus on correlators of charge currents in

To access the "strongly disordered" regime, massive gravity [?, ?, ?, ?] and other methods [?, ?, ?, ?, ?, ?, ?, ?] with similar phenomenology have been developed. See [?] for older approaches based on Dirac-Born-Infeld theory. We refer to these models as "mean-field disordered", as the geometry is completely homogeneous, despite the fact that momentum relaxes, and so microscopic translational symmetry has been broken. Holographic mean-field disordered insulators, where $\sigma(T) \sim T^p$ with p > 0, are not disorder-driven: i) σ saturates at a finite value for fixed T independent of the disorder strength (e.g. [?]); ii) insulating behavior in these models is caused by the depletion of charge carriers as $T \to 0$. Hence, this broad class of holographic approaches predicts the absence of a disorder-driven metal-insulator transition. So far, there has been no explicit confirmation of this prediction.

Our letter verifies this prediction of mean-field disordered models. In doing so, it gives an explicit example of an "incoherent metal" (but not insulator) in a disordered, isotropic system. We derive a universal lower bound on the conductivity of certain quantum field theories in two spatial dimensions, which are holographically dual to (classical) Einstein-Maxwell theory, a bulk theory with no free parameters. Our bound is independent of temperature, the average charge density and its fluctuations. The new technical developments we exploit are non-perturbative hydrodynamic methods [?] along with an exact reduction of the holographic transport problem in the Einstein-Maxwell system to a hydrodynamic linear response problem in an inhomogeneous fluid [?]. Both techniques generalize and we expect that our qualitative result ruling out disorder-driven insulators is generic and holds in more complicated holographic models.

Results

We consider classical solutions to the 3+1 dimensional Einstein-Maxwell system with a negative cosmological constant. The action of this theory is

$$S_{\text{bulk}} = \int d^4x \sqrt{-g} \left(\frac{R}{16 \ 10 \ -.18 \ \text{#G}} + \frac{6}{16 \ 10 \ -.18 \ \text{#GL}^2} - \frac{F^2}{4e^2} \right). \tag{6.1}$$

L is the AdS radius, e is the charge of the gauge field, and G is Newton's constant; $L = e = 16 - 10 - .18 \, \text{#}G = 1 \, \text{henceforth}$. Note that e is not the unit of charge in the boundary theory [?]. The bulk graviton is dual to the stress-energy tensor of the holographic dual QFT, and the gauge field is dual to a conserved U(1) (electrical) current. We consider a static background geometry [?]:

$$ds^{2} = g_{MN}dx^{M}dx^{N} = -U(r)V(r, \mathbf{x})dt^{2} + U(r)^{-1}W(r, \mathbf{x})dr^{2} + G_{ij}(r, \mathbf{x})dx_{i}dx_{j},$$

$$(6.2)$$

where $\mathbf{x} = (x, y)$ denotes the spatial directions in the boundary theory (denoted with Latin indices i, j), t the time coordinate, and r the bulk radial coordinate. This background is supported by a non-vanishing gauge field:

$$A = \Phi(r, \mathbf{x}) dt. \tag{6.3}$$

The background is not arbitrary: it obeys the Einstein-Maxwell equations of motion. We shall not need its explicit form, but we assume that it asymptotes to AdS at the boundary $r=\infty$, and that it possesses a connected black hole horizon at r=0. For such a static black hole, the Hawking temperature T of the black hole must be constant and homogeneous since it has a Killing horizon [?, ?]. This is the gravitational equivalent of the zeroth law of thermodynamics: an equilibrated system has a constant temperature. Aside from requiring regularity and constancy of T (all functions are finite at r=0, and $U\approx 4$ 10 -.18 $tTr+\ldots$), bulk fields can have arbitrarily large spatial variations. Such spatially variations are sourced by a boundary chemical potential $\phi(\mathbf{x}) = \Phi(\infty, \mathbf{x})$, whose explicit form again we shall not need. We take the spatial dimensions of the dual theory to be compact and flat, with metric 10 -.18 δ_{ij} : x and y obey periodic boundary conditions $x \sim x + L$ and $y \sim y + L$. We denote (boundary) spatial averages with $\mathbb{E}[\cdots]$: namely, $\mathbb{E}[f] = L^{-2} \int d^2\mathbf{x} f$.

The expectation value of the electrical current $\langle j^i \rangle$ in the boundary theory dual to the Einstein-Maxwell system, where $i \in \{x, y\}$, will generically be non-zero when a constant, static, external electric field E_i is applied. In the bulk, we add infinitesimal perturbations to the fields, linear in E_i . The direct current (DC) conductivity σ^{ij} is a (boundary) linear response coefficient:

$$\mathbb{E}\left[\langle j^i \rangle\right] \equiv J^i = \sigma^{ij} E_j. \tag{6.4}$$

As the boundary theory lives on flat space, there is no trouble freely raising and lowering spatial indices for boundary quantities such as σ^{ij} . In the thermodynamic limit $L \to \infty$, a disordered but on average isotropic theory with time reversal symmetry has $\sigma^{ij} = \sigma + 10$ -.18 δ^{ij} .

What we prove in this letter is that for any holographic system with the above assumptions,

$$\sigma \ge \frac{1}{e^2} = 1. \tag{6.5}$$

In the boundary theory, the conductivity σ is measured in units of q^2/\hbar , with q the U(1) charge of j^i . Furthermore, $\sigma = 1$ exactly for any uncharged black hole, even with additional bulk matter, so long as it is uncharged under the U(1) sector in (??), and no higher derivative terms in F are included. Eq. (??) is neither valid in more general Einstein-Maxwell-dilaton theories, where the F^2 term in (??) couples to the dilaton as well, nor in theories with higher derivative terms. However, if deviations from (??) are "small", as they should be in well-defined higher derivative theories, we similarly expect corrections to (??) to be "small", and that the conductivities do not vanish when small higher derivative terms are included.

Our results have been anticipated by mean-field treatments of disorder in holography. A particular example is holographic massive gravity [?], with a consistent graviton mass m added to the bulk action (??), where⁴².

$$\sigma = \frac{1}{e^2} + \frac{4 \cdot 1 \cdot 0 - .18 \, \# \mathcal{Q}_0^2}{\mathcal{S}_0 m^2},\tag{6.6}$$

where Q_0 is the homogeneous charge density of the dual theory, and S_0 is the homogeneous entropy density. This formula also obeys (??), with the bound saturated on uncharged black holes ($Q_0 = 0$). This result anticipates (??), but its reliability for all values of m is surprising. While the quantitative equivalence between massive gravity and explicitly disordered models has been shown in the limit where bulk deformations which break translation invariance are perturbatively small [?, ?, ?], it has been an open question whether or not such models are sensible in the limit of strong disorder. This letter points out that some predictions of mean-field disorder in holography are quantitatively correct. Such justification is useful for a large body of recent holographic work which relies on this approximation to model strong disorder.

A heuristic understanding of our bound follows from hydrodynamic considerations, first emphasized in [?]: if the theory thermalizes on short length scales compared to the correlation length of disorder, a theory with locally positive quantum critical conductance cannot be an insulator. The remarkable results of [?] suggest that this hydrodynamic intuition is mathematically sound in holographic models, regardless of the wavelength of disorder. This formalism, which allows us to derive (??), may be a consequence of the holographic large N limit which neglects quantum fluctuations, and has no lattice UV cutoff. Our result contrasts with conventional lattice realizations of quantum critical models, which are always insulators at strong enough disorder. In lattice models, our bound may be realized at intermediate disorder scales, and our theory may be compared in this regime with quantum Monte Carlo computations of the conductivity σ

⁴²Similar results are found using other mean field ways to model disorder in Einstein-Maxwell theory [?, ?].

[?].

Our holographic models may serve as a candidate theory for an incoherent metal with badly-broken translational symmetry [?]. Incoherent metals are proposed states whose conductivities are intrinsically bounded from below. Remarkably, our holographic models do have bounded electrical conductivity. [?] argued that the disappearance of a Drude peak in the finite frequency conductivity of some experimental systems may be evidence for such an incoherent metal. Our work demonstrates that Einstein-Maxwell systems transition from coherent metals (where momentum is long-lived and there is a sharp Drude peak in the conductivity) to incoherent metals, which remain conductors despite substantial local inhomogeneities. This defies the conventional phenomenology for strong disorder, and indicates the potential utility of our approach. To make further connection to experimentally realized bad metals, $\sigma \sim T^{-1}$ is required [?], instead of $\sigma \sim T^0$. Our explicit realization of incoherent metals serves as an important first step.

Finally, we note that finely tuned models with disconnected black hole topologies [?, ?] exist, but we do not allow for this: randomly disordered black holes appear to stay connected and have uniform temperature [?, ?]. A fragmented black hole may be a holographic many-body localized [?] state, and may evade our bound.

Technical Details

The remainder of this letter contains the proof of (??). We begin by re-interpreting physically the results of [?]. They found, following the general membrane paradigm technique of [?, ?], that if the asymptotic expansion of G_{ij} and Φ near the horizon is

$$\Phi = rS(\mathbf{x})Q(\mathbf{x}) + \cdots, \quad G_{ij} = \gamma_{ij}(\mathbf{x}) + \cdots,$$
 (6.7)

with $S(\mathbf{x}) = V(0, \mathbf{x})$, whilst a constant infinitesimal electric field E_j (note index is lowered) and its thermal analogue ζ_j (similar to to $-\partial_j \log T$) are applied to the boundary theory, then the following equations hold (we change notation from [?]):

$$\nabla_i \left(T \mathcal{S} v^i \right) = \nabla_i \left(\mathcal{Q} v^i + \sigma_{\mathcal{Q}} \left(E^i - \partial^i \mu \right) \right) = 0, \tag{6.8a}$$

$$Q(E_i - \partial_i \mu) + S(T\zeta_i - \partial_i \Theta) + 2\eta \nabla^i \nabla_{(i} v_{i)} = 0, \tag{6.8b}$$

with covariant derivatives taken with the metric γ_{ij} . The coefficients μ , Θ and v_i are interpreted as the chemical potential, temperature (difference) and velocity of an emergent horizon fluid, and may be expressed

in terms of perturbations of the bulk fields [?]; their specific forms are irrelevant for our purposes. $\eta = \sigma_Q = 1$ and S = 4 + 10-.18 $\rlap{/}{\pi}$ are constants. It is, however, helpful to not substitute these explicit values in just yet, as in the form (??) it is straightforward how to apply the formalism of [?]. Eqs. (??) encode heat and charge conservation in a fluid with a constant entropy density S, variable charge density Q, and constant isotropic quantum critical thermoelectric conductivities $\sigma_Q = 1$, $\alpha_Q = \bar{\kappa}_Q = 0$, living on a curved space with metric γ_{ij} . Eq. (??) is the analogue of the Navier-Stokes equation for an isotropic, relativistic fluid with shear viscosity η (the value of bulk viscosity is not important, due to incompressibility (??)).

Consider now the spatial average of the currents associated with this horizon fluid:

$$J^{i} = \mathbb{E}\left[\sqrt{\gamma}Qv^{i} + \sigma_{Q}\sqrt{\gamma}\gamma^{ij}\left(E_{i} - \partial_{i}\mu\right)\right],\tag{6.9a}$$

$$Q^{i} = \mathbb{E}\left[\sqrt{\gamma}T\mathcal{S}v^{i}\right]. \tag{6.9b}$$

The Einstein-Maxwell equations imply that these spatial averages are independent of the holographic radial direction and that they encode the spatially averaged charge and heat currents of the boundary theory. We can therefore compute transport coefficients in the disordered boundary theory by solving a linear response problem in the disordered horizon fluid for the electrical current J^i and heat current Q^i as a function of E_i and ζ_i .

The holographic DC transport problem has thus reduced to a hydrodynamic computation in the framework of [?] (after a straightforward generalization to curved space). One direct consequence of hydrodynamics is Onsager reciprocity: the thermoelectric conductivity matrix is symmetric. This is distinct from positive-definiteness, which was shown in [?].

We first compute the conductivity of uncharged black holes, where Q = 0. Generically, this will only occur when A = 0 in the background solution. In this case charge and heat transport decouple and (??) simplifies to

$$\partial_i \left(\sqrt{\gamma} \gamma^{ij} \left(E_j - \partial_j \mu \right) \right) = 0, \tag{6.10}$$

with $\Theta = v^i = 0$ consistently set to vanish. (??) has a unique solution for μ , up to an unimportant constant, and is also unchanged by additional bulk matter so long as it does not couple to the Maxwell term in (??).

As (??) is linear, we may write $\mu = \mu^j E_j$. It follows that for some constants ψ_i^j and a (periodic) function Ψ^i :

$$\sqrt{\gamma}\gamma^{ij} \left(1 \ 0 \ -.18 \ \delta^k_j - \partial_j \mu^k \right) = \epsilon^{ij} \left(\psi^k_j - \partial_j \Psi^k \right) \tag{6.11}$$

with $\epsilon^{xy}=-\epsilon^{yx}=1,\,\epsilon^{xx}=\epsilon^{yy}=0.$ (??) is equivalent to

$$-\epsilon^{ij} \left(1 \ 0 \ -.18 \ \delta^k_j - \partial_j \mu^k \right) = \sqrt{\gamma} \gamma^{ij} \left(\psi^k_j - \partial_j \Psi^k \right), \tag{6.12}$$

and taking another spatial derivative:

$$\partial_i \left(\sqrt{\gamma} \gamma^{ij} \left(\psi_i^k - \partial_i \Psi^k \right) \right) = 0. \tag{6.13}$$

Uniqueness and linearity fix

$$\partial_i \Psi^k = \psi_i^k \partial_i \mu^j. \tag{6.14}$$

Combining (??) and (??), we find

$$\sqrt{\gamma}\gamma^{ij} \left(1 \ 0 \ \text{-.}18 \ \delta^k_j - \partial_j \mu^k \right) = -\epsilon^{ij} \left(1 \ 0 \ \text{-.}18 \ \delta^m_j - \partial_j \mu^m \right) \left(\psi^{-1} \right)_m^k. \tag{6.15}$$

Contracting with E_k and integrating over the torus, the left hand side equals J^i . Using (??), we find

$$\epsilon^{ik}\psi_k^j = \sigma^{ij}. ag{6.16}$$

Eqs. (??) and (??) are only consistent if

$$\det(\sigma^{ij}) = 1. \tag{6.17}$$

This holds for any theory, regardless of the assumption of isotropy. But if we further assume isotropy, we conclude

$$\sigma = 1. \tag{6.18}$$

This confirms that the lower bound of (??) is satisfied whenever the black hole is uncharged.

Eq. (??) is reminiscent of a known result that random resistors arranged on a square lattice, with the logarithmic resistances symmetrically distributed around 0, have an exact conductivity of 1 in the thermodynamic limit [?]. If we suppose for simplicity that $\gamma_{xy} = 0$, then a discretized approximation to the diffusion equation (??) would consist of resistors on a square lattice of resistance $R = \sqrt{\gamma_{yy}/\gamma_{xx}}$ when oriented in the x-direction, and resistors of resistance $R = \sqrt{\gamma_{xx}/\gamma_{yy}}$ when oriented in the y-direction. In a theory which is on average isotropic, it is clear that $\log R$ is symmetrically distributed around 0, for every resistor. This gives a heuristic justification for (??). Such exact results for resistor networks are rare. Likewise, we do not expect the generalization of (??) to higher dimensional uncharged black holes to exactly

match the non-perturbative prediction of massive gravity.

Bulk Maxwell self-duality [?] provides further physical insight into (??). Define a bulk dual Maxwell tensor

$$\mathcal{F}^{MN} = -\frac{1}{2}\varepsilon^{MNPQ}F_{PQ},\tag{6.19}$$

with $\varepsilon^{rtxy} = 1/\sqrt{-g}$. Note that:

$$\mathcal{F}^{rj} = \frac{1}{\sqrt{-g}} \epsilon^{ji} F_{ti} \tag{6.20}$$

and that as $r \to \infty$, (??) implies that (from the dual Maxwell tensor) there is a constant dual current density $\mathcal{I}^i = \epsilon^{ij} E_j$ in the boundary theory. $\nabla_M F^{Mi} = 0$, whose spatial average leads to $\partial_r J^i = 0$, is the Bianchi identity for \mathcal{F} , and implies $\partial_r \mathbb{E}[\mathcal{F}_{it}] = 0$. Using \mathcal{F} at r = 0,⁴³

$$\mathbb{E}[\mathcal{F}_{it}] \equiv \mathcal{E}^i = \epsilon^{ij} J^j. \tag{6.21}$$

The spatially averaged dual electric field \mathcal{E}_i is independent of bulk radius and may be evaluated at the horizon. Denoting with \mathfrak{r} the dual resistivity tensor, we conclude that $\mathcal{E}^i = \mathfrak{r}^{ij}\mathcal{I}^j$. Relating \mathcal{E} and \mathcal{I} to \mathcal{E} and \mathcal{I} leads to

$$J^{i} = -\epsilon^{ij} \mathfrak{r}^{jk} \epsilon^{kl} E^{l}. \tag{6.22}$$

If we assume that the disordered boundary theory is particle-vortex dual, then we expect $\mathfrak{r}^{-1} = \sigma$. This assumption, along with (??), leads to (??). Theories with holographic duals with bulk Maxwell electromagnetism thus appear to have remnants of particle-vortex duality even when translational symmetry is strongly broken.

We now prove the bound (??) for charged black holes using a variational technique from [?]. In our holographic model, the following inequalities are satisfied:

$$\frac{\bar{\mathcal{J}}^2}{\sigma} \leq \frac{\bar{\mathcal{J}}^2 T \bar{\kappa}}{T \sigma \bar{\kappa} - T^2 \alpha^2} \leq \mathbb{E} \left[2 \nabla^{(i} \mathcal{V}^{j)} \nabla_{(i} \mathcal{V}_{j)} \sqrt{\gamma} + \left(\mathcal{J}^i - \mathcal{Q} \mathcal{V}^i \right) \left(\mathcal{J}_i - \mathcal{Q} \mathcal{V}_i \right) \sqrt{\gamma} \right],$$
(6.23)

with $\bar{\kappa}$ the thermal conductivity when $E_i = 0$, α the Seebeck coefficient, both assumed to be isotropic, and \mathcal{J}^i and \mathcal{V}^i arbitrary vector fields such that

$$\nabla_i \mathcal{V}^i = \nabla_i \mathcal{J}^i = 0, \tag{6.24}$$

 $^{^{43}}$ Recall that for the boundary theory quantities referenced below, indices may be raised and lowered freely with 10-.18 δ_i^j .

$$\bar{\mathcal{J}}^i = \mathbb{E}\left[\sqrt{\gamma}\mathcal{J}^i\right], \qquad \mathbb{E}\left[\sqrt{\gamma}\mathcal{V}^i\right] = 0.$$
 (6.25)

Note that $\bar{\mathcal{J}}^i$ is the averaged current measured in the boundary theory on our trial current \mathcal{J}^i , and so the index in $\bar{\mathcal{J}}^i$ is raised and lowered with 10-.18 δ_{ij} . The second inequality in (??) is satisfied only by the exact solutions of the equations of motion, when

$$\mathcal{V}^i = v^i, \qquad \mathcal{J}^i = \mathcal{Q}v^i + E^i - \partial^i \mu. \tag{6.26}$$

Furthermore, the last constraint in (??) ensures there is no net heat flow [?].

The inequality (??) follows from studying the power that would be dissipated if we tried to force electrical current \mathcal{J}^i , and velocity \mathcal{V}^i , through the fluid. The fact that the dissipated power is minimized by the true solution to the equations of motion is analogous to the fact that the power dissipated in a resistor network, allowing arbitrary current flows through each resistor, up to current conservation, is minimized on the true solution where both of Kirchoff's Laws are obeyed [?].

For any charged black hole, we may set $\mathcal{V}^i = 0$, which trivially satisfies our constraints. For \mathcal{J}^i , we choose

$$\mathcal{J}^i = E^i - \partial^i \tilde{\mu} \equiv \tilde{\mathcal{J}}^i, \tag{6.27}$$

where $\tilde{\mu}$ is the exact solution to the diffusion equation (??), using the metric γ_{ij} of the charged black hole. $\tilde{\mathcal{J}}^i$ is the exact electric current that would flow upon application of the electric field, if we remove all charge density from the horizon fluid, but keep the same γ_{ij} . If $\tilde{\mathcal{J}}^i$ is normalized by (??),

$$\bar{\mathcal{J}}^2 = \mathbb{E}\left[\sqrt{\gamma}\tilde{\mathcal{J}}^i\tilde{\mathcal{J}}_i\right]. \tag{6.28}$$

To derive this result, we use that $\alpha = 0$ for an uncharged black hole, along with (??) and the fact that the bound (??) is saturated on the true electrical current for the uncharged black hole, which is $\tilde{\mathcal{J}}^i$, along with $\mathcal{V}^i = 0$. The ansatz $\mathcal{J}^i = \tilde{\mathcal{J}}^i$ and $\mathcal{V}^i = 0$ is no longer the true solution when $\mathcal{Q} \neq 0$, but we may still use it as a variational ansatz; however, in this case, we expect $\alpha \neq 0$, and that each inequality in (??) is strict. Using (??) in (??), we obtain our main result, (??).

Chapter 7

Lower bound on thermal conductivity

Below we present the original text of [?]. Reprinted with permission from S. Grozdanov, A. Lucas and K. Schalm, "Incoherent thermal transport from dirty black holes", Physical Review **D93** 061901 (2016). Copyright (2016) by the American Physical Society.

Introduction

One of the most dramatic and unique consequences of quantum mechanics is the localization of electronic wave functions in disordered systems [?], which leads to exponentially suppressed thermal (and electrical) conductivity in non-interacting theories at finite temperature [?]. In recent years, there has been an intense effort to study whether localization extends to interacting theories [?]. Under many circumstances, at least in one spatial dimension [?, ?, ?], this has been shown to be the case, and the resulting phase is coined many-body localization. It is of great interest to understand whether this phenomenon persists in strongly interacting quantum systems in higher dimensions.

One of the only analytical techniques to study higher dimensional strongly coupled systems is gauge-gravity duality [?, ?, ?]. In particular, finite temperature computations become tractable. In the past few years, numerous holographic models with heuristic "mean field" approximations to disorder have conjectured (perhaps inadvertently) that the simplest holographic models are thermal conductors at all disorder strengths, in two or more spatial dimensions [?, ?, ?, ?]. Such models correctly approximate weak disorder [?, ?, ?], as the theories are in a hydrodynamic regime. Numerical work on holographic thermal transport [?, ?, ?] has also been performed by explicitly constructing disordered black holes [?, ?]. What remains an open question is whether mean field results are also sensible when disorder is strong.

Recently, the tools to analytically address this problem have been developed. Firstly, the computation of

thermal DC conductivity has been reduced to a hydrodynamics problem for an "artificial" fluid on the black hole horizon [?, ?]. Secondly, a general hydrodynamic framework has been developed which can provide non-perturbative bounds on transport coefficients [?]. Recently, these formalisms have been combined to prove that the DC electrical conductivity of Einstein-Maxwell holographic models in two spatial (boundary) dimensions is strictly finite [?], so long as the black hole horizon is connected. The goal of this letter is to obtain similar results for the thermal conductivity of disordered Einstein-Maxwell-dilaton (EMD) holographic models.

Results

We bound the thermal conductivity κ of a relativistic (at high energies) theory dual to a disordered black hole in EMD gravity in d+2 spacetime dimensions, for d=1,2. These holographic models are dual to field theories at finite density and temperature, deformed by a charge-neutral relevant scalar operator. The dual theory is sourced by arbitrarily strong disorder, so long as in the bulk, the horizon remains connected. Assuming isotropy on long length scales, κ is defined as

$$\kappa \equiv -\frac{Q_x}{\partial_x T}\bigg|_{J_x=0},\tag{7.1}$$

where Q_x is the heat current, J_x is the charge current, and $-\partial_x T$ is an externally imposed uniform temperature gradient. Note that κ is positive by the second law of thermodynamics, has (relativistic) mass dimension $[\kappa] = [M]^{d-1}$, and that it is defined under the boundary condition that no average electric current flows. The boundary theory is at a uniform temperature T.

Analytically computing bounds on κ , in d=1 we find

$$\kappa \ge 16 \ 10 - .18 \, t^3 \left(\frac{1}{1 - \frac{1}{2} V_{\min}} \right) \frac{T}{s} \times \frac{k_{\rm B}^2}{\hbar} \left(N^2 \right)^2, \tag{7.2}$$

where s is the (spatially averaged) entropy density in the boundary theory, N^2 is a large prefactor due to the many degrees of freedom in holographic models, and V_{\min} denotes the global minimum of the dilaton potential; note that $V_{\min} \leq 0$ by construction. In d=2 we find

$$\frac{\kappa}{T} \ge \frac{4 \cdot 1 \cdot 0 - .18 \, t^2}{3} \left(\frac{1}{1 - \frac{1}{6} V_{\min}} \right) \times \frac{k_{\rm B}^2}{\hbar} N^2. \tag{7.3}$$

Hence, if the dilaton potential is bounded from below, the (relativistically) dimensionless number κ/T is strictly finite. Such sharp exact results for κ have never before been obtained in higher dimensions in a

theory where (generic) disorder and interactions are both treated non-perturbatively at finite temperature and density. Henceforth, we work in units where $\hbar = k_{\rm B} = c = 1$.

Let us briefly compare (??) with our previous result [?] showing that in d=2, σ is strictly finite in Einstein-Maxwell models. The bound on σ derived in [?] relies entirely on curious properties of holographic "horizon fluids" governing transport, but not on details of the near-horizon geometry! Crudely speaking, the horizon fluid is always a local conductor, and so is necessarily a global conductor, as is the dual theory. No such local bound exists for κ ; the bulk Einstein's equations play an essential role in enforcing the bound (??). For this reason, it is much more subtle. It is also more powerful: while in general EMD models $\sigma(T) \sim T^p$ can be either metallic (p < 0) or insulating (p > 0) [?, ?, ?, ?], we show that many EMD models are never better thermal insulators than naive dimensional analysis predicts. Many models with IR hyperscaling-violating exponent $\theta \geq 0$ have $V_{\min} > -\infty$ [?]; for these models (??) is non-trivial.

Our result (??) in d=2 is reminiscent of the proposal for "incoherent" metallic transport presented in [?], whereby a metal with badly broken translational invariance may remain a conductor of thermal (and electric) currents. The incoherent metal was proposed as a conceptual framework to understand how a strongly interacting system, such as the strange metal phase of the high- T_c superconductors [?], remains a conductor even when disorder is strong enough to destroy the Drude peak. In an incoherent metal, transport is diffusion-limited, and remains finite even with strong disorder. This phenomenon is challenging to realize using traditional condensed matter approaches, as interaction strength and disorder strength cannot both be treated non-perturbatively. Mean field holographic approaches have recovered incoherent thermal transport before [?]. Our results demonstrate that generic disordered holographic models can realize incoherent thermal transport.

Evidence for hydrodynamic electronic flow in a strongly coupled metal has emerged in experiments on clean graphene [?, ?]. However, this hydrodynamic behavior is limited by disorder in real systems, and the possibility for holography to capture transport physics beyond the hydrodynamic limit of [?] is intriguing. Our qualitative bound $\kappa/T \gtrsim$ constant in d=2 may therefore be relevant to "messier" materials. It also is interesting to extend these ideas to transport at finite frequency and magnetic field [?, ?, ?, ?, ?, ?, ?, ?, ?, ?].

Returning to our opening question of whether holographic models may realize a many-body localized state, our work rules this out under a broad set of circumstances: κ/T is bounded, regardless of disorder strength, and not vanishing with increasing disorder. Indeed, it appears likely that the only possible holographic model of localization contains black holes with horizons of disconnected topologies. Although some progress has been made in this direction [?, ?, ?], this phenomenon has not been shown to be generic, nor are the properties of such holographic models well understood. Hence, further analyses and constructions of such fragmented black holes remain an interesting and important direction for future work.

Dirty Black Holes

We now present the details of our derivation of the bounds (??) and (??) on the thermal conductivity κ . We will consider a family of theories dual to EMD holographic models, for which the Lagrangian is

$$\mathcal{L} = R - 2\Lambda - \frac{1}{2}(\partial\Phi)^2 - \frac{V(\Phi)}{\ell^2} - \frac{Z(\Phi)F^2}{4e^2},$$
(7.4)

with $\Lambda = -d(d+1)/2\ell^2$ a negative cosmological constant. Here Φ is the scalar dilaton and F is the Maxwell tensor for a U(1) gauge field. The prefactor N^2 defined previously is $N^2 = \ell^2/16 - 10 - .18 \, \text{π} G_{\rm N}$. We assume $Z(\Phi = 0) = 1$ and $V(\Phi = 0) = 0$; $V_{\rm min}$ as defined previously is $V_{\rm min} = \min_{\Phi}(V(\Phi))$, which is assumed to be finite, i.e. the dilaton potential is everywhere bounded from below. We have set 16 - 10 - .18 $\text{$\pi$} G_{\rm N} = 1$, and will also set $e = \ell = 1$ henceforth ⁴⁴.

It is most convenient to consider static background black hole geometries in Gaussian normal coordinates:

$$ds^2 = -f(r, \mathbf{x})^2 dt^2 + dr^2 + G_{ij}(r, \mathbf{x}) dx^i dx^j,$$

$$(7.5)$$

with a connected black hole horizon at r = 0 ⁴⁵. The coordinate r denotes the holographic radial direction (r increases towards the boundary, which we take to be asymptotically AdS), and (t, \mathbf{x}) are boundary theory directions. The (uniform) temperature of the black hole horizon is T, which is also the temperature of the dual field theory. This follows from the zeroth law of black hole thermodynamics and is true for any amount of disorder. Assuming a smooth horizon, we can constrain the near-horizon expansion of f and G (see e.g. [?]):

$$f(r, \mathbf{x}) = 2 \cdot 1 \cdot 0 - .18 \, \text{t} Tr + \frac{F(\mathbf{x})}{6} r^3 + \cdots,$$
 (7.6a)

$$G_{ij}(r, \mathbf{x}) = \gamma_{ij}(\mathbf{x}) + \frac{h_{ij}(\mathbf{x})}{2}r^2 + \cdots$$
(7.6b)

A d-dimensional diffeomorphism symmetry $x_i \to X_i(x_j)$ is still remaining, and we may use this to our advantage. The dilaton admits the near-horizon expansion

$$\Phi(r, \mathbf{x}) = \phi(\mathbf{x}) + \dots \tag{7.7}$$

⁴⁴Note that $\ell^2/16$ 10-.18 $\pi G_N = N^2$, but since N^2 only enters the computation as an overall prefactor in κ , it is not necessary to keep track of it explicitly.

⁴⁵To obtain the near-horizon Gaussian normal coordinates from the coordinates $(t, \tilde{r}, \tilde{\mathbf{x}})$ that were used in [?, ?, ?], we write $\tilde{r} = \Gamma_0(\mathbf{x})r^2 + \Gamma_1(\mathbf{x})r^3 + \mathcal{O}\left(r^4\right)$, $\tilde{x}^i = x^i + \Omega_0^i(\mathbf{x})r^2 + \mathcal{O}\left(r^3\right)$ and appropriately adjust the functions $\Gamma_n(\mathbf{x})$ and $\Omega_n^i(\mathbf{x})$. Importantly, this process does not alter γ_{ij} or ϕ , nor the leading order behavior in A_t up to a simple rescaling.

and the Maxwell field

Although our choice of radial coordinate is a bit different than what is used in [?], since this metric obeys all general constraints demanded in their paper, we may still use their results in our new coordinate system. We assume our boundary theory and black hole horizon have topology T^d , and so we can introduce normalized spatial averaging over the horizon, which we denote by

$$\mathbb{E}[\circ] = \frac{1}{L^d} \int d^d \mathbf{x} \circ . \tag{7.9}$$

In the above definition, we have not included a factor of the induced horizon metric. This convention follows [?]. The boundary spatial torus has a length L in each direction, and spatial metric 1 0 -.18 δ_{ij} , for simplicity.

The requirement that the Ricci scalar curvature of the induced horizon metric be non-singular implies that the extrinsic curvature of the horizon must vanish. As a result, the horizon is the hypersurface (at constant t) with minimal area A_{hor} (see e.g. [?]). In our setup, the black hole horizon is a d-dimensional hypersurface of topology T^d on a fixed time slice. Let us now consider the hypersurface of points lying along the curve $r = \varepsilon R(\mathbf{x})$, with $R(\mathbf{x}) \geq 0$ and ε an infinitesimally small positive number. This hypersurface thus lies just outside of the horizon for all \mathbf{x} and must as a consequence of our above discussion obey

$$A_{\text{hor}} \le A_R. \tag{7.10}$$

When ε is small, the area A_R is

$$A_R \approx \int d^d \mathbf{x} \sqrt{\det\left(\gamma_{ij} + \frac{\varepsilon^2}{2} h_{ij} R^2 + \varepsilon^2 \partial_i R \, \partial_j R\right)}.$$
 (7.11)

Note that A_{hor} is obtained by setting R = 0. Expanding (??) to leading order in ε and using (??) gives

$$0 \le \mathbb{E}\left[\sqrt{\gamma} \left(\gamma^{ij} \partial_i R \,\partial_j R + \frac{\gamma^{ij} h_{ij}}{2} R^2\right)\right],\tag{7.12}$$

which should hold for all possible choices of $R(\mathbf{x}) \geq 0$. The inequality in Eq. (??) allows us to place non-trivial constraints on the possible h_{ij} , and will play a crucial role in finding bounds on κ .

One Dimension

We begin by considering boundary theories with one spatial dimension, where it has recently been shown [?] that given any EMD theory (??):⁴⁶

$$\kappa = \frac{16\pi^2 T}{\mathbb{E}\left[\gamma^{-1/2}(\partial_x \phi)^2 + \gamma^{1/2} Z(\phi) Q^2\right]}.$$
(7.13)

In this case, the Gaussian normal coordinates used in (??), (??) and (??) prove to be particularly convenient. By using the leading order coefficients of the tt component of Einstein's equations near the horizon, we find the following:

$$\mathbb{E}\left[\frac{(\partial_x \phi)^2}{\sqrt{\gamma}} + \sqrt{\gamma} Z(\phi) \mathcal{Q}^2\right]$$

$$= \mathbb{E}\left[4\sqrt{\gamma} - \frac{2h_{xx}}{\sqrt{\gamma}} - 2\sqrt{\gamma} V(\phi)\right].$$
(7.14)

By substituting the ansatz R = 1 into the bound (??), we find

$$\mathbb{E}\left[\frac{h_{xx}}{\sqrt{\gamma}}\right] \ge 0. \tag{7.15}$$

Using $s = 4 + 1 + 0 - .18 \, \text{t}\mathbb{E}[\sqrt{\gamma}]$ and $V \geq V_{\min}$ directly implies (??).

Two Dimensions

Let us now consider the thermal conductivity of a disordered black hole in EMD gravity when d = 2. We assume the black hole geometry is isotropic (in the boundary spatial directions) on thermodynamically large length scales. Following [?, ?], it is straightforward to derive a variational bound on the thermal conductivity. [?] showed that the DC transport coefficients may be computed as follows: solve the following equations

$$\nabla_i \mathcal{I}^i = \nabla_i \mathcal{J}^i = 0, \tag{7.16a}$$

$$\mathcal{I}_{i} = Z(\phi) (E_{i} - \nabla_{i}\mu) + (4 \ 1 \ 0 - .18 \ \text{t}T)^{-1} Z(\phi) \mathcal{Q} \mathcal{J}_{i}, \tag{7.16b}$$

$$Z(\phi)Q(\nabla_i\mu - E_i) + 4 \quad 1 \quad 0 \quad -.18 \quad \pi(\nabla_i\Theta - T\zeta_i) =$$

$$(4\pi T)^{-1} \left[2\nabla^j \nabla_{(j} \mathcal{J}_{i)} - \mathcal{J}^j \nabla_j \phi \nabla_i \phi \right], \tag{7.16c}$$

⁴⁶In this formula, and in (??), we have already transformed the expression to our coordinate system.

where ϕ and \mathcal{Q} are the horizon data defined previously, covariant derivatives are taken with respect to the induced horizon metric γ_{ij} , μ and Θ are scalar functions and E_i and ζ_i are an applied electric field and thermal "drive" (ζ_i is analogous to $-\partial_i \log T$) in the boundary theory. The spatially averaged boundary charge and heat currents are

$$J_{\text{charge}}^{i} = \mathbb{E}[\sqrt{\gamma}\mathcal{I}^{i}], \qquad J_{\text{heat}}^{i} = \mathbb{E}[\sqrt{\gamma}\mathcal{J}^{i}]. \tag{7.17}$$

The Joule heating in the boundary theory is given by

$$\mathcal{P} = E_{i} J_{\text{charge}}^{i} + \zeta_{i} J_{\text{heat}}^{i} = \frac{1}{16 \cdot 1 \cdot 0 \cdot .18 \, \pi^{2} T^{2}} \mathbb{E} \left[2 \sqrt{\gamma} \nabla^{(i} \mathcal{J}^{j)} \nabla_{(i} \mathcal{J}_{j)} + \sqrt{\gamma} \left(\mathcal{J}^{i} \nabla_{i} \phi \right)^{2} + \sqrt{\gamma} Z(\phi) \left(\mathcal{Q} \mathcal{J}_{i} - \frac{4 \cdot 1 \cdot 0 \cdot .18 \, \pi T}{Z(\phi)} \mathcal{I}_{i} \right) \left(\mathcal{Q} \mathcal{J}^{i} - \frac{4 \cdot 1 \cdot 0 \cdot .18 \, \pi T}{Z(\phi)} \mathcal{I}^{i} \right) \right],$$

$$(7.18)$$

as is simple to check by integrating each term in the above expression by parts, and employing (??) and (??).

We now think of \mathcal{P} as a functional of arbitrary currents \mathcal{I}^i and \mathcal{J}^i which are conserved. If $\overline{\mathcal{I}}$ and $\overline{\mathcal{J}}$ are the currents that solve (??) for fixed J_{charge} and J_{heat} , then writing an arbitrary current as $\mathcal{I} = \overline{\mathcal{I}} + \tilde{\mathcal{I}}$ and $\mathcal{J} = \overline{\mathcal{J}} + \tilde{\mathcal{J}}$ we find that (using that $\overline{\mathcal{I}}$ and $\overline{\mathcal{J}}$ obey (??))

$$\mathcal{P}\left[\mathcal{I},\mathcal{J}\right] = \mathcal{P}\left[\overline{\mathcal{I}},\overline{\mathcal{J}}\right] + \mathcal{P}\left[\tilde{\mathcal{I}},\tilde{\mathcal{J}}\right] + \mathbb{E}\left[2\sqrt{\gamma}\left(E_{i}\tilde{\mathcal{I}}^{i} + \zeta_{i}\tilde{\mathcal{J}}^{i}\right)\right]. \tag{7.19}$$

The last term vanishes if we fix normalization (??). As (??) is positive definite, we conclude that $\mathcal{P} \geq \mathcal{P}[\overline{\mathcal{I}}, \overline{\mathcal{J}}]$. Furthermore, the power dissipated in the absence of electric current is $J_{\text{heat}}^2/T\kappa$. Hence, if \mathcal{I} and \mathcal{J} are trial currents which are conserved and normalized to $J_{\text{heat}} = 1$ and $J_{\text{charge}} = 0$, we may employ (??) to find an upper bound on $1/\kappa$. A simple guess for \mathcal{I} and \mathcal{J} is

$$\mathcal{I}^i = 0, \qquad \qquad \mathcal{J}^i = \frac{1}{\sqrt{\gamma}} \ 1 \ 0 - .18 \ \delta_x^i. \tag{7.20}$$

It is helpful to use the residual diffeomorphism invariance to fix

$$\gamma_{ij} = 10 - .18 \, \delta_{ij} e^{\omega(\mathbf{x})}.$$
 (7.21)

Because of the emergent isotropy of our model, this diffeomorphism should not change the length of the spatial torus in either direction in the thermodynamic limit (we may add a constant to ω to achieve this).

Combining our variational ansatz (??) with the induced horizon metric choice (??), we obtain the bound

$$\frac{T}{\kappa} \leq \frac{1}{16 \cdot 1 \cdot 0 - .18 \, \pi^2} \, \mathbb{E} \left[e^{-\omega} \left((\partial_x \omega)^2 + (\partial_y \omega)^2 + (\partial_x \phi)^2 \right) + Z(\phi) \mathcal{Q}^2 \right]
= \frac{1}{16 \cdot 1 \cdot 0 - .18 \, \pi^2} \, \mathbb{E} \left[-R_2 + e^{-\omega} (\partial_x \phi)^2 + Z(\phi) \mathcal{Q}^2 \right],$$
(7.22)

where R_2 is the induced Ricci scalar on the horizon:

$$R_2 = -e^{-\omega} \left(\partial_x^2 \omega + \partial_y^2 \omega \right). \tag{7.23}$$

We now derive an upper bound on $\mathbb{E}[R_2]$. The four dimensional Ricci scalar R_4 in the bulk is given by

$$R_4 = -12 + \frac{1}{2}(\partial \Phi)^2 + 2V(\Phi), \tag{7.24}$$

for any solution of the Einstein's equations that follow from the Lagrangian (??). General arguments [?] about geometries near black hole horizons, independent of the equations of motion, then allow us to relate R_4 to R_2 . At the horizon, i.e. at r = 0,

$$R_4 = R_2 - \frac{F}{10 - .18 \, \text{t}T} - 2e^{-\omega} (h_{xx} + h_{yy}). \tag{7.25}$$

Einstein's equations at leading order in the near-horizon expansion then force

$$\frac{F}{1 \cdot 0 - .18 \, \text{t}T} = 6 + \frac{Z(\phi)\mathcal{Q}^2}{2} - e^{-\omega} (h_{xx} + h_{yy}) - V(\phi). \tag{7.26}$$

Combining (??), (??) and (??) at r = 0, we obtain

$$R_2 = -6 + e^{-\omega} (h_{xx} + h_{yy}) + \frac{Z(\phi)Q^2}{2} + \frac{(\partial \phi)^2}{2} + V(\phi).$$
 (7.27)

Next, we plug the ansatz $R(\mathbf{x}) = e^{-\omega(\mathbf{x})/2}$ into (??), which gives us the inequality

$$0 \le \mathbb{E}\left[e^{-\omega}\left(\frac{1}{2}\left(\partial_x\omega\right)^2 + \frac{1}{2}\left(\partial_y\omega\right)^2 + h_{xx} + h_{yy}\right)\right]. \tag{7.28}$$

Recognizing R_2 from Eq. (??) after partial integration inside (??), we find

$$\mathbb{E}\left[R_2\right] \le 2\,\mathbb{E}\left[e^{-\omega}(h_{xx} + h_{yy})\right]. \tag{7.29}$$

Combining (??) and (??), along with $V \geq V_{\min}$, we obtain

$$\mathbb{E}\left[e^{-\omega}(\partial_x \phi)^2 + Z(\phi)Q^2 - R_2\right] \le \mathbb{E}\left[(\partial\phi)^2 + Z(\phi)Q^2 - R_2\right] \le 12 - 2V_{\min},\tag{7.30}$$

which can be used in (??) to establish (??). In both d=1 and d=2, we may replace V_{\min} by $\mathbb{E}[V(\phi)]$, if we are able to compute this quantity. In particular, even if $V(\Phi \to \pm \infty)$ is unbounded, κ is finite so long as ϕ is finite everywhere at finite T. There can be no analogue of many-body localization if $V(\phi)$ is finite on the horizon.

A simple extension of the model we have studied so far in this paper includes n > 1 scalar fields Φ^a in d = 2,

$$\mathcal{L} = R - 2\Lambda - \sum_{a=1}^{n} \frac{(\partial \Phi^{a})^{2}}{2} - V(\Phi^{a}) - \frac{Z(\Phi^{a})F^{2}}{4}.$$
 (7.31)

The bounds for the theory in (??) are still (??) and (??).

Mean Field Models

Let us now compare our exact results with the predictions of "mean field" models of disorder in holography. A simple model in d=2 consists of n=2 copies of the same scalar field, with Lagrangian (??), but with V=0 and Z=1 [?, ?]. Choosing the scalar fields to be $\Phi^i=mx^i$, one finds [?]

$$\kappa = \frac{4 \cdot 1 \cdot 0 - .18 \, \text{t/s}T}{m^2 + \mu^2},\tag{7.32}$$

where s is the entropy density and μ is the chemical potential. In order for the temperature of the dual theory to be non-negative,

$$2m^2 + \mu^2 \le \frac{3}{1.0 - .18 \, \pi} s. \tag{7.33}$$

As it must, our bound (??) is obeyed, as

$$\kappa \ge \frac{4 \cdot 1 \cdot 0 - .18 \, \dot{\pi}^2 T}{3} \frac{2m^2 + \mu^2}{m^2 + \mu^2} \ge \frac{4 \cdot 1 \cdot 0 - .18 \, \dot{\pi}^2 T}{3} \tag{7.34}$$

The fact that mean field models capture the correct behavior of κ in explicitly disordered models is a pleasing surprise to us.

Part IV

Hydrodynamics in graphene

Chapter 8

Observation of the Dirac fluid

Below we present the original text of [?]. Reprinted with permission from AAAS.

Understanding the dynamics of many interacting particles is a formidable task in physics, complicated by many coupled degrees of freedom. For electronic transport in matter, strong interactions can lead to a breakdown of the Fermi liquid (FL) paradigm of coherent quasiparticles scattering off of impurities. In such situations, the complex microscopic dynamics can be coarse-grained to a hydrodynamic description of momentum, energy, and charge transport on long length and time scales [?]. Hydrodynamics has been successfully applied to a diverse array of interacting quantum systems, from high mobility electrons in conductors [?], to cold atoms [?] and quark-gluon plasmas [?]. As has been argued for strongly interacting massless Dirac fermions in graphene at the charge-neutrality point (CNP) [?, ?, ?, ?], hydrodynamic effects are expected to greatly modify transport coefficients as compared to their FL counterparts.

Many-body physics in graphene is interesting due to electron-hole symmetry and a linear dispersion relation at the CNP [?, ?]. Together with the vanishing Fermi surface, the ultrarelativistic spectrum leads to ineffective screening [?] and the formation of a strongly-interacting quasi-relativistic electron-hole plasma, known as a Dirac fluid [?]. The Dirac fluid shares many features with quantum critical systems [?]: most importantly, the electron-electron scattering time is fast [?, ?, ?, ?], and well suited to a hydrodynamic description. Because of the quasi-relativistic nature of the Dirac fluid, this hydrodynamic limit is described by novel equations [?] quite different from non-relativistic counterparts. A number of exotic properties have been predicted including nearly perfect (inviscid) flow [?] and a diverging thermal conductivity resulting in the breakdown of the Wiedemann-Franz law [?, ?].

Away from the CNP, graphene has a sharp Fermi surface and the standard FL phenomenology holds. By tuning the chemical potential, we may measure thermal and electrical conductivity in both the Dirac

Figure 28: **Temperature and density dependent electrical and thermal conductivity.** (A) Resistance versus gate voltage at various temperatures. (B) Electrical conductivity (blue) as a function of the charge density set by the back gate for different bath temperatures. The residual carrier density at the neutrality point (green) is estimated by the intersection of the minimum conductivity with a linear fit to $\log(\sigma)$ away from neutrality (dashed grey lines). Curves have been offset vertically such that the minimum density (green) aligns with the temperature axis to the right. Solid black lines correspond to $4e^2/h$. At low temperature, the minimum density is limited by disorder (charge puddles). However, above $T_{\rm dis} \sim 40$ K, a crossover marked in the half-tone background, thermal excitations begin to dominate and the sample enters the non-degenerate regime near the neutrality point. (C-E) Thermal conductivity (red points) as a function of (C) gate voltage and (D-E) bath temperature compared to the Wiedemann-Franz law, $\sigma T \mathcal{L}_0$ (blue lines). At low temperature and/or high doping ($|\mu| \gg k_{\rm B}T$), we find the WF law to hold. This is a non-trivial check on the quality of our measurement. In the non-degenerate regime ($|\mu| < k_{\rm B}T$) the thermal conductivity is enhanced and the WF law is violated. Above $T \sim 100$ K, electron-phonon coupling becomes appreciable and begins to dominate thermal transport at all measured gate voltages. At this temperature, the half-tone background ends. All data from this figure is taken from sample S2 (inset 1E).

fluid (DF) and the FL in the same sample. In a FL, the relaxation of heat and charge currents is closely related as they are carried by the same quasiparticles. The Wiedemann-Franz (WF) law [?] states that the electronic contribution to a metal's thermal conductivity $\kappa_{\rm e}$ is proportional to its electrical conductivity σ and temperature T, such that the Lorenz ratio \mathcal{L} satisfies

$$\mathcal{L} \equiv \frac{\kappa_{\rm e}}{\sigma T} = \frac{\pi^2}{3} \left(\frac{k_{\rm B}}{e}\right)^2 \equiv \mathcal{L}_0 \tag{8.1}$$

where e is the electron charge, $k_{\rm B}$ is the Boltzmann constant, and \mathcal{L}_0 is the Sommerfeld value derived from FL theory. \mathcal{L}_0 depends only on fundamental constants, and not on specific details of the system such as carrier density or effective mass. As a robust prediction of FL theory, the WF law has been verified in numerous metals [?]. However, in recent years, an increasing number of non-trivial violations of the WF law have been reported in strongly interacting systems such as Luttinger liquids [?], metallic ferromagnets [?], heavy fermion metals [?], and underdoped cuprates [?], all related to the emergence of non-Fermi liquid behavior.

The WF law is expected to be violated at the CNP in a DF due to the strong Coulomb interactions between thermally excited charge carriers. An electric field drives electrons and holes in opposite directions; collisions between them introduce a frictional dissipation, resulting in a finite conductivity even in the absence of disorder [?]. In contrast, a temperature gradient causes electrons and holes to move in the same direction inducing an energy current, which grows unimpeded by inter-particle collisions (Fig. 3C inset). The thermal conductivity is therefore limited only by the rate at which momentum is relaxed due to residual impurities.

Realization of the Dirac fluid in graphene requires that the thermal energy be larger than the local chemical potential $\mu(\mathbf{r})$, defined at position \mathbf{r} : $k_{\rm B}T \gtrsim |\mu(\mathbf{r})|$. Impurities cause spatial variations in the local

chemical potential, and even when the sample is globally neutral, it is locally doped to form electron-hole puddles with finite $\mu(\mathbf{r})$ [?, ?, ?, ?]. Formation of the DF is further complicated by phonon scattering at high temperature which can relax momentum by creating additional inelastic scattering channels. This high temperature limit occurs when the electron-phonon scattering rate becomes comparable to the electron-electron scattering rate. These two temperatures set the experimental window in which the DF and the breakdown of the WF law can be observed.

To minimize disorder, the monolayer graphene samples used in this report are encapsulated in hexagonal boron nitride (hBN) [?]. All devices used in this study are two-terminal to keep a well-defined temperature profile [?] with contacts fabricated using the one-dimensional edge technique [?] in order to minimize contact resistance. We employ a back gate voltage V_g applied to the silicon substrate to tune the charge carrier density $n = n_e - n_h$, where n_e and n_h are the electron and hole density, respectively (see supplementary materials (SM)). All measurements are performed in a cryostat controlling the temperature T_{bath} . Fig. 1A shows the resistance R versus V_g measured at various fixed temperatures for a representative device (see SM for all samples). From this, we estimate the electrical conductivity σ (Fig. 1B) using the known sample dimensions. At the CNP, the residual charge carrier density n_{min} can be estimated by extrapolating a linear fit of $\log(\sigma)$ as a function of $\log(n)$ out to the minimum conductivity [?]. At the lowest temperatures we find n_{min} saturates to $\sim 8 \times 10^9$ cm⁻². We note that the extraction of n_{min} by this method overestimates the charge puddle energy, consistent with previous reports [?]. Above the disorder energy scale $T_{\text{dis}} \sim 40 \text{ K}$, n_{min} increases as T_{bath} is raised, suggesting thermal excitations begin to dominate and the sample enters the non-degenerate regime near the CNP.

The electronic thermal conductivity is measured using high sensitivity Johnson noise thermometry (JNT) [?,?]. We apply a small bias current through the sample that injects a joule heating power P directly into the electronic system, inducing a small temperature difference $\Delta T \equiv T_{\rm e} - T_{\rm bath}$ between the graphene electrons and the bath. The electron temperature $T_{\rm e}$ is monitored independent of the lattice temperature through the Johnson noise power emitted at 100 MHz with a 20 MHz bandwidth defined by an LC matching network. We designed our JNT to be operated over a wide temperature range 3–300 K [?]. With a precision of \sim 10 mK, we measure small deviations of $T_{\rm e}$ from $T_{\rm bath}$, i.e. $\Delta T \ll T_{\rm bath}$. In this limit, the temperature of the graphene lattice is well thermalized to the bath [?] and our JNT setup allows us to sensitively measure the electronic cooling pathways in graphene. At low enough temperatures, electron and lattice interactions are weak [?, ?], and most of the Joule heat generated in graphene escapes via direct diffusion to the contacts (SM). As temperature increases, electron-phonon scattering becomes appreciable and thermal transport becomes limited by the electron-phonon coupling strength [?, ?, ?]. The onset temperature of appreciable electron-phonon scattering, $T_{\rm el-ph}$, depends on the sample disorder and device geometry: $T_{\rm el-ph} \sim 80$ K

Figure 29: Breakdown of the Wiedemann-Franz law in the Dirac fluid regime. The Lorenz ratio is shown as a function of the charge carrier density and bath temperature. Near the CNP and for temperatures above the disorder (charge puddle) regime but below the onset of electron-phonon coupling, the Lorenz ratio is measured to be an order of magnitude greater than the Fermi liquid value of 1 (blue). The WF law is observed to hold outside of the Dirac fluid regime. All data from this figure is taken from sample S1.

[?, ?, ?, ?] for our samples. Below this temperature, the electronic contribution of the thermal conductivity can be obtained from P and ΔT using the device dimensions (SM).

Fig. 1C plots $\kappa_{\rm e}(V_{\rm g})$ alongside the simultaneously measured $\sigma(V_{\rm g})$ at various fixed bath temperatures. Here, for a direct quantitative comparison based on the WF law, we plot the scaled electrical conductivity as $\sigma T \mathcal{L}_0$ in the same units as $\kappa_{\rm e}$. At low temperatures, $T < T_{\rm dis} \sim 40$ K, where the puddle induced density fluctuations dominate, we find $\kappa_{\rm e} \approx \sigma T \mathcal{L}_0$, monotonically increasing as a function of carrier density with a minimum at the neutrality point, confirming the WF law in the disordered regime. As T increases ($T > T_{\rm dis}$), however, the measured $\kappa_{\rm e}$ begins to deviate from the FL theory. We note that this violation of the WF law only appears close to the CNP, with the measured thermal conductivity maximized at n = 0 (Fig 1C). The deviation is the largest at 75 K, where $\kappa_{\rm e}$ is over an order of magnitude larger than the value expected for a FL. The non-monotonicity of $\kappa_{\rm e}(T)$ is consistent with acoustic phonons relaxing momentum more efficiently than impurities as T increases [?], while for $T \gtrsim 100$ K in our samples, activation of optical phonons adds an additional electron-phonon cooling pathway [?], and the measured thermal conductivity is larger than $\kappa_{\rm e}$. This non-FL behavior quickly disappears as |n| increases; $\kappa_{\rm e}$ returns to the FL value and restores the WF law. In fact, away from the CNP, the WF law holds for a wide temperature range, consistent with previous reports [?, ?, ?] (Fig. 1E). For this FL regime, we verify the WF law up to $T \sim 80$ K.

Our observation of the breakdown of the WF law in graphene is consistent with the emergence of the DF. Fig 2 shows the full density and temperature dependence of the experimentally measured Lorenz ratio in order to highlight the presence of the DF. The blue colored region denotes $\mathcal{L} \sim \mathcal{L}_0$, suggesting the carriers in graphene exhibit FL behavior. The WF law is violated in the DF (yellow-red) with a peak Lorenz ratio 22 times larger than \mathcal{L}_0 . The green dotted line shows the corresponding $n_{\min}(T)$ for this sample; the DF is found within this regime, indicating the coexistence of thermally populated electrons and holes. Disorder and electron-acoustic phonon scattering serve as lower and upper limits respectively on the temperature range over which the DF can be observed.

We investigate the effect of impurities on hydrodynamic transport by comparing the results obtained from samples with varying disorder. Fig. 3A shows n_{\min} as a function of temperature for three samples used in this study. $n_{\min}(T=0)$ is estimated as 5, 8, and 10×10^9 cm⁻² in samples S1, S2, and S3, respectively. All devices show qualitatively similar Dirac fluid behavior; the largest value of $\mathcal{L}/\mathcal{L}_0$ measured in the Dirac

Figure 30: **Disorder in the Dirac fluid.** (A) Minimum carrier density as a function of temperature for all three samples. At low temperature each sample is limited by disorder. At high temperature all samples become limited by thermal excitations. Dashed lines are a guide to the eye. (B) The Lorentz ratio of all three samples as a function of bath temperature. The largest WF violation is seen in the cleanest sample. (C) The gate dependence of the Lorentz ratio is well fit to hydrodynamic theory of Ref. [?, ?]. Fits of all three samples are shown at 60 K. All samples return to the Fermi liquid value (black dashed line) at high density. Inset shows the fitted enthalpy density as a function of temperature and the theoretical value in clean graphene (black dashed line). Schematic inset illustrates the difference between heat and charge current in the neutral Dirac plasma.

fluid regime is 22, 12 and 3 in samples S1, S2, and S3, respectively (Fig 3B). For a direct comparison, we show $\mathcal{L}(n)$ for all three samples at the same temperature (60 K) in Fig 3C. We find that cleaner samples not only have a more pronounced peak but also a narrower density dependence, as predicted [?, ?].

More quantitative analysis of $\mathcal{L}(n)$ in our experiment can be done by employing a quasi-relativistic hydrodynamic theory of the DF incorporating the effects of weak impurity scattering [?, ?, ?]:

$$\mathcal{L} = \frac{\mathcal{L}_{DF}}{(1 + (n/n_0)^2)^2}$$
 (8.2)

where

$$\mathcal{L}_{\rm DF} = \frac{\mathcal{H}v_{\rm F}l_{\rm m}}{T^2\sigma_{\rm min}} \quad \text{and} \quad n_0^2 = \frac{\mathcal{H}\sigma_{\rm min}}{e^2v_{\rm F}l_{\rm m}}.$$
 (8.3)

Here $v_{\rm F}$ is the Fermi velocity in graphene, $\sigma_{\rm min}$ is the electrical conductivity at the CNP, \mathcal{H} is the fluid enthalpy density, and l_m is the momentum relaxation length from impurities. Two parameters in Eqn. (??) are undetermined for any given sample: l_m and \mathcal{H} . For simplicity, we assume we are well within the DF limit where l_m and \mathcal{H} are approximately independent of n. We fit Eqn. (??) to the experimentally measured $\mathcal{L}(n)$ for all temperatures and densities in the Dirac fluid regime to obtain l_m and \mathcal{H} for each sample. Fig 3C shows three representative fits to Eqn. (??) taken at 60 K. l_m is estimated to be 1.5, 0.6, and 0.034 μ m for samples S1, S2, and S3, respectively. For the system to be well described by hydrodynamics, l_m should be long compared to the electron-electron scattering length of \sim 0.1 μ m expected for the Dirac fluid at 60 K [?]. This is consistent with the pronounced signatures of hydrodynamics in S1 and S2, but not in S3, where only a glimpse of the DF appears in this more disordered sample. We also observe in S1 that $\mathcal{L}(n)$ dips substantially below \mathcal{L}_0 : its minimum is $\sim \mathcal{L}_0/3$. $\mathcal{L} < 1$ is predicted to occur in Eq. (??) for $n \gg n_0$. Our analysis also allows us to estimate the thermodynamic quantity $\mathcal{H}(T)$ for the DF. The Fig. 3C inset shows the fitted enthalpy density as a function of temperature compared to that expected in clean graphene (dashed line) [?], excluding renormalization of the Fermi velocity. In the cleanest sample \mathcal{H} varies from 1.1-2.3 eV/ μ m² in the hydrodynamic regime. This enthalpy density corresponds to \sim 20 meV or \sim 4kBT

per charge carrier — about a factor of 2 larger than the model calculation without disorder [?]. The sharp temperature and impurity dependence observed in \mathcal{L} is a prediction of these hydrodynamic models. These effects and the magnitude of \mathcal{L} are inconsistent with alternative models for WF violations, including bipolar diffusion in graphene [?]. Furthermore, recent experiments report monotonic behavior in thermopower as a function of T [?], implying phonon drag is not responsible for the peak in κ_e that we observe as a function of T.

To fully incorporate the effects of disorder, a hydrodynamic theory treating inhomogeneity non-perturbatively is necessary [?, ?]. The enthalpy densities reported here are larger than the theoretical estimation obtained for disorder free graphene, consistent with the picture that chemical potential fluctuations prevent the sample from reaching the Dirac point. While we find thermal conductivity well described by Ref. [?, ?], electrical conductivity increases slower than expected away from the CNP, a result consistent with hydrodynamic transport in a viscous fluid with charge puddles [?].

In a hydrodynamic system, the ratio of shear viscosity η to entropy density s is an indicator of the strength of the interactions between constituent particles. It is suggested that the DF can behave as a nearly perfect fluid [?]: η/s approaches a conjecture by Kovtun-Son-Starinets: $(\eta/s)/(\hbar/k_B) \gtrsim 1/4\pi$ for a strongly interacting system [?]. A non-perturbative hydrodynamic framework can be employed to estimate η , as we discuss elsewhere [?]. A direct measurement of η is of great interest.

We have experimentally discovered the breakdown of the WF law and provided evidence for the hydrodynamic behavior of the Dirac fermions in graphene. This provides an experimentally realizable Dirac fluid and opens the way for future studies of strongly interacting relativistic many-body systems. Beyond a diverging thermal conductivity and an ultra-low viscosity, other peculiar phenomena are expected to arise in this plasma. The massless nature of the Dirac fermions is expected to result in a large kinematic viscosity, despite a small shear viscosity η . Observable hydrodynamic effects have also been predicted to extend into the FL regime [?]. The study of magnetotransport in the DF will lead to further tests of hydrodynamics [?, ?].

Chapter 9

Hydrodynamic transport in the Dirac fluid

Below we present the original text of [?]. Reprinted with permission from A. Lucas, J. Crossno, K. C. Fong, P. Kim and S. Sachdev, "Hydrodynamic transport in quantum critical fluids and in the Dirac fluid in graphene", Physical Review **B93** 075426 (2016). Copyright (2016) by the American Physical Society.

Introduction

Over a half century ago, the theory of electronic transport in "standard" metals such as iron and copper was developed. The key pillar of this approach is the validity of Fermi liquid theory, which states that the interacting electrons in solids form nearly free-streaming quasiparticles [?]. At finite temperature, these quasiparticles form a weakly interacting quantum gas which is well described by quantum kinetic theory. The transport properties of these quantum gases are by now very well understood. A particularly important property of Fermi liquids is the Wiedemann-Franz law, which states that ⁴⁷

$$\mathcal{L} \equiv \frac{\kappa}{\sigma T} = \frac{10 - .18 \, t^2}{3} \frac{k_{\rm B}^2}{e^2} \equiv \mathcal{L}_{\rm WF}.$$
 (9.1)

Here κ is the electronic contribution to thermal conductivity, σ is the electrical conductivity, T is the temperature, and \mathcal{L} is the Lorenz ratio. Implicit in the above equation is that the dominant interactions are between impurities or phonons and quasiparticles, and in most metals this is true: the interaction time

 $^{^{47}}$ Below we have assumed that the charge of the quasiparticles is $\pm e$, with e the charge of the electron – this is essentially always the case.

between quasiparticles is typically 10^4 times longer than the interaction times between quasiparticles and impurities or phonons [?].

Also over a half century ago, a study of the consequences of hydrodynamic behavior on correlation functions and transport in interacting quantum systems was initiated [?]. Hydrodynamics is a framework for understanding the collective motion of the quasiparticles in a solid, or any other interacting quantum or classical system, so long as the microscopic degrees of freedom reach thermal equilibrium locally. In a solid, this interaction time must be the fastest time scale in the problem to see hydrodynamic behavior, but since quasiparticles in a Fermi liquid interact with each other only very weakly, observing hydrodynamics in electron fluids is notoriously hard. Even in the purest metals where hydrodynamic behavior can be observed, such as in GaAs [?, ?, ?], the resulting fluid is often a Fermi liquid. The resulting dynamics is the fluid dynamics of (quantum) gases. More recent theoretical work on hydrodynamics in Fermi liquids includes [?, ?, ?, ?, ?, ?], and recent experimental work includes [?, ?].

Fermi liquid theory is known to fail in a variety of experimentally realized metals in two or more spatial dimensions – most famous among these is the strange metal phase of the cuprate superconductors [?, ?, ?] which does not have quasiparticle excitations. A slightly more theoretically controlled and better understood example of a state of quantum matter without quasiparticles is the quasi-relativistic Dirac fluid in the semimetal graphene. The Dirac fluid, which effectively lives in two spatial dimensions, has also been argued to be strongly interacting at experimentally achievable temperatures [?, ?, ?, ?] due to ineffective Coulomb screening [?]. Although it is separated from the Fermi liquid by a crossover, and not a (thermal) phase transition, its proximity to a (simple) zero temperature quantum critical point at charge neutrality means that the phenomenology of the Dirac fluid is expected to differ strongly from Fermi liquid theory. Due to the high spatial dimensionality, 48 the development of a predictive quantitative theory of these systems is notoriously hard. A major theme in recent work has been quantum criticality [?, ?], which opens up the possibility for borrowing powerful techniques from high energy physics, but even in this case very little is known about experimentally relevant regime of finite temperature and density. One of the only remaining techniques for understanding these systems is hydrodynamics, as many features of hydrodynamics are universal and model independent, and the strongly interacting quantum physics is captured entirely by the coefficients in otherwise classical differential equations. Such fluids are quantum analogues of classical liquids such as water, which are strongly interacting (albeit with negligible quantum entanglement) insofar as they do not admit a controllable description via kinetic theory. Furthermore, it has been shown [?] that strongly interacting quantum critical fluids have a somewhat different hydrodynamic description than the canonical

⁴⁸Quantum dynamics in one dimension, which is often integrable, is described using very different techniques and has qualitatively distinct features.

Fermi liquids described above, and this can lead to very different hydrodynamic properties, including in transport [?, ?, ?, ?, ?, ?, ?], as we will review in this paper.

Using novel techniques to measure thermal transport [?, ?, ?], the Dirac fluid has finally been observed in monolayer graphene, and evidence for its hydrodynamic behavior has emerged [?], as we will detail. However, existing theories of hydrodynamic transport are not consistent with the simultaneous density dependence in experimentally measured thermal and electrical conductivities. In this paper, we improve upon the hydrodynamic theory of [?], describe carefully effects of finite density, and develop a non-perturbative relativistic hydrodynamic theory of transport in electron fluids near a quantum critical point. Under certain assumptions about the equations of state of the Dirac fluid, our theory is quantitatively consistent with experimental observations. The techniques we employ are included in the framework of [?], which developed a hydrodynamic description of transport in relativistic fluids with long wavelength disorder in the chemical potential. [?] was itself inspired by recent progress employing the AdS/CFT correspondence to understand quantum critical transport in strange metals [?, ?, ?, ?, ?, ?, ?, ?, ?, ?], but as we will discuss, this theory is also well suited to describe the physics of graphene.

Summary of Results

The recent experiment [?] reported order-of-magnitude violations of the Wiedemann-Franz law. The results were compared with the standard theory of hydrodynamic transport in quantum critical systems [?], which predicts that

$$\sigma(n) = \sigma_{Q} + \frac{e^{2}v_{F}^{2}n^{2}\tau}{\mathcal{H}},$$
(9.2a)

$$\kappa(n) = \frac{v_{\rm F}^2 \mathcal{H}\tau}{T} \frac{\sigma_{\rm Q}}{\sigma(n)},\tag{9.2b}$$

where e is the electron charge, s is the entropy density, n is the charge density (in units of length⁻²), \mathcal{H} is the enthalpy density, τ is a momentum relaxation time, and σ_{Q} is a quantum critical effect, whose existence is a new effect in the hydrodynamic gradient expansion of a relativistic fluid. Note that up to σ_{Q} , $\sigma(n)$ is simply described by Drude physics. The Lorenz ratio then takes the general form

$$\mathcal{L}(n) = \frac{\mathcal{L}_{DF}}{(1 + (n/n_0)^2)^2},$$
(9.3)

where

$$\mathcal{L}_{\rm DF} = \frac{v_{\rm F}^2 \mathcal{H}\tau}{T^2 \sigma_{\rm o}},\tag{9.4a}$$

Figure 31: A comparison of our hydrodynamic theory of transport with the experimental results of [?] in clean samples of graphene at T=75 K. We study the electrical and thermal conductances at various charge densities n near the charge neutrality point. Experimental data is shown as circular red data markers, and numerical results of our theory, averaged over 30 disorder realizations, are shown as the solid blue line. Our theory assumes the equations of state described in (??) with the parameters $C_0 \approx 11$, $C_2 \approx 9$, $C_4 \approx 200$, $\eta_0 \approx 110$, $\sigma_0 \approx 1.7$, and (??) with $u_0 \approx 0.13$. The yellow shaded region shows where Fermi liquid behavior is observed and the Wiedemann-Franz law is restored, and our hydrodynamic theory is not valid in or near this regime. We also show the predictions of (??) as dashed purple lines, and have chosen the 3 parameter fit to be optimized for $\kappa(n)$.

Figure 32: A comparison of our hydrodynamic theory of transport with the experimental results of [?] in clean samples of graphene at the charge neutrality point (n = 0). We use no new fit parameters compared to Figure ??. The yellow shaded region denotes where Fermi liquid behavior is observed; the purple shaded region denotes the likely onset of electron-phonon coupling.

$$n_0^2 = \frac{\mathcal{H}\sigma_{\mathcal{Q}}}{e^2 v_{\mathcal{D}}^2 \tau}.\tag{9.4b}$$

 $\mathcal{L}(n)$ can be parametrically larger than $\mathcal{L}_{\mathrm{WF}}$ (as $\tau \to \infty$ and $n \ll n_0$), and much smaller $(n \gg n_0)$. Both of these predictions were observed in the recent experiment, and fits of the measured \mathcal{L} to (??) were quantitatively consistent, until large enough n where Fermi liquid behavior was restored. However, the experiment also found that the conductivity did not grow rapidly away from n=0 as predicted in (??), despite a large peak in $\kappa(n)$ near n=0, as we show in Figure ??. Furthermore, the theory of [?] does not make clear predictions for the temperature dependence of τ , which determines $\kappa(T)$.

In this paper, we argue that there are two related reasons for the breakdown of (??). One is that the dominant source of disorder in graphene – fluctuations in the local charge density, commonly referred to as charge puddles [?, ?, ?, ?] – are not perturbatively weak, and therefore a non-perturbative treatment of their effects is necessary.⁴⁹ The second is that the parameter τ , even when it is sharply defined, is intimately related to both the viscosity and to n, and this n dependence is neglected when performing the fit to (??) in Figure ??. We develop a non-perturbative hydrodynamic theory of transport which relies on neither of the above assumptions, and gives us an explicit formula for τ in the limit of weak disorder. The key assumption for the validity of our theory is that the size of the charge puddles is comparable to or larger than the electron interaction length scale, which is about 100 nm. Experimental evidence suggests this is marginally true in graphene samples mounted on hexagonal boron nitride [?], as was done in [?]. Although we cannot analytically solve our theory non-perturbatively, we perform numerical computations of the transport coefficients in disordered fluids, and compare the results to the experimental data in Figure ??. Our simultaneous fit to $\kappa(n)$ and $\sigma(n)$ shows improved quantitative agreement with both sets of data in the

⁴⁹See [?, ?] for a theory of electrical conductivity in charge puddle dominated graphene at low temperatures.

Figure 33: A cartoon of a nearly quantum critical fluid where our hydrodynamic description of transport is sensible. The local chemical potential $\mu(\mathbf{x})$ always obeys $|\mu| \ll k_{\rm B}T$, and so the entropy density $s/k_{\rm B}$ is much larger than the charge density |n|; both electrons and holes are everywhere excited, and the energy density ϵ does not fluctuate as much relative to the mean. Near charge neutrality the local charge density flips sign repeatedly. The correlation length of disorder ξ is much larger than $l_{\rm ee}$, the electron-electron interaction length.

Dirac fluid regime. We further compare in Figure ?? the temperature dependence of κ and σ between our numerics and the experiment, using no new fitting parameters, and find satisfactory quantitative agreement in the Dirac fluid regime.

Figure ?? shows a cartoon of the regime of validity of our hydrodynamic theory. The fact that the charge puddles may be substantial, while the entropy and energy densities are much more constant, helps to explain why the perturbative description of transport is much better for κ than σ , as the perturbative approach works well in a nearly homogeneous fluid. In coming years the quality of graphene samples will improve, and the charge puddle size may grow larger than 100 nm, allowing us to observe the clean hydrodynamic limit described by (??). As present day samples are just clean enough to observe hydrodynamics, our determination of the equations of state should be understood as preliminary.

Although the focus of this paper is on the Dirac fluid in graphene, this is because of the experimental motivation for this work. Our theory has broader validity, and we will introduce it in the more general context of transport in a disordered electronic fluid near a quantum critical point with manifest Lorentz invariance, with the microscopic Fermi velocity v_F playing the role of the speed of light. The Dirac fluid is not strictly Lorentz invariant, but we will justify the validity of our approach even in this system. While the Dirac fluid in graphene is currently the only experimentally realized strongly interacting condensed matter system with evidence for electronic hydrodynamics [?], in the future surface states in topological insulators in three spatial dimensions may host strongly interacting electron fluids [?]. Strongly interacting three dimensional materials including Weyl semimetals [?, ?, ?] may also give rise to novel phenomena relevant for transport [?, ?].

Outline

The outline of this paper is as follows. We briefly review the definitions of transport coefficients in Section ??. In Section ?? we develop a theory of hydrodynamic transport in the electron fluid, assuming that it is Lorentz invariant. We discuss the peculiar case of the Dirac fluid in graphene in Section ??, and argue that deviations from Lorentz invariance are small. We describe the results of our numerical simulations of this theory in Section ??, and directly compare our simulations with recent experimental data from graphene

[?]. The experimentally relevant effects of phonons are qualitatively described in Section ??. We conclude the paper with a discussion of future experimental directions. Appendices contain technical details of our theory.

In this paper we use index notation for vectors and tensors. Latin indices $ij\cdots$ run over spatial coordinates x and y; Greek indices $\mu\nu\cdots$ run over time t as well. We will denote the time-like coordinate of A^{μ} as A^{t} . Indices are raised and lowered with the Minkowski metric $\eta^{\mu\nu} \equiv \operatorname{diag}(-1,1,1)$. The Einstein summation convention is always employed.

Transport Coefficients

Let us begin by defining the thermoelectric response coefficients of interest in this paper. Suppose that we drive our fluid by a spatially uniform, externally applied, electric field E_i (formally, an electrochemical potential gradient), and a temperature gradient $-\partial_i T$. We will refer to $-\partial_j T$ as $T\zeta_j$, with $\zeta_j = -T^{-1}\partial_j T$, for technical reasons later. As is standard in linear response theory, we decompose these perturbations into various frequencies, and focus on the response at a single frequency ω . Time translation invariance implies that the (uniformly) spatially averaged charge current $\langle J_i \rangle$ and the spatially averaged heat current $\langle Q_i \rangle$ are also periodic in time of frequency ω , and are related to E_i and ζ_i by the thermoelectric transport coefficients:

$$\begin{pmatrix} \langle J_i \rangle \\ \langle Q_i \rangle \end{pmatrix} e^{-i\omega t} = \begin{pmatrix} \sigma_{ij}(\omega) & T\alpha_{ij}(\omega) \\ T\bar{\alpha}_{ij}(\omega) & T\bar{\kappa}_{ij}(\omega) \end{pmatrix} \begin{pmatrix} E_j \\ \zeta_j \end{pmatrix} e^{-i\omega t}.$$
 (9.5)

In a typical disordered system, we expect that σ_{ij} , α_{ij} , $\bar{\alpha}_{ij}$ and $\bar{\kappa}_{ij}$ are all proportional to 1 0 -.18 δ_{ij} . In our numerics, finite size effects introduce some anisotropy; our theory is valid in this more general scenario.

In fact, (??) is somewhat subtle. Implicit in the definitions of the transport coefficients are a set of boundary conditions. In the definitions in (??), we have assumed that we tune E_i and ζ_i , and then measure J_i and Q_i . However, usually in experiments one fixes J_i , as electronic measurements are far easier to control. One then can fix either E_i or ζ_i . So while it is straightforward to measure σ_{ij} by setting $\zeta_i = 0$, one measures not $\bar{\kappa}_{ij}$ but instead κ_{ij} , defined as

$$\langle Q_i \rangle |_{\langle J_i \rangle = 0} = T \kappa_{ij} \zeta_j.$$
 (9.6)

Straightforward manipulations give that $\sigma_{ij}E_j = -T\alpha_{ij}\zeta_j$, and therefore that

$$\kappa_{ij} = \bar{\kappa}_{ij} - T\bar{\alpha}_{ik}\sigma_{kl}^{-1}\alpha_{lj}. \tag{9.7}$$

These definitions are general and independent of our hydrodynamic theory.

Relativistic Hydrodynamics

We now develop a theory of relativistic hydrodynamics of the electronic plasma in a disordered metal, where the disorder is introduced by a spatially dependent chemical potential $\mu_0(\mathbf{x})$. So long as the length scale $\xi \sim |\mu_0|/|\partial_x \mu_0|$ over which this function varies is much larger than the electron-electron scattering length $l_{\rm ee} \sim \hbar v_{\rm F}/k_{\rm B}T$, it is sensible to treat the fluid as locally homogeneous, with parameters such as energy density and viscosity locally being functions of μ_0 alone. This external chemical potential acts as an external source of energy and momentum for the electronic plasma, and can be sourced by lattice defects or impurities, either in the (semi)metal itself, or in the substrate it is placed on, for two-dimensional materials such as graphene [?, ?]. Our theory here is analogous to [?], and similar to the earlier work [?] in non-relativistic fluids. However, [?] focused mostly on the mathematical consequences of relativistic hydrodynamics, particularly in regards to holographic models. Our focus here is on practical consequences in realistic quantum critical fluids where $\mu \ll k_{\rm B}T$, and where the equations of state are tightly constrained by scale invariance (see Appendix ??).

Previous theories of hydrodynamic transport assumed that disorder was parametrically weak, and so momentum is a nearly conserved quantity [?, ?]. Such theories can be shown to be a perturbative limit of the more general approach that we advocate below: see [?] and Appendix ??. However, near the charge-neutrality point, non-perturbative effects can become important [?]. Since this is the regime where [?] observed evidence for hydrodynamic behavior, it is necessary to treat transport in the charge-neutral fluid carefully and to study non-perturbative physics. We begin with a general discussion of the equations of state of a relativistic plasma, and then outline our non-perturbative hydrodynamic description of transport.

Though our focus in this paper is on the case of two spatial dimensions, it is straightforward to generalize our theory to higher dimensions.

Hydrodynamic Equations

Let us review the structure of relativistic hydrodynamics, which was derived carefully in [?]. Hydrodynamics is a general framework which describes the relaxation of an ergodic and locally thermalizing (classical or quantum) system to global thermal equilibrium, or as close to global equilibrium as boundary conditions or external sourcing allow. The assumption of local thermalization implies that the only quantities with dynamics on long time scales (compared to the local thermalization time $l_{\rm ee}/v_{\rm F}$) are quantities that are globally conserved, up to external sources. In a typical theory, these will be charge, energy and momentum,

and we will assume this to be the case for graphene as well. Hydrodynamics is a systematic way to truncate equations of motion for the local charge density n(x), energy density $\epsilon(x)$ and momentum density $\Pi_i(x)$, by treating the perturbative parameter as $l_{ee}\partial_{\mu}$. In fact, it is typical to instead study the dynamics of the thermodynamic conjugate variables: chemical potential $\mu(x)$, temperature T(x) and relativistic velocity $u^{\mu}(x)$, respectively. u^{μ} is subject to the usual constraint $u_{\mu}u^{\mu} = -v_{\rm F}^2$.

Note that throughout this paper, "charge density" n refers to the number density of electrons, minus the number density of holes: $n = n_{\text{elec}} - n_{\text{hole}}$. Thus, there are no factors of e in the definition of n, or chemical potential μ .⁵⁰

The equations of motion of hydrodynamics are the local conservation laws, up to external sources. We apply an external chemical potential μ_0 via an external electromagnetic field $A_{\rm ext}^t = -\mu_0(\mathbf{x})/e$, $A_{\rm ext}^i = 0$. We employ relativistic notation with $v_{\rm F} = 1$ temporarily. The equations of hydrodynamics are

$$\partial_{\mu}T^{\mu\nu} = eF^{\mu\nu}_{\text{ext}}J_{\nu},\tag{9.8a}$$

$$\partial_{\mu}J^{\mu} = 0, \tag{9.8b}$$

where $F_{\rm ext}^{ti} = -F_{\rm ext}^{it} = \partial_i \mu_0$ are the only non-vanishing components, $T^{\mu\nu}$ represents the expectation value of the local stress-energy density, and J^{μ} the expectation value of the local charge density. $T^{\mu\nu}$ and J^{μ} must be expressed in terms of μ , T and u^{μ} in order to obtain a closed set of equations. One can show that there is a static solution to the hydrodynamic equations with $u^{\mu} = (1,0,0)$, $T = T_0 = \text{constant}$, and $\mu(\mathbf{x}) = \mu_0(\mathbf{x})$ [?]. Recall that $\mu_0(\mathbf{x})$ is slowly varying on the length scale ξ . We will take this solution as the background state of our fluid.

Hydrodynamics is a perturbative expansion of (??), where the perturbative expansion parameter is the number of derivatives of space and time. At zeroth order, the equations of state are simply that $T^{\mu\nu}$ and J^{μ} are given by the thermodynamic relations we derived above:

$$T^{\mu\nu} = (\epsilon + P)u^{\mu}u^{\nu} + P\eta^{\mu\nu}, \tag{9.9a}$$

$$J^{\mu} = nu^{\mu},\tag{9.9b}$$

with ϵ the energy density and P the pressure. In the fluid's rest frame, $T^{tt} = \epsilon$, $T^{ij} = P + 1 + 0$ -.18 δ^{ij} , and $J^t = n$, with all other components vanishing. At first order, [?] showed that the most general first derivative

⁵⁰Therefore $[n] = [length]^{-d}$ and $[\mu] = [energy]$.

corrections to $T^{\mu\nu}$ and J^{μ} consistent with symmetries and the local second law of thermodynamics are

$$T^{\mu\nu} = (\epsilon + P)u^{\mu}u^{\nu} + P\eta^{\mu\nu} - 2\mathcal{P}^{\mu\rho}\mathcal{P}^{\nu\sigma}\eta\partial_{(\rho}u_{\sigma)} - \mathcal{P}^{\mu\nu}(\zeta - \eta)\partial_{\rho}u^{\rho}, \tag{9.10a}$$

$$J^{\mu} = nu^{\mu} - \frac{\sigma_{\mathcal{Q}}}{e^2} \left(\eta^{\mu\nu} + u^{\mu} u^{\nu} \right) \left(\partial_{\nu} \mu - \frac{\mu}{T} \partial_{\nu} T - e F_{\nu\rho, \text{ext}} u^{\rho} \right), \tag{9.10b}$$

with $\eta, \zeta, \sigma_{\rm Q} > 0$, and $\mathcal{P}^{\mu\nu} = \eta^{\mu\nu} + u^{\mu}u^{\nu}$. Here η and ζ are the shear and bulk viscosity respectively, and $\sigma_{\rm Q}$ is a "quantum critical" conductivity [?]. Note that the external electromagnetic fields show up in the hydrodynamic gradient expansion in the charge current; this happens because the charged fluid is sensitive only to the gradient in the total electrochemical potential [?]. We allow for P, n, η , ζ and $\sigma_{\rm Q}$ to all be position-dependent, with their position dependence related to $\mu_{\rm ext}$, as we will describe shortly in more detail.

It has long been appreciated [?] that σ_Q plays a fundamental role in hydrodynamic transport near quantum critical points. More recently [?] argued that η could play a role in transport. We will carefully detail how η affects transport in this paper, analytically and numerically.

In our extension of this theory to graphene, we will also allow for Coulomb interactions of the fluid to be substantial enough to enter the hydrodynamic equations. However, this should only alter the equations of state, as well as add a further contribution to $F_{\mu\nu,\text{ext}}$ [?], and we will detail this in the subsequent section. The constraints imposed on hydrodynamics from local positivity of entropy production [?] are unchanged in the presence of Coulomb interactions, which are entirely accounted for via a modified $F_{\text{ext}}^{\mu\nu}$.

It is sufficient in our calculation of σ , α and κ to simplify $T^{\mu\nu}$ and J^{μ} and retain only the terms linear in velocity. One finds, in d=2:

$$T^{ti} = (\epsilon + P)v^i, \tag{9.11a}$$

$$T^{ij} = P \ 1 \ 0 - .18 \ \delta^{ij} - \eta \left(\partial^{i} v^{j} + \partial^{j} v^{i}\right) - (\zeta - \eta) \ 1 \ 0 - .18 \ \delta^{ij} \partial_{k} v^{k}, \tag{9.11b}$$

$$J^{i} = nv^{i} - \frac{\sigma_{Q}}{e^{2}} \left(\partial_{i} (\mu - \mu_{0}) - \frac{\mu}{T} \partial_{i} T \right). \tag{9.11c}$$

We stress the novel role of $\sigma_{\rm Q}$, a new dissipative transport coefficient in a relativistic fluid, without a direct analogue in the canonical non-relativistic fluid. This term is related to the underlying thermally excited electron-hole plasma, and the fact that electrons and holes can move in opposite directions under an applied electric field, contributing a net electric current.⁵¹ There is no microscopic thermal conductivity – instead, all microscopic dissipation related to electric and thermal gradients is controlled by $\sigma_{\rm Q}$.

⁵¹It is qualitatively similar to the bipolar diffusion effect [?, ?] – however, in hydrodynamics the quasiparticle lifetimes are limited by $\hbar/k_{\rm B}T$, whereas in the bipolar diffusion effect these lifetimes are parametrically long, as in a Fermi liquid.

Hydrodynamic Theory of Transport

We are now ready to detail our hydrodynamic calculation of the transport coefficients defined in Section ??. We place our fluid in a box of length L in each direction, with periodic boundary conditions on the fluid in every direction. We then apply a constant background E_i and ζ_i . The static solution above is no longer a solution to the hydrodynamic equations of motion, sourced by these gradients. Now, we generically expect to excite both a spatial electric current J^i , and a spatial heat current

$$Q^i \equiv T^{ti} - \mu J^i. \tag{9.12}$$

We can expand out J^i and Q^i locally as a Taylor series in E_i and ζ_i . The transport coefficients in Section ?? are defined by retaining only the linear terms in E_i and ζ_i , and spatially averaging over the local charge and heat currents. It is sufficient to perform a linear response calculation about our previously identified static solution:

$$\mu \approx \mu_0(\mathbf{x}) + 10 - .18 \, \delta \mu(\mathbf{x}) e^{-i\omega t}, \tag{9.13a}$$

$$T \approx T_0 + 10 - .18 \, \delta T(\mathbf{x}) e^{-i\omega t},$$
 (9.13b)

$$u^t \approx 1,$$
 (9.13c)

$$u^i \approx 10 \text{ -.}18 \, \delta v^i(\mathbf{x}) e^{-i\omega t},$$
 (9.13d)

and then solve the linearized hydrodynamic equations – this is equivalent to only keeping terms linear in E_i and ζ_i in the full solution. For ease of notation, we drop the " 1 0 -.18 δ " in front of the linear response perturbations in the remainder of the paper, but one should keep in mind that $\mu(\mathbf{x})$, $T(\mathbf{x})$, and v^i are henceforth perturbatively small quantities.

Following [?], the linearized hydrodynamic equations (??) can be shown to take the following form:⁵³

$$\begin{pmatrix}
-e^{-2}\partial_{i}\sigma_{Q}\partial_{i} & e^{-2}T_{0}^{-1}\partial_{i}\mu_{0}\sigma_{Q}\partial_{i} & \partial_{j}n \\
e^{-2}\partial_{i}\mu_{0}\sigma_{Q}\partial_{i} & -e^{-2}T_{0}^{-1}\partial_{i}\mu_{0}^{2}\sigma_{Q}\partial_{i} & T_{0}\partial_{j}s \\
n\partial_{i} & s\partial_{i} & -\partial_{i}(\zeta-\eta)\partial_{j}-\partial_{i}\eta\partial_{j}-\partial_{j}\eta\partial_{i}
\end{pmatrix}
\begin{pmatrix}
\mu \\
T \\
v_{j}
\end{pmatrix}$$

⁵²The application of a constant ζ_j on a periodic space is the reason why we cannot talk about driving the system with a constant temperature gradient, since the temperature is a periodic function in space. One can formally implement ζ_i through deformations of the spacetime metric and external gauge fields [?].

53In this equation, derivatives act on all fields to the right, so $\partial_x \eta \partial_x v^x$ should be read as $\partial_x (\eta \partial_x v^x)$.

$$= \begin{pmatrix} -e^{-1}\partial_i \sigma_{\mathcal{Q}}(E_i - \mu_0 \zeta_i/e) \\ e^{-1}\partial_i \sigma_{\mathcal{Q}} \mu_0(E_i - \mu_0 \zeta_i/e) \\ enE_i + T_0 s \zeta_i \end{pmatrix}$$
(9.14)

Here

$$s = \frac{\epsilon + P - \mu_0 n}{T_0} \tag{9.15}$$

is the entropy density of the background fluid. s and n are not independent, and are related by thermodynamic Maxwell relations: see Appendix ??. We have also employed

$$\partial_i P = n \partial_i \mu + s \partial_i T. \tag{9.16}$$

In particular, s and n are position dependent functions whose position dependence is entirely determined by the local chemical potential: $s(\mathbf{x}) = s(T_0, \mu_0(\mathbf{x}))$, and similarly for n, η , and all other coefficients in the hydrodynamic equations. The proper boundary conditions to impose on μ , T and v_j are periodicity. This forms a well-posed elliptic partial differential equation and can be numerically solved: see Appendix ??. Combining (??) and (??), along with μ , T and v^i as found from solving the linear system (??), we obtain $J_i(E_j, \zeta_j)$ and $Q_i(E_j, \zeta_j)$. Spatially averaging these quantities and employing (??), we obtain σ_{ij}, α_{ij} and $\bar{\kappa}_{ij}$.

We cannot exactly compute these transport coefficients in general. However, one can prove [?] that Onsager reciprocity holds. This is a non-trivial consistency check on the validity of our approach. Furthermore,
there exist scaling symmetries combining re-scalings of μ , T and v_i , as well as the equations of state; these are
listed in Appendix ??. These are helpful when we fit this theory to the data of [?]. These scaling symmetries
are also present in the theory of [?], with the exception of a further scaling symmetry which only affects the
viscosity and the length scale of disorder in this theory.

In the limit where

$$\mu_0 = \bar{\mu}_0 + u\hat{\mu}(\mathbf{x}),\tag{9.17}$$

with $\hat{\mu}$ an O(1) function but $u \ll \bar{\mu}_0$, the transport coefficients may be perturbatively calculated analytically, and for $\mu \ll k_{\rm B}T$, we find that

$$\sigma \approx \frac{e^2 v_{\rm F}^2 n^2 \tau}{\epsilon + P},\tag{9.18a}$$

$$\alpha \approx \frac{ev_{\rm F}^2 ns\tau}{\epsilon + P},$$
(9.18b)

$$\bar{\kappa} \approx \frac{v_{\rm F}^2 T s^2 \tau}{\epsilon + P},$$
(9.18c)

and we find an analytical expression for τ with the following approximate form near the Dirac point:

$$\frac{1}{\tau} \approx \frac{v_{\rm F}^2 u^2}{2} \left(\frac{\partial n}{\partial \mu}\right)^2 \left[\frac{e^2}{\sigma_{\rm Q}(\epsilon + P)} + \frac{\eta + \zeta}{\xi^2} \frac{4\mu^2}{(\epsilon + P)^3}\right]. \tag{9.19}$$

Details of this calculation and a more precise (and complicated) formula are given in Appendix ??. The requirement that we are "far" from the Dirac point is that $\sigma_{\rm Q} \ll e^2 v_{\rm F}^2 n^2 \tau/(\epsilon + P)$. Everything in (??) except for u is evaluated in the clean fluid with $u \to 0$. (??) makes clear that if η/ξ^2 is large, the n and μ dependence of τ is not negligible even when $\mu \ll k_{\rm B}T$, and we will verify this in numerical simulations in Section ??. The validity of (??) for κ is not guaranteed far from the Dirac point in this perturbative limit, but can often be quite good in practice, when the density dependence of all parameters is accounted for. Combining (??) and (??), we obtain the relativistic analogue of the perturbative results of [?].

Noting that $n \sim \mu$ as $\mu \to 0$, careful study of (??) shows that the Lorentzian form of $\kappa(n)$ is not altered by plugging in this hydrodynamic formula for τ , while the form of $\sigma(n)$ can be quite distinct, with $\sigma(n)$ no longer growing quadratically at larger n. This helps explain why in Figure ??, (??) gave a quantitatively good fit to $\kappa(n)$, but not to $\sigma(n)$.

The Dirac Fluid in Graphene

The previous section developed a general theory for relativistic fluids. It is often said that the Dirac fluid in graphene is a "quantum critical" system in two spatial dimensions [?, ?, ?], and exhibits behavior analogous to the quantum critical regime at finite temperatures above the superfluid-insulator transition, although technical differences arise. Let us review elementary features of the quantum critical behavior of graphene, and argue that our formalism remains appropriate for transport computations.

Assuming that the electrons in graphene are non-interacting, standard band theory calculations on a honeycomb lattice in two spatial dimensions with nearest-neighbor hopping give two species of Dirac fermions with low-energy dispersion relation

$$\epsilon(\mathbf{q}) \approx \hbar v_{\rm F} |\mathbf{q}|,$$
 (9.20)

Convincing experimental evidence for these massless Dirac fermions was given in [?, ?]. There is a quantum critical point between electron and hole Fermi liquids at zero temperature in graphene, as the chemical potential μ is tuned through the Dirac point, $\mu = 0$. At (any experimentally accessible) finite temperature T, and at $\mu \ll T$, an effectively relativistic plasma of electrons and holes forms, interacting via a 1/r Coulomb

potential. The strength of these Coulomb interactions is captured by a dimensionless number α_0 analogous to the fine structure constant:

$$\alpha_0 = \frac{e^2}{4 \cdot 10^{-.18} \, \text{th} \epsilon_0 \epsilon_r \hbar v_F} \approx \frac{1}{137} \frac{c}{\epsilon_r v_F},\tag{9.21}$$

where $\epsilon_{\rm r} \sim 4$ is a dielectric constant, $c \approx 3 \times 10^8$ m/s is the speed of light, $v_{\rm F} \approx 1.1 \times 10^6$ m/s is the Fermi velocity in graphene and e is the charge of the electron. In experiments, $\alpha_0 \sim {\rm O}(1)$, and so unlike quantum electrodynamics ($\alpha_{\rm QED} \approx 1/137$), interactions are *strong*. $v_{\rm F}$ plays the role of the speed of light in an effectively relativistic electron-hole plasma, and in an experimentally accessible regime which we describe below, one can use relativistic hydrodynamics to model thermoelectric transport in graphene.

The exception to the emergent Lorentz invariance is the photon-mediated Coulomb interactions, which are the standard 1/r interaction of three spatial dimensions. Further, because $v_{\rm F} \sim c/300$, the Coulomb interaction is essentially non-local and instantaneous in time. Despite this, graphene shares many features with a truly relativistic plasma with "speed of light" $v_{\rm F}$, including a "quantum critical" diffusive conductivity $\sigma_{\rm Q}$ [?].

Analogously to in quantum electrodynamics, α is a marginally irrelevant interaction, and so the effective coupling constant runs. At temperature $T \to 0$, we should replace α_0 with [?]

$$\alpha_{\text{eff}} = \alpha_0 \left(1 + \frac{\alpha_0}{4} \log \frac{\Lambda}{T_0} \right)^{-1} \tag{9.22}$$

where $\Lambda \sim 8.4 \times 10^4$ K is a cutoff related to the graphene band structure (the energy scale at which the dispersion is no longer linear). Note that although the running of $\alpha_{\rm eff}$ causes a logarithmically increasing velocity $v_{\rm F}$ in (??), when we write $v_{\rm F}$ in this paper, we are always referring to the bare velocity, 1.1×10^6 m/s.

At the experimentally accessible temperatures ($T_0 \sim 70$ K) where the plasma described above is most likely not suppressed by local disorder in μ [?], (??) gives $\alpha_{\rm eff} \sim 0.25$. And so the experiments likely probe the dynamics of a strongly interacting quasi-relativistic plasma. It is such a regime where hydrodynamics is a good approximation. More carefully, the electron-electron scattering length has quantum critical scaling [?]

$$l_{\rm ee} \sim \frac{\hbar v_{\rm F}}{\alpha_{\rm eff}^2 k_{\rm B} T_0} \sim 100 \text{ nm},$$
 (9.23)

where we have plugged in for experimentally reasonable values of the parameters. Indeed, pump-probe experiments provide evidence that the electron-electron interaction time, $l_{\rm ee}/v_{\rm F} \sim 10^{-13}$ s, is consistent with (??) [?, ?]. Furthermore, it is believed that the dominant source of disorder in graphene are charge puddles, which are fluctuations in the local charge density. It is now possible to find samples of graphene where these

fluctuations are correlated on the length scale (??) [?]. In these cleanest samples, the experimental evidence thus points to the validity of a hydrodynamic description, such as the one we advocate in this paper.

Most computations of the thermodynamic and hydrodynamic coefficients in graphene are based on kinetic theory, which requires a quasiparticle description to be sensible, and so are valid as $\alpha_{\rm eff} \to 0$ ($T_0 \to 0$), when the plasma becomes weakly interacting. However, the experiments are likely not in this weakly interacting regime, and $\log \alpha_{\rm eff}$ corrections to these properties are not negligible. As such, we will allow *all* coefficients in the equations of motion to be fit parameters. We will also neglect the fact that the running of $\alpha_{\rm eff}(T_0)$ allows for certain thermodynamic relations for a strictly scale invariant, relativistic fluid to be violated. This assumption is justified in Appendix ??.

We must also take into account the long range Coulomb interactions in our hydrodynamic description. This can be done following [?]. The Coulomb potential introduces a local electric field and must be included in $F_{\text{ext}}^{\mu\nu}$:

$$A_{\text{ext}}^t = \mu_{\text{ext}} - \varphi = \mu_{\text{ext}} - \varphi_{\text{ext}} - 10 - .18 \, \delta \varphi \tag{9.24}$$

where

$$\varphi(\mathbf{x}) = \int d^2 \mathbf{y} \ K(\mathbf{x} - \mathbf{y}) \ n(\mathbf{y}), \tag{9.25}$$

with K a Coulomb kernel whose specific form [?] is not necessary for our purposes, and the n the charge density. At $T_0 = 0$, $K(r) = \alpha_{\rm eff}/r$; at finite T_0 , this is cut-off at long wavelengths due to thermal screening [?]. In (??) we have separated the effects of Coulomb screening into two contributions: $\varphi_{\rm ext}$, which alters the background disorder profile, so that $\mu_0 \neq \mu_{\rm ext}$, and $1 \, 0$ -.18 $\delta \varphi$, which is the infinitesimal Coulomb potential created by the change in charge density $1 \, 0$ -.18 δn , proportional to E_i and ζ_i .

The time-independent equations of motion depend only on T, v_i , the sources E_i and ζ_i , and the electrochemical potential

$$1 \ 0 - .18 \ \delta \Phi \equiv 1 \ 0 - .18 \ \delta \mu + 1 \ 0 - .18 \ \delta \varphi. \tag{9.26}$$

This is a direct consequence of the tightly constrained way that F_{ext} and μ enter the hydrodynamic gradient expansion. If we solve for 1.0-.18 $\delta\Phi$ instead of 1.0-.18 $\delta\mu$, we find that Coulomb screening does not affect dc transport at all: more precisely, the equations of motion are identical to those in Section ??, but with 1.0-.18 $\delta\Phi$ replacing 1.0-.18 $\delta\mu$. That dc transport is insensitive to Coulomb screening of the hydrodynamic degrees of freedom was also noted in [?] in a homogeneous fluid by appealing to the random phase approximation.⁵⁴ It is therefore appropriate to directly apply the formalism of Section ?? to study dc thermal and electric transport in the Dirac fluid in graphene. To maintain notation with Section ??,

⁵⁴See also the discussion in [?, ?].

we will continue to refer to Φ as μ in our linear response theory, with the understanding that this includes corrections due to Coulomb screening.

Numerical Results

Having argued that the theory of Section ?? is an acceptable approximation for dc transport in the Dirac fluid in graphene, we now present the results of numerical simulations of (??). In our numerics, we assume that the equations of state of the graphene fluid are as follows:

$$n(\mu_0) = \left(\frac{k_{\rm B}T_0}{\hbar v_{\rm F}}\right)^2 \left[C_2 \frac{\mu_0}{k_{\rm B}T_0} + C_4 \left(\frac{\mu_0}{k_{\rm B}T_0}\right)^3 \right],\tag{9.27a}$$

$$s(\mu_0) = \frac{k_{\rm B}^3 T_0^2}{(\hbar v_{\rm F})^2} \left[C_0 + \frac{C_2}{2} \left(\frac{\mu_0}{k_{\rm B} T_0} \right)^2 - \frac{C_4}{4} \left(\frac{\mu_0}{k_{\rm B} T_0} \right)^4 \right],\tag{9.27b}$$

$$\eta(\mu_0) = \frac{(k_{\rm B}T_0)^2}{\hbar v_{\rm F}^2} \eta_0,$$
(9.27c)

$$\zeta(\mu_0) = 0, \tag{9.27d}$$

$$\sigma(\mu_0) = \frac{e^2}{\hbar} \sigma_0, \tag{9.27e}$$

with $C_{0,2,4}$, σ_0 and η_0 dimensionless constants. The form of n and s are consistent with thermodynamic Maxwell relations – see Appendix ??. We take the disorder profile to be random sums of sine waves, and normalize the disorder distribution so that

$$\langle (\mu_0 - \bar{\mu}_0)^2 \rangle = u_0^2 (k_B T_0)^2.$$
 (9.28)

The shortest wavelength sine wave in the problem is taken to have wavelength $\xi = l_{\rm ee}$ in all of our numerics. There is an exact symmetry of the problem under which ξ can be made arbitrary, so long as we rescale η and ζ by a factor of $(\xi/l_{\rm ee})^2$ – see Appendix ??. We have chosen this value of ξ as it is roughly consistent with previous experimental observations [?], and also the smallest value for which a hydrodynamic description is sensible. More details on numerical methods are in Appendix ??.

An example of our numerical results is shown in Figure ??, where the results of varying the dimensionless viscosity η_0 are shown. When the charge puddle sizes are ~ 20 K, as in experiment [?], the value of η_0 dramatically alters the transport coefficients as a function of density. In particular, the $\sigma(n)$ and $\alpha(n)$ curves are substantially flattened, an effect which is predicted using (??). Further, the peak in $\kappa(n)$ is substantially smaller than predicted perturbatively, and $\kappa(n)$ does not shrink to 0 as $n \to \infty$, as predicted in [?]. In contrast, in a limit of extremely weak disorder (temperature at which the Dirac fluid emerges

Figure 34: Numerical computations of transport coefficients with $C_1 = C_2 = \sigma_0 = 1$ and $C_4 = 0$. The top row has $u_0 = 0.2$, and the bottom row has $u_0 = 0.002$. Solid lines are our theoretical results (using the particular disorder realizations studied) and the circular markers are numerical results. Averages are taken over 20 disorder realizations. $T_0 = 75$ K and we employ the value of v_F in graphene.

Figure 35: Numerical computations of transport coefficients with varying C_4 , $C_1 = \sigma_0 = 1$, $\eta_0 = 3$, $C_2 = 0.2$ and $u_0 = 0.2$. The sharp change in behavior when $C_4 < 0$ is a consequence of $n(\mu)$ not being monotonically increasing at large μ . Averages are taken over 20 disorder realizations. $T_0 = 75$ K and we employ the value of v_F in graphene.

 ~ 0.2 K), the transport coefficients are relatively insensitive to the viscosity (assuming that $\eta_0/C_0 \sim 1$, as expected for a strongly interacting quantum fluid).

We also show the consequences of a non-zero C_4 in Figure ??. The most important effect of C_4 is that n and $\bar{\mu}_0$ are no longer proportional – in particular, when $C_4 > 0$ we see that at larger n both σ and α decrease much more slowly with n. Whenever $C_4 \neq 0$, the equations of state become badly behaved at large μ , because $s(\mu)$ or $n(\mu)$ becomes a non-monotonically increasing function. At lower temperatures ($T \lesssim 50$ K) in Figure ??, this begins to be an issue in the codes for the equations of state we use to compare to experiment. This implies that higher order terms in the equations of state (associated with more fit parameters) are necessary.

Comparison to Experiment

We now describe in more details the lessons to be drawn from our fit to experimental data, shown in Figures ?? and ??. Due to a total of 6 fit parameters (3 which determine the overall scales in the plots, and 3 which alter the shapes of curves), we did not perform an exhaustive analysis and find a statistically optimal fit. We found that most choices of parameters do not agree well with data, and the fit we have presented serves as a proof of principle that hydrodynamics can explain many important features of the experiment [?], as we now discuss.

To obtain data at lower temperatures, we have taken disorder realizations from $T_0 = 75$ K, using our standard assumption $\xi = l_{\rm ee}(T_0 = 75$ K), and simply lowered the temperature. We also keep u_0T_0 constant as a function of T_0 . Formally, this implies that at lower temperatures $\xi < l_{\rm ee}$, as $l_{\rm ee} \sim T^{-1}$; this may be problematic for the validity of hydrodynamics. A conservative solution, employing the rescaling symmetries of our theory, is to simply double ξ , and quadruple η_0 : all data is exactly identical, except that for all data points taken in Figure ??, $\xi > l_{\rm ee}$ and η_0 increases.

Figure ?? revisits the T-dependence in κ . Assuming that disorder is weak, we employ (??) and (??) to determine the scaling of κ : since $s \sim T^2$, $\epsilon + P \sim T^3$, $\partial n/\partial \mu \sim T$, and the viscosity dependence in τ is negligible, we obtain $\tau \sim T$ and $\kappa \sim T^3$. That numerics and experiment are not consistent with this

Figure 36: A comparison of our numerical computation of $\kappa(T)$ with experimental results of [?] at the charge neutrality point (n=0). The red data points are experimental data from [?], the blue curve is our disorder-averaged simulation (using identical parameters to Figure ??), and the green dashed curve is the perturbative prediction $\kappa \sim T^3$ for comparison. Data is shown on a log-log scale. The yellow shaded region denotes where Fermi liquid behavior is observed; the purple shaded region denotes the likely onset of electron-phonon coupling.

Figure 37: A comparison of $\kappa(T)$ in simulations with varying C_4 . We take $C_0 = 1$, $C_2 = \eta_0 = 0.1$, $\sigma_0 = 1$, $u_0 = 0.1$ (at $T_0 = 75$ K). At large T both scenarios have $\kappa \sim T^3$; at lower T the fluid with $C_4 > 0$ undergoes a dramatic drop in $\kappa(T)$, similar to that observed in experiment.

power law is a sign of the strong non-perturbative effects, and suggests that observing power law signatures of hydrodynamics may only be possible in the cleanest samples: see Figure ??. Figure ?? suggests that the sharp dependence in T observed in experiment is a consequence of $C_4 > 0$ and is not a robust scaling regime.⁵⁵ As noted in [?], this dramatic T-dependence of κ , in contrast with the very weak T-dependence of σ , at the Dirac point, is a tell-tale sign of hydrodynamics that is not captured by competing theories, such as the bipolar diffusion effect.

The fits to $\sigma(n)$ and $\sigma(T)$ are not as good as the fits to κ . Nonetheless, our theory does help to explain the slow growth in σ away from the Dirac point, as a consequence of a fluid with both non-negligible viscosity and large disorder, as in Figure ??. Our simulations also correctly predict that the conductivity is an increasing function of T, an entirely non-perturbative effect, in Figure ??. This is at odds with predictions from kinetic theory in the Dirac fluid, which predict that $\sigma(n=0,T) \sim \alpha_{\text{eff}}^{-2}$ should be decreasing with T due to the T-dependence in α_{eff} [?]. Any residual contact resistance [?] will also increase the growth rate of $\sigma(n)$ away from the Dirac point, and as such will be closer fit by our numerical results in Figure ??.

The most surprising thing about the fit is the large values of all coefficients, compared to previous theories. For example, it is predicted [?, ?] that $C_0 \lesssim 3.4$, and we find $C_0 \sim 10$. This is a direct consequence of the large values of the density n over which the Dirac fluid is present (as measured by where strong deviations from the Wiedemann-Franz law occur). The naive theoretical estimate is that the Dirac fluid should not extend past about $n \sim 40 - 1.0 - .25 \,\mu\text{m}^{-2}$, 56 yet we see the Dirac fluid all the way to about $n \sim 200 - 1.0 - .25 \,\mu\text{m}^{-2}$; we will comment more on this issue shortly. As in non-relativistic fluid dynamics, our hydrodynamic theory has a large number of rescaling symmetries (Appendix ??), and these rescaling symmetries turn out to lead to very large values for all hydrodynamic coefficients as a consequence of the large scale on the density axis in Figure ??.

 $[\]overline{^{55}}$ For this particular simulation, the disorder becomes large enough at $T \lesssim 7.5$ K that disorder realizations with $C_4 = 0.1$ sometimes have unphysical thermodynamic behavior.

 $^{^{56}}$ We have used theoretically predicted values of C_0 and C_2 [?], and assumed that the Dirac fluid ends when the μ -dependent contribution to s is comparable to the T-dependent contribution.

Another consequence of this rescaling is a dramatically large shear viscosity: $\eta_0 \sim 100$. It is now canonical to normalize this by the entropy density, and so the "proper units" to measure η in are $\eta_0/C_0 \approx 10$. This scaling is a consequence of a proposition [?] that strongly coupled theories would have $\eta/s \approx \hbar/4 + 10$ -.18 $\hbar/8$, or $\eta_0/C_0 \approx 1/4 + 10$ -.18 $\hbar/8$. The viscosity is a helpful measure of the interaction strength in a theory; if the interactions are perturbatively controlled by a small parameter g, then we expect $\eta \sim g^{-2}$; only when the interaction strength is large can $\eta \sim s$, up to a prefactor of order unity. Hence, coming close to saturating the bound of [?] is a signature that the fluid is strongly interacting. Our estimate for η_0/C_0 is about 100 times larger than the bound of [?]. Smaller values of $\eta/s \sim 0.5\hbar/k_{\rm B}$ have been reported in other experiments in cold atomic gases [?] and quark-gluon plasma [?]. The possibility of adding the Dirac fluid to a list of strongly interacting quantum fluids is tantalizing, and a more direct measure of η in the Dirac fluid is of interest.

One possibility is that our bare coefficients C_0 , η_0 etc. are anomalously large because [?] has measured the average charge density in the entire sample. However, some regions of the sample (notably close to the contacts on the edges [?], or regions very close to impurities) may have such large local values of μ_0 that they are always in a Fermi liquid regime. So long as these Fermi liquid regimes do not percolate across the entire sample, our hydrodynamic description of transport may be quite reasonable in the bulk. However, these regions have a much smaller compressibility, and so can absorb a lot of charge relative to a clean Dirac fluid. It may be that the total averaged charge density is then not equal to the averaged hydrodynamic charge density, leading us to overestimate n. Rescaling $n \to \lambda n$ would rescale $C_0 \to \lambda C_0$ and $\eta_0 \to \lambda^2 \eta_0$. Choosing $\lambda = 0.2$, in accordance with our previous estimates on the regime of the Dirac fluid at $T_0 \sim 75$ K, we obtain $C_0 \sim 2$ and $\eta_0/C_0 \sim 2$, which are both reasonable for a strongly interacting fluid.

As noted previously, we expect that future measurements in cleaner samples may give a wider separation between l_{ee} and ξ . Together with a better understanding of edge effects and the charge puddle profile, we expect this approach to lead to cleaner estimates of $C_{0,2,4}$, η_0 and σ_0 .

Phonons in Graphene

Throughout this work we have neglected the effects of electron-phonon coupling in graphene [?, ?]. In this section, we provide some brief qualitative comments on the role of electron-phonon coupling in the experiment [?], and discuss signatures for future experiments.

Generically, phonons extract both energy and momentum from the electronic fluid, and in doing so hamper a hydrodynamic description.⁵⁷ In graphene, the acoustic branch(es) of phonons have dispersion

⁵⁷The hydrodynamic description of transport reduces to a diffusion equation for the conserved electrical current. Historically,

relation [?]

$$\omega_{\rm ac}(\mathbf{q}) \approx \hbar v_{\rm a} |\mathbf{q}| \tag{9.29}$$

with $v_a \approx 2 \times 10^4$ m/s and so $v_a \ll v_F$. By considering conservation of energy and momentum in electronphonon scattering events, one finds that the phonon energies are negligible, and thus the scattering event can be treated as elastic from the point of view of the electrons.

If only acoustic phonons couple to the electronic fluid, we may approximate that the momentum conservation equation is modified, following the phenomenology of [?]:

$$\partial_{\mu} T^{\mu i} \approx F_{\text{ext}}^{\nu i} J_{\nu} - \frac{T^{ti}}{\tau_{\text{a}}}.$$
(9.30)

The latter term implies that the momentum of the electronic fluid degrades at a constant rate $\tau_{\rm a}^{-1}$, which we take to be

$$\frac{1}{\tau_{\rm a}} = \mathcal{B}T^a,\tag{9.31}$$

where a>0 and $\mathcal{B}>0$ are constants that are phenomenological. [?] computed their values using kinetic theory and found a=4 far from the Dirac point. This effect has been observed experimentally [?], but a is expected to change near the Dirac point. Following arguments similar to [?, ?], we can estimate a by assuming a quasiparticle description of transport, and that the dominant events are absorption or emission of a single phonon. Since acoustic phonons cannot effectively carry away energy, a Dirac quasiparticle of energy ϵ can scatter into $\sim \epsilon$ states. All phonons with relevant momenta are thermally populated, and we estimate the scattering rate to be proportional to the momentum of the phonon. Thus we estimate, using that the typical quasiparticle energy is $\epsilon \sim T$, $a=1+1=2.^{58}$

Assuming that the charge puddles are small and can be accounted for perturbatively, κ is approximately given by (??) at the Dirac point, with

$$\frac{1}{\tau} \approx \frac{u^2}{2\sigma_{\mathcal{Q}}(\epsilon + P)} \left(\frac{\partial n}{\partial \mu}\right)^2 + \mathcal{B}T^a = \frac{\mathcal{A}u^2}{T^b} + \mathcal{B}T^a. \tag{9.32}$$

Our analytic theory predicts b = 1. The contribution κ from electron-phonon coupling is negligible so long as

$$T \ll T^* \equiv \left(\frac{\mathcal{A}}{\mathcal{B}}u^2\right)^{\frac{1}{b+a}}.$$
 (9.33)

Note that $T^*(u)$ is an increasing function – the weaker the disorder, the lower the temperature at which

this was modeled via resistor networks [?, ?].

 $^{^{58}}$ As there is no large Fermi surface with $\mu \gg k_{\rm B}T$, no further corrections to a are necessary, as in usual metals.

Figure 38: A sketch of $\kappa(T)$, accounting for coupling to acoustic phonons, for samples of graphene with three different amounts of disorder (measured by u). We take a=3, b=1 in this plot.

electron-phonon coupling cannot be neglected in the Dirac fluid. The thermal conductivity scales as

$$\kappa \sim \begin{cases}
T^{2+b} & T \ll T^* \\
T^{2-a} & T \gg T^*
\end{cases}$$
(9.34)

If a > 2, we find phenomenology quite similar to that observed in [?], with $\kappa(T)$ growing non-monotonically. We also find that

$$\kappa(T^*) = \mathcal{C}(T^*)^{2-a},\tag{9.35}$$

a result which can be tested in experiment by measuring T^* via the peak in κ for different samples. The prefactor of this proportionality \mathcal{C} may not be very sensitive to the particular sample, since it is independent of u. Figure ?? shows a sketch of $\kappa(T)$, accounting for acoustic phonons, in three samples with different disorder strengths u. This mechanism is also consistent with the fact that the cleaner samples in [?] had peaks in $\kappa(T)$ at lower temperatures, which suggests our proposed mechanism for the non-monotonicity in $\kappa(T)$ is sensible. Although our perturbative quasiparticle-based argument found a=2 above, the presence of local charge puddles may increase the effective value of a to somewhere between 2 and 4, and lead to $\kappa(T^*)$ be a decreasing function. A careful analysis of electron-phonon coupling in disordered Dirac fluids is worth more study.

At higher temperatures, we expect optical phonons to couple non-negligibly to the electron fluid. These phonons can exchange both energy and momentum effectively, and at this point we expect the measured thermal conductivity to increase due to electron-phonon coupling. In [?], there is a sharp upturn in $\kappa(T)$ at all densities at temperatures of 100 K, which is likely due to activation of optical phonons in the boron nitride subtrate [?].

Conclusions

We have developed a theory of transport in realistic hydrodynamic electron fluids near a quantum critical point. This theory provides a substantially improved quantitative fit to $\kappa(n)$ and $\sigma(n)$ simultaneously. We have further found reasonable quantitative fits to $\sigma(T)$ and $\kappa(T)$ at the Dirac point, giving us valuable information about the mechanism of momentum relaxation beyond the theory of [?].

Although we have managed to find fluids where the growth in $\sigma(n)$ is quite slow, there are still differences

between the shape of $\sigma(n)$ found numerically and in experiment. There are numerous possibilities for residual discrepancies. One of the most important possibilities is that the disorder is so strong that the full thermodynamic equation of state is necessary – in this paper, we have only kept the three leading order terms. Alternatively, we may simply not have found the correct equation of state of graphene. A disorder profile more subtle than superimposed sines and cosines may also be responsible for deviations with our theory, although our investigation into this possibility suggests that other disorder profiles cause $\sigma(n)$ to have more substantial density dependence. We have assumed that the disorder profile is unaltered both by changes in T and in $\bar{\mu}_0$. This is a very strong assumption and need not be true. Finally, there may be other sources of momentum relaxation, such as out-of-plane distortions in the graphene lattice, or interactions with phonons. An understanding of the aforementioned issues is an important future task, though may be quite challenging given the possibility that strong interactions in the Dirac fluid at $T \sim 70$ K may lead to the failure of standard perturbative techniques. The most fruitful direction for resolving at least some of these questions may be directly in experiments: for example, techniques to directly resolve the local charge density on length scales $\lesssim 10$ nm are well known [?], and can shed light into the evolution of μ_0 as a function of T, as well as the spatial correlations in μ_0 .

Experimentally, it may be possible to generate samples of graphene with much weaker charge puddles using suspended devices [?, ?]. Thermodynamic measurements can also be used to determine the coefficients $C_{0,2,4}$, though these measurements are complicated by the presence of disorder, as we discuss in Appendix ??. Nonetheless, measurements of the specific heat and compressibility in the Dirac fluid will serve as valuable guideposts for future hydrodynamic models. Such measurements have been made in the Fermi liquid [?], and their extension to the Dirac fluid form the basis for worthwhile experiments.

Previous experiments which measured the ac conductivity [?] were not in the hydrodynamic limit. Comparing the momentum relaxation time τ between measurements of κ , and a putative Drude peak in ac transport, may provide a quantitative test of our theory. Studying magnetotransport [?] may also be a fruitful direction in experiments. A theoretical discussion of transport at finite frequency and magnetic field beyond the weak disorder limit will appear elsewhere. The thermopower of graphene has recently been measured at $T \sim 200$ K [?], and it would be interesting to measure σ , α and κ in the same sample in the Dirac fluid and compare with our hydrodynamic formalism.

Appendix A

Appendix for Chapter 5

Here we discuss the matrix element $M_{P_x\partial_x n}$, when the operator \mathcal{O} which couples to the translational symmetry breaking field is not charge conjugation symmetric. From the definition of the memory matrix,

$$M_{P_x \partial_x n} = \frac{1}{\pi i} \int d\omega \int d^d \mathbf{q} \ h(\mathbf{q}) \frac{\operatorname{Im} \left(-i\omega G_{\mathcal{O}\partial_x n}^{R}(\mathbf{q}, k_x, \omega) \right)}{\omega(\omega - z)}, \tag{A.1}$$

where we have related \dot{P}_x to \mathcal{O} . Let us discuss the general structure of this Green's function. In fact, noting that z is just above the real axis, we find that

$$M_{P_x \partial_x n} = \int d^d \mathbf{q} \ h(\mathbf{q}) \operatorname{Re} \left(G_{\mathcal{O} \partial_x n}^{\mathrm{R}}(\mathbf{q}, k_x, 0) \right). \tag{A.2}$$

We know that $G_{\mathcal{O}\partial_x n}^{\mathrm{R}} \sim h$, as this Green's function does not obey translation invariance, and thus must be proportional to h. Furthermore, so long as charge is an exactly conserved quantity, and this Green's function is analytic in a neighborhood of $k_x = 0$, we conclude that $G_{\mathcal{O}\partial_x n}^{\mathrm{R}} \sim hk_x$. Thus we conclude that $M_{P_x\partial_x n} \sim h^2k_x$.

Next, let us consider the corrections to the conductivity. For simplicity, we focus on the case where B=0, but similar considerations will hold in the more general case. The full memory matrix \mathfrak{m} is block diagonal, and, considering only xx indices, is

$$\mathfrak{m} = \begin{pmatrix} h^2 \mathcal{B} & h^2 k_x \mathcal{A} \\ h^2 k_x \mathcal{A} & \sigma_Q k_x^2 \end{pmatrix}$$
(A.3)

with \mathcal{A} and \mathcal{B} chosen as functions which are not perturbatively small. We find

$$\mathfrak{m}^{-1} = \frac{1}{h^2 k_x^2 \mathcal{B} \sigma_{\mathcal{Q}} - k_x^2 h^4 \mathcal{A}^2} \begin{pmatrix} \sigma_{\mathcal{Q}} k_x^2 & -h^2 k_x \mathcal{A} \\ -h^2 k_x \mathcal{A} & h^2 \mathcal{B} \end{pmatrix} \approx \begin{pmatrix} 1/h^2 \mathcal{B} & -\mathcal{A}/\mathcal{B} \sigma_{\mathcal{Q}} k_x \\ -\mathcal{A}/\mathcal{B} \sigma_{\mathcal{Q}} k_x & 1/\sigma_{\mathcal{Q}} k_x^2 \end{pmatrix}$$
(A.4)

The correction to the conductivity as given in (??) is

$$\delta \sigma_{xx} = -\frac{2\mathcal{A}\mathcal{Q}}{\mathcal{B}}.\tag{A.5}$$

This is, in our limit, much smaller than either σ_Q or $Q^2\tau/\mathcal{M}$. Logically, we should think of this as much smaller than σ_Q since we argued previously that either σ_Q must be anomalously large, or Q must be very small, in order for $\sigma_Q \sim Q^2\tau/\mathcal{M}$ to be possible. (If τ is anomalously large and σ_Q is negligible, then we should generically expect $\delta\sigma_{xx}$ to also be negligible). Thus, it is consistent to ignore these corrections to the memory matrix at leading order.

Appendix B

Appendix for Chapter 8

Sample Fabrication

Single layer graphene is encapsulated in hexagonal boron nitride on an n-doped silicon wafer with 285 nm SiO₂ [?] and is subsequently annealed in vacuum for 15 minutes at 350 °C. It is then etched using reactive-ion-etching (RIE) to define the width of the device. A second etch mask is then lithographically defined to overlap with the sample edge, leaving the rest of the sample rectangular shaped with the desired aspect ratio. After the RIE is performed, the same etch mask is used as the metal deposition mask, upon which Cr/Pd/Au (1.5 nm / 5 nm / 200 nm) is deposited. The resulting Ohmic contacts show low contact resistances and small PN junction effects due to their minimum overlap with device edge.

Optimizing samples for high frequency thermal conductivity measurements

To measure the electronic thermal conductivity $\kappa_{\rm e}$ of graphene using high frequency Johnson noise the sample design should be made with three additional considerations: stray chip capacitance, resistance of the lead wires, and sample dimensions that enhance electron diffusion cooling over phonon coupling.

Johnson noise thermometry (JNT) relies on measuring the total noise power emitted in a specified frequency band and relating that to the electronic temperature on the device; to maximize the sensitivity, high frequency and wide bandwidth measurements should be made [?]. In the temperature range discussed here, the upper frequency limit for JNT is typically set by the amount of stray capacitance from the graphene, lead wires, and contact pads to the Si back gate. This is minimized by using short, narrow lead wires and small (50 $\,$ 1 0 -.25 μ m \times 50 $\,$ 1 0 -.25 μ m) bonding pads resulting in an estimated 4 pF stray capacitance.

The amount of Johnson noise emitted between any two terminals is proportional to the mean electronic

	S1	S2	S3
length (1 025 μ m)	3	3	4
width (1 025 /km)	9	9	10.5
mobility $(10^5 \text{ cm}^2 \cdot \text{V}^{-1} \cdot \text{s}^{-1})$	3	2.5	0.8
$n_{\rm min} \ (10^9 \ {\rm cm}^{-2})$	5	8	10

Table 2: Basic properties of our three samples.

temperature between them where each point in space is weighted by its local resistance. Therefore, to maximize the signal coming from the graphene, contact resistance should be kept at a minimum. To compensate for the narrow lead wires, we deposit a thicker layer (200 nm) of gold resulting in an estimated lead resistance of 50 Ω . This, combined with an estimated interfacial contact resistance of < 135 $\Omega \cdot 10$ -.25 μ m results in a total measured contact resistance of < 80 Ω . The interfacial contact resistance may be density dependent and we estimate it to be $\lesssim 100$ –300 $\Omega \cdot 10$ -.25 μ m. The most important effect of this contact resistance is likely the thermal resistance associated to the contacts, which may limit the maximal observable Lorenz ratio. As such, the true value of $\mathcal L$ is likely slightly higher than what we measure.

Lastly, to effectively extract κ_e from the total electronic thermal conductance $G_{\rm th}$ we want to enhance the electron diffusion cooling pathway with respect to the electron-phonon cooling pathway (see below). This can be accomplished by keeping the length of the sample short as the total power coupled into the lattice scales as the area of the device while diffusion cooling scales as 1/R. In addition, the device should be made wide to minimize the effects of disordered edges. We find these high aspect ratio samples ($\sim 3:1$) are ideal for our measurements and serve the additional purpose of lowering the total sample resistance allowing us to impedance match over a wider bandwidth.

Device Characterization

In this study we measure three graphene devices encapsulated in hexagonal boron nitride (hBN), whose basic properties are detailed in Table ??. All devices are two-terminal with mobility estimated as

$$\mu \approx \frac{L}{neRW},$$
(B.1)

where L and W are the sample length and width respectively, e is the electron charge, and n is the charge carrier density. The gate capacitance per unit area $C_{\rm g} \approx 0.11~{\rm fF}/~1~0~\text{-}.25~\mu{\rm m}^2$ is estimated considering the 285 nm SiO₂ and $\sim 20~{\rm nm}$ hBN dielectrics. From this we estimate the charge density

$$n = \frac{C_{\rm g}(V_{\rm g} - V_{\rm d})}{e} \tag{B.2}$$

Figure 39: 2-terminal resistance R vs. back gate voltage for the 3 samples used in this report.

Figure 40: Reflectance $\mathcal{R} = |S_{11}|^2$ for a graphene device impedance matched to 50 Ω near 125 MHz.

where $V_{\rm d}$ is the gate voltage corresponding to the charge neutrality point (CNP) estimated by the location of the maximum of the curve $R(V_{\rm g})$. Fig. ?? shows the resistance of all samples as a function of gate voltage.

Johnson Noise Thermometry

The full Johnson noise thermometry (JNT) setup used in this study is outlined in detail in [?]. Here, we only give a brief synopsis for completeness.

The electronic transport within a dissipative device can be determined by the high frequency noise power collected by a low noise amplifier as

$$\langle V^2 \rangle = k_{\rm B} T_{\rm e} \times \text{Re}(Z) \Delta f \left[1 - \left(\frac{Z - Z_0}{Z + Z_0} \right)^2 \right]$$
 (B.3)

where Z is the complex impedance of the device under test, Z_0 is the impedance of the measure circuit (typically 50 Ω) and Δf is the bandwidth. From this formula, we can see two critical components of JNT: impedance matching over a wide bandwidth and low noise amplification.

Graphene devices have a typical channel resistance on the order of $h/4e^2 \sim 6 \text{ k}\Omega$ near the CNP. To compensate for this, we use an inductor-capacitor (LC) tank circuit mounted directly on the sample package to impedance match the graphene to the 50 Ω measurement network. Fig. ?? shows the reflectance coefficient $\mathcal{R} = |S_{11}|^2$ for a typical graphene device after impedance matching. The bandwidth and measurement frequency of our JNT is set by the Q-factor and LC time of this matchingnetwork.

At 10 K, the power emitted by a resistor in a 1 Hz bandwidth is $\sim 10^{-22}$ W or -190 dBm. To amplify this signal we use a SiGe low noise amplifier (Caltech CITLF3) with a room temperature noise figure of about 0.64 dB in our measurement bandwidth, corresponding to a noise temperature of about 46 K. We operate the amplifier at room temperature, outside of the cryostat, to ensure it is unaffected by the 3–300 K temperature ramp used for thermal conduction measurements. After amplification, a homodyne mixer and low pass filter define the measurement bandwidth and the power is found by an analog RF multiplier operating up to 2 GHz (Analog Devices ADL5931). The result is a voltage proportional to the Johnson noise power which – after calibration – measures the electron temperature in the graphene device.

Calibration of our JNT device must be done on every sample as each device has a unique $R(T, V_g)$ and

Figure 41: Output voltage V_s from the JNT measuring a graphene device with no excitation current. This is used to calibrate the JNT to a given sample.

Figure 42: The electronic temperature in an encapsulated graphene device as a function of heating current for three different bath temperatures. $T_{\rm e} = T_{\rm bath} + I^2 R/G_{\rm th}$. The total thermal conductance between the electronic system and the bath is found through Fourier's Law (solid lines).

therefore couples differently to the amplifier. The graphene device being measured is placed on a cold finger in a cryostat with varying temperature T_{bath} . With no excitation current in the graphene, we collect the JNT signal $V_{\text{s}}(T, V_{\text{g}})$ for all temperatures and gate voltage needed in the study, as shown in Fig. ??. The linear temperature slope at each point gives a gain factor $g(T, V_{\text{g}}) = \partial V_{\text{s}}/\partial T$.

Measuring electronic thermal conductance

The procedure used to measure electronic thermal conductance is outlined in [?, ?, ?]. A small sinusoidal current $I(\omega)$ is run through the graphene sample, causing a Joule heating power $P(2\omega)$ to be injected directly into the electronic system. This causes a small temperature difference $\Delta T(2\omega)$ between the electronic temperature and the bath, described by Fourier's law:

$$P = G_{\rm th} \Delta T. \tag{B.4}$$

Here $G_{\rm th}$ is the total thermal conductance between the electronic system and the bath. The component of Johnson noise at frequency 2ω is measured by a lock-in amplifier and then converted to a temperature difference ΔT using the gain $g(T, V_{\rm g})$ described in the previous section. Fig. ?? shows $T_{\rm e}$ as a function of heating current I for a graphene device at three different bath temperatures: 3, 30 and 300 K.

Thermal model of graphene electrons

In the regime presented here, G_{th} is dominated by two electronic cooling pathways. Hot electrons can diffuse directly out to the contacts (G_{diff}) , or they can couple to phonons $(G_{\text{el-ph}})$:

$$G \approx G_{\text{diff}} + G_{\text{el-ph}}.$$
 (B.5)

In a typical metal, electron diffusion is described by the WF law which is linear in $T_{\rm e}$. The electron-phonon cooling pathway has two components: first, the electrons must transfer heat to the lattice via electron-phonon

Figure 43: Simplified thermal diagram of the electronic cooling pathways in graphene relevant for our experimental conditions. A current induces a heating power into the electronic system which conducts to the bath via two parallel pathways: diffusion and coupling to phonons.

Figure 44: Comparison of the measured thermal conductance to the heat transfer to phonons due to electronphonon coupling. Data (blue diamonds) from Sample S1 at charge carrier density of $3.3 \times 10^{11}/\text{cm}^2$. Red solid and green dashed lines are the expected thermal conductance of heat transfer from electrons to phonons.

coupling, and then the lattice must conduct the heat to the bath. Fig. ?? shows the simplified thermal diagram of the electronic cooling pathways in graphene, relevant to our experiment.

At low temperature, $G_{\rm th}$ is dominated by $G_{\rm diff}$, while at high temperature it is dominated by $G_{\rm el-ph}$. We plot in Fig. ?? our data compared to two different experimental reports. For our device parameters, the heat transferred to the lattice by the supercollision mechansim is much smaller (green solid line) as verified by three independent experiments in Ref. [?, ?, ?], based on the theories of Song-Reizer-Levitov [?] and Chen-Clerk [?]. Similarly, the heat transferred to acoustic phonons is also smaller than the electronic diffusion term for our device geometry (purple solid curve) as verified by three sets of experiments in Ref. [?], [?, ?, ?, ?] based on the theories of Bistritzer-MacDonald [?], Tse-DasSarma [?], Viljas-Heikkalla [?], and Kubakaddi [?]. Yigen and Champagne reported in Ref. [?] a similar graphene device dominated by the electronic thermal conductivity. Hence the electronic contribution to the thermal conductivity and the Lorenz number can be directly measured in Yigen-Champagne's [?] and our experiments without the influence of acoustic phonons below $\sim 100 \text{ K}$.

Measuring Thermal Conductivity

In the diffusion-limited regime, we extract the electronic thermal conductivity $\kappa_{\rm e}$ as follows. This is detailed in [?] and we review the basic calculation for clarity. The total power dissipated, P, is given by

$$P = \frac{J^2}{\sigma}LW = \mathcal{P}LW \tag{B.6}$$

where L is the length of the sample in the direction of current flow, W is the width in the perpendicular direction and \mathcal{P} is the local power dissipated. Because this calculation is done in linear response, and the external heat baths on either side of the sample are at the same temperature, the contributions to power dissipated $\sim \kappa(\Delta T)^2$ do not enter so long as $\Delta T \sim J^2$ is small. This is an appropriate assumption in the regime of linear response, where J is treated as a perturbatively small parameter. Fig. ?? shows our experiment is in this regime.

Figure 45: Cartoon illustrating the non-uniform temperature profile within the graphene-hBN stack during Joule heating in the diffusion-limited regime.

Let us now determine the change in the temperature profile. For simplicity we assume that the graphene sample is homogeneous, that the approximately uniform electrical current is given by

$$J = -\sigma \frac{\mathrm{d}V}{\mathrm{d}x} - \alpha \frac{\mathrm{d}T}{\mathrm{d}x},\tag{B.7}$$

and that the heat current is given by

$$Q = -\alpha T \frac{\mathrm{d}V}{\mathrm{d}x} - \bar{\kappa}_{\mathrm{e}} \frac{\mathrm{d}T}{\mathrm{d}x},\tag{B.8}$$

where

$$\bar{\kappa}_{\rm e} \equiv \kappa_{\rm e} + \frac{T\alpha^2}{\sigma} = \kappa_{\rm e}(1 + ZT).$$
 (B.9)

In the latter equation, ZT is the thermoelectric coefficient of merit. As $\alpha \approx 0$ at the CNP, we expect $ZT \approx 0$, and that $\bar{\kappa}_e \approx \kappa_e$.

 $\mathrm{d}T/\mathrm{d}x$ is the temperature gradient in the sample, and $-\mathrm{d}V/\mathrm{d}x$ is the electric field in the sample. α/σ is the Seebeck coefficient. We assume that the response of graphene is dominated only by the changes in voltage V and temperature T to a uniform current density J, which is applied externally. We also assume that deviations from constant V and T are small, so that the linear response theory is valid. Joule heating leads to the following equations:

$$0 = \frac{\mathrm{d}J}{\mathrm{d}x},\tag{B.10a}$$

$$\mathcal{P} = \frac{J^2}{\sigma} = \frac{\mathrm{d}Q}{\mathrm{d}x},\tag{B.10b}$$

which can be combined to obtain

$$\mathcal{P} = -\kappa_{\rm e} \frac{\mathrm{d}^2 T}{\mathrm{d}x^2},\tag{B.11}$$

assuming that $\kappa_{\rm e}$ is approximately homogeneous throughout the sample.

The contacts in our experiment are held at the same temperature T. Thus, writing

$$T(x) = T_{e} + \Delta T(x), \tag{B.12}$$

we find that

$$\Delta T(x) = \frac{\mathcal{P}}{2\kappa_{\rm e}} x(L - x). \tag{B.13}$$

The average temperature change in the sample, which is directly measured through JNT, is

$$\langle \Delta T \rangle = \int_{0}^{L} \frac{\mathrm{d}x}{L} \ \Delta T(x) = \frac{\mathcal{P}L^2}{12\kappa_{\mathrm{e}}}.$$
 (B.14)

This non-uniform temperature profile is illustrated in Fig. ??. Combining Eqs. (??), (??) and (??) we obtain

$$G_{\rm th} = \frac{12L}{W} \kappa_{\rm e}. \tag{B.15}$$

As we have pointed out in the main text, our samples are not perfectly homogeneous, but have local fluctuations in the charge density. Nevertheless, we do recover the WF law in the FL regime, suggesting that our measurement of $G_{\rm th}$ – and thus $\kappa_{\rm e}$ – using JNT, along with the above formalism, is valid.

Bipolar Diffusion

The bipolar diffusion effect occurs when different charge carriers of opposite sign move in the same direction under an applied temperature gradient. The thermal conductivity κ , as defined in the main text in the absence of net electric current flow, is given in Ref. [?]:

$$\kappa \equiv \left(\bar{\kappa}_{e} - \frac{T\alpha_{e}^{2}}{\sigma_{e}}\right) + \left(\bar{\kappa}_{h} - \frac{T\alpha_{h}^{2}}{\sigma_{h}}\right) + \frac{T\sigma_{e}\sigma_{h}}{\sigma_{e} + \sigma_{h}} \left(\frac{\alpha_{e}}{\sigma_{e}} - \frac{\alpha_{h}}{\sigma_{h}}\right)^{2}$$
(B.16)

The first two terms in the above equations are the thermal conductivity of electrons and holes respectively.

The third term is the bipolar diffusion term, and accounts for the possibility of electrons and holes flowing in the same direction.

Bipolar diffusion has been used to explain the thermal conductivity of narrow gap semiconductors, such as bismuth telluride, when the chemical potential is close to the midgap. Estimates of the Lorenz ratio in bismuth telluride have been reported as high as 7.2 \mathcal{L}_0 in Ref. [?]. In graphene, the two types of charge carriers correspond to above/below the Dirac point. To use the formula (??) requires the assumption that interactions between electrons and holes are negligible. If this is the case, it is reasonable to employ kinetic theory to estimate $\sigma_{e,h}$, $\alpha_{e,h}$ and $\bar{\kappa}_{e,h}$. This was shown in Ref. [?] and we state the formalism here for completeness.

Employing the ultrarelativistic band structure of graphene near the CNP, the transport coefficients are

Figure 46: Comparison of the Lorenz ratio in graphene between bipolar diffusion theory [?] and our experimental data. The sharp temperature dependence of \mathcal{L} is inconsistent with bipolar diffusion (see green dashed lines). This sharp behavior is predicted in hydrodynamics [?].

given by:

$$\sigma_{\rm e} = \int \frac{\mathrm{d}^2 \mathbf{k}}{2\pi^2} \tau_{\rm e}(\mathbf{k}) v_{\rm F}^2 \mathcal{F} \left(\frac{\hbar v_{\rm F} k \pm \mu}{k_{\rm B} T} \right), \tag{B.17a}$$

$$\alpha_{\rm e} = \pm \int \frac{\mathrm{d}^2 \mathbf{k}}{2\pi^2} \tau_{\rm e}(\mathbf{k}) (\hbar v_{\rm F} k \pm \mu) v_{\rm F}^2 \mathcal{F} \left(\frac{\hbar v_{\rm F} k \pm \mu}{k_{\rm B} T} \right), \tag{B.17b}$$

$$\bar{\kappa}_{e} = \int \frac{\mathrm{d}^{2} \mathbf{k}}{2\pi^{2}} \tau_{e}(\mathbf{k}) (\hbar v_{F} k \pm \mu)^{2} v_{F}^{2} \mathcal{F} \left(\frac{\hbar v_{F} k \pm \mu}{k_{B} T} \right), \tag{B.17c}$$

where $\tau_{e,h}$ are suitably defined energy relaxation times for electrons and holes, we use a \pm sign for electrons/holes, and

$$\mathcal{F}(x) \equiv \frac{1}{k_{\rm B}T} \frac{{\rm e}^x}{(1 + {\rm e}^x)^2}.$$
 (B.18)

Given a choice of τ , it is straightforward to numerically integrate these equations. This was done in Ref. [?] for some choices of τ ; we have checked additional choices. We compare the result of this two-band formalism at the CNP, to the same data for S1 used in Figure 3 of the main text. We can rule out the canonical bipolar diffusion (BD) explanation of our data for the following reasons:

- (1) The BD theory predicts that $\mathcal{L}/\mathcal{L}_{WF}$ is independent of temperature at the CNP in a clean sample. Adding disorder only adds a very weak temperature dependence [?]. This is in stark contrast to our data – see Figure ??. Hydrodynamic models do predict a sharp temperature dependence in \mathcal{L} [?].
- (2) Simple models of BD in the presence of charge puddles with local chemical potential fluctuations of 50 meV or higher predict factor of 2 violations of the WF law [?], and a weak dependence of \mathcal{L} on disorder, compared to hydrodynamics. In contrast we see a sharp dependence on disorder, comparing our three samples (Figure 3 of the main text). In samples where chemical potential fluctuations are comparable to 50 meV, the WF law is obeyed to within 40% [?].
- (3) Working under the theory of [?], $\tau(\mathbf{k}) \sim |\mathbf{k}|$, and hence the maximal Lorenz ratio $\mathcal{L}/\mathcal{L}_{\mathrm{WF}} \approx 4$ [?] well below to our experimental observation of $\mathcal{L}/\mathcal{L}_{\mathrm{WF}} \approx 22$.
- (4) The BD theory of [?] predicts $\mathcal{L}/\mathcal{L}_{\mathrm{WF}} \gtrsim 0.8$ under all conditions. Hydrodynamics predicts that this ratio can become arbitrarily small in a clean sample, and we have indeed observed $\mathcal{L}/\mathcal{L}_{\mathrm{WF}} \sim 1/3$ at finite

density in the DF in sample S1, only consistent with hydrodynamics.

Appendix C

Appendix for Chapter 9

Thermodynamics

In this appendix and in every subsequent appendix, we will work in units where $\hbar = k_{\rm B} = v_{\rm F} = e = 1$. It is straightforward using dimensional analysis to restore these units.

We consider the equations of state of the relativistic plasma in a relativistic strongly interacting fluid in d=2. Without specific microscopic details, these are very general facts about relativistic plasmas without an intrinsic mass scale (or gap). The discussion generalizes straightforwardly to other d. The only relevant energy scales are the temperature T and the chemical potential μ . We have the general Gibbs-Duhem relation:

$$\epsilon + P = \mu n + Ts,\tag{C.1}$$

where ϵ is the energy density, P is the pressure, s is the entropy density and n is the charge density (n = 0 at the particle-hole symmetric Dirac point). In a relativistic fluid,

$$P = T^3 \mathcal{F}\left(\frac{\mu}{T}\right) \tag{C.2}$$

for some dimensionless function \mathcal{F} . Thermodynamic identities imply that

$$n = \frac{\partial P}{\partial \mu} = T^2 \mathcal{F}' \left(\frac{\mu}{T}\right) \tag{C.3a}$$

$$s = \frac{\partial P}{\partial T} = 3T^2 \mathcal{F} - \mu T \mathcal{F}' \left(\frac{\mu}{T}\right) = \frac{3P - \mu n}{T}.$$
 (C.3b)

Combining (??) and (??) we obtain

$$\epsilon = 2P.$$
 (C.4)

The hydrodynamic description is only sensible for $\mu \ll T$ – for $\mu \gg T$ the standard Fermi liquid description applies. Furthermore, the equations of state of the Dirac fluid are charge conjugation symmetric, implying that \mathcal{F} is an even function of μ . So we Taylor expand:

$$\mathcal{F}\left(\frac{\mu}{T}\right) \approx \frac{C_0}{3} + \frac{C_2}{2} \left(\frac{\mu}{T}\right)^2 + \frac{C_4}{4} \left(\frac{\mu}{T}\right)^4. \tag{C.5}$$

Using (??):

$$n = C_2 \mu T + C_4 \frac{\mu^3}{T},\tag{C.6a}$$

$$s = C_0 T^2 + \frac{C_2 \mu^2}{2} - \frac{C_4 \mu^4}{4T^2}.$$
 (C.6b)

We also require that $C_0, C_2 \ge 0$, so that $s \ge 0$ and that n/μ is positive as $\mu \to 0$, as it should be.

Thermodynamics of Disordered Fluids

Already at this point we can make interesting predictions about the thermodynamics of the strongly interacting hydrodynamic regime in graphene. For concreteness, let us suppose that the background chemical potential is

$$\mu_0(\mathbf{x}) = \bar{\mu}_0 + \hat{\mu}(\mathbf{x}),\tag{C.7}$$

with $\bar{\mu}_0$ a constant and $\hat{\mu}$ a zero-mean random function; for simplicity, suppose that $\hat{\mu}$ is evenly distributed about zero, and has a disorder correlation length of $\xi \gtrsim l_{\rm ee}$, so that the hydrodynamic description applies. In this case, spatially averaging over μ_0 , we find

$$\langle \epsilon \rangle = \frac{2C_0}{3} T^3 + C_2 T \left(\bar{\mu}_0^2 + \langle \hat{\mu}^2 \rangle \right) + \frac{C_4}{2} \left(\bar{\mu}_0^4 + 6 \bar{\mu}_0^2 \langle \hat{\mu}^2 \rangle + \langle \hat{\mu}^4 \rangle \right) + \cdots$$
 (C.8)

The \cdots denotes higher order terms in the equation of state that we have neglected. A similar expression can be found for the charge density:

$$\langle n \rangle = C_2 T \bar{\mu}_0 + \frac{3C_4}{T} \bar{\mu}_0 \left\langle \hat{\mu}^2 \right\rangle + \cdots . \tag{C.9}$$

Let us focus on a clean limit where $\hat{\mu}$ is very small relative to T. Let us also assume that we are close to

the Dirac point, so that only C_0 and C_2 terms need to be kept. Thermodynamics then gives tight constraints on the behavior of measurable quantities: specific heat and compressibility, in an experimentally testable regime, due to the ability to easily tune both T and $\bar{\mu}_0$ (the average charge density) experimentally. In the limit above, the (spatially averaged) compressibility \mathcal{K} is

$$\frac{1}{\mathcal{K}} = \frac{\partial \langle n \rangle}{\partial \mu} = C_2 T. \tag{C.10}$$

where as before, we use $\langle \cdots \rangle$ to denote a uniform spatial average. Note that the independence of \mathcal{K} to $\bar{\mu}_0$ and $\hat{\mu}$ is simply a consequence of the fact that we did not expand (??) to quartic order. The spatially averaged specific heat

$$c = \frac{\partial \langle \epsilon \rangle}{\partial T} = 2C_0 T^2 + C_2 \left(\bar{\mu}_0^2 + \langle \hat{\mu}^2 \rangle \right). \tag{C.11}$$

The experimental consequence of this result is as follows. Very close to the Dirac point, we expect that \mathcal{K} is approximately constant. Restoring all dimensional prefactors, we can therefore set

$$C_2 \approx \frac{(\hbar v_{\rm F})^2}{\mathcal{K}k_{\rm B}T}$$
 (C.12)

and re-write

$$c \approx 2C_0 \frac{k_{\rm B}^3 T^2}{(\hbar v_{\rm F})^2} + 2 \frac{\bar{\mu}_0^2 + \langle \hat{\mu}^2 \rangle}{\mathcal{K}T} \approx 2C_0 \frac{k_{\rm B}^3 T^2}{(\hbar v_{\rm F})^2} + 2 \frac{\langle \hat{\mu}^2 \rangle}{\mathcal{K}T} + \frac{2\mathcal{K}n^2}{T}.$$
 (C.13)

We thus see that the quadratic dependence in c(n) gives us an independent measurement of \mathcal{K} through a measurement of the heat capacity. In principle, a quadratic polynomial fit to c(n) thus determines both \mathcal{K} and C_0 , up to the residual effects of disorder, which will lead to an overestimate of C_0 . Repeating measurements of \mathcal{K} directly, as well as c(n) at different T, provide non-trivial checks on the above theory. It is important to note that this argument does not rely on the validity of hydrodynamics, only that graphene is gapless, $\bar{\mu}_0 \ll T$, and that $\hat{\mu}$ is very small. Of these three requirements, the last poses the biggest experimental hurdle.

In the above argument, there is no reason a priori why to truncate the Taylor expansion to neglect C_4 and higher order corrections, beyond appealing to the weak disorder limit. In particular, inclusion of C_4 complicates our ability to obtain an accurate measure of $\bar{\mu}_0$ from n. The argument above is simply meant to give a flavor for the constraints on measurable quantities imposed by scale invariant thermodynamics. A more systematic treatment is likely necessary to make quantitative contact with future experiments.

Rescaling Symmetries of dc Transport

Solutions to (??) are invariant, up to global rescalings, under certain rescalings of the linearized hydrodynamic equations of motion. These symmetries are, assuming $\lambda > 0$ is a constant scaling parameter:

$$\eta \to \lambda^2 \eta, \ x \to \lambda x;$$
 (C.14a)

$$\eta \to \lambda \eta, \ \sigma \to \lambda \sigma, \ \alpha \to \lambda \alpha, \ \kappa \to \lambda \kappa, \ P \to \lambda P;$$
 (C.14b)

$$\alpha \to \lambda \alpha, \ \kappa \to \lambda^2 \kappa, \ \eta \to \lambda^{-2} \eta, \ \mu_0 \to \lambda \mu_0, \ C_2 \to \lambda^{-2} C_2, \ C_4 \to \lambda^{-4} C_4, \text{ etc.};$$
 (C.14c)

$$\alpha \to \lambda \alpha, \ \kappa \to \lambda \kappa, \ \sigma \to \lambda \sigma, \ \eta \to \lambda^{-1} \eta.$$
 (C.14d)

Everything not listed is invariant. ζ and η have the same scalings, as do σ and σ_Q , and so we have only listed some of these parameters.

These rescalings are useful to help us compare simulations to experimental data from graphene. The latter three rescalings can be used to help fix the overall magnitude of κ and σ , as well as the values of n, as measured in experiment. These are exactly analogous to the symmetries of the Navier-Stokes equation, which allow us to reduce all such hydrodynamic problems to a universal equation, up to a single dimensionless parameter. [?] neither measured the viscosity directly nor the charge puddle size, and the first scaling above implies that we cannot determine viscosity alone. So, as mentioned in the main text, we assume that $\xi = l_{\text{ee}}$, the shortest possibile value of ξ for which hydrodynamics seems sensible.

Weak Disorder

Many analytic results can be obtained in the limit where the disorder strength is "small". We provide detailed derivations of all such results in this appendix. We introduce disorder as in (??). Below we denote $n_0 = n(\bar{\mu}_0)$, etc.

The perturbative solution is found exactly as was done in [?]: we split the velocity field into a constant piece $\bar{v}_i \sim u^{-2}$, and a fluctuating zero-mean piece $\hat{v}_i \sim u^{-1}$; similarly, $\mu \sim T \sim u^{-1}$. It proves convenient to work in Fourier space. At $O(u^{-1})$, the momentum conservation equation becomes

$$-ik_i \left(n_0 \mu(\mathbf{k}) + s_0 T(\mathbf{k})\right) = \eta_0 k^2 \hat{v}_i(\mathbf{k}) + \zeta_0 k_i k_j \hat{v}_i(\mathbf{k}), \tag{C.15}$$

and the conservation laws become (at the same order)

$$0 = ik_i \left(\hat{n}(\mathbf{k})\bar{v}_i + n_0\hat{v}_i(\mathbf{k})\right) + \sigma_{Q0}k^2 \left(\mu(\mathbf{k}) - \frac{\mu_0}{T_0}T(\mathbf{k})\right), \tag{C.16a}$$

$$0 = ik_i T_0 \left(\hat{s}(\mathbf{k}) \bar{v}_i + s_0 \hat{v}_i(\mathbf{k}) \right) - \mu_0 \sigma_{Q0} k^2 \left(\mu(\mathbf{k}) - \frac{\mu_0}{T_0} T(\mathbf{k}) \right).$$
 (C.16b)

Combining these equations we obtain expressions for T, μ and $k_i\hat{v}_i$:

$$k_i \hat{v}_i(\mathbf{k}) = -\frac{\mu_0 \hat{n}(\mathbf{k}) + T_0 \hat{s}(\mathbf{k})}{\mu_0 n_0 + T_0 s_0} k_i \bar{v}_i, \tag{C.17a}$$

$$T(\mathbf{k}) = -\frac{\mathrm{i}k_i\bar{v}_i}{\sigma_{\mathrm{Q}0}k^2(\epsilon_0 + P_0)^2} \left(\sigma_{\mathrm{Q}0}k^2(\eta_0 + \zeta_0)(\mu_0\hat{n} + T_0\hat{s})T_0 - T_0n_0(T_0s_0\hat{n} - T_0n_0\hat{s})\right),\tag{C.17b}$$

$$\mu(\mathbf{k}) = -\frac{\mathrm{i}k_i \bar{v}_i}{\sigma_{Q0} k^2 (\epsilon_0 + P_0)^2} \left(\sigma_{Q0} k^2 (\eta_0 + \zeta_0) (\mu_0 \hat{n} + T_0 \hat{s}) \mu_0 + T_0 s_0 (T_0 s_0 \hat{n} - T_0 n_0 \hat{s}) \right). \tag{C.17c}$$

Spatially averaging over the momentum conservation equation at $O(u^0)$, and defining:

$$(\epsilon + P)\tau_{ij}^{-1}\bar{v}_j \equiv \sum_{\mathbf{k}} ik_i \left[\hat{n}(-\mathbf{k})\mu(\mathbf{k}) + \hat{s}(-\mathbf{k})T(\mathbf{k})\right], \qquad (C.18)$$

we find that

$$\tau_{ij}^{-1} = \sum_{\mathbf{k}} \frac{k_i k_j}{k^2} \frac{|T_0 s_0 \hat{n}(\mathbf{k}) - T_0 n_0 \hat{s}(\mathbf{k})|^2 + \sigma_{Q0} k^2 (\eta_0 + \zeta_0) |\mu_0 \hat{n}(\mathbf{k}) + T_0 \hat{s}(\mathbf{k})|^2}{\sigma_{Q0} (\epsilon_0 + P_0)^3}$$
(C.19)

and that the spatially averaged momentum equation reduces to

$$0 = n_0 E_i + T_0 s_0 \zeta_i - (\epsilon_0 + P_0) \tau_{ij}^{-1} \bar{v}_j.$$
 (C.20)

In this equation, we have used the fact that $J_i \approx n\bar{v}_i$ at leading order in perturbation theory. The resulting transport coefficients are analogous to $(\ref{equation})$:

$$\sigma_{ij} = \frac{n_0^2}{\epsilon_0 + P_0} \tau_{ij},\tag{C.21a}$$

$$\bar{\alpha}_{ij} = \alpha_{ij} = \frac{n_0 s_0}{\epsilon_0 + P_0} \tau_{ij}, \tag{C.21b}$$

$$\bar{\kappa}_{ij} = \frac{Ts_0^2}{\epsilon_0 + P_0} \tau_{ij}. \tag{C.21c}$$

In the expression for σ , we have not included a σ_{Q0} contribution, as was done in [?], as this is a subleading order in perturbation theory.

Using our Taylor expanded equations of state for the fluid and assuming $C_4 = 0$, since

$$\hat{s}(\mathbf{k}) \approx C_2 \mu_0 \hat{\mu}(\mathbf{k}) = \frac{\mu_0}{T_0} \hat{n}(\mathbf{k}),$$
 (C.22)

we can simplify (??) to

$$\tau_{ij}^{-1} = \sum_{\mathbf{k}} \frac{k_i k_j}{k^2} \frac{(T_0 s_0 - \mu_0 n_0)^2 + 4\sigma_{Q0} k^2 (\eta_0 + \zeta_0) \mu_0^2}{\sigma_{Q0} (\epsilon_0 + P_0)^3} |\hat{n}(\mathbf{k})|^2$$
 (C.23)

Similar results were presented (in a different format) in [?], though the practical consequences of this formula, as discussed in the main text, have not previously been understood.

We cannot take the naive limit where $\sigma_{\rm Q0} \sim u^{-2}$ in order to recover (??) in full generality. The simplest way to see that something goes wrong is to study $\bar{\kappa}$ near $\bar{\mu}_0 = 0$ (more precisely, $\bar{\mu}_0 \sim u$): if $\sigma_{\rm Q} \sim u^{-2}$ we find that $\tau \sim u^{-4}$, and this implies that the heat current (and thus $\bar{\kappa}$) would be parametrically larger than anticipated. Thus our perturbative scaling breaks down. The breakdown of the perturbative theory for $u \sim \bar{\mu}_0$ was also advocated in [?].

Although we have argued there are problems in principle with (??) when $\bar{\mu}_0 \sim u$, even when u is perturbatively small, in practice the mean-field model of [?] can be quite good in practice near $\bar{\mu}_0 \sim u$, as shown in Figure ??. Note that it is also important that $C_0T^2 \gg C_2u^2$ – when this limit is violated, we see substantial deviations from (??) at all $\bar{\mu}_0$, as shown in Figure ??. This may be a consequence of our assumption that σ_Q is independent of μ_0 .

Equations of State of the Dirac Fluid

The thermodynamics of graphene is similar to that presented in Appendix ??, with some minor differences. Perturbative computations and renormalization group arguments, valid as $T \to 0$, give [?, ?]

$$C_0 = \frac{9 \cdot 1 \cdot 0 - .15 \, \xi(3)}{1 \cdot 0 - .18 \, t} \left(\frac{\alpha_{\text{eff}}}{\alpha_0}\right)^2 \approx 3.44 \left(\frac{\alpha}{\alpha_0}\right)^2, \tag{C.24a}$$

$$C_2 = \frac{4\log 2}{10 - .18 \, \pi} \left(\frac{\alpha_{\text{eff}}}{\alpha_0}\right)^2 \approx 0.88 \left(\frac{\alpha}{\alpha_0}\right)^2. \tag{C.24b}$$

(??) can be derived by computing the thermodynamics of 2 species of non-interacting Dirac fermions, with Coulomb interactions leading to a logarithmically increasing Fermi velocity [?, ?]. As $\alpha_{\text{eff}}(T)$ is not a constant, this implies that the entropy has an additional contribution related to the logarithmic T dependence of $C_{0,2}(\alpha_{\text{eff}})$. Assuming C_0 and C_2 above, and assuming $C_4 = 0$ for simplicity as its value for free fermions

is quite small [?], we find:

$$s = C_0 T^2 \left[1 + \frac{\alpha_{\text{eff}}}{6} \right] + \frac{C_2}{2} \mu^2 \left[1 + \frac{\alpha_{\text{eff}}}{2} \right]$$
 (C.25)

This equation directly implies $\epsilon > 2P$. Using the estimate $\alpha_{\rm eff} \sim 0.25$ from above, we see that the corrections to s (and ϵ) are rather minor (< 10%); n is unchanged. In fact, (??) is not quite right: the computation of (??) is only a leading order perturbative computation: there are corrections to (??) at higher orders in $\log \alpha_{\rm eff}$. Nonetheless, our general conclusion that $\epsilon > 2P$ is possible in graphene continues to hold, given any logarithmic running of the Fermi velocity.

As noted above, these theoretical computations of the thermodynamic coefficients in graphene are all perturbative computations in $\alpha_{\rm eff}$, yet we only expect $\alpha_{\rm eff}/\alpha_0 \sim 0.5$: there is no reason to expect that higher order corrections, which can be as large as $\sim \log \alpha_{\rm eff}$, are negligible. More sensitive experiments may find discrepancies with Lorentz invariant hydrodynamics, associated with these peculiar properties of the Dirac fluid. Similar logarithms can appear in σ_Q [?] and η [?], and in both cases, for the reasons above, we neglect these logarithms and use the theory of Section ??.

Numerical Methods

We solved the hydrodynamic equations (??) on a periodic domain of size $L \times L$, employing pseudospectral methods [?] using a basis of N Fourier modes in each direction, with $25 \lesssim N \lesssim 43$. For simplicity, we set $T_0 = 1$, as this can be restored straightforwardly by dimensional analysis. Our numerical methods involves approximating continuous partial differential equations in the form

$$Lu = s. (C.26)$$

 ${\bf u}$ contains the linear response fields μ , T, v_x and v_y , evaluated on a uniformly distributed discrete grid, and ${\bf s}$ contains the source terms, linear in E_i and ζ_i , evaluated at the same points. ${\bf L}$ is a matrix with two zero eigenvectors, which correspond to constant shifts in μ and T respectively. We thus remove two rows of ${\bf L}$ and replace them with constraints that $\mu({\bf 0}) = T({\bf 0}) = 0$. A simple matrix inversion thus gives ${\bf u} = {\bf L}^{-1}{\bf s}$. Inverting this $(4N^2 - 2) \times (4N^2 - 2)$ matrix four times (once for sources $E_{x,y}$ and $\zeta_{x,y}$) limits the size of the domain we can analyze. More complicated algorithms exist [?] to solve such problems but we did not find finite size effects to qualitatively alter our comparison to experimental data, as we discuss below.

As mentioned in the main text, our disorder realizations consisted of random sums of sine waves. More

Figure 47: Finite size effects with $u_0 = 0.3$, $C_0 = 3$, $C_2 = 1$, $\sigma_0 = 1$, $\eta_0 = 20$. Numerical averages are performed over 100 disorder realizations.

Figure 48: Finite size effects with $u_0 = 0.3$, $C_0 = 1$, $C_2 = 1$, $C_0 = 1$, $C_0 = 1$. Numerical averages are performed over 100 disorder realizations.

precisely,

$$\mu_0(\mathbf{x}) = \bar{\mu}_0 + \sum_{|n_x|, |n_y| \le k} \hat{\mu}_0(n_x, n_y) \sin\left(\phi_x + \frac{2n_x + 1 \cdot 0 - .18 \, \pi x}{k\xi}\right) \sin\left(\phi_y + \frac{2n_y + 1 \cdot 0 - .18 \, \pi y}{k\xi}\right) \tag{C.27}$$

with $\bar{\mu}_0$ a constant, $\hat{\mu}_0(n_x, n_y)$ uniformly distributed on [-c, c] where $c = \sqrt{(2-10 \cdot .18 \, \delta_{n_x,0} - 10 \cdot .18 \, \delta_{n_y,0})/2}$, and $\phi_{x,y}$ uniformly distributed on $[0, 2 \ 10 \cdot .18 \, t)$. The lack of heavy tails in $\hat{\mu}_0(n_x, n_y)$, perhaps associated with point-like impurities, is consistent with experiment [?]. The form of c is chosen so that we do not add random charge density bias to our disorder (as the zero mode has no amplitude), and so that all Fourier modes included at finite wave number have the same average amplitude.

Finite Size Effects

The first source of finite size effects is simply related to the fact that we only have a finite number of disorder modes. Averaging over a large number of ensemble samples allows us to approximately, but not exactly, undo this effect: see Figures ?? and ??. In both cases, we used 8k + 3 grid points in each direction for various k. To the best of our knowledge, in all numerical simulations we have studied, it appears as though the result converges to a finite fixed answer as $k \to \infty$. However, residual error from finite size effects may lead to some error in our estimation of the thermodynamic and hydrodynamic coefficients of the Dirac fluid in graphene.

The other source of finite size effects is related to the finite number of grid points in our pseudospectral methods. However, we expect standard exponential accuracy [?] in the number of grid points per ξ , which we have taken to be at least 10 in all figures in the main text. Numerical evidence suggests that our spectral methods have converged to within about 0.1–1% of the correct answer by this relatively small number of grid points per ξ , depending on the precise equations of state used. In the case of the experimentally relevant parameters used in Figure ??, we see exponential convergence of our spectral methods with increasing grid points, with numerical error of only 0.1% by the time the number of grid points per ξ is 11, as shown in Figure ??. This spectral convergence is dramatically faster in the weak disorder limit.

Methods are known to improve our simple algorithms, which can reduce both types of finite size effects

Figure 49: Exponential convergence of our pseudospectral code with an increasing number of grid points. We computed κ and σ using our code, employing the "experimental" equations of state given in Figure ??, and the disorder profile $\mu_0(x) = \bar{\mu}_0 + 2u\cos(2 + 10 - .18 \pi x/L)\cos(2 + 10 - .18 \pi y/L)$. Red data points denote the error in κ , and blue points denote the error in σ . Circles denote data at $\bar{\mu}_0 = 2u$, and triangles at $\bar{\mu}_0 = 0.4u$. Absolute error is determined by (e.g.) $|\sigma(N) - \sigma(29)|/\sigma(29)$, where we use the data points at N = 29 as a reference point.

discussed above. Given the preliminary nature of the experiments to which we compare our simulations, we have found the numerical errors described above tolerable.

Dimensional Analysis

We have performed numerical computations in dimensionless units, since we can trivially restore the units to our numerical results via dimensional analysis. Setting $\hbar=k_{\rm B}=e=v_{\rm F}=T_0=1$ completely non-dimensionalizes the problem, while setting no dimensionless parameters to unity. We can now trivially restore the units as follows:

$$L = \frac{\hbar v_{\rm F}}{k_{\rm B} T_0} \times L_{\rm numerics} \sim (100 \text{ nm}) \times L_{\rm numerics}$$
 (C.28a)

$$\mu = k_{\rm B} T_0 \times \mu_{\rm numerics} \sim (5 \text{ meV}) \times \mu_{\rm numerics},$$
 (C.28b)

$$\sigma = \frac{e^2}{\hbar} \times \sigma_{\text{numerics}} \sim (0.25 \text{ k}\Omega^{-1}) \times \sigma_{\text{numerics}}, \tag{C.28c}$$

$$\alpha = \frac{k_{\rm B}e}{\hbar} \times \alpha_{\rm numerics} \sim \left(20 \, \frac{\rm nW}{\rm V}\right) \times \alpha_{\rm numerics},$$
(C.28d)

$$\kappa = \frac{k_{\rm B}^2 T_0}{\hbar} \times \kappa_{\rm numerics} \sim \left(0.1 \, \frac{\rm nW}{\rm K}\right) \times \kappa_{\rm numerics}. \tag{C.28e}$$

We have also noted the approximate scale of each important physical quantity in the problem for convenience.